JOURNAL OF THE Electrochemical Society

Vol. 107, No. 1 January 1960

AN IMPORTANT MESSAGE FOR ELECTROLYTIC CELL OPERATORS

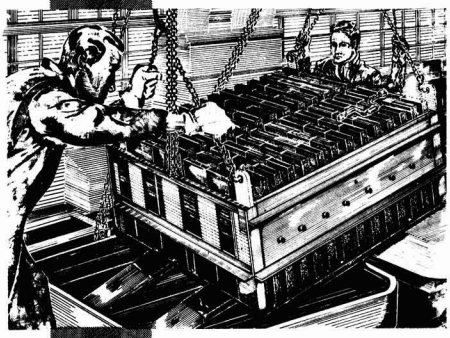

Extra dividends in the form of increased cell operating economies are now available to users of GLC Anodes.

These dividends have been developing during the past several years as a result of exchanges between GLC engineers and those of GLC customers.

Among the results, depending upon the requirements of the individual electrolytic cell operator, are longer anode life, longer diaphragm life, reduced power consumption, and reduced labor costs.

As you know, it takes months to translate technical objectives into anode characteristics—and many months more to check on the results of these changes in cell operations.

The time has now come when the hoped-for results are actually being achieved by GLC Anode customers.

If you, as an electrolytic cell operator, are not as yet fully informed about the GLC program of technical exchanges with GLC Anode customers, and the results of this program which are now becoming evident, we will be happy to furnish such information to you.

We feel sure you will find these facts a profitable step forward in improving the operating efficiency of your electrolytic cells also.

PRODUCTS ELECTRODE GLC DIVISION YOU CAN TRUST

GREAT LAKES CARBON CORPORATION

18 EAST 48TH STREET, NEW YORK 17, N. Y. OFFICES IN PRINCIPAL CITIES

Manuscripts submitted to the Journal should be sent, in triplicate, to the Editorial Office at 1860 Broadway, New York 23, N. Y. They should conform to the Instructions to Authors, last published in the August 1959 issue, pp. 232C-233C. Manuscripts so submitted become the property of The Electrochemical Society and may not be published elsewhere, in whole or in part, unless permission is requested and granted by the Editor.

Inquiries re positive microfilm copies of volumes should be addressed to University Microfilms, Inc., 313 N. First St., Ann Arbor, Mich.

Journal of the Electrochemical Society

JANUARY 1960 **VOL. 107 • NO. 1**

CONTENTS

Published monthly by The Electrochemical Society, Inc., from Manchester, N. H., **Executive Offices, Editorial Office** and **Circulation Dept.,** and **Advertising Office** at 1860 Broadway, New York 23, N. Y., combining the JOURNAL and TRANSACTIONS OF THE ELECTROCHEMICAL SOCIETY. Statements and opinions given in articles and papers in the JOURNAL OF THE ELECTROCHEMICAL SOCIETY are those of the contributors, and The Electrochemical Society assumes no responsibility for them. Nondeductible subscription to members $5.00; subscription to nonmembers $18.00. Single copies $1.25 to members, $1.75 to nonmembers.

Entered as second-class matter at the Post Office at Manchester, N. H., under the act of August 24, 1912.

SARGENT-SLOMIN ANALYZERS
are standard equipment
in prominent laboratories

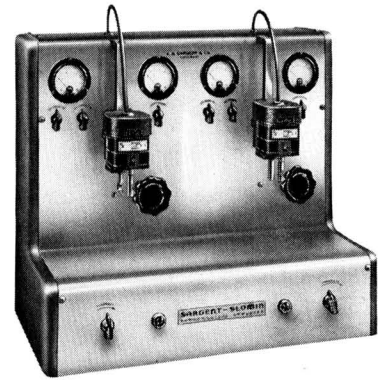

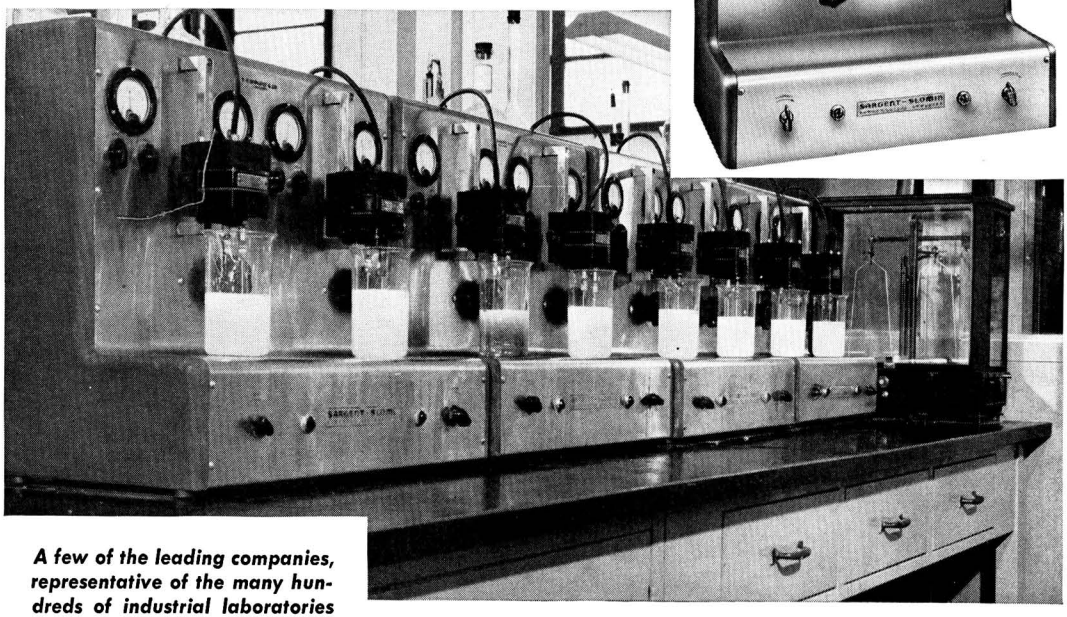

A few of the leading companies, representative of the many hundreds of industrial laboratories using the Sargent - Slomin and Heavy Duty Analyzers for control analyses . . .

AMPCO METAL, Inc.
ANDERSON LABORATORIES
CALERA MINING COMPANY
EUREKA WILLIAMS COMPANY
THE FEDERAL METAL CO.
FORD MOTOR COMPANY
THE GLIDDEN COMPANY—Chemical, Metal and Pigment Division
HOT POINT CO.
HOWARD FOUNDRY COMPANY
INTERNATIONAL HARVESTER COMPANY
KENNAMETAL Inc.
McQUAY - NORRIS MANUFACTURING CO.
NATIONAL LEAD COMPANY, Fredericktown, Missouri
PIASECKI HELICOPTER CORPORATION
REVERE COPPER & BRASS INCORPORATED
THE RIVER SMELTING & REFINING COMPANY
SILAS MASON COMPANY
THE STUDEBAKER CORPORATION
THOMPSON PRODUCTS, INC.

Photo Courtesy INTERNATIONAL HARVESTER COMPANY, Melrose Park, Illinois

Sargent-Slomin Electrolytic Analyzers are recommended for such electro analytical determinations as: Copper in—ores, brass, iron, aluminum and its alloys, magnesium and its alloys, bronze, white metals, silver solders, nickel and zinc die castings. Lead in—brass, aluminum and its alloys, bronze, zinc and zinc die castings. Assay of electrolytical copper, nickel and other metals.

Sargent analyzers are completely line operated, employing self-contained rectifying and filter circuits. Deposition voltage is adjusted by means of autotransformers, with meters indicating volts and amperes and controls on the panel. An easily replaceable fuse guards against circuit overload. Maximum D.C. current capacity is 5 to 15 amperes; maximum D.C. voltage available, 10 volts.

Sargent-Slomin Analyzers stir through a rotating chuck operated from a capacitor type induction motor, having a fixed speed of 550 r.p.m. with 60 cycle A.C. current or 460 r.p.m. with 50 cycle A.C. current. Motors are sealed against corrosive fumes and are mounted on cast metal brackets, sliding on ½" square stainless steel rods, permitting vertical adjustment of electrode position over a distance of 4". Pre-lubricated ball-bearings support the rotating shaft. All analyzers accommodate electrodes having shaft diameters no greater than 0.059 inch. Stainless steel spring tension chucks permit quick, easy insertion of electrodes and maintain proper electrical contact. Special Sargent high efficiency electrodes are available for these analyzers. Illustrated above is one model of the five types of Sargent-Slomin and Heavy Duty Analyzers.

S-29465 ELECTROLYTIC ANALYZER—Motor stirred, Two Position, 5 Ampere. With two adjustable heaters, pilot lights and control knobs. For operation from 115 volt, 50 or 60 cycle A.C. circuits.....**$530.00**

SARGENT *SCIENTIFIC LABORATORY INSTRUMENTS • APPARATUS • SUPPLIES • CHEMICALS*

E. H. SARGENT & COMPANY, 4647 W. FOSTER, CHICAGO 30, ILLINOIS
DETROIT 4, MICH. • DALLAS 35, TEXAS • BIRMINGHAM 4, ALA. • SPRINGFIELD, N. J.

Resolving the driver-car-road complex

The manner in which vehicles follow each other on a highway is a current subject of theoretical investigation at the General Motors Research Laboratories. These studies in traffic dynamics, coupled with controlled experiments, are leading to new "follow-the-leader" models of vehicle interaction.

For example, conditions have been derived for the stability of a chain of moving vehicles when the velocity of the lead car suddenly changes – a type of perturbation that has caused multiple collisions on modern superhighways. Theoretical analysis shows that the motion of a chain of cars *can be stable* when a driver accelerates in proportion to the relative velocity between his car and the car ahead. The motion is always unstable when the acceleration is proportional only to the relative distance between cars. Experimentally, GM Research scientists found that a driver does react mainly to relative velocity rather than to relative distance, with a sensitivity of reaction that increases with decreasing distance.

Traffic dynamics research such as this is adding to our understanding of intricate traffic problems – what causes them, how they can best be resolved. The study is an example of the ways GM Research works to make transportation of the future more efficient and safe.

General Motors Research Laboratories

Warren, Michigan

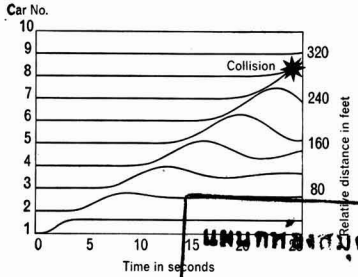

Relative positions of 10 hypothetical cars after lead car goes through maneuver. Amplitude of instability increases, resulting in a collision between 7th and 8th cars.

Editorial

The Preparation of a Manuscript

THE goal of a scientific article is to present a comprehensive, critical account of new experimental or theoretical work, with such discussion, interpretation, and even speculation as will make it of interest and value to an expert in the particular field. Even the student reader should find the presentation lucid and logical so that he can say: I could understand everything if I had more background, or if I could have certain points explained to me.

How can the author write his manuscript so that it approaches this goal? There, of course, is no simple and easy answer to this question, which itself has formed the basis of many excellent articles. We suggest that each author study the style of articles which he thinks are well written, and pay careful attention to the "Instructions to Authors" or its equivalent, published frequently by many journals, including *This Journal* and the *Journal of The American Chemical Society*. The American Institute of Physics publishes a Style Manual,[1] which not only discusses the scientific content of a manuscript but explains some of the problems of publication and shows how the author can ease the editorial task of preparing copy for the printer.

All of the Instructions agree that brevity and conciseness are desirable, not only for the sake of keeping publication costs down, but because the result is more interesting and understandable. Repetition should be avoided, and lengthy discussions should be examined critically to see if they cannot be improved by reduction in length. Many journals, because of the cost, will not publish the same data in both tabular and graphic forms, even though the latter illustrates a derived result. This is sometimes a pity: if one wishes to make new calculations he needs the original data, while graphs often convey much information quickly. Authors must keep these things in mind in deciding how to present data.

The author should remember that the typesetter will know nothing about the contents of an article and must have specific directions for every detail. The manuscripts are "styled" by a special editorial staff, who indicate type size, line and symbol spacing, size and position of headlines and subheadings, sub- and superscripts, Greek letters, special symbols, style of equations etc. The author can help by visualizing what will have to be done to put his manuscript in the smallest space while conforming to current journal style. Among other things, this means watching table headings and columns, figure captions, use of accepted spelling, and hyphenation. Mathematical equations should be written on one line if possible, otherwise should conform to the least expensive method of setting up for printing. Special attention should be given to the list of references—initials of authors are required, abbreviations of journal titles should conform to the Chemical Abstracts "List of Periodicals Abstracted," and if a title is not so listed it should be given in full. The object, of course, is to enable the reader to look up the reference, not to add to an already impressive list.

—CVK

[1] Available for $1.00 from American Institute of Physics, 57 East 55 St., New York 22, N. Y.

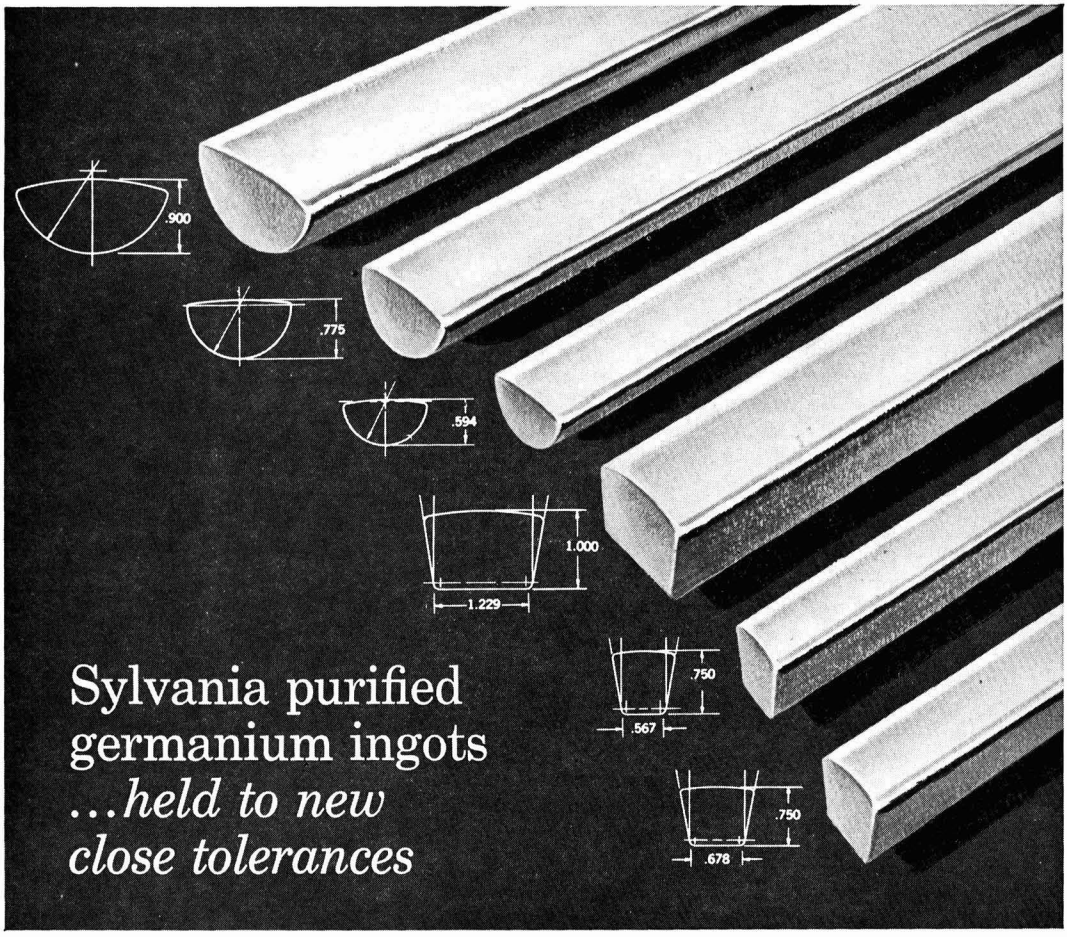

Sylvania purified germanium ingots ...held to new close tolerances

...new dimensions for precise crystal growing

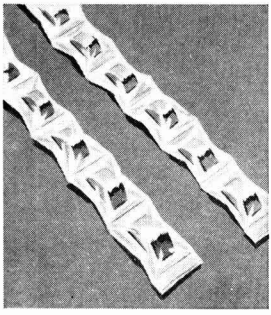

Sylvania germanium pieces, cut to specific size and weight for vertical crystal growing.

THROUGH THE YEARS, from early experimental projects to the place Sylvania now occupies as prime suppliers of as-reduced and purified germanium . . . Sylvania has constantly worked to provide ingots with the maximum yield potentials in single crystals.

Sylvania is now equipped to supply germanium ingots to the closest dimension-tolerances ever achieved. Shown here are the six standard shapes which fill practically every requirement. In each case, the dimensions are held to a new order of precision.

These new precise dimensions result in even melting, less shrinkage and almost negligible surface drop . . . all important factors in preventing waste through polycrystalline formation. You'll find that the unit cost of doped single crystals is lower too.

Special shapes of ingots can of course be supplied to your order if required, and users of the vertical growing method will like Sylvania germanium cut to specific size and weight. These pieces can be used as received, without processing.

Since Sylvania controls germanium purity from ore to ingot, you can't obtain better material. We'll be glad to send you a new technical bulletin on Sylvania germanium ingot dimensions, showing the new sizes, shapes and tolerances.

SYLVANIA GENERAL SYSTEM

Subsidiary of
GENERAL TELEPHONE & ELECTRONICS

Sylvania Electric Products Inc.
Chemical & Metallurgical Div.
Towanda, Penna.

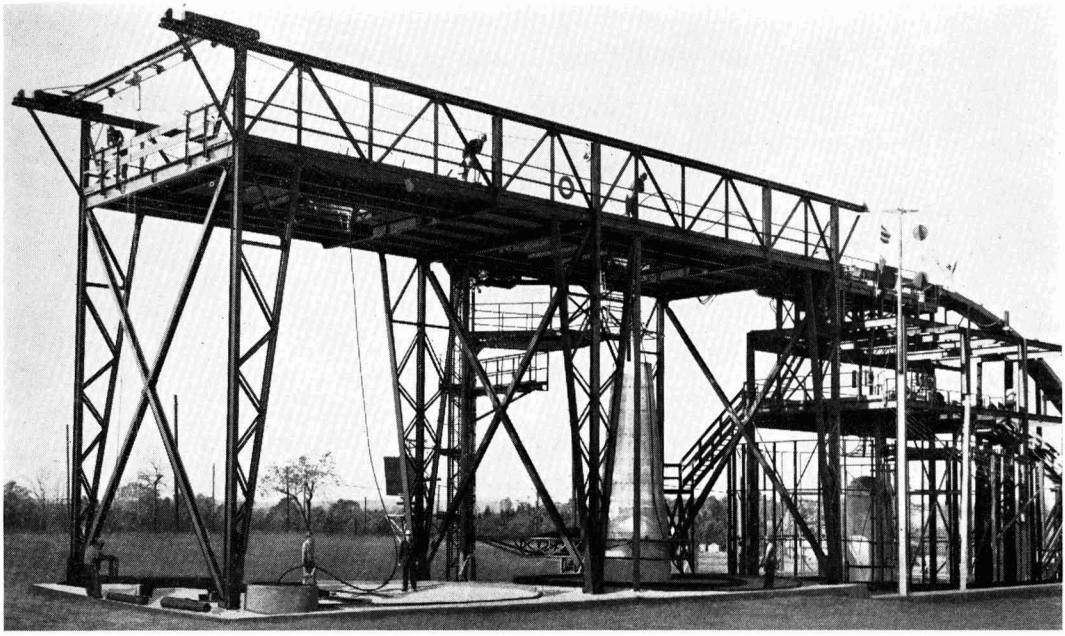

SHIP WITHOUT AN OCEAN

How do you lay a cable on the ocean floor—a cable that is connected to scores of large, heavy amplifiers? How do you "overboard" such a system in a continuous operation, without once halting the cable ship?

Bell Telephone Laboratories engineers must answer these questions in order to lay a new deep-sea telephone system designed to carry many more simultaneous conversations. They're experimenting on dry land because it is easier and more economical than on a ship. Ideas that couldn't even be attempted at sea are safely tested and evaluated.

In one experiment, they use a mock-up of the storage tank area of a cable ship (above). Here, they learn how amplifiers (see photo right), too rigid and heavy to be stored with the cable coils *below* decks, must be positioned *on* deck for trouble-free handling and overboarding.

Elsewhere in the Laboratories, engineers learn how best to grip the cable and control its speed, what happens as the cable with its amplifiers falls through the sea, and how fast it must be payed out to snugly fit the ocean floor. Oceanographic studies reveal the hills and valleys which will be encountered. Studies with naval architects show how the findings can be best put to work in actual cable ships.

This work is typical of the research and development effort that goes on at Bell Laboratories to bring you more and better communications services.

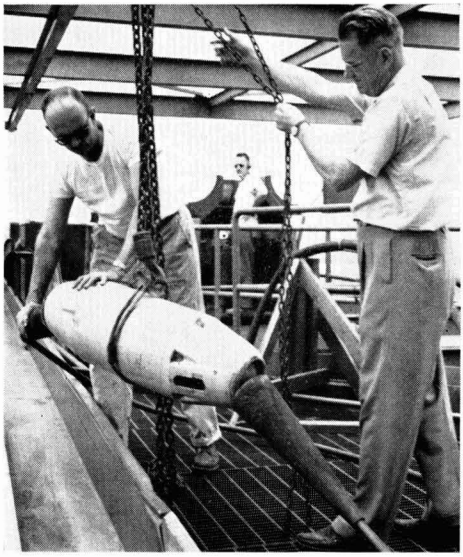

Experimental amplifier about to be "launched" from "cable ship." Like a giant string of beads, amplifiers and connecting cable must be overboarded without stopping the ship.

BELL TELEPHONE LABORATORIES

WORLD CENTER OF COMMUNICATIONS RESEARCH AND DEVELOPMENT

Wave-Length Dependence of the Quantum Efficiency and Absorption of Powder Phosphors

Yasuo Uehara, Iso Masuda, and Yoshimasa Kobuke

Matsuda Research Laboratory, Tokyo Shibaura Electric Company, Kawasaki, Japan

ABSTRACT

A number of powder phosphors have been measured by a direct optical method. Results are compared with other published values. Although slight discrepancies are found for magnesium and calcium tungstate at the 2537Å position, the maximum quantum efficiency for magnesium tungstate is in good agreement with the published values. Good agreement is also found for impurity-activated phosphors. New data are presented for a number of orthophosphates. The quantum efficiency curves decrease more rapidly than the absorption curves toward both longer and shorter wave lengths from the peak position. The peaks of the quantum efficiency curves lie at longer wave lengths than those of the absorption curves. Reasons for these differences are discussed.

Knowledge of the wave-length dependence of the quantum efficiency and absorption of phosphors provides an important foundation for the theoretical interpretation of luminescent properties as well as for the development or technical application of phosphors.

The quantum efficiency of powder phosphors has been measured by several methods (1), i.e., by direct optical, lamp efficiency calculation, calorimetric, and comparison methods. The second method used by Thayers and Barnes (2) and others (3-6) consists of comparing the measured luminous efficiency of a fluorescent lamp with its calculated maximum efficiency. This method involves some ambiguous assumptions concerning the optical characteristics of the phosphor layer in the fluorescent lamp. With the third or calorimetric method (1, 7) it is difficult to carry out the measurement over a wide range of exciting wave lengths, because an intense source of ultraviolet radiation is required but not available. The comparison method (1, 6, 8) is unsuitable to determine the absolute value of the quantum efficiency. In the present investigation, therefore, the first or direct optical method (9-11) was used to measure the wave-length dependence of many powder phosphors.

Experimental Apparatus

The arrangement of the experimental apparatus is similar to that reported by Botden and Kröger (10) and is shown schematically in Fig. 1. The radiation from a low-pressure hydrogen lamp L is reflected by two concave mirrors A and B, then falls on the entrance slit of a Beckmann type monochromator MN. The monochromatic beam from the exit slit is projected on the layer of phosphor P or magnesium oxide Q through a 5-mm circular hole in the ellipsoidal aluminum mirror M of 100 mm diameter. The samples are placed interchangeably on the first focus of the mirror whose position is 2 mm from the plane of aperture of the mirror in order to concentrate the entire flux of reflected light from the sample onto the second focus of the ellipsoidal mirror. The phosphor sample consists of a 3-mm thick layer prepared by compressing the phosphor powder into a rectangular recess of approximate size 3 x 10 x 18 mm which is cut or machined into a rectangular metal block of slightly larger size. The layer of magnesium oxide powder is in turn covered with a freshly smoked layer of magnesium oxide. Thus the thickness of the magnesium oxide layer is also about 3 mm. The two samples are interchangeable by 180° rotation about the rotation axis of the sample holder R. Their geometrical positions are adjustable so as to be accurately identical after rotation.

The radiation reflected from the phosphor or magnesium oxide is concentrated by the ellipsoidal mirror onto a photomultiplier PM (RCA 1P28) placed at the second focus of the mirror. With a phosphor in the measuring position, filters with a cut-off at about 3500Å or 4000Å are inserted between the photomultiplier and sample in order to separate the fluorescent light from the reflected radiation. The spectral sensitivity of the photomultiplier was determined by comparing it with a vacuum thermopile at various wave lengths in the spectral region from 2200 to 8500Å. In this experiment, a 500-w Xe lamp (Osram XB0501) and an incandescent lamp with a tungsten ribbon filament

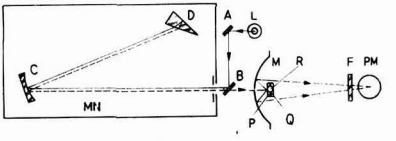

Fig. 1. Arrangement of experimental apparatus. L, light source A, B, and C, concave mirrors; D, quartz prism; MN, Beckmann type monochromator; M, ellipsoidal aluminum mirror; P, phosphor layer; Q, plaque of smoked magnesium oxide; R, axis of rotation of sample holder; F, filter; and PM, photomultiplier.

were used as the source for ultraviolet and visible radiation, respectively.

For the measurement of the spectral energy distribution of fluorescence, a Zeiss Three Glass Prism Spectrometer combined with a photomultiplier (RCA 1P22) was used, as reported in a previous paper (12). All of the experiments mentioned above were made at room temperature.

Experimental Procedure

In order to measure the relative reflectance of the aluminum mirror M, a fragment cut from its flange was placed at the position of sample P in Fig. 1, and the intensity of monochromatic radiation reflected by it and then by the ellipsoidal mirror was measured at various wave lengths relative to that of monochromatic radiation projected directly onto the photomultiplier. The relative spectral reflectivity of the plaque of smoked magnesium oxide was measured in the same manner. Let i, i_A, and i_o be the photocurrents produced by the incident monochromatic radiation, by the monochromatic radiation reflected from the piece of the aluminum mirror, and from the plaque of magnesium oxide, respectively, then the relative spectral reflectance of the aluminum mirror R_M and that of magnesium oxide R_1 are determined by the following relations:

$$R_M \equiv K_1 R_A = \left\{ \frac{i_A}{i} \right\}^{1/2} \qquad [1]$$

and

$$R_1 \equiv K_2 R_o = \frac{i_o}{i R_M} \qquad [2]$$

where R_A and R_o are the absolute values of the spectral reflectance of the aluminum mirror and magnesium oxide, respectively, and K_1 and K_2 are proportionality constants. In these equations, the influence of the multiple reflection between the samples and the mirror on the radiation reflected by the samples and then by the mirror was neglected. The measured results are shown in Fig. 2. Curve (2) for magnesium oxide shows no noticeable selectivity over a wide range of the spectrum from about 3500 to 6000Å, in contrast to curve (1) for the aluminum mirror. This result suggests that the influence of the multiple reflection on the measurement is negligibly small, as assumed above.

In order to determine the quantum efficiency of pure phosphors such as magnesium tungstate, it is necessary to know the absolute value of the spectral reflectivity of magnesium oxide, which is known to be close to unity in the visible region of the spectrum (13). One can, therefore, accept the spectral reflectivity of magnesium oxide normalized to unity as the absolute one with a probable error of about 0.2% (13).

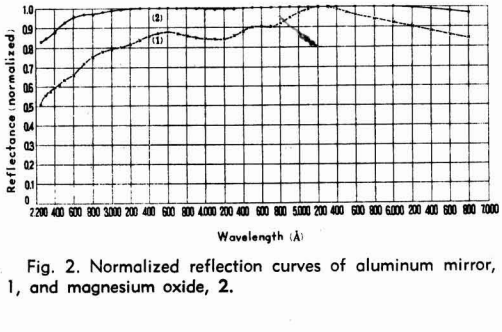

Fig. 2. Normalized reflection curves of aluminum mirror, 1, and magnesium oxide, 2.

It was verified by experiments that the transmittance for ultraviolet and visible light through a 3-mm thick layer of samples was practically zero. For such a layer, the relation between reflectivity R and absorptance A is given by

$$A = 1 - R \qquad [3]$$

Using this relation, one can determine the spectral absorptance by measuring the spectral reflectivity. The spectral reflectivity of unactivated phosphor base, of pure phosphor, and of impurity-activated phosphor is given by the following relations, respectively

$$R_b = \frac{i_b}{i_o} \cdot R_o \qquad [4a]$$

$$R_p = \frac{i_p}{i_o} \cdot R_o \qquad [4b]$$

and

$$R_a = \frac{i_a}{i_o} \cdot R_o \qquad [4c]$$

where i_b, i_p, *and* i_a are, respectively, the photocurrents produced with the layer of unactivated phosphor base, of pure phosphor, and of impurity-activated phosphor. Putting these relations in Eq. [3], the spectral absorptance of the pure and the impurity-activated phosphor is determined as follows:

$$A_p = 1 - R_p = \frac{i_o - i_p \cdot R_o}{i_o} \qquad [5a]$$

and

$$A_a = R_b - R_a = \frac{(i_b - i_a) R_o}{i_o} \qquad [5b]$$

Referring to Eq. [5b], it should be noted that A_a expresses the spectral absorptance due solely to the activators in the impurity-activated phosphor.

We shall define the quantum efficiency of the pure and the impurity-activated phosphors by the ratio of the emitted quanta to the quanta absorbed by the pure phosphor and by the activators in the impurity-activated phosphor, respectively. Then, the wave-length dependencies for the quantum efficiency of the pure and the impurity-activated phosphor are given by

$$\eta_p = \frac{i_{f,p} \cdot R_M \cdot S}{i_o / R_o - i_p} \times \frac{\int_o^\infty \lambda/\lambda e \cdot E_p \cdot d\lambda}{\int_o^\infty R_M \cdot S \cdot E_p \cdot d\lambda} \qquad [6a]$$

and

$$\eta_a = \frac{i_{f,a} \cdot R_M \cdot S}{i_b - i_a} \times \frac{\int_o^\infty \lambda/\lambda e \cdot E_a \cdot d\lambda}{\int_o^\infty R_M \cdot S \cdot E_a \cdot d\lambda} \qquad [6b]$$

where E_p and E_a are the respective energy distributions of the fluorescent emission, S is the spectral sensitivity of the photomultiplier, $i_{f,p}$ and $i_{f,a}$ are,

respectively, the photocurrents produced by the fluorescent emission with the pure and the impurity-activated phosphor, and λ and λ_e denote the wave length of the fluorescent and exciting radiation, respectively.

Since the spectral distribution of the emission of the phosphors measured was practically independent of the wave length of exciting radiation from 2200 to 4000Å, the integration of Eq. [6] can be carried out easily by numerical calculation. In order to measure the wave-length dependence of the quantum efficiency due to sensitizer and activator in the sensitized phosphors such as calcium halophosphate activated with Sb and Mn, the measured fluorescence spectrum was resolved into two bands due to sensitizer and activator. For example, the relative energy distribution curve of the Sb-band in calcium halophosphate activated with Sb and Mn was determined so as to fit it with that of the phosphor activated with Sb alone. By subtracting this curve from the energy distribution curve of the sensitized phosphor, the energy distribution of the Mn-band was determined.

In Eq. [6], the effect of absorption loss of fluorescent light through the powder on the measured quantum efficiency was neglected. Taking into account the absorption loss in the powder, Bril and Klasens (14) have already given the following approximate formula for the intrinsic quantum efficiency of fluorescence:

$$\eta_i = \frac{2}{1 + R_\infty}\,\eta_m \qquad [7]$$

where η_i and η_m are, respectively, the intrinsic and the measured quantum efficiency, and R_∞ is the reflectance of the thick phosphor layer for its fluorescent light. If the value for R_∞ is larger than 0.9, the correction factor according to Eq. [7] is less than 5%. On the other hand, the experimental errors in this experiment were about ±5%. The correction by Eq. [7], therefore, will be necessary only for phosphor layers whose reflectance in the visible region of the spectrum is smaller than 0.9.

Preparation of Phosphors and Experimental Results

Magnesium tungstate phosphors.—Three types of magnesium tungstate phosphors were measured. The first and second type had compositions of $MgWO_4$ and Mg_2WO_5, respectively. They were prepared by firing together the required proportions of magnesium nitrate and ammonium tungstate [$(NH_4)_2O \cdot 7WO_3 \cdot 6H_2O$], with or without Pb and Cd in amounts of 1 mole %. Firing was at 980°C for 30 min followed by intimate grinding and a second firing at 1000°C for 1 hr. The third type phosphors were commercial products obtained from Sylvania Electric Products Inc. and from our factory.

Results for the first series of phosphors with and without Pb are shown in Fig. 3. The data for the second and third types of phosphors without added impurities were practically identical with those labeled (1) in Fig. 3, except for the Sylvania product whose quantum efficiency was about 5% smaller than that of the other magnesium tungstate phosphors. Addition of 1 mole % Cd to magnesium

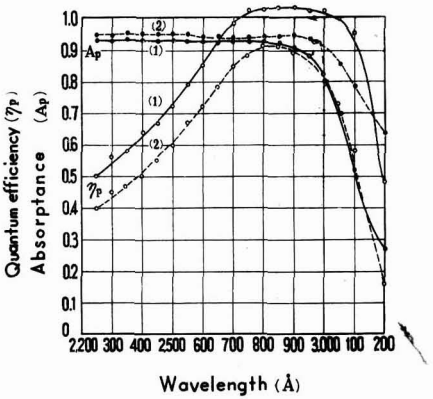

Fig. 3. Wave-length dependence of quantum efficiency and absorption for magnesium tungstate phosphors with or without Pb. 1, $MgWO_4$; 2, $MgWO_4$:Pb (10^{-2} mole).

tungstate of composition Mg_2WO_5 gave essentially the same curves as (2) in Fig. 3. Considering the experimental errors, the quantum efficiency of magnesium tungstate without added impurities is thus practically independent of its composition and close to unity in the spectral region from about 2750 to 3000Å. It is 0.75-0.80 at wave length 2537Å.

Calcium tungstate phosphors.—Six samples of calcium tungstate phosphors were measured. They were prepared by firing mixtures of 1 mole calcium nitrate and 1/7 mole ammonium tungstate with or without 0.4 mole calcium sulfate or 0.01 mole lead fluoride for two half-hour periods at 1000°C with intimate grinding between firings. In order to investigate the existence of nonluminescent compounds in the phosphor which absorb ultraviolet radiation uselessly (15), two samples of calcium tungstate phosphors with or without added calcium sulfate were washed with 5 wt % hot ammonium hydroxide aqueous solution.

Results for calcium tungstates are shown in Fig. 4. The phosphor with 0.4 mole calcium sulfate gave almost the same curves as those labeled (1) in Fig. 4. Washing with ammonium hydroxide decreases

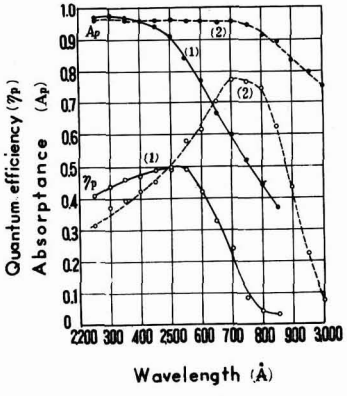

Fig. 4. Wave-length dependence of quantum efficiency and absorption for calcium tungstate phosphors with or without Pb. 1, $CaWO_4$; 2, WO_4:Pb (10^{-2} mole).

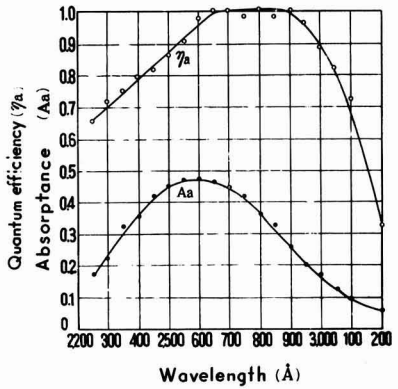

Fig. 5. Wave-length dependence of quantum efficiency and absorption for β-calcium orthophosphate activated with Cu, i.e., β-$Ca_{2.1}P_2O_8$:Cu (5×10^{-3} moles).

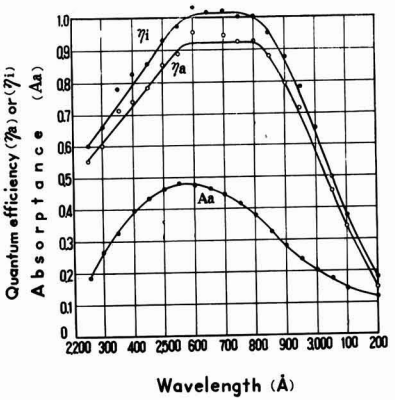

Fig. 6. Wave-length dependence of quantum efficiency and absorption for β-calcium-zinc orthophosphate activated Cu, i.e., β-$Ca_{2.7}Zn_{0.3}P_2O_8$:Cu(5×10^{-3} moles). η_a and η_i denote the measured and the intrinsic quantum efficiency, respectively.

the absorption of calcium tungstate phosphors with or without calcium sulfate slightly, while the quantum efficiency of both phosphors is increased by 5-10%. The maximum quantum efficiency of pure calcium tungstate phosphors, including the washed samples, is 0.50-0.62 at about 2537Å. The addition of 1 mole % Pb produces a remarkable increase in absorption and in the quantum efficiency in the spectral region above about 2500Å. In the spectral region below 2500Å, the quantum efficiency is slightly lowered by the addition of Pb. The maximum value of the quantum efficiency of calcium tungstate sensitized with Pb is about 0.77 at 2700Å.

Cu-activated β-calcium orthophosphate and related phosphors.—Data for Cu-activated β-calcium, β-calcium·magnesium, and β-calcium·zinc orthophosphate, together with those for pure orthophosphates without activators (used for the measurements) are shown in Fig. 5 and 6; the phosphors were prepared as reported in a previous paper (12).

The quantum efficiency of Cu-activated β-calcium orthophosphate is close to unity in the spectral region from about 2650 to 2900Å, as shown in Fig. 5, while that of Cu-activated β-calcium·zinc orthophosphate is about 0.92 in the same spectral region, as shown by the η_a-curve in Fig. 6. The spectral reflectivity of Cu-activated β-calcium and β-calcium magnesium orthophosphate averaged over the entire visible region of the spectrum was about 0.94, while that of Cu-activated β-calcium·zinc orthophosphate was about 0.81. Using Eq. [7], the intrinsic quantum efficiency of the latter phosphor was calculated. It is shown by the η_i-curve in Fig. 6. The curve for calcium·magnesium orthophosphate is quite similar to the η_i-curve in Fig. 6, but it is slightly lower; the maximum quantum efficiency of this phosphor is 0.99 around 2700Å. The absorption curve of this phosphor is in good agreement with that shown in Fig. 6.

Tin-activated calcium orthophosphate and related phosphors.—β-calcium orthophosphate phosphors activated with Sn and with Sn and Mn were prepared by firing mixtures of 1 mole calcium hydroxide, 2 moles dibasic calcium phosphate and 0.1 mole stannous chloride with or without 0.1 mole manganese carbonate for 30 min in air at 950°C and 1100°C, respectively, followed by firing in a reducing atmosphere (mixture of 25% H_2 and 75% N_2) for the same period and at the same temperature after an intimate grinding between firings. Pure β-calcium orthophosphate without activators was prepared by the same method.

Results are shown in Fig. 7. The curve for the quantum efficiency of the Sn-activated phosphor resembles somewhat that of the Cu-activated material, while the absorption curves are noticeably different. On the other hand, the absorption curves of the Sn and the (Sn + Mn) activated orthophosphate are quite close to each other, while the wave length dependencies of the quantum efficiencies are remarkably different.

As reported by Butler, the α-form of Sn-activated calcium orthophosphate is easily produced by firing at temperatures above 1175°C with low amounts of Sn, while the transition from the β- to the α-form of the phosphor is inhibited by the addition of

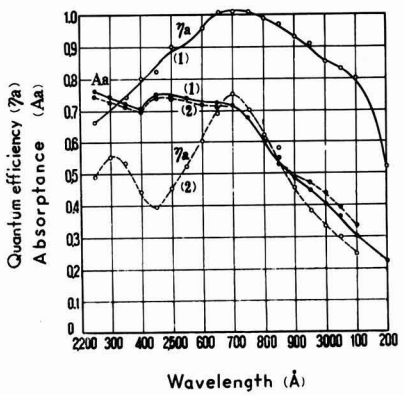

Fig. 7. Wave-length dependence of quantum efficiency and absorption for β-calcium orthophosphate phosphors activated with Sn and Mn.
1, $Ca_3P_2O_8$:Sn (0.1 mole); 2, $Ca_3P_2O_8$:Sn (0.1 mole), Mn (0.1 mole).

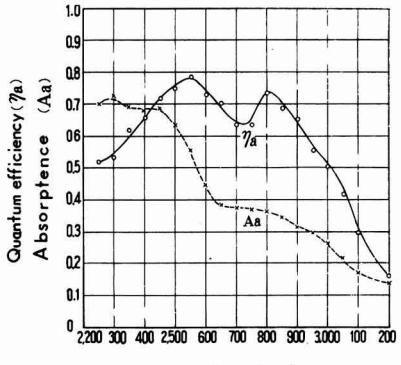

Fig. 8. Wave-length dependence of quantum efficiency and absorption for α-calcium orthophosphate activated with 4 mole % Sn and containing 0.45 mole silica, fired at about 1200°C.

rather large amounts of Sn of the order of 4 mole %. It was found by the present authors that the conversion from the β- to the α-form with rather large amounts of Sn was promoted by the addition of silica during the preparation of phosphors. A series of Sn-activated calcium orthophosphate phosphors containing various amounts of silica were prepared by firing mixtures of 2 moles dibasic calcium phosphate, 0.9 mole calcium carbonate, silica in various amounts from 0.01 to 0.8 moles, and 0.04 mole stannous chloride for 30 min at about 1200°C in air, and then in a reducing atmosphere for the same period and at the same temperature after an intimate grinding between firings. Pure α-calcium orthophosphates without activators were prepared by the same method.

Results for Sn-activated α-calcium orthophosphate containing 0.45 mole silica are shown in Fig. 8. It was proved by x-ray analysis and by measurement of the fluorescent spectrum that it was typical α-calcium orthophosphate. The wave-length dependence of the quantum efficiency for Sn-activated α-phosphors is practically independent of the amount of added silica. It is quite different from that for the Sn-activated β-phosphor and resembles the curve for β-calcium orthophosphate activated with Sn and Mn. The absorption curves for Sn-activated α- and β-phosphors are rather different, and the intensity of the absorption band peaking at about 2800Å for α-phosphor is lower than that for β-phosphor.

Calcium·cadmium silicate phosphor activated Pb *and* Mn.—Calcium·cadmium silicate containing less than 30 mole % Cd and activated with Pb and Mn was described by Schulman (16). The phosphors used for the present measurements were prepared by firing a mixture of 0.8 mole calcium carbonate, 0.2 mole cadmium carbonate, and 1.2 mole silica with or without 8 x 10^{-3} mole lead fluoride and 0.1 mole manganese chloride for two 2-hr periods at 1180°C with an intimate grinding between firings. Results are shown in Fig. 9. Also shown as a dotted line (2) is the corresponding curve for the total (Pb+Mn) emission of calcium silicate activated with

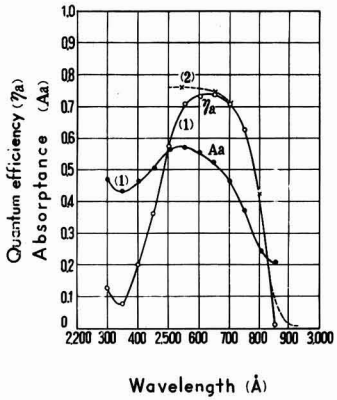

Fig. 9. Wave-length dependence of quantum efficiency and absorption for calcium · cadmium silicate activated with Pb and Mn, compared with Botden and Kroger's data on calcium silicate.
1, $Ca_{0.8}Cd_{0.2}$ · $1.2SiO_2$:Pb(8×10^{-3} moles), Mn (0.1 mole), (Mn-emission);
2, calcium silicate: Pb, Mn (observed by Botden and Kroger).

Pb and Mn, as reported by Botden and Kröger (10). The two curves for the quantum efficiency are in good agreement in the spectral region above about 2650Å.

Calcium halophosphate phosphors activated with Sb or with Sb and Mn.—Calcium halophosphate phosphors of composition $3\,Ca_x\cdot P_2O_8\cdot 0.6\,CaF_2\cdot 0.4\,CaCl_2$ $(x = 2.7 - 2.8)$ and activated with 0.3 mole Sb and various amounts of Mn ranging from 0 to 0.18 moles per mole calcium halophosphate, together with pure halophosphate without activators, were prepared by firing calcium carbonate and dibasic calcium phosphate with or without added Sb or Mn for two half-hour periods at 1100°C, with intimate grinding between firings.

Results for typical samples are shown in Fig. 10 and 11. The quantum efficiency of the phosphor

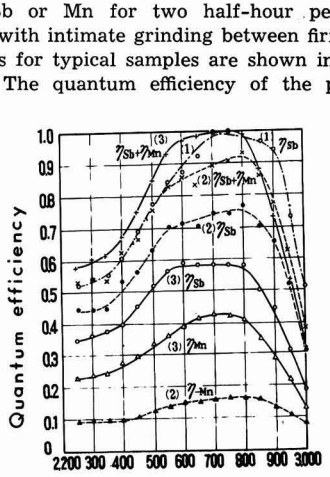

Fig. 10. Wave-length dependence of quantum efficiency for calcium halophosphate phosphors activated with Sb and with Mn. η_{Sb} and η_{Mn} denote the quantum efficiencies for the individual Sb-and Mn-bands.
1, 3 $Ca_{2.7}P_2O_8$ · 0.6 CaF_2 · 0.4 $CaCl_2$:Sb (0.3 moles),
2, 3 $Ca_{2.8}P_2O_8$ · 0.6 CaF_2 · 0.4 $CaCl_2$:Sb (0.3 moles), Mn (3×10^{-2} moles),
3, 3 $Ca_{2.8}P_2O_8$ · 0.6 CaF_2 · 0.4 $CaCl_2$:Sb (0.3 moles), Mn (9×10^{-2} moles).

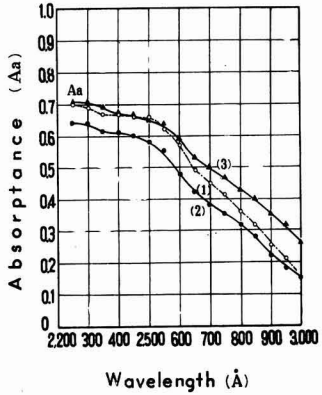

Fig. 11. Spectral distribution of absorption (Aa) due to activators for calcium halophosphate phosphors. The samples are the same as in Fig. 10.

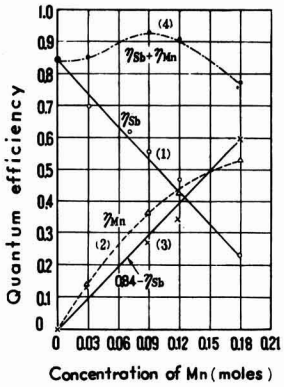

Fig. 12. Relation between quantum efficiency and concentration of Mn for calcium halophosphate phosphors activated with 0.3 mole Sb and various amounts of Mn from 0 to 0.18 mole per mole phosphor, excited with 2537Å. η_{Sb} and η_{Mn} denote the quantum efficiencies for the individual Sb- and Mn-bands.

activated with Sb alone is close to unity at wave lengths around 2750Å and 0.84 at 2537Å.

The relation between quantum efficiency and concentration of Mn for phosphors excited with 2537Å is shown in Fig. 12. With increasing concentration of Mn, the quantum efficiency for the Sb-emission, η_{Sb}, decreases almost linearly, while that for the Mn-emission, η_{Mn}, increases nonlinearly. Thus the total quantum efficiency of fluorescence, $\eta_{Sb} + \eta_{Mn}$, depends on the concentration of Mn. The straight line given by $0.84 - \eta_{Sb}$ expresses the concentration dependence of the quantum efficiency for the Mn-emission which might be obtained if the excitation energy absorbed by the Sb-centers were transferred to the Mn-centers with the same efficiency as that of Sb-centers alone. By comparing the observed with the calculated $(0.84-\eta_{Sb})$ values, it is seen that a part of the excitation energy, which is dissipated as heat energy in the Sb-centers, is transferred to Mn-centers in the sensitized phosphor and it leads to Mn-emission at concentrations below 15 mole % Mn; when the concentration of Mn ex-

Table I. Quantum efficiency of various phosphors

Phosphors	Quantum efficiency: Excited by 2537Å	Quantum efficiency: Maximum value	Wave length at maximum Q.E., Å	Method	Reference
Magnesium tungstate	0.7			Lamp efficiency	Thayer and Barnes, 1939 (2)
	0.9-1	1	2800	Direct	Fonda, 1944 (9)
	0.9			Lamp efficiency	Thayer, 1945 (2)
	0.84			Lamp efficiency	Jerome, 1953 (6)
	0.90			Lamp efficiency	Tregellas-Williams, 1958 (1)
$MgWO_4$ and Mg_3WO_6	0.75-0.80	1	2750-3000	Direct	This paper
:Pb	0.68	0.91	2750-2900	Direct	This paper
:Cd	0.70	0.95	2750-2900	Direct	This paper
Calcium tungstate	0.70			Lamp efficiency	Thayer and Barnes, 1939 (2)
	0.7			Direct	Kröger, 1948 (10)
	0.50-0.62	0.50-0.62	2537-2550	Direct	This paper
:Pb	0.55-0.60	0.77	2700	Direct	This paper
Calcium orthophosphate: Cu	0.91	1	2650-2900	Direct	This paper
Calcium·magnesium Orthophosphate: Cu	0.93	0.99	2650-2800	Direct	This paper
Calcium·zinc Orthophosphate: Cu	0.88	0.92	2650-2900	Direct	This paper
Calcium orthophosphate: Sn	0.92	1	2650-2750	Direct	This paper
Calcium orthophosphate: Sn, Mn	0.52	0.75	2700	Direct	This paper
Calcium orthophosphate: Sn	0.78-0.83	0.78-0.83	2500-2550	Direct	This paper
Calcium·cadmium silicate: Pb, Mn (Mn-em.)	0.70	0.73	2650	Direct	This paper
Calcium halophosphate					
:Sb	0.87-0.96	1	2600-2800	Comparison	Fonda, 1954 (8)
	0.95			Lamp efficiency	Tregellas-Williams, 1958 (1)
	0.84	1	2750	Direct	This paper
:Sb, Mn	0.52-0.76			Comparison	Fonda, 1954 (8)
	0.85			Comparison	Fonda, 1954 (8)
	0.74			Direct	Butaeva, *et al.* 1959 (18)
	0.77-0.92	1	2700-2750	Direct	This paper

ceeds 15 mole %, it is partly dissipated as thermal energy by the action of concentration quenching in the Mn-center. The absorption spectrum of these phosphors shown in Fig. 11 resembles that of Sn-activated α-calcium orthophosphate.

Discussion

Values for the measured quantum efficiency are summarized in Table I, compared with values reported in the literature. Our value for the quantum efficiency of magnesium tungstate at 2537Å is somewhat smaller than that reported by Fonda (9). This discrepancy does not seem to be due to phosphor differences but mainly due to the accuracy of measurements since the quantum efficiency of pure magnesium tungstate phosphors was independent of the samples used, as mentioned before. The maximum quantum efficiency and its wave length showed rather good agreement with the values reported by Fonda (9). The discrepancy of the quantum efficiency around 2537Å may be ascribed to the errors of the calibration of the photomultiplier or photocell used in these measurements. Furthermore, it should be noted that the quantum efficiency obtained by the lamp efficiency calculation method is likely to turn out too high because of neglect of the contribution of mercury lines other than the line 2537Å, for example, the line at 1850Å, to the luminous flux of the fluorescent lamp (18). Our value of the quantum efficiency of pure calcium tungstate is also somewhat smaller than that reported by the other authors. This discrepancy between these values may be due to the same reason as that for magnesium tungstate. The quantum efficiency of magnesium tungstate was decreased by the addition of Pb or Cd, while that of calcium tungstate was increased remarkably by the addition of Pb, as mentioned before. This fact is theoretically interesting with respect to the configuration of the luminescent center of tungstate phosphors.

In the impurity-activated phosphors, the quantum efficiency should be defined by the ratio of the emitted quanta to the quanta absorbed solely by activators, as shown by Eq. [6b]. Such a caution is especially important for the case in which the phosphor base shows a rather strong absorption in the ultraviolet region. It should be noted that the quantum efficiency of impurity-activated phosphors, based on the above definition, can be measured only by the direct optical method. Considering the sample differences, the quantum efficiency of halophosphate activated with Sb and with Sb and Mn shows good agreement with that reported by the other authors. The measured quantum efficiencies for the other impurity-activated phosphors seem to be reasonable.

In general, the quantum efficiency curves decrease more rapidly than the absorption curves at both longer and shorter wave lengths compared with the peak. For example, in the typical cases of magnesium and calcium tungstate, the quantum efficiency curves decrease gradually in the short wave-length region in which the absorption curves are flat, as shown in Fig. 3 and 4. The peaks of the quantum efficiency curves lie at a longer wave-length region than those of the absorption curves.

In principle, the wave-length dependence of the quantum efficiency of phosphors containing a single emitting state in the activator center should be flat over a wide range of the absorption spectrum, if the absorption is allowed only between the ground and the emitting state. If the absorption spectrum contains other absorption bands which are not responsible for the emission, the quantum efficiency should be reduced to small values in the corresponding spectral region. The rapid decrease of the quantum efficiency at longer wave lengths may be thus explained.

The decrease of the quantum efficiency at short wave lengths, however, seems to be attributable to another mechanism. It may be explained by a mechanism similar to that suggested by Dexter, Klick, and Russell (19) as an explanation for the low efficiency of F-center emission in alkali halides. We assume that the higher the vibration state in the excited state to which an electron makes a transition from the ground state, the larger becomes the nonradiative quenching of the excited state. The quantum efficiency will then decrease in the shorter wave-length region of the absorption spectrum. As a result, the peaks of the quantum efficiency curves will shift toward long wave lengths.

Acknowledgment

The authors wish to express their sincere thanks to Dr. Tsuneo Harada, the Director of Matsuda Research Laboratory of Tokyo Shibaura Electric Co., for his continuous support and encouragement. Part of this paper was presented at the Spring Meeting of The Physical Society of Japan, Fukuoka, April 9-11, 1957.

Manuscript received April 13, 1959.

Any discussion of this paper will appear in a Discussion Section to be published in the December 1960 JOURNAL.

REFERENCES

1. For general review and references see: J. Tregellas-Williams, *This Journal*, **105**, 173 (1958).
2. R. N. Thayer and B. T. Barnes, *J. Opt. Soc. Amer.*, **29**, 131 (1939); R. N. Thayer, *Trans. Electrochem. Soc.*, **87**, 413 (1945).
3. J. H. Schulman, *J. Appl. Phys.*, **17**, 902 (1946).
4. H. C. Froelich, *Trans. Electrochem. Soc.*, **91**, 241 (1947); *This Journal*, **93**, 101 (1948); *ibid.*, **98**, 402 (1951).
5. A. A. Shklover, *J. Techn. Phys. (USSR)*, **7**, 1239 (1947).
6. C. W. Jerome, *This Journal*, **100**, 586 (1953).
7. Z. Bodó, *Acta Phys. Acad. Sci. Hung.*, **3**, 23 (1953); Gy. Gergely, *J. Phys. radium*, **672**, 698 (1956).
8. G. R. Fonda, *J. Appl. Phys. Suppl.*, **4**, 69 (1954); *ibid.*, **4**, 17 (1954).
9. G. R. Fonda, *J. Phys. Chem.*, **43**, 561 (1939); *ibid.*, **48**, 303 (1944).
10. P. J. Botden and F. A. Kröger, *Physica*, **14**, 553 (1948); F. A. Kröger, "Some Aspects of the Luminescence of Solids," Elsevier Publishing Co., New York (1948); P. J. Botden, *Philips Research Repts.*, **6**, 425 (1951).
11. V. V. Antonov-Romanovsky and M. T. Epstein, *C. R. Acad. Sci. U.R.S.S.*, **64**, 483 (1949); V. V. Antonov-Romanovsky, *J. Phys. radium*, **17**, 694 (1956).
12. Y. Uehara, Y. Kobuke, and I. Masuda, *This Journal*, **106**, 200 (1959).

13. See, for example: M. G. Mellon, "Analytical Absorption Spectroscopy," p. 263, John Wiley & Sons, Inc., New York (1950).
14. A. Bril and H. A. Klasens, *Philips Tech. Rev.*, **15**, 63 (1953).
15. J. L. Ouweltjes and W. L. Wanmaker, *This Journal*, **103**, 160 (1956); W. A. Roberts, U.S. Pat. 2,312,267.
16. J. H. Schulman, U.S. Pat. 2,471,082.
17. F. A. Kröger, *Physica*, **6**, 774 (1939).
18. F. A. Butaeva, B. A. Fabricant, and A. L. Nedospasov, CIE XIV Sessions, Brussels (1959), Preprint P-59.4.
19. D. L. Dexter, C. C. Klick, and G. A. Russell, *Phys. Rev.*, **100**, 603 (1955).

Microscopic Observations on Electroluminescent Phosphors

A. Kremheller

Sylvania Research Laboratories, Bayside, New York

ABSTRACT

The electroluminescent brightness of single phosphor particles is studied microscopically in liquid dielectric cells. A simple visual technique in conjunction with a microscope permits one to analyze the brightness distribution within and among electroluminescent particles. Some experimental results are presented on the nonuniformity of the emission, the influence of ball milling and acid etching on the brightness, the improvement of brightness by particle separation, the analysis of the integrated light output as a function of the processing temperature, and the brightness changes due to particle orientation, contact, and irradiation.

Many investigations which aim at improving the brightness[1] of electroluminescent (EL) lamps are concerned with the integrated light output in evaluating the influence of the processing parameters in phosphor preparation. Although this approach is useful in testing and comparing finished products with each other, one does not learn much about the behavior of the single particles composing the EL layer. Even if one observes that a certain treatment improves the integrated light output, it is not evident how the improvement affects the phosphor particles, e.g., does an increased number of particles become electroluminescent, does every particle become brighter, or does the brightness distribution of particles change in some other way. These questions can be answered by observing the single EL particles. In this way, it is hoped that the analysis of the components of the integrated light output will finally lead to improved EL lamps by means of synthesis of the improved components. This paper shows in several examples that such an improvement can be attained by the microscopic study of single phosphor particles.

Experimental

Various EL phosphors have been studied in liquid, plastic, and glass dielectric cells. Some phosphors are of an experimental nature, while others are commercially available. Most brightness measurements are conducted with an adjustable-gap sandwich cell using castor oil as the liquid dielectric. The study of particle orientation, contact, and alignment is facilitated by using a gap-like cell. Its electrodes are about 0.5 mm high to avoid excessive edge effects with respect to the electric field.

[1] "Electroluminescent brightness" as used here is a measure of the luminous flux per unit emissive area of a single particle. (See also the definition of "brightness" in American Institute of Physics Handbook, Dwight E. Gray, New York, 1957, page 6-3.)

The particle brightness is determined by a method similar to that described by Zalm, Diemer, and Klasens (1) and has been adapted for our purpose. In this method, a relative estimate of the EL brightness of phosphor particles is obtained by employing photographic, neutral-density step filters in conjunction with a microscope. The filter is inserted into the optical path of the microscope until the EL particle remains just visible to the adapted eye; the step number is then a measure of the particle brightness. The opacity of the filter doubles with every two filter steps, so that 20 steps correspond to a change in particle brightness B by a factor of $2^{10} = 1024$. The logarithmic sequence of the opacity facilitates the plotting of log B if $2^{1/2}$ is used as the base of the logarithms. This simple visual technique permits comparison of the brightness from various regions within a single particle and among phosphor particles.

Nonuniformity of EL Emission

The importance of studying the EL brightness of single phosphor particles becomes apparent when an EL lamp is viewed under a microscope, and the considerable brightness variations from particle to particle are observed (Fig. 1). Only a minority of particles electroluminesces brightly, while some particles do not emit any EL light and others appear fairly dim.

Microscopic investigation of single particles permits one to measure their brightness and to produce a frequency diagram of the EL brightness (Fig. 2). The diagram indicates the degree of brightness variation. Since the base $2^{1/2}$ is used for log B, the brightness range is such that the brightest particles are about 50 times brighter than the dim ones. Actually, there are about 20% of the particles which do not

Fig. 1. Brightness variation among particles. Average particle diameter about 25 μ.

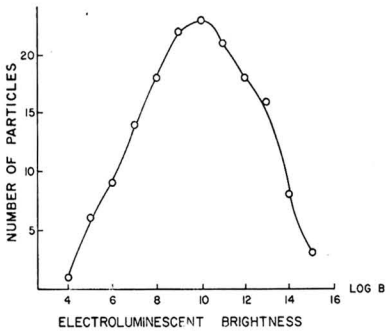

Fig. 2. Brightness distribution of electroluminescent phosphor particles; log B to the base $2^{1/2}$.

electroluminesce at all. Some of these "dead" particles do not show up in the photograph, others get some light from adjacent bright particles and can be seen. There is a most frequent particle brightness which is about 8 times the lowest brightness measured. The brightness-frequency diagram varies somewhat from phosphor to phosphor. In some cases a relatively flat peak or even 2 maxima have been observed.

Besides the brightness nonuniformity among particles, considerable brightness variation also occurs within single particles, as shown in Fig. 3. The emission seems to originate from particle regions[2] (usually the edges of particles) which appear opaque in transmitted visible light; it is also observed that the same opaque regions become photoluminescent under ultraviolet irradiation. The photoluminescence is, however, somewhat more uniform than the electroluminescence, as pointed out by other researchers (2). In addition to electroluminescent emission from extended areas, there is emission from spots (3); this spot emission is not observed during photoluminescence. The spot emission predominates at high frequencies (several kc) of the applied electric field. The spots occur usually in line arrange-

[2] In the review of this paper it was indicated that "the emission is, very likely, created only in small spots, and that the area emission is simulated mainly, or exclusively, by multiple reflections inside the crystals." The author feels that this statement is definitely valid at high frequencies, although primary area emission may occur at very low frequencies of the applied electric field.

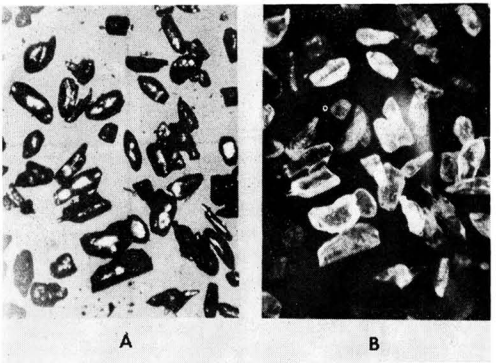

Fig. 3. Microscopic observation of phosphor particles: (a) in transmitted light; (b) under their own EL illumination. Average particle diameter about 120 μ.

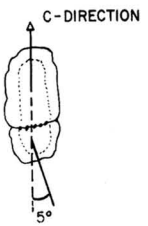

Fig. 4. Disorientation and spot emission along crystallite boundary.

ments, apparently located in fissures parallel to the c-plane (or 111-plane for cubic structure). It appears that these fissures separate contiguous crystallographic regions which are in many cases disoriented. The misalignment often amounts to 5° (Fig. 4), as the difference in extinction angle between crossed nicols indicates. Sometimes emission colors from spots and from areas are different; for instance, some (Zn,Cd) (S,Se):Cu,Cl phosphors emit greenish-orange area and greenish-blue spot electroluminescence. It is possible that these color differences are caused by the nonuniformity of the electric field (4), or by the preferential optical absorption of the short-wavelength light in the bulk of the crystallite.

Ball Milling and Acid Etching

Another series of EL phosphors differs in that they have been ball milled prior to a final thermal treatment. Microscopic observation indicates that the milled phosphors exhibit an improved uniformity in EL brightness among and within single particles. The integrated light output increases in a typical case by 30% due to milling. As an attendant effect, milling introduces enough damage to particles to make most of them appear opaque in transmitted light. It is plausible that the particle damage during milling may contribute to an improved activator distribution (5) in the thermal processing step. In addition to this effect, it appears that surface damage increases the EL brightness by facilitating light emission which is otherwise lost by absorption due to internal multiple reflections.

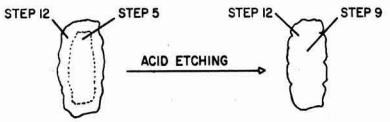

Fig. 5. Increase of emission uniformity by acid etching; the opacity values of the step filter indicate the relative brightness.

This hypothesis has been tested by acid etching of phosphor particles. A single phosphor particle (Fig. 5) is observed in a gap cell in castor oil. It is found that the edge has about 10 times greater EL brightness than the center region of the particle. The particle is removed from the cell, etched with concentrated HCl for a few minutes, and returned into the cell. The opacity of the center region in transmitted light is considerably increased by acid etching. The center region is now 4 times brighter electroluminescent than in the case of the original grain. The use of the step filter permits an estimate of the brightness improvement of the center region as a result of the acid treatment. The acid etching is not uniform over the whole grain; there is some preferential dissolution along grain boundaries, strained regions, and in strongly birefringent regions.

An increase in brightness and uniformity is also indicated by the slight shift of the brightness distribution (Fig. 6), which represents a large number of particles in the test cell. While there is no change in the maximum particle brightness, one obtains a slight increase in the most frequent brightness. The integrated light output is also measured, and an increase of 30% is observed which is due to the acid etching.

Particle Separation

Since the EL brightness of individual particles differs widely, attempts have been made to select bright particles for separate examination. This selection is sometimes comparatively simple; for instance, the bright particles may differ in size from the rest. A Zn(S,Se):Cu,I phosphor exhibited an unusual frequency diagram of the brightness distribution in that 2 peaks are observed (Fig. 7). The peak at high brightness is mainly due to the bright large particles. This green EL phosphor is fractionated so that particles above 80 and below 20 μ could be studied separately, since microscopic

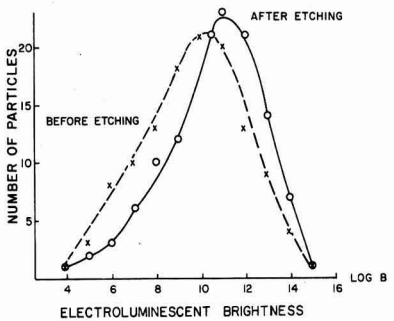

Fig. 6. Frequency diagram of brightness change with acid etching.

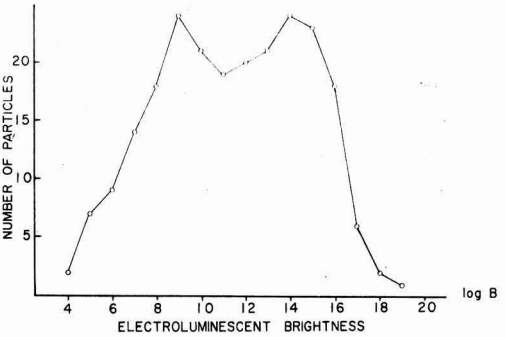

Fig. 7. Brightness distribution of a Zn(S,Se):Cu,I phosphor

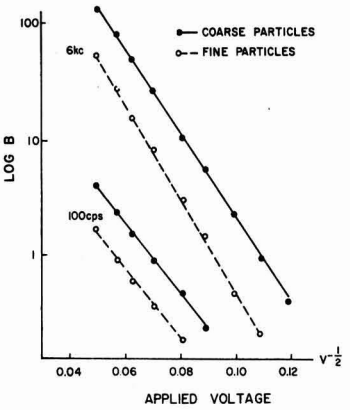

Fig. 8. Brightness vs. voltage for two particle fractions

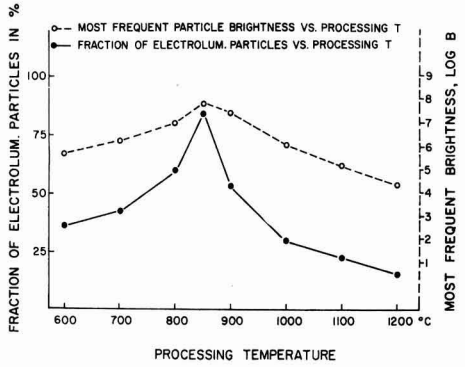

Fig. 9. Components of integrated light output vs. processing temperature.

observations had indicated that the large particles were brighter than the small ones. Measurements on the fractionated material show that the integrated light output from a liquid dielectric sandwich cell containing the coarse particles is up to 5 times as high as that from a cell containing the same weight of the fine particle size fraction (Fig. 8).[3]

Analysis of Integrated Light Output

Microscopic observation of single particles also permits analysis of the brightness characteristics as

[3] Measured by Dr. P. Goldberg of our laboratory.

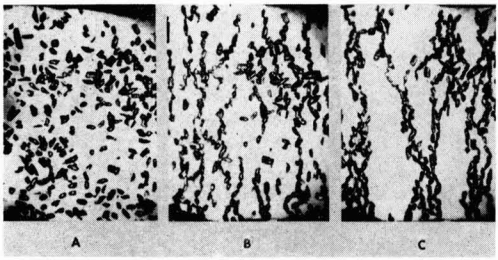

Fig. 10. Influence of electric field and irradiation on particle orientation: (a) random particle distribution, (b) orientation due to electric field, and (c) re-alignment due to irradiation with visible light. Average particle diameter about 70 μ.

a function of processing parameters, such as the preparation temperature. A series of blue-emitting EL phosphors has been studied for which the thermal treatment had been carried out at various temperatures between 600° and 1200°C. The integrated light output had been shown to be at a maximum for the material processed at 850°C. The study of the brightness of single particles reveals that this maximum in integrated light output results from optimization in two respects at this temperature, as indicated in Fig. 9. First, the fraction of particles which are electroluminescent peaks sharply at 850°C, and second, the most frequent particle brightness of the various frequency-brightness distribution curves is also at a maximum at this temperature.

Particle Orientation, Contact, and Irradiation

Phosphor particles in castor oil dielectric cells are readily oriented by electric a-c and d-c fields (6, 7). A change in voltage or frequency causes motion and reorientation of particles; some particles exhibit translational and rotational motion even at constant voltage and frequency. Especially the very small particles move erratically and appear to be charged and discharged by collisions with other particles. Randomly distributed particles (Fig. 10a) are oriented in an electric field; Fig. 10b shows the orientation with 1250 v/cm applied at 500 cps. During the orientational motion some particles become attached to one electrode while most particles become attached to other particles. The particles form oriented chains, with their elongation parallel to the electric field, and aggregates between the electrodes. Alignment and contact increase the EL brightness of many particles; although some particles remain nonelectroluminescent, others turn brightly electroluminescent. A brightness increase by a factor of 4 can be observed readily in many cases.

Although most particles align themselves with their elongation parallel to the applied electric field, there are some internally misaligned particles (some with adjacent crystallite regions disoriented by up to 10°, cf. Fig. 4) which align themselves with their aggregate elongation perpendicular to the electric field. It appears that this mode of alignment occurs when there is only little electrical contact between adjacent, elongated single crystal regions, which are consequently aligned with their single crystal elongation parallel to the electric field. This anomalous particle orientation is also connected with a marked increase in the EL brightness of such particles.

Irradiation with ultraviolet or visible light facilitates particle alignment and changes the brightness distribution. The threshold field for particle alignment under strong irradiation is considerably below that for the start of alignment in the dark. When partially aligned particles (Fig. 10b) are irradiated with visible light, the alignment as well as chain and aggregate formation continue until a new, fairly stationary arrangement is achieved, as shown in Fig. 10c. Besides this re-alignment, irradiation causes a redistribution of the local light emission from the phosphor particles in the test cell. The electroluminescence emission from single particles and particle regions frequently increases or decreases. It appears likely that most of these brightness changes, due to various parameters discussed above, are caused by the concomitant changes in the local electric field.

Summary and Conclusions

A simple visual method employing a logarithmically graded, neutral-density step filter enables one to study microscopically the brightness variation among and within single EL phosphor particles.

It has been shown that a relation exists between the opacity and the light emission from single particles, in that acid etching increases both. Sometimes it is possible to make use of the nonuniformity of light emission in improving the lamp brightness, for instance by particle separation. The integrated light output as a function of processing temperature is analyzed, and it is found that the phosphor sample of optimum integrated brightness contains the largest fraction of EL particles and the maximum brightness value for the most frequent particle fraction. Particle orientation, particle-to-particle and particle-to-electrode contact enhance the electroluminescence emission. External irradiation with visible or ultraviolet light exerts also a marked influence on the brightness distribution within and among single phosphor particles.

Microscopic studies consequently can contribute to the preparation and selection of bright particles, so that the integrated light output of EL lamps can also be increased. The method is that of analysis and synthesis. That is, one looks first at single particles and attempts to optimize the components contributing to the integrated light output. The second step is then the synthesis of the optimized components which leads to the improvement of the brightness of EL lamps, as has been demonstrated above in some typical cases.

Manuscript received Aug. 17, 1959. This paper was prepared for delivery before the Philadelphia Meeting, May 3-7, 1959.

Any discussion of this paper will appear in a Discussion Section to be published in the December 1960 JOURNAL.

REFERENCES

1. P. Zalm, G. Diemer, and H. A. Klasens, *Philips Research Repts.*, **10**, 205 (1955).

2. K. H. Butler, C. W. Jerome, and J. F. Waymouth, *Elec. Eng.*, **73**, 524 (1954).
3. J. F. Waymouth and F. Bitter, *Phys. Rev.*, **95**, 941 (1954).
4. L. Burns, *This Journal*, **100**, 572 (1953).
5. A. H. McKeag and E. G. Steward, *ibid.*, **104**, 41-4 (1957).
6. W. Lehmann, *ibid.*, **103**, 24 (1956); **105**, 585 (1958).
7. W. C. Gungle, *et al.* (to Sylvania Electric Products Inc.), U. S. Pat. 2,728,870, Dec. 27, 1955.

Hydrothermal Preparation of Two-Component Solid Solutions from II-VI Compounds

A. Kremheller, A. K. Levine,[1] and G. Gashurov

Sylvania Research Laboratories, A Division of Sylvania Electric Products Inc., Bayside, New York

ABSTRACT

The hydrothermal synthesis of binary solid solutions of inorganic phosphors and photoconductors is described. This method depends on the increased reactivity between the components and ease of crystal growth in an aqueous solution maintained at high temperature under a confining pressure. The hydrothermal method offers the advantages of a sealed system and easily reproducible experimental conditions. Solid solutions of ZnS-HgS, CdS-HgS, and ZnS-CdS have been prepared by this method. Results of optical absorption measurements, x-ray analysis, microscopic studies, and the spectral photoresponse of the solid solutions formed are presented.

The conventional preparation of binary solid solutions from group II—group VI systems recently has been of interest (1,2), since these materials (such as zinc-inter-chalcogenides, zinc sulfo-and seleno-tellurides) permit one to study the correlation between crystal structure and their electronic behavior as photoconductors and phosphors. The usual synthesis (3) of stoichiometrically controlled two-component solid solutions is difficult if the vapor pressures of the compounds involved differ greatly, so that preferential evaporation occurs. In such cases solid solution is sometimes achieved by a vapor phase process in high-pressure furnaces (4), or by coprecipitation in aqueous solutions (5).

Utilizing processing techniques introduced by Allen and Crenshaw (6), Kremheller and Levine (7) succeeded in hydrothermally preparing electronically active II-VI compounds, such as photoconductive cadmium sulfide and various related luminescent materials. This paper reports on the extension of these investigations to the synthesis of binary solid solutions of II-VI compounds. The hydrothermal method was chosen because it employs a lower temperature than is required in dry processing. Low-temperature synthesis is possible under hydrothermal conditions because the formation of mixed crystals is effected by solution transport, whereas in conventional processing crystal formation and growth take place mainly by vapor transport.

Experimental

The hydrothermal method has been described in some detail in previous publications (7); therefore, only a brief account of the method is given here. Hydrothermal synthesis employs aqueous or liquid solution of the component materials, sometimes with certain additives, at temperatures considerably above the normal boiling point of the solution and under pressures of several hundred atmospheres.

Hydrothermal synthesis is carried out by placing the finely divided component solids, say zinc sulfide and mercuric sulfide in a typical case, into a quartz vial which then is filled partially with deionized water and sealed. The quartz vial is enclosed in a high-pressure steel autoclave which also contains water. As long as there is a liquid phase in equilibrium with a vapor, the pressure will depend only on the temperature and not on the amount of each phase. Therefore, at temperatures below the critical temperature, the pressure outside of the quartz vial can be equal to the pressure inside even though the degree of filling of the autoclave is not the same as that in the vial. For example, the temperature-density diagram for water shows that two phases are present at 350°C as long as the degree of filling is in the range of about 20 to 50% (8). The autoclave is put in place, and its temperature is raised very slowly so that the temperature of the water in the vial is almost the same as that of the water outside it. Under these conditions the pressure inside the sealed quartz vial is sufficiently close to that in the autoclave so that the quartz vial neither explodes nor implodes. After the desired time at temperature, the autoclave is cooled slowly until the pressure is atmospheric; the vial is taken out and the processed material is removed. A large number of vials can be processed at the same time under identical conditions without danger of sample-to-sample contamination.

Results

Most experiments were carried out at temperatures around 350°C and under pressures of several

[1] Chemistry Department, Brooklyn College, Brooklyn, N. Y.; Consultant, Research Laboratories, Sylvania Electric Products Inc., Bayside, N. Y.

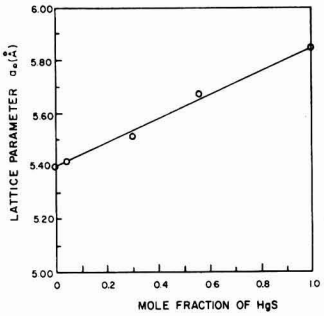

Fig. 1. Lattice parameter as a function of composition, ZnS-HgS system.

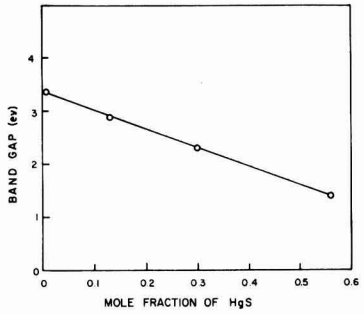

Fig. 2. Band gap as a function of composition, ZnS-HgS system.

hundred atmospheres. It was found that heat-treatment under these conditions for two or three days was sufficient usually to produce solid solutions of ZnS-HgS , CdS-HgS, and ZnS-CdS. In some experiments, equilibrium was reached in shorter time.

Solid solutions of ZnS-HgS.—Since the solubility rather than the vapor pressure is responsible for the formation of solid solutions by the hydrothermal processing technique, it is feasible to prepare quantitatively controlled solid solutions of components exhibiting greatly different vapor pressures under conventional processing conditions. For example, attempts were made conventionally to prepare solid solutions of (Zn,Hg)S by mixing ZnS with HgS and heating. However, after 30 min at 800°C, it was found that all the mercuric sulfide had volatilized leaving only ZnS. When a mixture of ZnS and HgS was processed hydrothermally for 50 hr at 350°C, solid solutions of (Zn,Hg)S were obtained, as indicated by the results of x-ray diffraction analysis of a series of such solid solutions (Fig. 1). These solid solutions are of the zinc blende structure, and within the limit of experimental error they exhibit a change of lattice constant with chemical composition in agreement with Vegard's law. A further proof of the formation of solid solution for the ZnS-HgS system was obtained from optical reflection measurements which show a shift in the absorption edge toward longer wave lengths as the mercury content increases. The reflection measurements were made with a Beckman Model DU Spectrophotometer with a MgO cell as the standard. The change of the energy band gap determined from these measurements

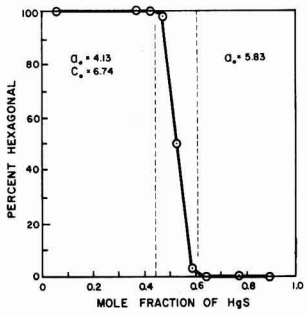

Fig. 3. Results of x-ray analysis, CdS-HgS system.

is shown in Fig. 2. The values of the band gap were calculated from the wave lengths corresponding to the intersection of the straight-line extrapolation above and below the short wave length knee of the reflectance curve, i.e., the same procedure was used as that employed by Larach, Shrader, and Stocker (2).

Solid solutions of CdS-HgS.—Solid solutions of (Hg,Cd)S can also be prepared readily by the hydrothermal synthesis. Figure 3 shows x-ray results for the CdS-HgS system. For HgS additions up to 43 mole % all the samples were of the wurtzite structure, and within the limit of experimental error no shift in the lattice parameters could be detected, the lattice parameters being essentially those of hexagonal CdS. The energy gap change in these samples (Fig. 4) indicates that formation of solid solutions was achieved, and it appears that CdS takes up HgS without any apparent structural changes.

For HgS additions of 60 mole % and higher only the zinc blende structure could be detected in CdS-HgS samples, and these cubic solid solutions have the same cell constant of 5.83Å. There is also an intermediate region in the CdS-HgS system extending from 43 to 60 mole % of HgS in which both the hexagonal (a = 4.13Å, c =6.74Å) and the cubic (a = 5.83Å) phases are present. The ratio of hexagonal phase to cubic appears to change gradually with the change in composition so that the sample to which 53 mole % of HgS were added contains both phases in equal amounts. To investigate further the nature of the intermediate region, microscopic observations were made on CdS-HgS samples and some results are given in Fig. 5. Figure 5a shows the sample con-

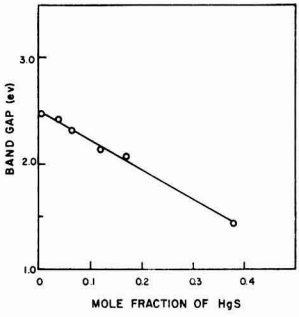

Fig. 4. Band gap as a function of composition, CdS-HgS system.

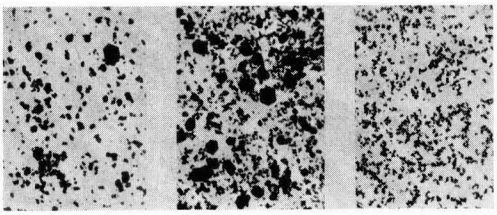

Fig. 5. Photomicrographs of CdS-HgS preparations: (a) (left) 43 mole % HgS (hexagonal), (b) (center) 53 mole % HgS (hexagonal:cubic, 1:1), and (c) (right) 77 mole % HgS (cubic). Figures have the same magnification; largest particle diameter about 50 μ.

taining 43 mole % of HgS in which only the hexagonal phase was found by x-ray analysis. One observes that the sample consists of large hexagons and small particles of indefinite shape. Under higher magnification it is observed that the small particles are also either hexagonal in shape or that they are fractions of large hexagons. The sample 5c containing 77 mole % of HgS consists of small particles which are found by x-ray analysis to be aggregates of cubic crystallites. The sample shown in the center, Fig. 5b, in which both hexagonal and cubic phases were found in equal amounts, consists of hexagons similar to those in Fig. 5a and small particles of the same kind as those in Fig. 5c. It appears that the sample containing 53% of HgS is a physical mixture of two solid solutions: the hexagonal ($a = 4.13$Å, $c = 6.74$Å) and the cubic ($a = 5.83$Å).

Solid solutions of ZnS-CdS.—Self-activated (Zn,Cd)S solid solutions have also been prepared by hydrothermal synthesis. The single crystallites exhibit good crystallinity; they are below 5μ in diameter, which is considerably smaller than the size of particles prepared by dry processing. Their luminescence and photoconductivity properties are comparable to those of conventionally prepared solid solutions. Luminescence under ultraviolet excitation (3650Å) shifts from blue to red with the increase in CdS concentration, while photosensitivity decreases with increasing ZnS concentration.

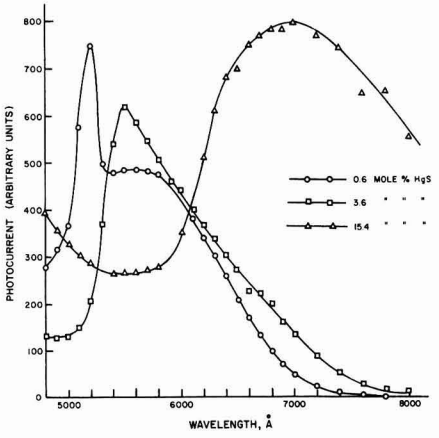

Fig. 6. Spectral response of photoconductive (Cd,Hg)S:Cu, Cl.

Activated solid solutions.—Solid solutions of (Zn,Hg)S, (Zn,Cd)S, and (Cd,Hg)S were made photoconductive or luminescent by proper activation. Activation was accomplished by adding copper or silver together with chlorine or aluminum to the host components. The luminescence of (Zn,Hg)S solid solutions under ultraviolet excitation (3650Å) shifts from green to red with the increase in HgS concentration. No visible photoluminescence is exhibited by (Zn,Hg)S solid solutions containing over 30 mole % of HgS because of a shift to the infrared. (Cd,Hg)S solid solutions were found to show photoluminescence and photoconductivity. Figure 6 shows the spectral response curves for this system. In every case 0.3 mole % of copper, 1 mole % of chlorine, relative to the sulfide was added to the solution in the vial. The photoconductivity peak shifts toward longer wave lengths with increasing HgS, as one would expect from the decrease in the width of the energy gap (Fig. 4). The photosensitivity in general decreases and the dark current increases with increase in HgS concentration.

Conclusions

Complete solid solution is obtained throughout the whole range for the ZnS-HgS system. These solid solutions appear to show a linear variation of lattice constant with composition. Corresponding to the continuous range of solid solution in this system, there occurs a linear variation of the energy gap at least up to 56 mole % of HgS. It is clear, however, that the energy gap cannot vary linearly in the whole range since the straight line in Fig. 2 extrapolates to a negative value for the band gap of pure cubic HgS.

HgS and CdS form solid solutions over the entire range, but the crystal system depends on the composition. Hexagonal solid solution of the wurtzite structure is obtained in the 0-43 mole % HgS range, while cubic solid solution of the zinc blende type is obtained for HgS additions above 60 mole %. Within the limits of experimental error neither of these solid solutions showed any shift in lattice parameters with composition. Hexagonal and cubic solid solutions are present in the 43-60 mole % region, the ratio of cubic to hexagonal solid solutions increasing continuously with increasing HgS concentration. These results agree essentially with those reported by Rittner and Schulman (5), who obtained (Cd,Hg)S solid solutions by coprecipitating CdS and HgS in concentrated ammonium sulfide solution. Solid solutions of (Zn,Hg)S, (Zn,Cd)S, and (Cd,Hg)S were made photoconductive and luminescent by proper activation.

Acknowledgment

Grateful acknowledgment is made to V. A. Brophy for carrying out the x-ray determinations, and to J. T. Ragusin and S. Faria for valuable assistance with the experimental work.

Manuscript received Aug. 24, 1959. This paper was prepared for delivery at the Philadelphia Meeting, May 3-7, 1959.

Any discussion of this paper will appear in a Discussion Section to be published in the December 1960 JOURNAL.

REFERENCES

1. S. Larach, W. H. McCarroll, and R. E. Shrader, *J. Phys. Chem.*, **60**, 604 (1956).
2. S. Larach, R. E. Shrader, and C. F. Stocker, *Phys. Rev.*, **108**, 587 (1957).
3. H. W. Leverenz, "Luminescence of Solids," Chap. 3, John Wiley & Sons, Inc., New York (1950).
4. L. Wesch, "Leuchten und Struktur fester Stoffe," R. Tomaschek, Editor, pp. 124-146, R. Oldenburg (publisher), Munich and Berlin (1943).
5. E. S. Rittner and J. H. Schulman, *J. Phys. Chem.*, **47**, 537 (1943).
6. E. T. Allen and J. L. Crenshaw, *Am. J. Sci.*, **34**, 341 (1912).
7. A. Kremheller and A. K. Levine, Spring Meeting of the ACS, Miami, April 9, 1957; *J. Appl. Phys.*, **28**, 746 (1957); *Sylvania Technologist*, **10**, 67 (1957).
8. A. Neuhaus, *Chemie-Ing.-Techn.*, **5**, 355 (1956).

Tin-Activated Alkaline-Earth Pyrophosphate Phosphors

R. C. Ropp and R. W. Mooney

Chemical and Metallurgical Division, Sylvania Electric Products Inc., Towanda, Pennsylvania

ABSTRACT

The preparation and properties of the Group II metal pyrophosphates activated by tin are described. It is shown that the fluorescent emission is strongly dependent on the matrix shifting toward higher wave lengths with increasing size of the cation of the pyrophosphate. Excitation and emission spectra of many of the phosphors are given. The most useful of these phosphors is $Sr_2P_2O_7$:Sn, a very efficient blue phosphor emitting at 452 mμ.

During the past few years there have been several investigations of tin-activated phosphates. These phosphors present certain problems in preparation since the tin atoms function as activators only when in a partially reduced state, commonly thought to be the Sn^{2+} oxidation state. Except for this minor problem, the tin-activated phosphates are easily prepared and a wealth of new phosphors may be obtained by changing the cationic constituent of the lattice and the crystal structure if the compound exists in polymorphic forms.

The tin-activated orthophosphates were studied in detail by Butler (1) and several efficient phosphors discovered. Starting from titanium-activated barium pyrophosphate (2), Ranby and co-workers (3) made a study of the tin-activated alkaline-earth pyrophosphates giving the visually detected luminescent colors obtained by, varying the ratio of one cation to another in the three binary systems and the spectral energy distributions of selected pyrophosphates activated by tin and manganese. All three alkaline-earth pyrophosphates were found to be polymorphic, but only in the barium pyrophosphate system did a change in structure from the low-temperature to the high-temperature form produce a change in emission, specifically from green to red. The high-temperature forms (commonly referred to as the α-forms) and the low-temperature or β-forms of calcium and strontium pyrophosphate both were stated to fluoresce blue under 254 μ excitation. A concurrent study of the tin-activated strontium and barium pyro- and tetraphosphates by McKeag and Steward (4) yielded several different phosphors in the barium system, but the blue emission of the strontium system was relatively unaffected by changes in the Sr/P ratio or firing temperature.

The present study was undertaken to investigate in greater detail the optical properties of the tin-activated alkaline-earth pyrophosphates and modifications thereof, especially with regard to the effects of crystal structure changes on the emission and excitation spectra of these phosphors. It will be shown that the spectral properties are even more dependent on crystal structure than was previously realized, thus leading to the discovery of several new phosphors. The most useful phosphor in this system is $Sr_2P_2O_7$:Sn, a deep-blue emitter, which has found practical application in fluorescent lamps.

Experimental Method

The pyrophosphates of calcium, strontium, and barium were readily obtained by ignition of their respective secondary phosphates. The compounds $CaHPO_4$ and $BaHPO_4$ were precipitated by the usual methods of adding a solution of $(NH_4)_2HPO_4$ to a solution of $CaCl_2$ or $BaCl_2$, each solution having been previously purified by sulfide separation of the heavy metals. Anomalies in the precipitation of $SrHPO_4$ led to an investigation of this material from which it was found that $SrHPO_4$ is dimorphic with each polymorph exhibiting slightly different behavior on ignition (5). In general, a slight excess of phosphate ion was used and the tin concentration varied from 0.01-0.20 gram-atom tin per gram-mole of pyrophosphate. It was found that phosphor characteristics were independent of activator concentration over this range, and therefore all phosphors were prepared at the same added concentration of 0.05 gram-atom tin per gram-mole of pyrophosphate. For the magnesium- and zinc-modified phosphors, the compounds $MgNH_4PO_4$ and $ZnNHPO_4$ were precipitated by standard techniques (13). The firing techniques used in the preparation of these phosphors followed the methods described in detail by several previous authors (1-3) and are not described here, except to state that various requisite

temperatures were employed to form the diverse polymorphic crystalline forms.

The crystal structures of the phosphors were determined by conventional x-ray diffraction techniques using CuKα radiation from a Philips Norelco unit. In the majority of cases, identification was made by means of Debye-Scherrer powder patterns taken on large diameter (114.6 mm) cameras. In a few cases, diffractometer tracings were taken on a Norelco wide-range goniometer at a scanning speed of ¼°/min. As would be expected, the two methods were in excellent agreement.

The excitation-emission radiometer[1] used for the measurements of excitation and emission spectra will be described in detail elsewhere (6). Basically, it is a double monochromator system with a high-pressure xenon arc source and a 1P28 photomultiplier detector. A combination of optical and electrical components provides for constant-energy-level illumination of the sample during excitation measurements and gives an emission spectrum which is proportional to the true energy output of the sample regardless of source fluctuations or detector sensitivity as a function of wave length. The relative efficiency measurements were made on a plaque tester of conventional design (7).

Experimental Results in Single-Component Pyrophosphates

Spectral characteristics of the tin-activated polymorphic modifications of calcium, strontium, and barium pyrophosphate are summarized below. In general, there were no changes in spectra with tin content.

Calcium pyrophosphates.—Excitation and emission spectra of β- and α-$Ca_2P_2O_7$:Sn are shown in Fig. 1. (λ_x refers to the wave length of excitation, and λ_e, the emission wave length at which the excitation was measured.) No fluorescence was observed for γ-$Ca_2P_2O_7$:Sn.

The low-temperature or β-form of $Ca_2P_2O_7$:Sn is primarily an ultraviolet emitter with a broad band peaking at 369 mμ. The excitation spectrum is also broad with the primary band peaking at 238 mμ. Both the emission and excitation spectra suggest the presence of a second band in each at lower energies. However, the emission spectrum remained essentially as shown in Fig. 1 for all energies of excitation which gave fluorescence. These results agree with the emission spectrum for β-$Ca_2P_2O_7$:Sn presented by Bril and Klasens (8).

As the crystal structure changed from β-$Ca_2P_2O_7$ to α-$Ca_2P_2O_7$, the high-temperature form, the spectra also varied. With high excitation energies, the emission spectrum closely resembled that of β-$Ca_2P_2O_7$:Sn with the peak shifted very slightly to higher energies at 364 mμ. The excitation spectrum for this band was, however, different with the strongest absorption band at 254 mμ and a weaker band at about 232 mμ. As the energy of excitation decreased, a second band appeared in the emission spectrum at about 430 mμ until with $\lambda_x = 276$ mμ the fluorescent spectrum shown in Fig. 1 was obtained. The excitation spectrum obtained for emission in this band also showed two peaks, the stronger at 240 mμ and the weaker at 260 mμ. An inspection of Fig. 1 shows that the positions of the bands in the excitation spectra are not equivalent for the two different emission bands.

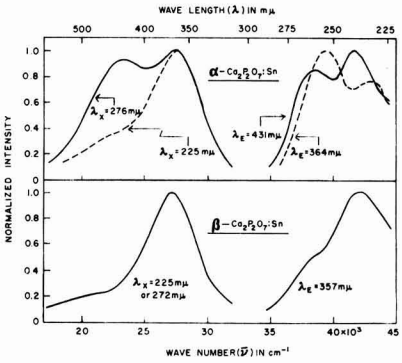

Fig. 1. Excitation-emission spectra for $Ca_2P_2O_7$:Sn phosphors. Firing temperature, 1300° and 1175°C, respectively.

Strontium pyrophosphates.—The low-temperature or β-form of $Sr_2P_2O_7$:Sn is also primarily an ultraviolet emitter (see Fig. 2) with its main band at 364 mμ and evidence of another weaker band in the visible. Its excitation spectrum has two bands, the stronger peaking at 234 mμ and the weaker at about 260 mμ. The similarities between the excitation and emission spectra of β-$Ca_2P_2O_7$:Sn and β-$Sr_2P_2O_7$:Sn are striking with the bands shifted very slightly to higher energies for β-$Sr_2P_2O_7$:Sn.

The α-form of $Sr_2P_2O_7$:Sn has a single emission band peaking at 464 mμ and the usual two excitation bands at 256 mμ and approximately 238 mμ. Again, a similarity may be noted between α-$Sr_2P_2O_7$:Sn and the lower-energy emission band in α-$Ca_2P_2O_7$:Sn with the spectrum of the strontium compound shifted to lower energies. The bands in the excitation spectra of α-$Sr_2P_2O_7$:Sn and α-$Ca_2P_2O_7$:Sn for $\lambda_E = 431$ mμ occur at almost identical energies although the relative intensities of the bands are reversed.

Barium pyrophosphates.—The low-temperature form of $Ba_2P_2O_7$, which Ranby (3) has designated as α-$Ba_2P_2O_7$ has a single weak emission band peaking

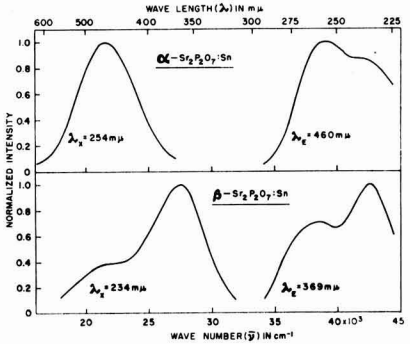

Fig. 2. Excitation-emission spectra for $Sr_2P_2O_7$:Sn phosphors. Firing temperature, 1100° and 650°C, respectively.

[1] Built by the Perkin-Elmer Corporation, Norwalk, Conn.

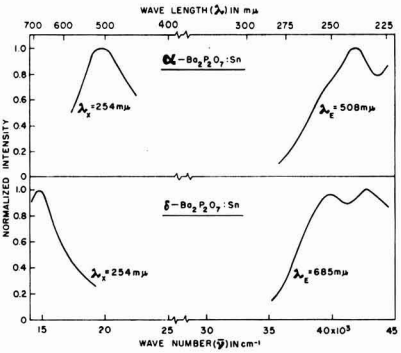

Fig. 3. Excitation-emission spectra for $Ba_2P_2O_7$:Sn phosphors. Firing temperature, 650° and 980°C, respectively.

at 505 mμ (see Fig. 3). The main excitation band peaks at 239 mμ and there is evidence of a weaker band at lower energies in the general vicinity of 256 mμ. Thus this phosphor also has spectral characteristics in common with α-$Ca_2P_2O_7$:Sn and α-$Sr_2P_2O_7$:Sn with the emission peak shifted to lower energies, but the positions of the two excitation bands relatively unchanged.

The δ-$Ba_2P_2O_7$ structure is unique and has no simple relationship to the other alkaline-earth pyrophosphates. Therefore, it is not surprising that the phosphor δ-$Ba_2P_2O_7$:Sn is also unique having a single emission band peaking in the deep red at 676 mμ and two excitation bands at 233 mμ and 250 mμ.

Experimental Results on Binary Metal Pyrophosphates

The effect of varying the ratio of one cation to another in the three possible binary combinations of the alkaline-earth pyrophosphates is shown in Fig. 4 in which the relative red and blue plaque readings, using Corning 2424 and 5543 plus 3389 filters, respectively, (7) are plotted against composition. The data given in Fig. 4 represent three separate systems. On the right is shown the binary combinations of the strontium calcium pyrophosphates activated by tin. The section in the middle represents barium strontium pyrophosphates activated by tin, and the left hand section represents barium calcium pyrophosphate activated by tin. In general, the combination of a pair of red and blue plaque readings represents the response of a single phosphor composition. Changes in fluorescent color were observed, and these changes are represented at the top of the figure. An increase or decrease in blue or red plaque readings should be correlated together to determine the relative chromaticities of the three systems to each other. The firing temperature was selected to give the high-temperature modification of each pyrophosphate, i.e., the α-modifications of $Ca_2P_2O_7$ and $Sr_2P_2O_7$ and the δ-modification of $Ba_2P_2O_7$ since the high-temperature forms were more efficient, visually, than their low-temperature modifications. Data on each system are summarized below.

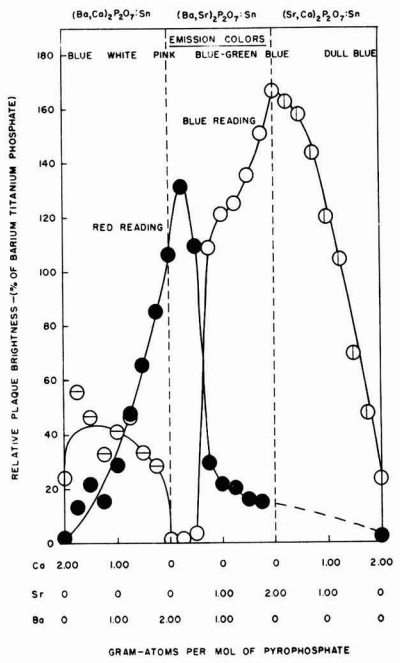

Fig. 4. Variation of relative plaque response with change in cationic constituents in three binary systems. Firing temperature, 1100°C.

Calcium-strontium pyrophosphates.—The plaque data of Fig. 4 show a continuous increase in blue emission as the Sr/Ca ratio is increased in $(Sr,Ca)_2P_2O_7$:Sn (right portion of Fig. 4). Identification of the compounds present by x-ray diffraction showed that the phosphors were mixtures of α-$Ca_2P_2O_7$ and α-$Sr_2P_2O_7$ with the relative amount of each being determined by the relative amounts of the cations. Therefore, it was not surprising that the emission spectra also showed the ultraviolet emission band at about 361 mμ characteristic of α-$Ca_2P_2O_7$:Sn and the visible band at about 464 mμ characteristic of α-$Sr_2P_2O_7$:Sn. Again, the amount of each emission band present was determined by the relative amount of the particular compound in the mixture. The excitation spectra were not examined in detail.

Strontium-barium pyrophosphates.—The fluorescent color of $(Ba,Sr)_2P_2O_7$:Sn changed from blue to blue-green to pink in agreement with Ranby, *et al.* (3) as the Ba/Sr ratio increased (middle portion of Fig. 4). It is evident that there is a sharp change in fluorescent color in going from $Sr_{0.75}Ba_{1.25}P_2O_7$:Sn to $Sr_{0.50}Ba_{1.50}P_2O_7$:Sn. The emission spectra of the system exhibited only a single band whose peak wave number varied with the alkaline-earth ratio. The discontinuity mentioned above is readily shown in Fig. 5 where the peak emission energy is plotted against this ratio. The x-ray data paralleled the optical measurements. Thus the diffraction pattern showed a continuous change from α-$Sr_2P_2O_7$ to a pattern closely resembling α-$Ba_2P_2O_7$ in going from $Sr_2P_2O_7$ to $Sr_{0.75}Ba_{1.25}P_2O_7$. Phosphors with higher barium contents than the latter had essentially the δ-$Ba_2P_2O_7$ structure and the characteristic red emission of δ-$Ba_2P_2O_7$:Sn. The data of Fig. 4 seem to imply that the phosphor $Sr_{0.25}Ba_{1.75}P_2O_7$:Sn has more emission in the red than δ-$Ba_2P_2O_7$:Sn. However, this result is due to the greater sensitivity of the photo-

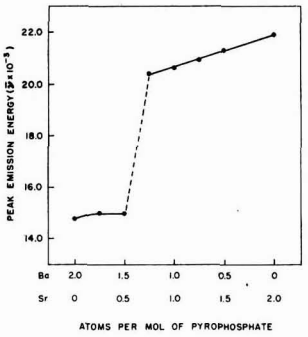

Fig. 5. Peak emission changes in the $(Sr,Ba)_2P_2O_7$:Sn systems.

multiplier as the peak emission shifts toward the green. In this system also, there was no detailed study of excitation spectra.

Barium-calcium pyrophosphates.—It is apparent from the results given in Fig. 4 (left portion) that the $(Ba,Ca)_2P_2O_7$:Sn phosphors are low in efficiency. For this reason, and since they melted very easily giving fused materials, this sytem was not studied in detail.

Other binary pyrophosphates.—With two exceptions, other Group II binary pyrophosphates activated by Sn were generally inefficient and uninteresting. The exceptions were $(Sr, Mg)_2P_2O_7$:Sn and $(Sr,Zn)_2P_2O_7$:Sn. These phosphors displayed a decrease in blue plaque efficiency similar to that shown in Fig. 4 for $(Sr,Ca)_2P_2O_7$:Sn as the Sr/Mg or Sr/Zn ratio decreased. Measurements of emission spectra disclosed that although $Mg_2P_2O_7$:Sn and $Zn_2P_2O_7$:Sn are essentially inert, the addition of small amounts of strontium produces ultraviolet-emitting phosphors. As an example, the emission and excitation spectra of $Mg_{1.75}Sr_{0.25}P_2O_7$:Sn and $Zn_{1.75}Sr_{0.25}P_2O_7$:Sn are given in Fig. 6. Both have a strong emission band peaking at 333 mμ and evidence of the α-$Sr_2P_2O_7$:Sn band appearing at lower energies. As the Sr/Mg ratio or Sr/Zn is increased, this band at about 464 mμ increases in intensity while the one at 333 mμ decreases. The excitation spectra are composed of two bands, on at about 248 mμ and a second at about 226 mμ. X-ray identification showed the presence of α-$Sr_2P_2O_7$ as well as compounds having diffraction patterns similar, but not identical, to $Mg_2P_2O_7$ and $Zn_2P_2O_7$. A comparison of the emission spectra data in Fig. 1 and 2 with those in Fig. 5 reveals no interrelation or similitude to previous data.

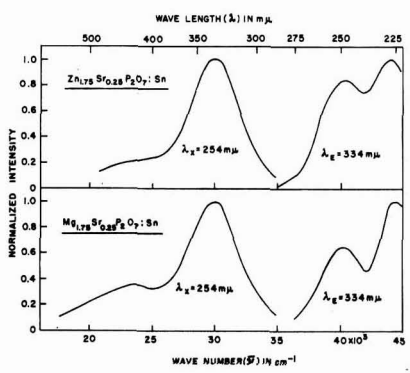

Fig. 6. Excitation-emission spectra for $(Mg,Sr)_2P_2O_7$:Sn and $(Zn,Sr)_2P_2O_7$:Sn phosphors. Firing temperature, 1120°C.

Discussion

The results of this investigation are in general agreement with those reached earlier by Ranby, *et al.* (3), namely, that the emission spectra are determined primarily by the crystal structure of the matrix. This conclusion is also applicable to the excitation spectra. However, while there is general agreement with previous work, there are several areas in which previous views must be modified. For instance, the tin-activated calcium strontium pyrophosphates exhibit considerable change in emission in going from $Ca_2P_2O_7$:Sn to $Sr_2P_2O_7$:Sn and in going from the β-form to the α-form. Thus, both β-$Ca_2P_2O_7$:Sn and β-$Sr_2P_2O_7$:Sn are primarily ultraviolet emitters, but neither is very efficiently excited by 254 mμ excitation. On the contrary, α-$Sr_2P_2O_7$:Sn is a blue phosphor and is very efficiently excited by 254 mμ, while α-$Ca_2P_2O_7$:Sn is both a blue and an ultraviolet emitter, but the blue band is only weakly excited by a low-pressure mercury-vapor arc. Therefore, under this excitation the $(Sr,Ca)_2P_2O_7$:Sn phosphors show changes in relative intensity but little change in position of the emission bands. The band at 464 mμ attributed to α-$(Ca,Sr)_2P_2O_7$:Sn (3) is therefore, in reality, due to α-$Sr_2P_2O_7$:Sn as shown in Fig. 2. The emission data on the barium pyrophosphates are in fair agreement with previous results (3,4).

The $(Sr,Ba)_2P_2O_7$:Sn system is interesting in view of its continuous change in the position of the emission peak with composition as shown in Fig. 5. Starting from α-$Sr_2P_2O_7$:Sn and replacing strontium by barium, the emission peak energy decreased linearly approaching that of the α-$Ba_2P_2O_7$:Sn phosphor. The d-spacings in the x-ray diffraction patterns showed a similar continuous shift, and therefore it is concluded that $Sr_2P_2O_7$ and $Ba_2P_2O_7$ form a continuous series of solid solutions up to an alkaline-earth content of 75% barium. At this point, the α-phase is no longer stable and the δ-$Ba_2P_2O_7$:Sn phosphor is formed as evidenced by the x-ray diffraction pattern and the spectra. It should be noted that the most efficient phosphors having the blue-green emission characteristic of α-$Ba_2P_2O_7$:Sn are prepared by stabilizing this structure with strontium as, for instance, in the phosphor $Ba_{1.25}Sr_{0.75}P_2O_7$:Sn, since it is difficult to prepare α-$Ba_2P_2O_7$:Sn with high efficiency due to the tendency to form δ-$Ba_2P_2O_7$:Sn at temperatures necessary to promote the requisite crystallinity and ultraviolet response of the phosphor.

The $(Sr,Ba)_2P_2O_7$:Sn system is therefore very different from the $(Sr,Ca)_2P_2O_7$:Sn, $(Sr,Mg)_2P_2O_7$:Sn, and $(Sr,Zn)_2P_2O_7$:Sn systems where the x-ray diffraction patterns of each individual component are readily discernible and where the emission spectra of both components appear, as for example the bands due to α-$Sr_2P_2O_7$:Sn and α-$Ca_2P_2O_7$:Sn in $(Sr,Ca)_2P_2O_7$:Sn. One is therefore led to believe that in these systems the phosphor components

Table I. Ultraviolet emission bands

Phosphor	Peak wave length in mμ		
	Emission	Excitation	
β-$Ca_2P_2O_7$: Sn	369	260	238
β-$Sr_2P_2O_7$: Sn	364	260	234
α-$Ca_2P_2O_7$: Sn	362	253	232

Table II. Visible emission bands

Phosphor	Peak wave length in mμ		
	Emission	Excitation	
α-$Ca_2P_2O_7$: Sn	429	261	240
α-$Sr_2P_2O_7$: Sn	463	256	238
α-$Ba_2P_2O_7$: Sn	505	256	239

exist as separate species, in contrast to the $(Sr,Ba)_2P_2O_7$: Sn system.

It was noted earlier that the emission spectra of the β-forms of $Ca_2P_2O_7$: Sn and $Sr_2P_2O_7$: Sn were similar and apparently related to one of the bands in α-$Ca_2P_2O_7$: Sn. This relationship is easily seen by a compilation of the peak energies.

Inspection of Table I shows that the peaks in the emission and excitation bands occur at almost identical energies. A corresponding tabulation of the peak energies of the α-forms of calcium, strontium and barium pyrophosphate is given in Table II. These three forms are closely related structure-wise and have orthorhombic symmetry (3).

For the visible emission bands there is a definite trend toward lower energies with increasing size of the alkaline-earth cation; however, again the excitation bands peak at almost identical energies.

The relative heights of the two excitation bands given in Tables I and II vary for each phosphor. If one assumes that the lower-energy emission bands, i.e., the visible, are associated with the lower-energy excitation bands, and the higher-energy emission bands, i.e., the ultraviolet, are associated with the higher-energy excitation bands, one obtains a direct correspondence between the strong excitation and the strong emission bands with both strontium systems and with β-$Ca_2P_2O_7$: Sn. However, the correspondence is very poor for α-$Ba_2P_2O_7$: Sn where the phosphor absorbs in the higher-energy band and emits in what we have arbitrarily called the lower-energy band, i.e., at 505 mμ. A similar, but even more puzzling anomaly exists in the α-$Ca_2P_2O_7$: Sn system where, considering only the excitation data, one would predict that irradiation with low-energy ultraviolet would yield the ultraviolet band. Actually, just the reverse results were obtained for the emission spectra, i.e., irradiation with 225 mμ energy gave the ultraviolet band and irradiation with 276 mμ energy gave both ultraviolet and visible bands. Thus the emission data are, by themselves, consistent with the other calcium and strontium systems.

In order to illustrate the trends in emission spectra with changes in structure, the peak emission energies of all phosphors are plotted against the alkaline-earth cationic radii in Fig. 7. The grouping

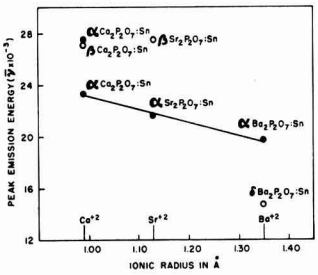

Fig. 7. Effect of cationic radius and structure on emission of tin-activated alkaline-earth pyrophosphate phosphors.

together of the ultraviolet bands is obvious as is the linear relationship between the peak energies in the α-pyrophosphates vs. cationic radii. The emission of δ-$Ba_2P_2O_7$: Sn falls into neither grouping. It is very apparent from Fig. 7 that there is an over-all trend toward lower emission energies or longer wave lengths with increasing cationic size. Unfortunately, this is in direct conflict with the results on several other phosphor systems as summarized by Fonda (9). However, with three exceptions all of the phosphors listed by Fonda were activated by manganese either as a primary or secondary activator. These exceptions were the alkaline-earth sulfides activated by europium (10), the self-activated vanadates of the alkaline-earth metals (11), and the alkaline-earth orthophosphates activated by tin (1). However, in the latter case the results were conflicting since, in one case, an increase in cationic size shifted the emission to shorter wave lengths, whereas in the other a shift to longer wave lengths was observed.

Fonda also points out several exceptions to his general rule that the spectral position of the emission band should shift to longer wave lengths as the lattice spacing is decreased. For these exceptions, the activators are thallium, silver, copper and in two cases, manganese. It is interesting that, ignoring the two manganese cases above, all of the other activators together with tin share the property that their bonding electrons are s-electrons, not d-electrons as is the case with manganese and europium. We are, therefore, led to agree with Fonda that the effects of polarizability lead to the reversal of his general rule stated above, but going a step further we believe that the effects of polarizability are more apt to be found in systems with activators whose bonding electrons are symmetrical s-electrons than in those whose bonding electrons are d-electrons, as for instance, manganese. The results on the tin-activated alkaline-earth pyrophosphates are explained, therefore, by assuming that the tin in a barium site has a greater effective radius than in a calcium site and is, therefore, more easily polarizable leading to a greater overlapping of the electronic orbits and a consequent shrinkage in the energy difference between the excited and ground states. Generalizing, it would appear that it is dangerous to treat all activator centers as identical and, specifically, it is very dangerous to use manganese-activated systems as typical. This conclusion is equally applicable to properties other than optical spectra

since, for instance, it has been shown that the tin- and manganese-activated phosphates do not exhibit the same type of variation of fluorescent efficiency with temperature (12).

Finally, one might assign the visible emission bands in the α-structures to the $^3P_1^0 \rightarrow {}^1S_0$ transition of the tin center and the ultraviolet emission bands to the $^1P_1^0 \rightarrow {}^1S_0$ transition. Corresponding assignments in the reverse direction could also be made to the excitation bands, although there are many unexplained phenomena that do not correspond exactly to these assignments.

Acknowledgment

The authors are indebted to T. J. Veleker and C. W. W. Hoffman for their x-ray identifications of the structures.

Manuscript received July 6, 1959. This paper was prepared for delivery before the Philadelphia Meeting, May 3-7, 1959.

Any discussion of this paper will appear in a Discussion Section to be published in the December 1960 JOURNAL.

REFERENCES

1. K. H. Butler, *This Journal*, **100**, 250 (1953).
2. S. T. Henderson and P. W. Ranby, *ibid.*, **98**, 479 (1951).
3. P. W. Ranby, D. H. Mash, and S. T. Henderson, *Brit. J. Appl. Phys.*, Supplement #4, S18 (1955).
4. A. H. McKeag and E. G. Steward, *ibid.*, Supplement #4, S26 (1955).
5. R. W. Mooney, M. A. Aia, C. W. W. Hoffman, and R. C. Ropp, *J. Am. Chem. Soc.*, **81**, 826 (1959).
6. W. Slavin, R. W. Mooney, and D. T. Palumbo, To be published.
7. K. H. Butler and R. W. Mooney, *Sylvania Technologist*, **9**, 121 (1956).
8. A. Bril and H. A. Klasens, *Philips Research Repts.*, **7**, 421 (1952).
9. G. R. Fonda, *J. Opt. Soc. Amer.*, **47**, 877 (1957).
10. P. M. Jaffe and E. Banks, *This Journal*, **102**, 518 (1955).
11. H. Gobrecht and G. Heinsohn, *Z. Physik*, **147**, 350 (1957).
12. R. W. Mooney, *This Journal*, **105**, 456 (1958).
13. I. M. Kolthoff and E. B. Sandell, "Textbook of Quantitative Inorganic Analysis," Macmillan Co., New York, p. 362, (1949).

Voltage Dependence and Particle Size Distribution of Electroluminescent Phosphors

Willi Lehmann

Research Department, Westinghouse Electric Corporation, Bloomfield, New Jersey

ABSTRACT

The particle sizes of electroluminescent zinc sulfide phosphors prepared by common firing techniques usually range over broad distributions which always have the same shape. Every phosphor of this "normal" particle size distribution shows a voltage (V) dependence of electroluminescent brightness (L) which, over many decades of L, can closely be described by $L = L_o \exp [-(V_o/V)^{0.5}]$. Every deviation of the particle size distribution from the "normal" form also causes a deviation of the measurable $L(V)$ dependence from this expression. Measurements on phosphor particles and on uniform phosphor films indicate that the basic excitation mechanism of electroluminescence follows the voltage dependence $L = L_o \exp [-(V_o/V)]$ and that the square root in the exponent of the usual equation is due mainly to the broad particle size distribution of regular phosphors. This view is supported also by a mathematical analysis.

The time-average of the emission intensity, L, of electroluminescent (EL) zinc sulfide powders generally increases rather rapidly with increasing amplitude of the exciting alternating voltage, V. Based on rough theoretical considerations, Destriau originally proposed to describe this dependence by

$$L = L_o \exp [-(V_o/V)] \qquad [1]$$

with L_o and V_o as constants (1). It developed, however, that the fit of this equation to experimental results is not too good, and a great variety of other mathematical forms have been proposed by various workers since that time (2-17). One of them

$$L = L_o \exp [-(V_o/V)^{0.5}] \qquad [2]$$

differs from Eq. [1] only by the square root in the exponent, and its agreement with experimental results is amazingly good in many cases and can extend over six or more decades of L. This agreement has repeatedly been considered to be a proof for the validity of the exhaustion barrier theory (9, 18-20) from which Eq. [2] originally was deduced (9). It cannot be denied, however, that deviations from Eq. [2] have been observed frequently.

The suggestion by Lehmann (21) that Eq. [2] is a result of the well-known nonuniformity of the emission in a phosphor powder could not, at that time, be supported by experimental results.

A somewhat unexpected answer to the problem came from investigations of particle size effects on

EL. If a common phosphor having the usual broad particle size distribution is separated into fractions of different mean particle sizes, then these fractions also show different $L(V)$ dependences. The first reliable experimental results in this respect apparently were reported by Milch and Mazenko (22). They separated their phosphor into fractions of fairly small distribution widths and used a generalized modification of Eq. [2]

$$L = L_0 V^n \exp\ [-(V_0/V)^{0.5}] \qquad [3]$$

to describe their measured $L(V)$ dependences. They found that not only L_0 and V_0 in Eq. [3] depend on the mean particle size, but also that a proper fit could be obtained only with values of the exponent, n, ranging between $n = -11$ and $n = +0.67$. Later, Goldberg (23) and Lehmann (24) independently made similar experiments with apparently less sharply separated phosphor fractions and described the $L(V)$ dependence of these fractions by Eq. [2]. They found, too, that both constants in Eq. [2], L_0 and V_0, depend on the mean particle size of the phosphor.

These experimental results immediately permit a conclusion. If the $L(V)$ dependence of a single phosphor particle depends in some fashion on its size, and if a phosphor has a broad particle size distribution (which is normally always the case), then the $L(V)$ dependence of the whole phosphor must be determined not only by the $L(V)$ dependence of a single particle but also by the form of the particle size distribution of the phosphor. In other words, there must be a correlation between the particle size distribution of a phosphor and its measurable $L(V)$ dependence, i.e., the $L(V)$ dependences of two otherwise identical phosphors, one of a broad and the other of a narrow particle size distribution, should be different even if the mean particle sizes of both samples are equal. The $L(V)$ dependence of normal phosphors with broad particle size distributions can be described fairly well by Eq. [2]. Consequently, a phosphor with a very narrow particle size distribution can be expected to show an $L(V)$ dependence which does not closely follow Eq. [2]. The significance of an experimental confirmation of this conclusion for all theoretical efforts to understand the mechanism of electroluminescence is obvious.

Particle Size Distributions of Regular Phosphors

Particle size distributions of normal phosphors, as obtained by common preparation procedures, were determined by means of a projection microscope. The approximate diameters of some 200-300 particles of each sample were measured. The resulting distributions of all these phosphors had essentially the same shape. An example in the form of a frequency-diameter histogram is shown in Fig. 1. Such a typical distribution curve has been shown earlier by Leverenz (25). It is not symmetrical and cannot be described closely by a Gaussian function, but a relatively good fit was obtained empirically by the function

$$y = ax^2 \exp\ (-2x/x_0) \qquad [4]$$

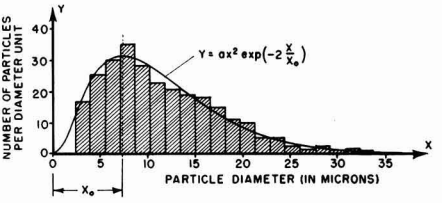

Fig. 1. Typical particle size distribution of a normal (i.e., unseparated) phosphor.

where x is the particle diameter, x_0 that particular particle diameter which corresponds to the peak of the function $y(x)$, a is a constant, and ydx is the number of particles between the size limits x and $x + dx$. The close fit of this function to the experimental distribution is shown also in Fig. 1. Variations of the several parameters of preparation (e.g., firing temperature and time, concentration of impurities, etc.) seem to cause only a shift of the peak size, x_0, to smaller or larger values but do not alter the general form of the particle size distribution. To what extent Eq. [4] may find a theoretical foundation (possibly in statistical considerations) is unknown. Nevertheless, it is at least a good approximation.

The $L(V)$ dependence of the phosphor sample whose particle size distribution is shown in Fig. 1 is given in Fig. 2. The agreement of the experimental points with straight lines, i.e., the agreement of the $L(V)$ dependence with Eq. [2], is almost exact over the whole measured range.

Behavior of Phosphor Fractions of Very Narrow Particle Size Distributions

The most desirable goal, fractions of almost uniform particle sizes separated out of common phosphor powders, could not be reached because of a lack of available techniques. There seems to be no

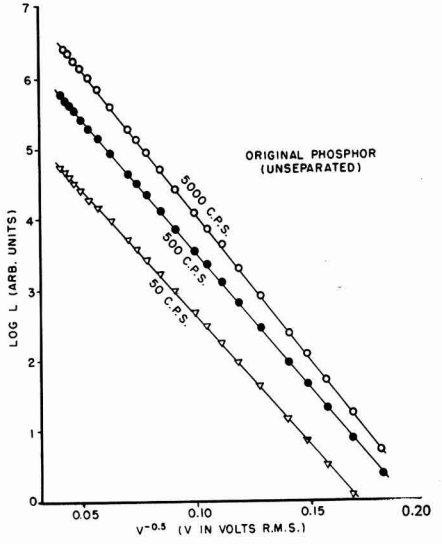

Fig. 2. The L(V) dependence of a normal phosphor can closely be described by Eq. [2].

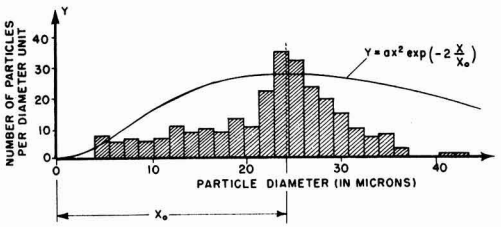

Fig. 3. Particle size distribution of a small fraction separated out of the normal phosphor of Fig. 1.

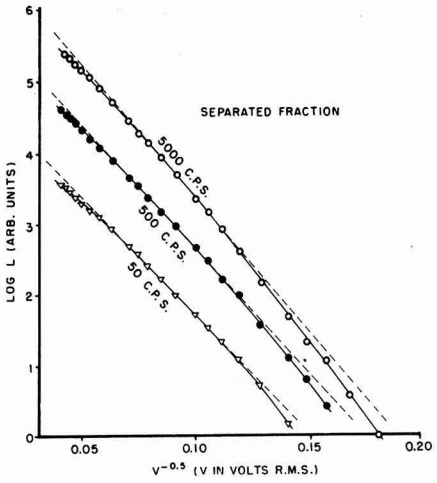

Fig. 4. The L(V) dependence of the separated fraction of Fig. 3 cannot closely be described by Eq. [2].

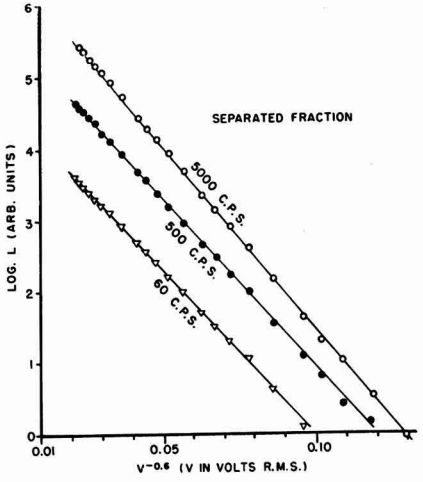

Fig. 5. The L(V) dependence of the separated fraction of Fig. 3 can closely be described by Eq. [5] with $\alpha = 0.6$.

known method permitting such narrow separations. As an example of what actually could be obtained in these experiments, Fig. 3 shows the distribution of a fraction of large diameter separated out of the phosphor whose original distribution is shown in Fig. 1. Although the distribution of Fig. 3 still has a considerable width, it is much smaller than that of the original, and it is obvious that there is no longer agreement with Eq. [4] as shown by the smooth curve in Fig. 3. The $L(V)$ dependence of this separated fraction is given in Fig. 4 as log L as a function of $V^{-0.5}$. The experimental points are not on straight lines here, so that this $L(V)$ dependence cannot be described closely by Eq. [2]. But if Eq. [2] is arbitrarily generalized by replacing the exponent 0.5 by an arbitrary constant

$$L = L_o \exp\left[-(V_o/V)^\alpha\right] \qquad [5]$$

it turns out that $\alpha = 0.6$ now gives a good fit, much better than $\alpha = 0.5$, as shown in Fig. 5. This value of $\alpha = 0.6$, of course, is purely incidental and has no physical meaning except that it indicates the influence of the still present width of the particle size distribution on the $L(V)$ dependence of the phosphor.

An extrapolation may be permitted here. If the $L(V)$ dependence of the original phosphor with its broad particle size distribution can be described by $\alpha = 0.5$ while the separated sample with the smaller but still considerable particle size distribution gives a better fit with $\alpha = 0.6$, then a phosphor with a still narrower particle size distribution probably would require a still higher value of α. An approach to $\alpha = 1$, i.e., toward Eq. [1], for ideally uniform particles seems likely but cannot, of course, be deduced rigorously from an extrapolation.

Behavior of Single Phosphor Particles

Most of all the geometrical complexity of a phosphor powder can be eliminated by consideration of single particles. However, a part of the complexity remains here also. Real single particles always have somewhat irregular shapes, may contain lattice disorders, and may be differently oriented with respect to the direction of the electric field. It is also known that the emission inside the phosphor crystals mainly originates from relatively small spots (5, 26, 27), and microscopic examination shows that every particle may contain one or more such emitting spots. Sometimes, the spots appear to be extended to lines, and the direction of these lines seems to follow the direction of some striped pattern, probably stacking faults (28-30), which can be seen when the crystal is illuminated by white light. Figure 6 shows a typical example of such nonuni-

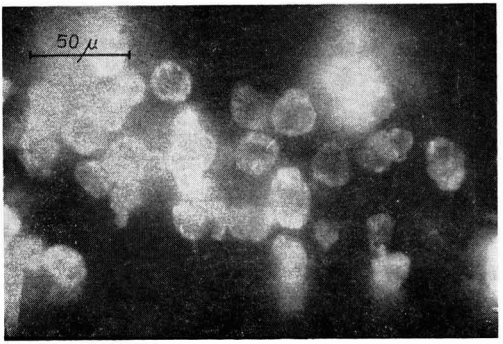

Fig. 6. Typical nonuniform distribution of emission, largely concentrated in "spots," of EL zinc sulfide particles.

form emission, largely concentrated in spots of single phosphor particles. Despite these complications, an $L(V)$ dependence of single particles somewhat simpler than that of complete phosphor powders can be expected.

The light emission of one single phosphor particle is too weak to be measured over a wide range by usual photomultipliers. Therefore, a visual method was used in these experiments. The phosphor to be measured (a few particles only) was placed in an oil cell and viewed through a microscope with low magnification. The starlike image of one luminescent particle was compared with the controlled and calibrated brightness of an artificial star (a pinhole in a piece of black paper illuminated by an incandescent lamp). Since a judgment of equality of the visual brightnesses of the two spots, even if they are visible side by side, always has a considerable uncertainty, each measurement was repeated ten times and the final value obtained by the arithmetic average of the ten single values. This technique gave fairly accurate results but was rather tiring to the eyes and time consuming so that only six single particles were completely measured.

The results obtained differ somewhat from particle to particle and are somewhat in contrast to results reported by Waymouth and Bitter (5) and by Zalm, Diemer, and Klasens (26). One particle out of the six had an $L(V)$ dependence which, over the whole measured range, can be described by Eq. [1] but not by Eq. [2] (see Fig. 7). Three other particles had $L(V)$ dependences which could not be described completely by either Eq. [1] or [2] but which can be understood easily by a superposition of two terms each of which has the form of Eq. [1]. Obviously in these three cases the curves are due to two emitting spots, with different voltage characteristics, inside the particles. Finally, the last two particles had $L(V)$ dependences which could be described in either way, by two terms of Eq. [1] or by one term of Eq. [2]. Since it seems unlikely that two totally different excitation mechanisms would be present in different particles of the same phosphor, we draw the conclusion that the emission of these two particles was due to two (or more) emitting spots inside the particles.

Behavior of Thin Phosphor Films

A uniform continuous film is obviously the simplest geometrical structure an EL phosphor can have. Its "particle size" is identical with its thickness, and variations of the thickness have the same effect as a finite particle size distribution of a powder phosphor; they cause a nonuniform distribution of the emission over the film area. The over-all emission of such nonuniform films in many cases can be described also by Eq. [2] fairly well, although deviations from this dependence occur rather frequently (31).

Most significant in this respect is, of course, the behavior of highly uniform films. Results obtained on specially selected uniform films[1] are shown in Fig. 8 and 9. These particular films (blue and green-emitting ZnS:Cu,Cl) were relatively thin (1 or 2 μ) and directly in contact with both electrodes (evaporated aluminum and the SnO_2 layer of conducting glass). The films appeared uniform and glassy under the microscope. Their electroluminescence was also uniform over their whole areas and without any emitting "spots" as are observed in powder phosphors. The experimental points deviate strongly from straight lines in Fig. 8 where log L is plotted as a function of $V^{-0.5}$. The points are on straight

[1] Made and kindly furnished by W. A. Thornton of this laboratory.

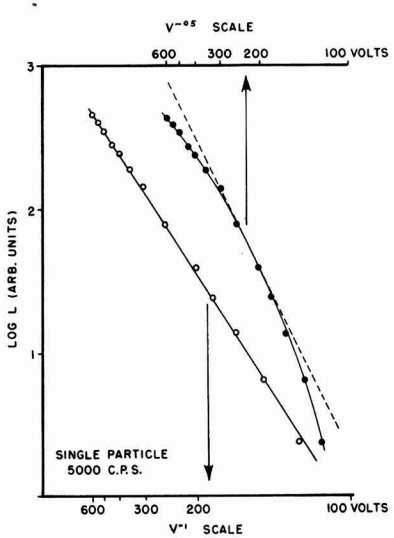

Fig. 7. The L(V) dependence of one single particle measured can closely be described by Eq. [1] but not by Eq. [2].

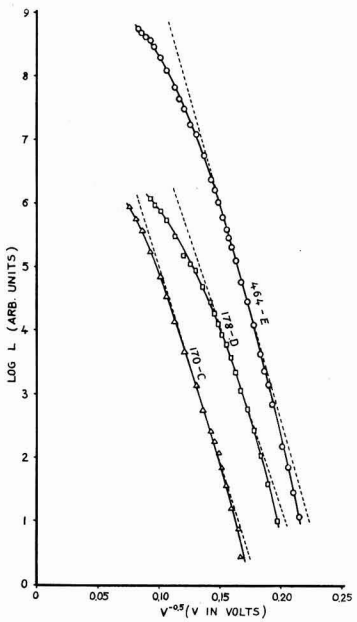

Fig. 8. The L(V) dependences of uniform zinc sulfide films do not follow Eq. [2].

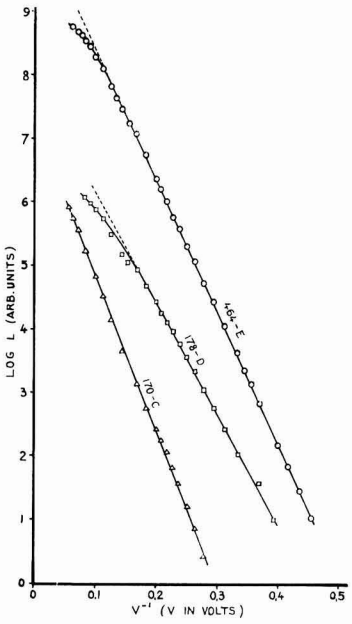

Fig. 9. The L(V) dependences of uniform zinc sulfide films follow Eq. [1] over many decades of L.

lines[3] in Fig. 9 over many decades of L, however, if log L is plotted as a function of V^{-1}.

Mathematical Treatment

The above experimental results indicate that, most likely, the process of excitation and emission of electroluminescence closely follows Eq. [1] if geometrical complexities are eliminated, and that the square root in Eq. [2] results only by the nonuniform geometry of the phosphor, i.e., mainly by the finite particle size distribution. Neglecting other possible reasons of nonuniformity (e.g., irregular particle shapes, orientations of stacking faults and barriers, etc.), it is possible even to draw a direct mathematical connection between the distribution function [4] and the emission function [1] on the one hand, and function [2] on the other hand.

A model phosphor may have a particle size distribution according to Eq. [4]. Every particle of this model phosphor may emit a light intensity described by

$$l = l_o \exp\ (-v_o/v) \qquad [6]$$

where l_o and v_o are constants and where v denotes the voltage drop across the whole particle. The two equations [1] and [6] are essentially identical concerning the voltage dependence. The particle size dependence enters Eq. [6] in two terms. The pre-exponential factor, l_o, may depend on the particle size, x, in a way which approximately may be described by $l_o = cx^m$ where c is a constant and where m is in the order of unity. Much stronger, however, seems to be the dependence v (x) since it enters Eq. [6] in the exponent. The ratio of the particle voltage, v, to the cell voltage, V, is essentially the ratio of the particle size, x, to the cell spacing, S, modified only by a factor, K, in the order of unity denoting the influence of the different dielectric constants of phosphor and embedding material

$$Kv/V = x/S \qquad [7]$$

The emission intensity of the whole phosphor is given by the integral

$$L = \int_o^\infty y(x)\ l(x,V)\,dx \qquad [8]$$

and introduction of [4], [6], and [7] into [8] gives

$$L = ac \int_o^\infty x^n \exp\left[-\left(2\frac{x}{x_o} + \frac{Kv_oS}{xV}\right)\right]dx \qquad [9]$$

where $n = m + 2$.

No simple analytical solution of this integral seems to exist, so a numerical integration was made with the assumption of reasonable values for the constants. The assumed values were $x_o = 8.7$ μ, and $(Kv_oS) = 2.3 \times 10^4$ vμ (this corresponds, for instance, to $v_o = 100$ v, $S = 100$ μ, and $K = 2.3$). The value of the factor ac in Eq. [9] is unimportant. With these values, the integrand in Eq. [9], i.e., of

$$Y = x^n \exp\left[-\left(2\frac{x}{x_o} + \frac{Kv_oS}{xV}\right)\right] \qquad [10]$$

was computed for different values of n and of V. It develops that the value of the exponent, n, is only of very minor influence so that the presentation of the case $n = 2$ in Fig. 10 may be sufficient here (the curves for the cases $n = 0$, 1, or 3 are almost the same). The results of the numerical integrations are shown in two different ways, in Fig. 11 as log L as a function of $V^{-0.5}$ and in Fig. 12 as log L as a function of V^{-1}. In Fig. 11, the curves very closely approach straight lines over many decades of L, almost independent of the particular value of n. The curves deviate from straight lines at the highest voltages,

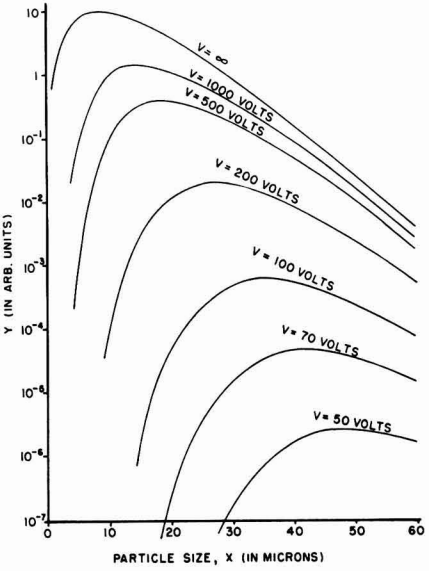

Fig. 10. The function Y (x,V) of Eq. 10 for n = 2, x_o = 8.7 μ, and (Kv_oS = 2300 Vμ.

[3] The deviation of two curves at the highest voltages in Fig. 11 is probably due to thermal quenching. The films became noticeably warm under the highest loads and the emission changed from blue to greenish.

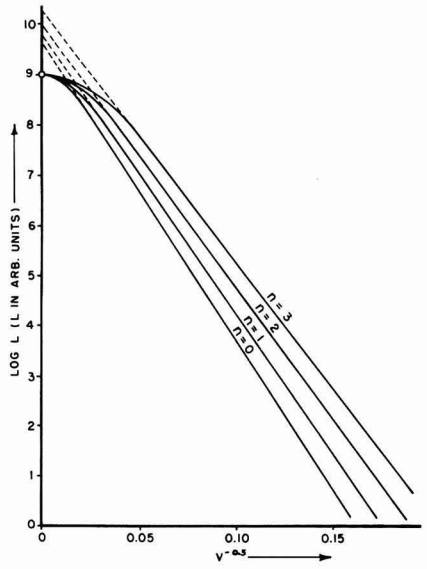

Fig. 11. The function $L = \int_0^\infty Y dx$ (Eq. [9]) approaches Eq. [2] very closely for low and moderate voltages.

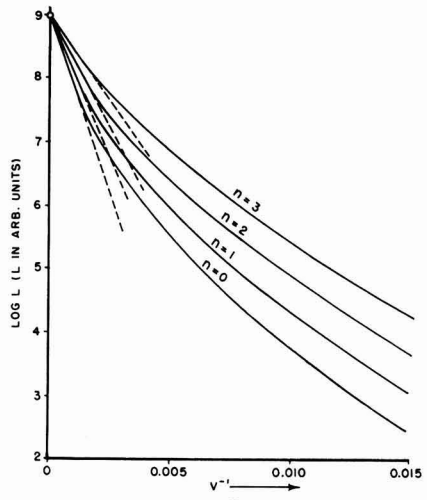

Fig. 12. The function $L = \int_0^\infty Y dx$ (Eq. [9]) does not closely follow Eq. [1] except at the highest voltages.

however, approaching "saturation" values considerably below the intersections of the straight lines with the axis $V = \infty$ (i.e., below the constant L_o in Eq. [2]). In Fig. 12, on the other hand, the curves do not approach straight lines at all except at the very highest voltages. This behavior is in agreement with experimental observations (15, 21).

Figure 10 also shows another effect, namely, a shift of these particle sizes which contribute most to the over-all light emission with a variation of the voltage, V. At low voltages, only the few largest particles contribute noticeably to the over-all light emission while the many fine particles are still practically dead. Increasing voltage causes the emission from the fine particles to increase faster than that from the coarse particles so that the fine particles dominate at high voltages because they are more numerous. This different contribution of the particles of a real phosphor at different voltages is qualitatively well known (3, 27).

Conclusions

The main results outlined in this paper permit the following conclusion:

(*a*) There is a correlation between the particle size distribution of an EL phosphor and the form of its $L(V)$ dependence. The particle size distribution of common EL zinc sulfide phosphors can be described closely by Eq. [4], and the $L(V)$ dependence of such phosphor follows closely Eq. [2] over many decades of L. Every deviation of the particle size distribution from Eq. [4] also causes a deviation of the $L(V)$ dependence from Eq. [2]. It is possible by a suitable form of the particle size distribution to obtain, within certain limits, any desired form of the $L(V)$ dependence of a phosphor.

(*b*) The fundamental process of electroluminescence, if geometrical complexities are eliminated, most likely follows Eq. [1].

Manuscript received July 29, 1959. This paper was prepared for delivery before the Philadelphia Meeting, May 3-7, 1959.

Any discussion of this paper will appear in a Discussion Section to be published in the December 1960 JOURNAL.

REFERENCES

1. G. Destriau, *J. chim. phys.*, **34**, 117 (1937).
2. G. Destriau, *Compt. rend.*, **209**, 36 (1939).
3. P. Zahm, G. Diemer, and H. A. Klasens, *Philips Research Repts.*, **9**, 81 (1954).
4. B. T. Howard, H. F. Ivey, and W. Lehmann, *Phys. Rev.*, **96**, 799 (1954).
5. J. F. Waymouth and F. Bitter, *ibid.*, **95**, 941 (1954).
6. R. Goffaux, *Bull. acad. roy. Belg., Cl. Sci.*, **40**, 808 (1954).
7. H. Gobrecht, D. Hahn, and H. E. Gumlich, *Z. Phys.*, **136**, 612 (1954).
8. G. F. Alfrey, *Brit. J. Appl. Phys., Suppl. No. 4*, p. 44 (1955).
9. J. B. Taylor, *ibid.*, 45 (1955).
10. P. Zahm, *ibid.*, 48 (1955).
11. W. W. Piper and F. E. Williams, *ibid.*, 39 (1955).
12. F. A. Schwertz, J. J. Mazenko, and E. R. Michalik, *Phys. Rev.*, **98**, 1133 (1955).
13. B. T. Howard, *ibid.*, **98**, 1544 (1955).
14. E. E. Loebner, *ibid.*, **98**, 1545 (1955).
15. G. Destriau and H. F. Ivey, *Proc. I.R.E.*, **43**, 1911 (1955).
16. S. Nudelman and F. Matossi, *This Journal*, **103**, 34 (1956).
17. E. Nagy, *Acta Phys. Acad. Sci. Hung.*, **6**, 153 (1956).
18. P. Zalm, *Philips Research Repts.*, **11**, 417 (1956).
19. G. Diemer, H. A. Klasens, and P. Zalm, *This Journal*, **104**, 130C (1957).
20. G. F. Alfrey and K.N.R. Taylor, *Helv. Phys. Acta*, **30**, 206 (1957).
21. W. Lehmann, *This Journal*, **103**, 667 (1956).
22. A. Milch and J. J. Mazenko, Quarterly Report No. 9, Second Series Computer Components Fellowship No. 347, Mellon Institute, Dec. 31, 1955, page V-40 (Contract No. CLN-AF19(604)-943).
23. P. Goldberg, *This Journal*, **106**, 34 (1959).

25. H. W. Leverenz, "An Introduction to Luminescence of Solids," p. 50, John Wiley and Sons, New York (1950).
26. P. Zalm, G. Diemer, and H. A. Klasens, *Philips Research Rept.*, **10**, 205 (1955).
27. A. Kremheller, Paper presented at Electrochem. Soc. Meeting, Philadelphia, May 1959 (Abstract 49).
28. M. A. Short, E. G. Steward, and T. B. Tomlinson, *Nature*, **177**, 240 (1956).
29. A. H. McKeag and E. G. Steward, *This Journal*, **104**, 41 (1957).
30. L. W. Strock; Intern. Union of Crystallography, Montreal, July 1957; *Acta Crystal.*, **10**, 840 (1957).
31. W. A. Thornton, *J. Appl. Phys.*, **30**, 123 (1959).

Gallium-Arsenide Diffused Diodes

J. Lowen and R. H. Rediker

Lincoln Laboratory, Massachusetts Institute of Technology, Lexington, Massachusetts

ABSTRACT

Gallium arsenide has been used to fabricate variable reactance and computer diodes which compare favorably with the best commercially available of germanium and silicon. The diodes have been fabricated by zinc diffusion into n-type gallium arsenide. Ohmic contact to the n-type material has been made with an antimony-gold alloy and to the p-type side with indium. Etching is used to remove the p-type diffused skin from everywhere but under the indium contact, thereby forming the mesa and defining the p-n junction area. Rectification ratios (at 2 v) as high as 10^{10} have been achieved. The diodes have been operated successfully in a variable reactance amplifier at S-band (2800 mcps) and in millimicrosecond-switching computer circuits.

Gallium arsenide, because its energy gap is larger than that of silicon, its electron mobility larger than that of germanium, and its dielectric constant smaller than both germanium and silicon, is a very attractive material for use in high-frequency as well as high-temperature devices. Recently it has been reported (1) that the electron lattice scattering mobility in GaAs may be as high as 12,000 $cm^2\ v^{-1}\ cm^{-1}$ and that material with electron mobilities as high as 6000 $cm^2\ v^{-1}\ cm^{-1}$ is now being produced. Point-contact gallium arsenide microwave diodes have been reported by Jenney (2) and Sharpless (3). These point-contact diodes have operated efficiently as first detectors at 6 Kmc (2), and at 11 Kmc and 60 Kmc (3). Jenney (4) has described the very low lifetime of the minority carriers in presently available gallium arsenide and the consequent difficulties in the fabrication of conventional bipolar transistors from the material. This very low lifetime, however, is one of the reasons for the very short switching times (10^{-9}-10^{-10} sec) reported (2, 3) for the point-contact gallium arsenide diode.

This paper describes the fabrication techniques and electrical properties of gallium arsenide diffused diodes. These diodes were designed for use as variable capacitors in parametric amplifiers. Because of the low lifetime for minority carriers in the gallium arsenide, the diodes also could be used in high-speed computer applications, since their switching times were in the order of 10^{-9} sec. The rectification ratios for these diodes are orders of magnitude larger than those for point-contact (2, 3) or alloy junction (5) gallium arsenide diodes previously reported.

Fabrication

The fabrication of the gallium arsenide diffused diodes can be divided into two sets of processes, the first set related to the diffusion step, the second including the assembly of the diode and the making of the ohmic contacts.

Diffusion is accomplished in a sealed quartz ampoule as shown in Fig. 1. All components are carefully etched and washed before being introduced into the ampoule. Referring to Fig. 1, the n-type gallium arsenide wafer which is about 0.050 cm thick has been cut from single crystal material so that its faces are perpendicular to the <111> direction. The face sitting on the flat quartz plate has been polished with 600 mesh SiC, but the exposed face has been polished to a mirror finish, the final abrasive being 0.1 μ alumina. The flat quartz plate is used to avoid the possibility of producing strains in the wafer during the diffusion cycle. About 250 mg of coarse crushed gallium arsenide is added below the quartz plate to provide an arsenic atmosphere and preserve the mirror-like finish during the diffusion. Without this added gallium arsenide the surface becomes stained and under extreme conditions of temperature and vacuum shows droplets of gallium. About 200 millionths of a gram of zinc, the p-type dopant, has been weighed into a quartz capillary which is inserted into the ampoule with due precaution to prevent contact between the zinc and the gallium arsenide. The quartz ampoules which have been used have a volume of about 20

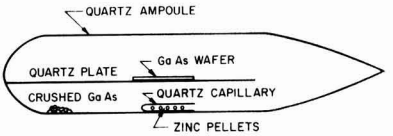

Fig. 1. Sealed diffusion ampoule just prior to being inserted into furnace.

ml; thus, the concentration of zinc in the vapor phase during diffusion is approximately 10^{17} atoms/ml. The loaded quartz ampoule is attached to a high vacuum system, pumped down to about 5 x 10^{-7} mm Hg, and then sealed off under vacuum. The heating cycle is programmed to heat to temperature rapidly, remain at that temperature for the desired period of time, and to allow for a slow cool down, between 1-2°C/min. Diodes have been fabricated from gallium arsenide indiffused with zinc at 650° and 700°C, and times of diffusion have been varied from 3 to 72 hr. There are indications that temperatures as low as 600°C can be used. For a 66-hr diffusion run at 650°C, we measured a junction depth of 8 μ, using a potassium hydroxide, potassium ferricyanide etch to delineate the junction.

The zinc indiffused gallium arsenide wafer then is diced and the rough side lapped to remove the p-type skin and to reduce the wafer thickness to between 0.003 to 0.005 in. Ohmic contact to this n-type side is made by bonding in a hydrogen atmosphere at about 450°C to an antimony gold plated Kovar rod. Ohmic contact to the p-type skin is made by alloying in an indium sphere 0.003-0.005 in. in diameter at 250°-300°C in a hydrogen atmosphere with aluminum chloride as a flux. The wafer is cleaned and then etched with a solution of equal parts of HNO_3, HAc, and HF. In this etching the p-n junction area is defined since the p-type skin is removed from the die everywhere but where it is masked by the indium alloy contact. An artist's conception of a section through a completed diode is shown in Fig. 2. This figure shows a pressure contact to the indium.

Electrical Properties

The voltage-current characteristic of a diode fabricated as described above is shown in Fig. 3. This characteristic has been plotted to logarithmic scale to show clearly the operating range of the diode. Note that below 5 v the reverse current is less than 2 x 10^{-11} amp and at 2 v the rectification ratio is about 10^{10}. For the diode of Fig. 3, the current in the forward direction obeys to a close approximation an $I = I_o \exp(qV/2kT)$ law between 10^{-11} and 10^{-2} amp. Larger area diodes have exhibited forward characteristics where, as the current is increased the exp $(qV/2kT)$ relationship changes to exp (qV/kT) before the ohmic series resistance masks the junction properties. This change in exponential behavior is consistent with the theory of Sah, Noyce, and Shockley (6).

The variation of diode capacitance with voltage is illustrated in Fig. 4. Plotted as abscissa is the applied voltage plus an assumed junction built-in-potential of 1.2 v. This assumed built-in-potential has been determined from the internal contact potential calculated from the impurity distribution. It is well known, however, that for germanium (7) and silicon the built-in-potential is usually less than this internal contact potential. The capacitance-voltage data is not sufficiently detailed to exclude by reason of poor fit to a power law the use of built-in-po-

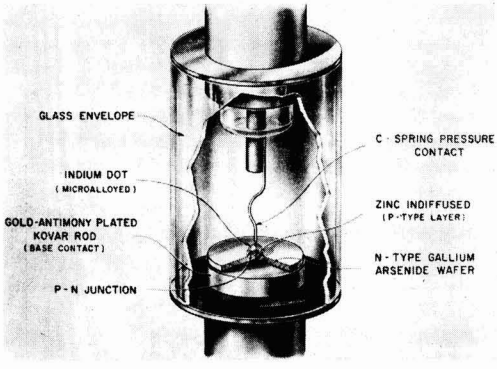

Fig. 2. Artist's representation of a packaged diode

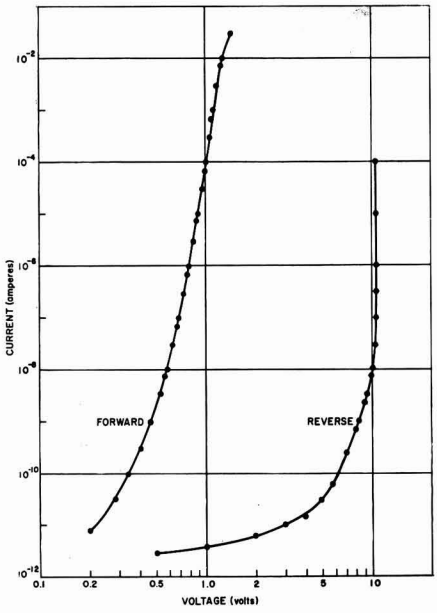

Fig. 3. Logarithmic presentation of voltage-current characteristics of GaAs diode. This diode was fabricated from material with a net donor density of 3.5 x 10^{16} cm^{-3} and electron mobility ~4000 cm^2/v sec. The diameter of the p-n junction was about 0.005 in.

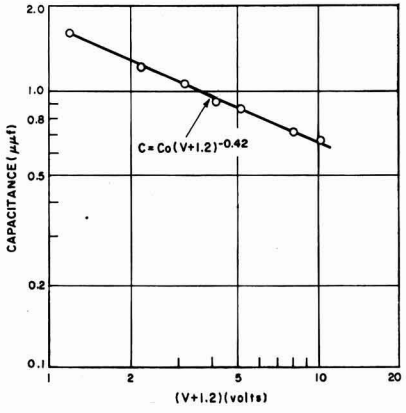

Fig. 4. Capacitance as a function of voltage for diode of Fig. 3.

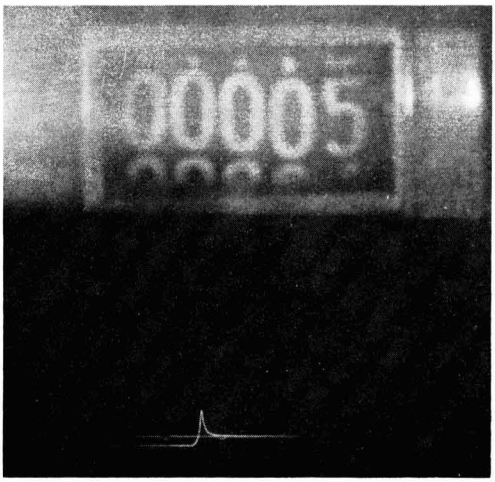

Fig. 5. Traveling-wave oscilloscope presentation of the reverse recovery transient for conditions described in text for diode of Fig. 3. Also shown is the zero diode current line on which two markers 6 mμsec apart have been superimposed.

tentials as low as 0.6 v. Using 1.2 v as shown in Fig. 5, the capacitance can be approximated by

$$C = \frac{C_o}{(V + 1.2)^{0.42}} \qquad [1]$$

indicating that the p-n junction is intermediate between an abrupt junction where the $V^{-1/2}$ law applies and the linear junction where the $V^{-1/3}$ law applies. If a built-in-potential of 0.7 v is used, on the other hand, the capacitance-voltage data can be fit by a $V^{-1/3}$ law.

Use as a Variable Capacitor

A figure of merit that has been proposed (8) for variable reactance diodes is the cutoff frequency

$$f_c = (2\pi R_s C_{\min})^{-1} \qquad [2]$$

where $C_{\min}$ is the diode capacitance (given in Eq. [1]) just short of breakdown and R_s is the semiconductor series bulk resistance through which the capacitance charging current must flow. This cutoff frequency is the highest frequency for which the quality factor Q of the variable reactance can be unity or larger. The intrinsic value of gallium arsenide as the semiconductor in variable reactance diodes lies in its high electron mobility even at high doping levels, which makes possible lower values of series resistance, R_s, than can be achieved in either germanium or silicon. The ratio of the cutoff frequency for diffused diodes of different semiconducting materials but of identical geometry and impurity concentration is

$$\frac{f_{c1}}{f_{c2}} = \frac{\mu_1}{\mu_2} \cdot \frac{\epsilon_2}{\epsilon_1} \qquad [3]$$

where ϵ is the dielectric constant and μ is the mobility of majority carriers in the bulk material. The cutoff frequency should be larger for GaAs than for Si or Ge because (a) the dielectric constant of 11 for GaAs is smaller than the values of 12 for Si and 16 for Ge, and (b) the electron mobility in GaAs is significantly larger, and for very heavily doped material ($n > 10^{18}$ cm^{-3}) almost an order of magnitude larger, than that in germanium and silicon. The comparison of cutoff frequencies has been given in Eq. [3] assuming the breakdown voltage for a given impurity distribution is independent of the semiconducting material. Actually, for the more heavily doped material ($n > 10^{18}$ cm^{-3}) diodes made of gallium arsenide seems to exhibit a higher breakdown voltage than similar diodes of germanium or silicon.

The diode whose electrical characteristics are shown in Fig. 3 and 4 has been used successfully in a variable reactance amplifier at S-band (2800 mcps). It had a cutoff frequency measured at 5 v reverse bias of about 30 Kmc which corresponds to a series bulk resistance of about 6.5 ohms. This value of resistance can be explained in terms of a true bulk resistance alone if one remembers that near the diffused junction the resistivity is much higher than the 0.04 ohm-cm resistivity of the starting material and that it is in this region (which is in the mesa) that the diode cross section is limited. On the other hand, contributions to the resistance by the contacts cannot be excluded.

By further refinements of technique we have been able, using the same resistivity material, to fabricate diodes with about 3 times the high frequency capabilities of the diode described above (9). This resistivity, however, is by no means optimum for diodes to be used as variable capacitors. For a given semiconductor the figure of merit, given in Eq. [2], is related to the material properties by

$$f_c \propto n^{1/2} \mu \qquad [4]$$

where n is the net impurity concentration and μ is the mobility. Lower resistivity gallium arsenide than has been used here should yield significantly better figures of merit. The full exploitation of the advantages of this relatively new intermetallic semiconductor for variable capacitors and other applications awaits a more abundant supply of good single crystal gallium arsenide of controlled resistivity. One application, however, for which present day gallium arsenide with its very low minority carrier lifetime is eminently suited is the fast-switch computer diode.

Use as a Computer Diode

Because of the very low lifetime in the GaAs now available, minority carrier storage which limits the switching speed in most germanium and silicon diodes is minimized. Diodes, which were fabricated as described above primarily for use as variable capacitors, when used in computer circuits have had switching times of the order of millimicroseconds. Figure 5 is a photograph of the reverse recovery transient as seen on a traveling wave oscilloscope of the diode whose characteristics are illustrated in Fig. 3 and 4. The diode was switched from 10 ma forward current to 5 v reverse bias with a loop impedance of 120 ohms. The time to recover to 1 ma reverse current is less than 3 mμsec.

Acknowledgments

The authors wish to thank Mrs. M. Barney and F. Sullivan for help in fabricating the diodes, and R. H. Kingston for evaluating the diodes in his S-band variable reactance amplifier. For our supply of single crystal gallium arsenide we are indebted to the RCA Semiconductor Division and the RCA Laboratories and to the Wright Air Development Center and the Air Materiel Command who sponsored their work, as well as to P. Moody and Mrs. C. Kolm of our laboratory.

Manuscript received June 24, 1959. This paper was prepared for delivery at the Philadelphia Meeting, May 3-7, 1959. The work reported in this paper was performed by Lincoln Laboratory, a center for research operated by Massachusetts Institute of Technology with the joint support of the U.S. Army, Navy, and Air Force.

Any discussion of this paper will appear in a Discussion Section to be published in the December 1960 JOURNAL.

REFERENCES

1. F. J. Reid and R. K. Willardson, *J. of Electronics and Control*, **5**, 54 (1958); see also, L. R. Weisberg, J. R. Woolston, and M. Glicksman, *J. Appl. Phys.*, **29**, 1514 (1958).
2. D. A. Jenney, *Proc. IRE*, **46**, 717 (1958).
3. W. M. Sharpless, *Bell System Tech. J.*, **38**, 259 (1959).
4. D. A. Jenney, *Proc. IRE*, **46**, 959 (1958).
5. S. M. Ku and H. T. Minden, Paper presented at ECS Meeting, Philadelphia, May 1959.
6. C. T. Sah, R. N. Noyce, and W. Shockley, *Proc. IRE*, **45**, 1228 (1957).
7. D. R. Muss, *J. Appl. Phys.*, **26**, 1514 (1955).
8. A. Uhlir, Jr., *Proc. IRE*, **46**, 1099 (1958).
9. J. Halpern, Private communication.

Purification of $SiCl_4$ by Adsorption Techniques

H. C. Theuerer

Bell Telephone Laboratories, Inc., Murray Hill, New Jersey

ABSTRACT

Silicon tetrachloride may be purified using adsorption columns filled with hydrous oxides or silicates. Hydrogen reduction of this purified halide leads to higher purity silicon than is obtainable otherwise. Data for the adsorption efficiency of various materials are presented using infrared spectroscopy and radioactive tracer techniques as the basis of comparison.

Several methods currently in use for the preparation of high-purity silicon require silicon tetrachloride as a source material. The quality of the silicon obtained depends on the purity of the silicon tetrachloride used, boron and phosphorus chlorides being the residual impurities of most concern. Removal of these impurities usually has been accomplished by distillation methods in conjunction with complexing additives (1-3). Such additives react with boron and phosphorus chlorides to form low vapor pressure compounds which remain in the still during distillation.

A new method for the purification of silicon tetrachloride using columns filled with hydrous adsorbents has led to significantly better results. It has been found that boron and phosphorus, as well as heavy metal chlorides, are removed efficiently by adsorption. Hydrogen reduction of the purified silicon tetrachloride to produce silicon rods, followed by floating-zone refining, has resulted in p-type crystals with resistivities above 8000 ohm-cm and minority carrier lifetimes of 1 msec. Using distillation methods for purification, comparative rods have resistivities of about 1000 ohm-cm and lifetimes of the same order as those obtained with the purer silicon.

In establishing the best adsorption techniques for the purification of silicon tetrachloride, it was necessary to evaluate various classes of adsorbents. Since hydrogen reduction and floating-zone refining are time consuming, several analytical methods were developed for these evaluations. Infrared absorption spectroscopy was used for the detection of BCl_3 and PCl_3 in $SiCl_4$. In the case of phosphorus, PCl_3 containing radioactive P32 with a half life of 14 days also was used for detection.

Evaluation of Adsorbents by Infrared Analysis for BCl_3 and PCl_3 in $SiCl_4$

Infrared spectra revealed that BCl_3 had a characteristic band at 1313 cm^{-1}, and PCl_3 had a series of bands at 1415, 1368, and 1345 cm^{-1}. $SiCl_4$ does not absorb in these regions. For calibration purposes, a series of $SiCl_4$ standards containing known amounts of BCl_3 and PCl_3 was prepared and analyzed. Strict adherence to Beer's law was not observed due to molecular interaction between BCl_3 and PCl_3, and the results are therefore semiquantitative with a detection sensitivity of 0.01%. Using this detection method and working with $SiCl_4$ containing 1% each of BCl_3 and PCl_3, it was possible to evaluate the relative efficiencies of various adsorbents for the removal of these impurities. Although the concentrations of impurities normally found in $SiCl_4$ are much lower than the detection limit of 0.01%, the above method gave much valuable information concerning the purification efficiency of various adsorbents.

In initial experiments, silica gel, activated alumina, coconut charcoal, and "molecular sieves" (sodium-calcium-alumino silicate) were evaluated for

Table I. Purification of $SiCl_4$ containing 1% PCl_3 and BCl_3 by various adsorbents

Adsorbent	First 10 cc eluted		Remaining drainable fractions	
	BCl_3, %	PCl_3, %	BCl_3, %	PCl_3, %
Silica gel 6-16 mesh	<0.01	<0.01	<0.01	<0.01
Activated alumina 8-14 mesh	<0.01	<0.01	<0.01	<0.01
Coconut charcoal 6-14 mesh	<0.01	0.1	0.1	0.1
Molecular sieves (sodium calcium alumino silicate) 1/16 in. pellets	1.0	<0.01	1.0	1.0

the removal of BCl_3 and PCl_3 from $SiCl_4$. Prior to use, the adsorbents were activated by treating in air at 270°C for 16 hr. The adsorbents then were added to 50 ml burettes to form columns 0.4 in. in diameter and 10 in. long. Thirty milliliters of $SiCl_4$ containing 1% each of BCl_3 and PCl_3 were allowed to drip into the columns at the rate of 1 ml/min. After standing 1 hr, 10 ml samples were drained from the burettes at a rate of 0.8 ml/min. A second set of samples comprising the remaining drainable $SiCl_4$ (approximately 12 ml) was collected also. All samples then were analyzed by the infrared absorption technique, with the results shown in Table I. It is apparent from these results that the hydrous oxides of silica and alumina are quite effective for removal of BCl_3 and PCl_3 from $SiCl_4$, the other adsorbents being relatively ineffective.

In addition to the above, various classes of adsorbents, including ion exchange resins, were tested for adsorption of BCl_3 and PCl_3 from $SiCl_4$ using the infrared technique. In a number of instances desired materials were not readily available, and in these cases, they were prepared specially. Where possible, the adsorbents were precipitated in gelatinous form for maximum surface area. The methods of preparation used are listed in Appendix I.

In the case of ion exchange resins, while $SiCl_4$ solutions are essentially nonionic, physical adsorption of impurities on these resins seemed possible, since they are porous and have a high surface area. Because such resins normally are furnished in a moist condition, prior to use with $SiCl_4$, it was necessary to remove the water by drying in a vacuum desiccator. After several days of pumping, these materials no longer hydrolyzed $SiCl_4$ and were then in satisfactory condition for adsorption studies.

In testing the adsorption efficiencies of the various materials, 5 cc of solid adsorbent, activated as listed in Table II, were added to 20 ml of $SiCl_4$ containing 1% each of BCl_3 and PCl_3. The mixtures were shaken intermittently for 1 hr, after which the $SiCl_4$ was filtered through glass wool and analyzed by infrared spectroscopy. Results are summarized in Table II.

It will be seen that hydrous oxides and silicates adsorb both BCl_3 and PCl_3 from $SiCl_4$. Those materials which were in gel form were most effective, probably due to their large surface area. Dehydration of several of the active oxides destroyed their adsorption efficiency, suggesting that chemisorption involving OH groupings is at least a part of the purification mechanism. Ion exchange resins were inoperative for the removal of boron and phosphorus chlorides.

Adsorption Studies Using Radioactive PCl_3 and PCl_5 in $SiCl_4$

In determining the effectiveness of adsorption columns for the removal of phosphorus chlorides

Table II. Purification of $SiCl_4$ containing 1% BCl_3 and PCl_3 by various adsorbents

Adsorbent	Activation	PCl_3, %	BCl_3, %
Silica gel 6-14 mesh	270°C-18 hr	0.01	<0.01
Silica gel 6-14 mesh deactivated	1000°C-18 hr	1	1
Silica gel from hydrolyzed $SiCl_4$	270°C-18 hr	<0.01	<0.01
$Mg(OH)_2$ powdered	120°C-4 hr	0.01	0.01
MgO anhydrous	120°C-18 hr	1	1
CaO	270°C-30 hr	1	1
$CaCO_3$	270°C-30 hr	1	1
$Fe(OH)_3$ gel	270°C-4 hr	<0.01	<0.01
TiO_2 gel	270°C-18 hr	<0.01	<0.01
Fullers earth	120°C-18 hr	<0.01	<0.01
Tungstic acid	—	0.1	0.1
Cellite #545 (treated diatomaceous earth)	120°C-18 hr	0.1	0.1
Decalso (alumino silicate gel)	120°C-18 hr	0.1	0.1
Zeo Dur (hydrous silicate greensand)	25°C-vacuum dried	0.01	0.01
Permutet H-70 (carboxylic acid resin)	25°C-vacuum dried	1	1
Permutet Q (sulfonated polystyrene)	25°C-vacuum dried	1	1
Permutet S-2 (quarternary amine polystyrene)	25°C-vacuum dried	1	1

from $SiCl_4$, solutions containing 0.001% by volume of PCl_3 containing radioactive P32 were used. Where desired, the PCl_3 was converted to PCl_5 by the addition of Cl_2 to the $SiCl_4$ solution. In these studies, samples of the eluent were analyzed, and autoradiographs of the columns were made. The detection sensitivity for phosphorus in the $SiCl_4$ was initially 1×10^{-8} mole %. In this work, activated alumina and silica gel were used as the adsorbents; these were activated by heating in air prior to use at 270°C for 18 hr. The initial exploratory work was done with 0.4 in. diameter x 10 in. long columns in 50 ml burettes using 6-14 mesh adsorbents. In these experiments, autoradiographs showed that the PCl_3 was dispersed throughout the adsorbents, suggesting that channeling of the liquid was occurring in the columns resulting in some elution of PCl_3. To prevent channeling, finer adsorbents were required, and all subsequent experiments were done with 80-200 mesh adsorbents. For these experiments, columns, such as the one shown in Fig. 1, were used. With these columns, the $SiCl_4$ was allowed to drip through the adsorbent at a rate of about 1 cc/min until a liquid head formed in the top of the tube. The column then was allowed to equilibrate for several hours before sample collection was begun at a rate of 1 ml/min, controllable with the Teflon valve in the apparatus. Radioactivity measurements on samples of eluent taken during the purification, and autoradiographs of the columns were made at the end of each experiment. Table III gives a summary of the analytical data obtained with variations of the adsorption practice. It will be seen that using 60-200 mesh silica gel or activated alumina eliminated the channeling found with the 6-14 mesh adsorbents, and in consequence, better phosphorus removal was obtained. Autoradiographs of the columns containing the finer adsorbents showed that the phosphorus was banded for a distance extending 3 in. down from the top, no phosphorus being detected below this point.

In the course of this work, as shown in Table III, it was found that best results were obtained when the $SiCl_4$ contained free chlorine or a combination of chlorine and aluminum chloride prior to adsorption purification. In these cases, 10 ml of liquid chlorine per liter of $SiCl_4$ were added; where $AlCl_3$ was used, 30 g/l of granular anhydrous $AlCl_3$ were added. After standing overnight, the undissolved $AlCl_3$ was filtered off. The purpose of the chlorine addition was to convert PCl_3 to PCl_5. The use of $AlCl_3$ results in the formation of the coordination compound, $PCl_5 \cdot AlCl_3$ (2, 4). Using either of these pretreatments, with activated alumina as the adsorbent, no phosphorus was detected in the eluent after 3525 ml had passed through the columns. In both cases tight banding of the phosphorus was observed at the top of the columns. The width of this band increased with the quantity of $SiCl_4$ eluted and after 3525 ml had passed through extended down from the top of the column for a distance of about 1 in. For phosphorus removal, no advantage was found in adding $AlCl_3$ in conjunction with the chlorine. However, for reasons not completely understood, use of the combination of $AlCl_3$ and Cl_2 in the purification of $SiCl_4$ leads to silicon lower in boron. It has been observed that both PCl_3 and PCl_5 form coordination compounds with BCl_3. The complex $BCl_3 \cdot PCl_5$ has a solubility of about 0.033 mole % in $SiCl_4$ and sublimes below 100°C. It may be that the $AlCl_3$ breaks this complex by forming $AlCl_3 \cdot PCl_5$, thus freeing the BCl_3

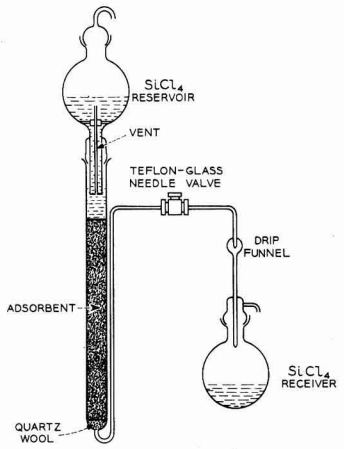

Fig. 1. Adsorption column for purification of $SiCl_4$

Table III. Purification of $SiCl_4$ containing 0.001% radioactive PCl_3 by adsorption on silica gel and activated alumina

Adsorbent	Additive	Quantity of $SiCl_4$ eluted, ml	Mole % P in eluent	Autoradiograph results
Silica gel 6-16 mesh	—	185	9.8×10^{-5}	Adsorption spotty throughout column channeling of $SiCl_4$
Activated alumina 6-14 mesh	—	185	—	As above
Silica gel 60-200 mesh	—	185	6.9×10^{-6}	Banding of PCl_3 top 3 in. of column
Activated alumina 80-200 mesh	—	185	Not detected $<7.7 \times 10^{-8}$	As above
		1500	4.2×10^{-6}	
Activated alumina 80-200 mesh	Cl_2*	3525	Not detected $<8.6 \times 10^{-7}$	Tight band extending 1 in. down column
Activated alumina 80-200	Cl_2, $AlCl_3$*	3525	Not detected $<8.4 \times 10^{-8}$	As above

* 10 ml of liquid chlorine per liter, and 30 g $AlCl_3$ per liter of $SiCl_4$ were used.

for more effective adsorption. These complexes of phosphorus and boron chlorides also may be the source of the difficulty normally encountered in distillation procedures for the removal of these impurities.

Removal of Heavy Metal Chlorides and Sulfur Compounds from $SiCl_4$

In operating adsorption columns, such as shown in Fig. 1, filled with either activated alumina or silica gel, it is observed that after several liters of $SiCl_4$ have been eluted, a brown band forms at the top of the column for a distance of about ½ in. This band gradually broadens with continued use. Spectrochemical analysis of the adsorbent in the banded region shows traces of B, Cu, Fe, Mn, and Mg. These impurities are not detected lower in the column and are not detectable in hydrolyzed samples of the initial $SiCl_4$. These results clearly indicate that the adsorption technique is quite effective in removing heavy metal chlorides from $SiCl_4$.

Commercially available $SiCl_4$ may contain sulfur compounds at mole ratios as high as 1.1×10^{-4}. These compounds, probably $SiCl_3HS$ and $SiCl_2S$, liberate H_2S on hydrolysis of the $SiCl_4$, and this may be used as a basis of detection. While adsorption methods remove these compounds, it is expedient to reflux the $SiCl_4$ with copper turnings for 16 hr prior to column purification, which effectively removes the sulfur. Sulfur compounds in $SiCl_4$ react with copper to form black CuS. In the absence of sulfur, the copper turnings remain bright.

Summary

It has been shown that adsorption columns filled with hydrous oxides or silicates offer an attractive method of purifying $SiCl_4$ for use in the preparation of very high-purity silicon. In using the method, the $SiCl_4$ is first refluxed with copper turnings to remove sulfur compounds. It is then preferably treated with $AlCl_3$ and Cl_2 and passed through an adsorption column containing either activated alumina or silica gel. The purified $SiCl_4$ contains Cl_2 which, if objectionable, may be removed by refluxing in a stream of dry nitrogen or hydrogen. On reduction of the purified $SiCl_4$ in hydrogen on tantalum tubes, polycrystalline rods suitable for floating-zone refining are obtained. After removal of the tantalum, such rods, if given several zone passes in dry hydrogen, are n-type with a resistivity of 50-100 ohm-cm in the region of the crystal where refining does not occur. Subsequent zone refining to eliminate the donors, principally phosphorus, results in p-type silicon with resistivities above 8000 ohm-cm. After two zone passes, the lifetimes of the crystals are of the order of 1 msec and no evidence of trapping centers is found. Subsequent refining does not further improve the lifetime.

The source of the phosphorus in this silicon is not known. It is unlikely that the phosphorus originates from the purified $SiCl_4$ in view of the radioactivity results, which show tight banding of phosphorus at the top of the column and no detectable phosphorus in the eluent. It seems probable that the donors are introduced during the reduction process either from the reactants or the apparatus itself.

Although a detailed study has not been made, exploratory experiments indicate that column methods using hydrous oxides as adsorbents can purify other halides such as $SiHCl_3$ and $GeCl_4$ effectively. Attempts to purify SiI_4 by passing through a heated column, or by dissolving the iodide in n-heptane or toluene prior to column elution, have not been promising. SiI_4 reacts with the adsorbents tried (activated alumina and silica gel) with the liberation of iodine.

Acknowledgments

The author is greatly indebted to a number of his colleagues at Bell Telephone Laboratories for much of the work in this investigation. D. L. Wood and J. P. Luongo were responsible for the infrared spectroscopy; J. D. Struthers was responsible for the radioactive tracer analyses; J. E. Jamieson purified the silicon tetrachloride and made the hydrogen reduced silicon; and D. D. Bacon did the zone refining work.

Manuscript received July 10, 1959. This paper was prepared for delivery before the Philadelphia Meeting, May 3-7, 1959.

Any discussion of this paper will appear in a Discussion Section to be published in the December 1960 JOURNAL.

REFERENCES

1. I. J. Krchma, U.S. Pat. 2,820,698.
2. J. M. Whelan, U.S. Pat. 2,821,460.
3. F. H. Winslow, U.S. Pat. 2,812,235.
4. W. Fischer and O. Juberman, *Z. anorg. u. allgem. Chem.*, **235**, 337 (1938).

APPENDIX I

Method of Preparing Various Adsorbents

Silica gel from hydrolyzed $SiCl_4$.—Fifty milliliters of $SiCl_4$ were hydrolyzed in 500 ml of deionized water at 0°C. An opalescent liquid was obtained which set to a gel in about 2 hr. After aging overnight, the gel was broken up and washed copiously to remove the HCl formed during hydrolysis. The gel was dried for 2 days in a vacuum desiccator followed by air drying at 100°C for 24 hr and activation at 270°C for 18 hr.

Silica gel anhydrous.—Commercial silica gel, 6-14 mesh, was deactivated at 1000°C for 18 hr in air with a weight loss of 5.2%.

MgO *and* $Mg(OH)_2$.—Anhydrous MgO powder was heated for 18 hr at 120°C prior to use as an adsorbent. To hydrate this oxide, a batch of the above MgO was dissolved in 6*N* HCl and filtered. The clear solution was made alkaline with ammonium hydroxide to precipitate $Mg(OH)_2$. This was filtered, washed, and dried at 120°C. The resulting hard cake of $Mg(OH)_2$ was crushed in an agate mortar and dried for 4 hr at 120°C before use.

Titania gel.—Twenty-five milliliters of tetraisopropyl titanate were stabilized against rapid hydrolysis with 5 ml of 12*N* HCl. To the above solution, 75 ml of H_2O were added and the mixture heated to 80°C. Ammonium hydroxide then was added until a curdy gelatinous precipitate formed. After standing for several hours, the gelatinous mass was made strongly alkaline with ammonium hydroxide. The curd then was aged overnight, washed free of ammonia, and dried for 24 hr in a vacuum desiccator. This was followed by air drying at 120°C and activation for 18 hr at 270°C.

$Fe(OH)_3$ *gel.*—$Fe(OH)_3$ was dissolved in a small excess of 6*N* HCl and the solution filtered. This was made strongly alkaline with NH_4OH precipitating gelatinous $Fe(OH)_3$. After aging overnight, the precipitate was filtered, washed free of NH_4OH and NH_4Cl, and dried overnight. It then was dried for 24 hr at 120°C and activated at 270°C for 4 hr

Purification of Tantalum Obtained by Vacuum Arc Melting

M. L. Torti

National Research Corporation, Cambridge, Massachusetts

ABSTRACT

The purest commercially available tantalum powder was consolidated by a single, vacuum, consumable-arc melting operation yielding ingots of considerably higher purity than the original powder. Interstitial and metallic impurity analyses are presented for a large number of heats made under consistent conditions of ingot and electrode size, arc current, and furnace pressure. The effect of carbon addition to an oxygen-rich starting material was investigated, and the optimum carbon-oxygen ratio for maximum refinement has been located approximately. Under favorable conditions, the oxygen content is reduced by approximately one order of magnitude.

Tantalum metal has traditionally been produced by the powder metallurgy route in which a lengthy high-temperature vacuum sintering treatment is utilized for refining to the purity necessary for fabrication.

The general extension of vacuum arc melting as a method for consolidating the refractory metals has prompted a wide interest in the arc melting of tantalum. Although fabricable ingots have been produced from tantalum powder of conventional purity, the purity and ductility of these ingots has not matched good sintered bar material. Indeed, doubt is commonly expressed as to whether any refinement at all occurs during arc melting.

When a relatively pure tantalum powder became commercially available the arc melting procedure gained new promise. Ingots are now being produced by a single melt which can be fabricated cold from ingot to 0.0005 in. thick strip without intermediate anneals. The excellent ductility and superior purities are due in a large degree to the initial purity of the tantalum powder. However, substantial purification does occur during arc melting with respect to both interstitial and metallic impurities.

Description of Equipment and Procedure

All melting was done in a conventional cold-mold arc furnace. Power was supplied by a bank of welding generators capable of supplying 5600 amp. A 1000 CFM mechanical-booster high-vacuum pump, backed by a 100 CFM mechanical pump, comprised the pumping system. This system blanks off below 1 μ and has a pumping speed of over 1000 CFM between 10 and 1000 μ. A nominal 4 in. diameter cold mold was used. Since double extra heavy copper pipe was installed as the mold liner, the actual inner mold diameter was 3.5 in. Melt stock was National Research Corporation melting grade tantalum powder −12 +325 mesh. Bars 1¾ to 2 in. in diameter were hydrostatically pressed from this powder. These bars were given a quick premelting treatment in which direct resistance heating was used to heat the bars to 1500°C for approximately 1 min in vacuum. This operation dimensionally stabilizes the bars and improves the already excellent green strength. No significant purification is obtained for such a short heating period. The bars are then welded into the electrode using a tungsten permanent electrode in an argon atmosphere. Strong, ductile welds are obtained on high-purity powder. Brittle welds may occur if powder containing over 1000 ppm total interstitial impurities is used.

Melts were run at 30 v, 4500-5000 amp under 2-5 μ pressure measured in the furnace body. A melting rate of 0.5 lb/min resulted. This corresponds to a power input of approximately 4.5 kwh/lb. The molten pool was stirred by a 500 turn d-c adjustable-amperage stirring coil. Normally 3 amp was sufficient to stabilize the arc and gently stir the pool without undue agitation. At that amperage the measured magnetic field in the center of the empty mold is 40 gauss.

During melting the arc is observed visually. A thin film of deposited vapor is seen above the melt. This layer is partially driven ahead of the melt level and partially redissolved in the melt, resulting in the higher impurity levels reported for the ingot tops.

The 70-90 lb ingots are lathe conditioned, then slices are cut from the top and bottom for analytical samples. Chunks from the interior of the samples are used for the oxygen and nitrogen samples. Dry drillings are used for the other samples. For some elements both spectrographic and wet analyses are reported, and two spectrographic procedures were employed.

Experimental Results

Table I reports carbon and oxygen analysis for 2-in. diameter pressed-bar electrodes and the resulting 3½ in. diameter ingot. In this series no carbon was added to the melt stock. Note that signifi-

cant amounts of oxygen are removed, particularly at the ingot bottom. The oxygen is probably removed as tantalum oxides which deposit on the mold wall above the melt. Since this oxide film must be either driven up or redissolved in the melt it is not surprising that the oxygen level at the ingot top, although slightly lower than the melt stock, is double the oxygen content at the ingot bottom. The carbon present in the melt stock is decreased to or below the analytical limits indicating that some carbon removal, probably as carbon monoxide, is occurring. Occasional analyses report higher oxygen content for the ingot than for the melt stock. This is attributed to individual sampling and analytical determination errors, and indicates the necessity for averaging the results from a large number of heats.

Table I also reports analytical data for 1¾-in. diameter electrodes to which fine graphite powder was added. Since the melt rate, pressure, ingot condition, and metallic refinement were the same as for the 2-in. diameter electrodes, it is assumed that except for the carbon addition, melting conditions for this series are identical to those for the 2-in. electrodes. The initial carbon content of the tantalum was 10-20 ppm. Additional carbon in the form of fine graphite powder was thoroughly mixed with the tantalum powder. Sufficient carbon was added to raise the carbon-oxygen ratio to 50% of the stoichiometric ratio for carbon monoxide.

The average oxygen content in the electrode was 239 ppm, the average oxygen content in the ingots was 65 ppm top and 34 ppm bottom. The total carbon in the electrode was 111 ppm which was reduced to 23 ppm top and 30 ppm bottom for the ingots. Thus an average of 73% of the oxygen content of the electrode was removed at the top of the ingots and 85% at the ingot bottom. This compares to a 25% oxygen reduction at the ingot top and 67% at the ingot bottom for the melts (Table I) to which no carbon was added. Furthermore, carbon additions appear to cut down the fluctuations in oxygen content from ingot to ingot.

Table I. Tantalum vacuum arc melting

I. Oxygen and carbon refinement for no carbon addition, average of 14 melts

	O (ppm)		C (ppm)	
	Top	Bottom	Top	Bottom
Electrode	140		10-20	
Ingot	106	46	<10	13

II. Oxygen and carbon refinement with 50% stoichiometric carbon addition, average of 11 melts

	O (ppm)		C (ppm)	
	Top	Bottom	Top	Bottom
Electrode	239		111	
Ingot	65	34	23	30

III. Oxygen and carbon refinement with 100% stoichiometric carbon addition, average of 2 melts, high oxygen powder used

	O (ppm)		C (ppm)	
	Top	Bottom	Top	Bottom
Electrode	950		800	
Ingot	120	—	360	—

IV. Other impurity refinement (ppm), average of 25 melts

	N	Fe	Cr	Ni	Nb	Si
Electrode	28	95	86	111	112	<250
Ingot	27	30	14	28	40	30

The final carbon-oxygen ratio appears quite good, particularly at the ingot bottom. Earlier in the program tantalum powder of 1000 ppm oxygen content was mixed with sufficient carbon to bring the carbon-oxygen ratio to 100% of the stoichiometric ratio for carbon monoxide removal. Table I shows the results of two melts. Considerable oxygen was removed, but the final carbon content was 2-3 times that of the oxygen. When one of these ingots was remelted, the decrease in oxygen was less than expected.

Table I reports analytical data for several other elements. The ingot analyses were taken at the ingot top. Three analytical procedures are used; wet chemical, pellet spectrographic, and carrier spectrographic.

Very little difference is noted between the nitrogen analysis for the ingots and electrodes so that it appears that little, if any, nitrogen removal occurs during melting at the low nitrogen levels encountered in this program.

Iron is definitely removed on melting, being reduced by a factor of two or three. The amount of refinement is somewhat vague for several melts due to the starting concentration being below the level of detection for the method used.

Nickel is present in the same amounts as iron and is removed to the same degree.

Chromium is quite volatile and considerable refinement occurs, generally resulting in an ingot content below the level of detection.

The data indicate a removal of niobium on the same level as iron and nickel. This is somewhat surprising since the vapor pressure of niobium is considerably lower than that of iron at the tantalum melting point. Two possible mechanisms may be postulated. The vapor pressure of the niobium suboxides may be higher than that tantalum suboxide vapor pressure resulting in the preferential removal of niobium oxides. Unfortunately, values of the vapor pressures have not been reported in the published literature. Iron and nickel form intermetallic compounds with tantalum while niobium does not. Thus the activity coefficient of niobium in tantalum may be higher than that for iron or nickel in tantalum. The resulting impurity partial pressures may then be more nearly equal.

The data for silicon unfortunately do not locate the silicon level in the electrode until the last few runs. However, these rather sparse data do indicate significant removal during melting.

Hydrogen analyses were not always run, but the electrode hydrogen content varies between 25 and 50 ppm, while the ingot hydrogen varies between 1 and 5 ppm.

Conclusions

Consumable arc melting of tantalum can, under favorable conditions, result in considerable refine-

ment of the metal. Oxygen can be removed both as tantalum oxides and as carbon monoxide. Of the combinations studied, the lowest, most uniform oxygen analyses in the ingot result when the carbon in the electrode is 50% of the stoichiometric carbon-oxygen ratio for carbon monoxide removal.

Nitrogen is not significantly reduced at the low nitrogen levels encountered. Metallic impurities with vapor pressures equal to or greater than nickel are significantly reduced. Niobium appears to be partially removed although the mechanism is not completely clear.

Acknowledgment

Grateful acknowledgment is given for the analytical services of Messrs. F. Pink, L. McGowan, and J. Martin, the analytical supervision of Dr. F. Benner, the melting operations of Mr. R. Malatesta, and the invaluable consultations of Mr. John Ham.

Mansucript received June 29, 1959. This paper was prepared for delivery before the Philadelphia Meeting, May 3-7, 1959.

Any discussion of this paper will appear in a Discussion Section to be published in the December 1960 JOURNAL.

Heat Transfer Rates of an Argon Plasma Jet

C. S. Stokes, W. W. Knipe,[1] and L. A. Streng

The Research Institute of Temple University, Philadelphia, Pennsylvania

ABSTRACT

Heat flux measurements were made on a small argon plasma jet. Experimental values as high as 4.5 kcal/cm² sec were obtained for the transient-heating rate of a small copper slug. The heat-flux variation with energy supplied and the energy distribution to cathode, anode, and plasma are presented.

Arcs have been of interest as high-temperature sources for a number of years. The development of the plasma jet has provided a convenient tool for studying gases at these temperatures, without electrode interference. A number of investigators (1-3) have devised plasma-jet apparatus of various kinds. This paper presents the measurements of the heat transfer rates of an argon plasma jet.

Apparatus and Procedure

A drawing of the plasma generator is shown in Fig. 1. The generator consists of a water-cooled ⅛ in.-2% thoriated tungsten cathode with an annulus for feeding the argon gas. The copper anode, which has a 0.157 in.-hole for the plasma jet, is water cooled. A ¼ in.-Teflon gasket insulates the anode from the cathode.

A 600-amp d-c welder was used as the power source. Appropriate electrical meters guided the operation. Argon[2] was metered through a Fisher and Porter flowmeter. The plasma jet was approximately 1 in. long and expanded to a diameter of about ¼ in.

The heat transfer measurements were made with a transient probe consisting of a piece of copper ⅛ in. in diameter and ¼ in. long, embedded in a ⅝ in.-diameter piece of "Transite" ½ in. long. This assembly was placed in a 1½ in.-diameter by 1 in.-long piece of laminated fiberglass (see Fig. 2). The probe was mounted on a high-speed air-piston cylinder which thrust the probe into the jet approximately 1 mm below the anode. A 30-gauge iron-constantan thermocouple was inserted into the copper slug 0.050 in. from the back surface.

Two separate high-speed measuring apparatus were used to obtain the time-temperature curves for the copper slugs. One consisted of a d-c-modulated high response time potentiometer. The low voltage from the thermocouple modulated a 160-kc carrier wave which was shown on an oscilloscope with a triggered-sweep duration of 2 sec. The other system used was a Tektronix type-533 oscilloscope with a type-53/54D calibrated high-gain d-c preamplifier.

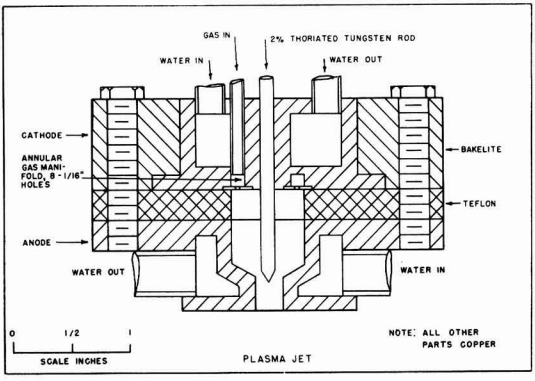

Fig. 1. Schematic of plasma jet apparatus

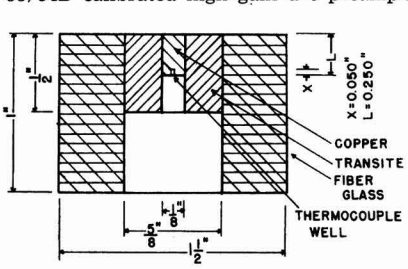

Fig. 2. Transient heat probe

[1] Present address: Pennsalt Chemicals Corp., Philadelphia, Pa.
[2] Obtained from Air Reduction Co.

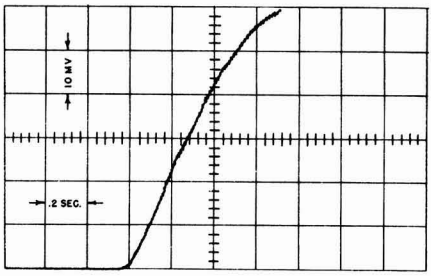

Fig. 3. Trace of the tektronix system. Ordinate, 10 mv per large division; abscissa, 0.2 sec per large division.

Both systems produced similar results. The modulation system cut out most of the "noise" produced by the arc but was more difficult to calibrate than the other. A typical trace of the Tektronix system is given in Fig. 3.

Calculation of Heat Transfer Rates

The general method of data reduction used is described by Sutton (4).

The equations for a transient one-dimensional system are:

$$\frac{T - T_o}{Q} = \frac{L}{K} Z \qquad [1]$$

$$Z = 2\sqrt{X} \sum_{0}^{\infty} (\text{ierfc } z + \text{ierfc } z') \qquad [2]$$

$$X = \frac{Kt}{dL^2 C_p} \qquad [3]$$

$$N = x/L \qquad [4]$$

$$z = (2r + 1 - N)/2\sqrt{X} \qquad r = 0, 1, 2, \ldots$$

$$z' = (2r + 1 + N)/2\sqrt{X}$$

Where: Q is heat transfer rate; T_o, initial temperature; T, temperature after time t; L, length of slug; K, thermal conductivity; N, position ratio; d, density of slug; C_p, heat capacity of slug at constant pressure; and x, distance of thermocouple from back of slug. Tables of Z have been tabulated by Kaye and Yeh (5) as a function of X and N.

The change in temperature was read from the photographs for the time increment 0.1 to 0.2 sec, making t equal to 0.1 sec. Values of X and N then were calculated and Z was read from the tables. From this value Q was computed. An example follows for the copper slug described previously: For copper: K, is 0.842 cal/cm sec °C; d, 8.94 g/cm³; C_p, 0.1057 cal/g °C; L, 0.635 cm; x, 0.127 cm; t, 0.1 sec;

X is $\dfrac{(0.842)(0.1)}{(8.94)(0.1057)(0.635)^2} = 0.222$; and N, $\dfrac{0.127}{0.635} = 0.20$.

For the above values of X and N, $Z = 0.095$. Therefore,

$$\frac{T - T_o}{Q} = \frac{L}{K}(0.095) = \frac{(0.635)(0.095)}{0.842} = 0.0715$$

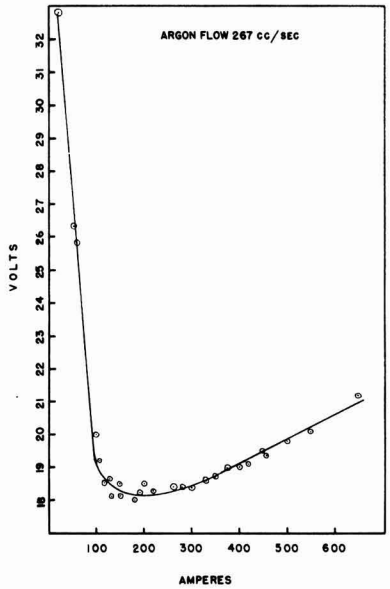

Fig. 4. Electrical characteristics of the argon plasma jet

letting $\Delta T = T - T_o$

$$Q = 1.4 \times 10^{-2} \Delta T \text{ in kcal/cm}^2 \text{ sec}$$

where ΔT is in °C.

Figure 4 shows the electrical characteristics of the arc jet. It will be noted that the high-intensity region starts at approximately 200 amp. Measurements of heat flux were made only in the high-intensity region because the jet becomes unsteady on the low-intensity side.

Results

The results of the heat transfer measurements are given in Fig. 5 and Table I. As can be seen, for the range of power used and for an argon flow of 16 liters/min, the heat flux falls between 0.5 and 4.5 kcal/cm² sec. These values are about 4 or 5 times those obtained from rocket motors and make possible tests on the stability of materials at extremely high temperatures and high heat fluxes. The values obtained are compared with the theoretical heat balance of the arc as shown in Fig. 6. The theoretical

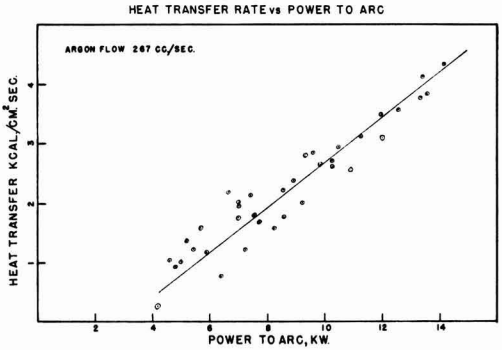

Fig. 5. Heat transfer rates vs. power to arc

Table I. Heat transfer rates of the argon plasma jet at a constant argon flow of 16 liters/min

Power to Arc, kw	Heat transfer rates, kcal/cm² sec
4.13	0.28
4.60	1.03
4.80	0.94
5.00	1.00
5.15	1.38
5.41	1.22
5.66	1.60
5.90	1.18
6.40	0.75
6.65	2.19
6.95	1.79
7.01	1.96
7.05	2.04
7.24	1.22
7.41	2.14
7.56	1.78
7.69	1.71
8.25	1.58
8.60	2.24
8.62	1.76
8.94	2.38
9.25	2.02
9.40	2.80
9.61	2.90
9.90	2.64
10.20	2.65
10.30	2.71
10.49	2.94
11.06	2.50
11.30	3.19
12.00	3.50
12.25	2.85
12.60	3.59
13.40	3.79
13.45	4.16
13.60	3.84
14.20	4.35

curve was calculated by dividing the power to the plasma in kcal/sec by the average cross-sectional area of the plasma jet in cm². Experimental values fall below the theoretical as would be expected, since some of the energy is dissipated by radiation and other processes. The energy in the plasma was arrived at by evaluating the losses to the water-cooling system. It was found that approximately 56% of the total energy to the arc goes into the plasma jet, 5% to cathode heating and the remainder to heating the anode. Figure 7 shows the experimental points.

By using the Saha ionization equation (6), average plasma temperatures were calculated. These

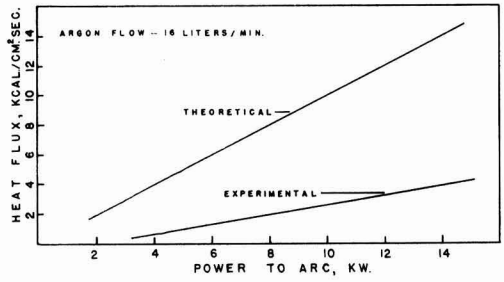

Fig. 6. Heat flux, theoretical maximum vs. experimental

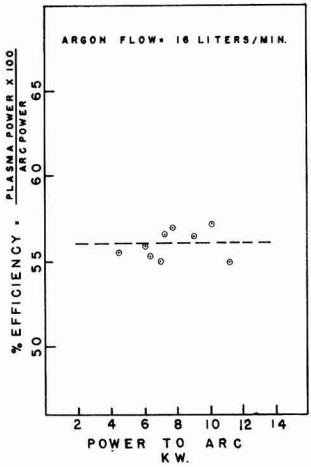

Fig. 7. Efficiency of arc

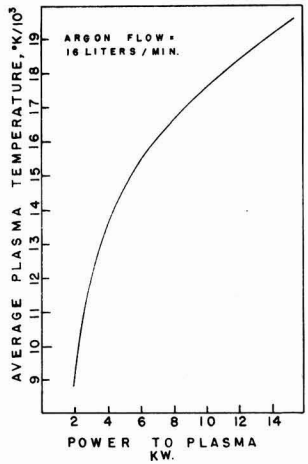

Fig. 8. Calculated temperature of the arc

temperatures are based on the total argon flow and the amount of energy actually in the plasma (56%). Figure 8 shows the results of these calculations. The temperatures range from 9000°K at 2 kw to 19000°K at 14 kw. There is some doubt whether these temperatures are actually the true ones, because a "frozen" composition of the jet is required by the Saha equation.

Acknowledgment

The authors wish to thank Dr. A. V. Grosse and Mr. W. L. Doyle for their helpful suggestions.

The research was supported by the U. S. Army through the U. S. Army Ballistic Missile Agency under Contract No. DA-36-034-ORD-2328.

Manuscript received May 4, 1959. This paper was prepared for delivery before the Ottawa Meeting, Sept. 28-Oct. 2, 1958.

Any discussion of this paper will appear in a Discussion Section to be published in the December 1960 JOURNAL.

REFERENCES

1. "The Symposium on Arcs in Inert Atmospheres and Vacuum," W. E. Kuhn, Editor, John Wiley & Sons, Inc., New York, (1956).
2. "High Intensity Arc Symposium," S. D. Mark, Jr., Editor, The Carborundum Co., Niagara Falls, N. Y. (1958).
3. "Conference on Extremely High Temperatures," Fisher and Mansur, Editors, John Wiley & Sons Inc., New York (1958).
4. G. W. Sutton, Real Gas Technical Memorandum No. 10, General Electric Company, MOSD, Philadelphia, Pa., May 23, 1956.
5. J. Kaye and V.C.M. Yeh, *J. Aeronaut. Sci.*, **22**, 755 (1955).
6. Saha, *Phil. Mag.*, **1**, 1025 (1920).

The Preparation of a New Crystalline Modification of Boron, and Notes on the Synthesis of Boron Triiodide

L. V. McCarty[1] and D. R. Carpenter

Research Laboratory, General Electric Company, Schenectady, New York

ABSTRACT

Boron triiodide has been made in yields as high as 70% from boron and iodine at 900°C. An equilibrium apparently limits the yield to 49% at 1050°C. An approximate free energy equation, $\Delta F°_T = -43{,}000 + 31\ T$ cal/mole of BI_3, has been derived for the reaction $B_{(c)} + 3/2\ I_{2(g)} \leftrightarrows BI_{3(g)}$. Molybdenum metal may catalyze the reaction.

A new and denser form of crystalline boron has been deposited on tantalum in the temperature range 800°-1000°C from boron triiodide. Small portions of the deposit occur as red crystals with a density of 2.459_5 at 22.6°. The main impurity is 0.04% iodine. The red boron is composed of units of nearly regular icosahedra in a slightly deformed cubic close packing.

The preparation and properties of pure boron prior to 1942 have been reviewed by Laubengayer, Newkirk, and Brandauer (1). A short time later Laubengayer, Hurd, Newkirk, and Hoard (2) published their preparation of pure boron by the hydrogen reduction of purified boron tribromide. This technique probably makes the purest boron that has been described to date.

At least three other methods have been described since. These include sodium reduction of boron trichloride or boron trifluoride (3, 4), the electrolytic reduction of fused salt baths of fluoborates and alkali borates (5), and the hydrogen reduction of boron trichloride on hot carbon (6, 7) or titanium (7) rods. The first two of these three and the deposition on titanium lead to contamination of the boron with other metals which can be leached from the samples at least in part. Boron prepared on carbon rods may have as much as 5% carbon contamination, which is difficult to remove.

One of the chief advantages of the hydrogen reduction of boron tribromide is that it can be accomplished at temperatures as low as 600°C, and contamination by alloying with the filament substrate is not as serious a problem. Thermodynamic estimates indicate that boron triiodide would not be reduced as readily, but it would be expected to decompose directly to iodine and boron below 1000°C.

A possible advantage might be realized in the purification of boron triiodide (bp 209.5°C) by distillation. Aside from tetraiodoethylene (bp 187°C) iodine is the next lower boiling material (bp 184.35°C). The possible presence of tetraiodoethylene cannot be dismissed lightly because of the importance of carbon as an impurity, but its formation seems unlikely in our method of preparing boron triiodide. Phosphorus triiodide (bp approx. 220°C) is the nearest higher boiling iodide. Its removal may be difficult because there is only a 10° or 11° difference in the boiling points. During the decomposition of boron triiodide, phosphorus might react to form boron phosphide which would not volatilize as readily as elemental phosphorus. The next higher boiling compound anticipated is silicon tetraiodide (bp 301.5°C) which should not be difficult to remove.

Since phosphorus will not affect the electrical properties as much as silicon or carbon, its presence in our product is perhaps not as serious as the latter two. Efforts to make very pure boron from fractionally distilled boron triiodide resulted in a new crystalline modification some of which occurred as small, transparent red crystals.

Preparation and Purification of Boron Triiodide

Boron triiodide was made from the elements according to the method described by Moissan (8). U.S. Borax crystalline grade boron was placed in vertical reactors, and reagent grade iodine was vaporized slowly by boiling into a stream of about 50 cc/min of argon.

Boron triiodide vapor attacks quartz and alumina reactors at the optimum temperature of preparation. This problem was solved only partially by lining

[1] Present address: Lamp Development Department, General Electric Company, Nela Park, Cleveland, Ohio.

Table I. Iodination of U. S. Borax crystalline boron

Reaction temp, °C	Reaction time, hr	Wt of boron in bed, g	Wt of I_2 vaporized, g	I_2 converted to crude BI_3, %
Batch No. 1 (−4 to +100 mesh)				
800*	25	173	2869	22
900‡	31.3	151	2060	62
900*	18.3	165	2639	70
1050*	14	177	1416	49
Batch No. 3 (−20 to +100 mesh)				
900*	14	187	2032	57
900**	34	812	10,550	17
900†	9	124	3473	9

* Boron contained in vertical quartz reactor 1⅛ in. OD by 12 in. lined with molybdenum sheet.
‡ Boron contained in vertical quartz reactor 1 in. OD by 12 in.
** Boron contained in vertical quartz reactor 2 in. OD by 12 in. lined with molybdenum sheet.
† Boron contained in vertical quartz reactor 1⅛ in. OD by 12 in. with graphite liner ¾ in. ID.

quartz reactors with molybdenum sheet, because a brittle molybdenum boride was formed which crumbled eventually in use. Graphite was also used, but it is so porous that it did not protect the quartz. Thermodynamic estimates indicate that beryllia reactors might be stable to boron triiodide, but these were not tried.

The product contained considerable quantities of unreacted iodine which was stripped off in preliminary distillations in a 30-plate Pyrex distillation column. Material remaining in the still pot was weighed as crude boron triiodide.

Table I presents data from several runs. In the series with boron batch No. 1 the yield of crude boron triiodide goes through a maximum at 900°C. We interpret the decrease in yield at 1050° to be the result of having achieved equilibrium conditions for an exothermic reaction. An identical yield was observed with another grade of boron powder at 1050°C. As the temperature increases for an exothermic reaction the equilibrium constant normally decreases. By combining these data with Brewer's (9) estimate of the free energy of formation of crystalline boron triiodide, an approximate free energy equation

$$\Delta F^\circ_T = -43{,}000 + 31\,T \text{ cal/mole of } BI_3$$

$$(T = {}^\circ\text{K};\ \text{range } 298^\circ\text{-}1323^\circ)$$

can be derived based on the reaction $B_{(c)} + 3/2\ I_{2(g)} \leftrightarrows BI_{3(g)}$, after allowing for the decrease in molecular iodine concentration due to dissociation.[2] Equilibrium constants calculated from this free energy equation indicate that our yields at 900°C could be improved upon.

Boron batch No. 3 was somewhat less reactive than batch No. 1 in the usual reactors, but astonishingly less reactive in larger reactors and graphite lined reactors. Molybdenum is quite likely acting as a catalyst even though it is one of the most inert materials toward iodine attack.

Several lots of crude boron triiodide were combined in a 2-liter Pyrex distillation flask which could be attached to a 1-in. OD Pyrex distillation column by means of a Teflon gasketed standard taper joint. The remaining parts of the column were sealed together in such a way that liquid boron triiodide was delivered through a heated tube to a receiving flask with a nitrogen blanket maintained around the connection. The column was packed with helices and had an estimated efficiency equivalent to about 30 theoretical plates. The reflux ratio was never less than 30/1. About 10-15% was taken off in the first cut which was rejected and 60-70% in the heart cut for decomposition to boron.

Purified boron triiodide was discolored by the presence of iodine which seemed to form in small amounts throughout the distillation. The still pot became very dark colored and essentially opaque during distillation. Undoubtedly it contained the B_xI_y, where $x > y$, that Schumb, Gamble, and Banus (10) described. Little, if any, of this latter compound appeared in the distillate which sublimed cleanly and completely in the experiments described below.

Decomposition of Boron Triiodide

The decomposition reaction occurs on an electrically heated wire or rod in an evacuated apparatus similar to that used for the decomposition of silicon tetraiodide (11, 12). Temperatures were read with an optical pyrometer and have not been corrected for transmission of quartz or emissivity of the boron. The temperature of the boron triiodide was adjusted to maintain estimated vapor pressures in the range 0.1-1.0 mm.

Tantalum, molybdenum, and tungsten as deposition substrates.—Previous work (2, 7) is in conflict with respect to tantalum as a satisfactorily nonreactive surface for the preparation of very pure boron. Conditions in this work differ from the work with boron tribromide or trichloride in that hydrogen was not used in the reduction. Hydrogen might influence the formation of tantalum boride indirectly, so three kinds of wires were coated with boron in order to determine their suitability for iodide boron deposition. Hairpins formed from 20 in. of 10-mil diameter wires were heated to 1000° for 1 hr in boron triiodide vapor coming from a reservoir at 0°C (vapor pressure of the order of 0.1 mm). About 17-18 mg of boron was deposited on each wire. They were sectioned, polished, and a photomicrograph of each was prepared.

In Fig. 1 two distinct layers have formed on the tantalum. The inner zone is quite well defined and is very probably a tantalum-boron alloy, but no work was done to try to identify it. Other evidence obtained later indicates that the outer, rather irregular zone is pure boron. It is so brittle that it has fractured rather badly during the sectioning. A close examination indicates the boron has a crystalline appearance.

Figure 2 is a similar photomicrograph for boron on molybdenum filaments. The alloy zone is much broader, and relatively little free boron is evident. Figure 3 shows the results obtained with tungsten. No adherent alloy zone is evident, and the nature of the material that has separated from the tungsten sur-

[2] The authors are indebted to Mr. A. C. Loonam for suggesting the correct method of calculating the free energy from the equilibrium constant at 1050°C.

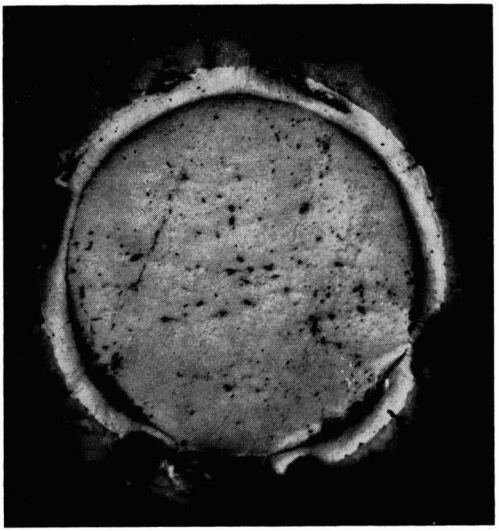

Fig. 1. Section of iodide boron deposit on 10-mil tantalum wire.

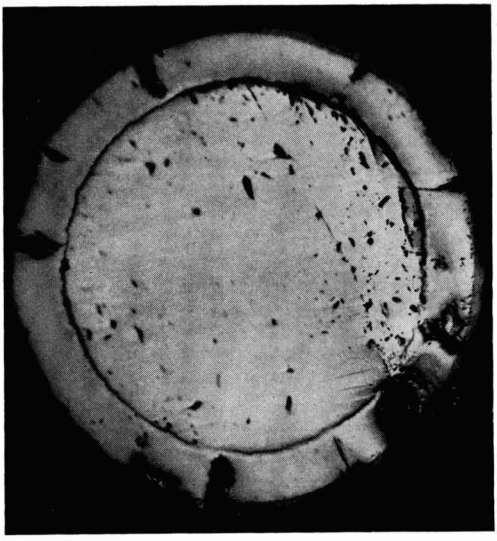

Fig. 2. Section of iodide boron deposit on 10-mil molybdenum wire.

face is unknown. Later work with tantalum at a lower temperature produced a similar flaky deposit that contained substantial amounts of tantalum. Since a densely adherent deposit was desired, the flaky type of product was unattractive.

Tantalum metal is not an ideal deposition substrate for this work, but it seems to be the best of the three refractory metals investigated. Tungsten might make a satisfactory surface at higher temperatures, but it would require further investigation.

Deposition of iodide boron on tantalum wire.— Two 4½ in. pieces of 3-mil tantalum wire were heated at 1000°C for 4½ hr in the vapor from boron triiodide kept at room temperature. The wire grew

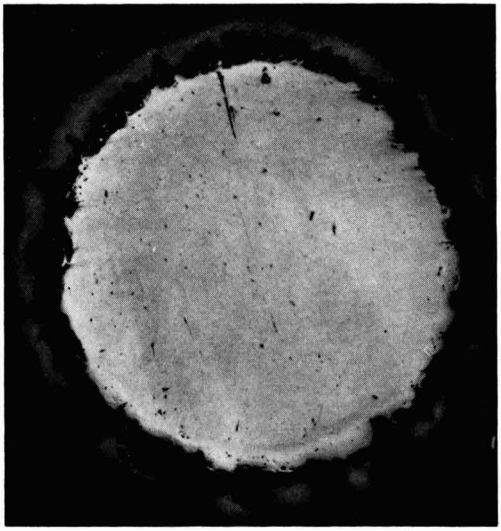

Fig. 3. Section of iodide boron deposit on 10-mil tungsten wire.

to approximately 70 mils in diameter when it broke revealing a cluster of red crystals surrounding the tantalum wire which were clearly visible to the unaided eye. In this same sample Horn (19) found a wedge-shaped band of orange-colored boron in a fractured portion of the rod which started as a narrow band at the tantalum core and expanded as it grew out to the surface. Neither the orange-colored band nor the red crystals were evident from the external appearance.

Deposition of iodide boron on tantalum rods.— Boron was deposited from boron triiodide on ⅛-in. x 36-in. tantalum rods in the form of a hairpin at the three temperatures shown in Table II. The deposit at 800°C was black, or nearly so, and very flaky. It peeled off the rod throughout the run and fell into the boron triiodide reservoir. X-ray powder photographs disclosed the presence of two components in this material: a low temperature crystal form of boron (13, 14), and considerable amounts of a tantalum boride. X-ray emission analysis of this sample confirmed the presence of approximately 78% tantalum, which was unexpected. The original purpose in preparing this sample was to compare its x-ray powder pattern with the 900°C sample which

Table II. Thermal decomposition of boron triiodide (tantalum rods)

Temp,* °C	BI_3 temp, °C	Time, hr	Wt of deposit, g	Yield, %
800	0-~25	73½	10.3	Not determined**
900	20	23	11	43
1000	~25	16	56.6†	78
1000	~25	48.3		

* Uncorrected temperature read with an optical pyrometer.
** Boron did not adhere well to the tantalum in this run and kept peeling and falling off.
† Combined weight of deposit.

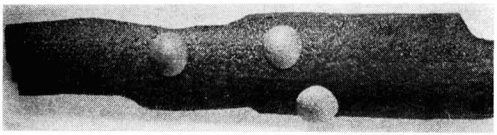

Fig. 4. Fragment of iodide boron made at 900°C

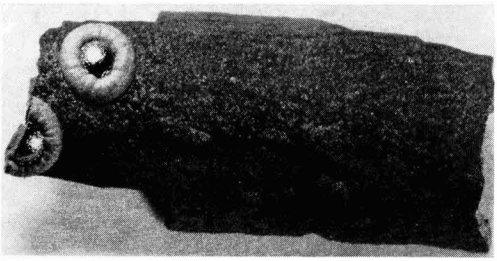

Fig. 5. Fragment of iodide boron made at 900°C

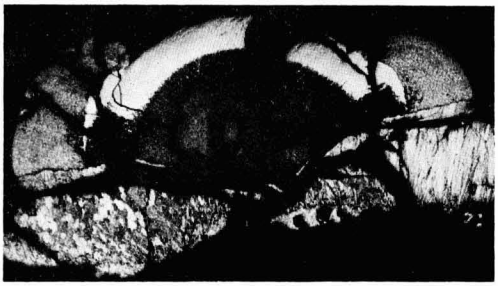

Fig. 6. Section across left end of boron fragment from Fig. 5.

was actually prepared first. There was no difference in the powder pattern from the boron, but the 900°C sample had only a very small amount of tantalum boride in it.

The boron sample prepared at 900°C adhered to the rod well during deposition and exhibited several features not seen at higher or lower temperatures. Two kinds of very regular growths about 0.060 in. in diameter developed on the surface of the boron during the run which are shown in Fig. 4 and 5. The two kinds of growth are probably related, but those shown in Fig. 4 have not been investigated for their structure. The central portion of the kind shown in Fig. 5 appeared to be a dark-colored glassy phase when viewed from above. A fracture in the boron deposit across one of the spots permitted examination of a cross section of the growth. The most dramatic feature revealed was that the glassy layer was clear red by transmitted light.

This particular sample was mounted by the Metallography Section of the G.E. Research Laboratory, polished, and photographed as shown in Fig. 6. The boron is so brittle that it has fractured during the polishing operation, but enough of the structure remains so that the chief features are easily discerned. The glassy layer referred to previously is the well-defined curved portion near the top about 4 mils in width.

The major portion of the exterior of the boron deposited at 900°C had a dull, matte-like texture with a brownish, slightly purple cast to it which contrasted sharply with the more metallic, crystalline appearance of the hemispherical growths of Fig. 4 and deposits made at higher temperatures.

The sample was subjected to several kinds of analysis after removing it from the tantalum rod by wrapping it in a polyethylene sheet and flexing gently. The analytical results are: carbon, 0.007 ±0.002%;[3] tantalum, 0.03%; iodine, present by x-ray emission analysis; nickel, trace by x-ray emission analysis, but not detected by spectrographic emission analysis, <0.01%. The tantalum was estimated from an uncalibrated x-ray emission analysis.

The sample of boron deposited on the tantalum rod at 1000°C warped the hairpin so badly that it moved close to the quartz wall of the deposition chamber and would have touched it if the experiment had continued. The experiment was interrupted to reposition the tantalum rod and then continued. The boron was removed from the tantalum by wrapping in aluminum foil and flexing in order to eliminate polyethylene as a source of carbon contamination. The carbon content of this sample was determined as 0.003 ±0.002%.

X-ray powder photographs of the 1000° sample showed some differences in line intensities compared to the 900°C sample, but the characteristic phase seemed to be the low temperature form of boron. Horn (19) found that the solid seemed to consist of several phases when examined under a microscope. By leaching with warm concentrated nitric acid he recovered red sandy, red glassy, and red microcrystalline material. Clear red crystals about 0.25 mm long were collected from this product. When examined by x-ray emission the red crystals showed about 0.04 wt % of iodine, but no other impurities of atomic number 13 or larger in concentration greater than 0.001% (the limit of detection for the amount of sample available). The density was measured as 2.459_5 at 22.6°C which is considerably greater than the density of the high temperature rhombohedral form obtained from melted boron, 2.33 at 22.6°C (13).

X-ray powder patterns of the various types of colored crystals present showed no significant differences (19), but there are very large differences in the electrical resistivities (15). The red colored crystals of the low-temperature rhombohedral form of boron apparently have impurities occupying very shallow levels near the band edge which contrasts with the deeper levels found in boron made at higher temperatures. The black portions of the deposits of low-temperature rhombohedral boron are probably more impure than the clear red crystals.

Kasper and Decker determined the crystal structure (14) of the red boron which is composed of units of nearly regular icosahedra in a slightly deformed cubic close-packing. The space group is $R\bar{3}m$ with $a_o = 5.07$Å and $\alpha = 58°1'$. The theoretical density calculated from the dimensions of this structure agrees very well with Horn's experimental values.

[3] Carbon analyses performed by a combustion-conductimetric technique fluxed with iron in a commercially available apparatus.

Discussion

The marked amount of tantalum contamination observed in the 800° deposition (cf. Table II) contrasts sharply with the experience of Laubengayer, Hurd, Newkirk, and Hoard in their work on the hydrogen reduction of boron tribromide (2). The formation of tantalum boride at 800°C in the present work may involve the formation of a tantalum iodide compound that is unstable at higher temperatures, while the corresponding tantalum bromide may simply never form because of the reducing action of hydrogen.

On the other hand, the small amount of contamination experienced in the 900° and 1000°C deposits on tantalum contrasts just as markedly with the experience of Stern and Lynds [cf. Table II, ref. (7)], who observed considerable diffusion of tantalum into boron at 975°-1025°C. Greater temperature gradients in the latter work could have increased the rate of diffusion in the solid phases, and, logically, at least comparable amounts of tantalum should have been found in Stern and Lynds' 1200°-1250°C sample, but it is not reported. It is difficult to reconcile the various observations on the basis of a physical mechanism such as simple diffusion. The chemistry of the various phases that can form at the tantalum surface may depend very strongly on the particular halide used and the presence or absence of hydrogen.

Among the elements not covered by our analytical techniques, the most probable contaminants are nitrogen and oxygen. Nitrogen should not be a problem during the deposition of the boron in an evacuated system. Richter (16) has shown that evaporated boron films will react with nitrogen of the air, however, to form crystalline boron nitride. It would not be surprising to find a surface film of nitrogen on most boron samples.

Oxygen is more of a problem because of the difficulty of removing water vapor completely from a quartz vessel. The reactor and boron triiodide container was prepared for use by flaming it with an air-gas mixture while it was being flushed with dry nitrogen with a dew point of less than −50°C. Boron triiodide vapor would be expected to react with most of the residual water vapor at or near the walls of the vessel. The work of Kaiser, Keck, and Lange (17) on the quantity of oxygen dissolved in floating zone purified silicon, suggests that iodide boron may contain less than 0.001% oxygen.

The band gap in the high-temperature rhombohedral boron formed from the melt is about 1.6 ev (18), and this kind of boron should be transparent to visible light in the far red end of the visible spectrum when pure enough. The "low-temperature" form of boron obtained as clear red crystals in this work may have a band gap as high as 2 ev (15), which could be the chief reason for the red transparency. It is true that high purity may be necessary too, but the purity requirements are, perhaps, not as stringent as for the "high-temperature" form in order to insure red transparency.

The red crystals observed within the deposit on the 3-mil tantalum wire were clustered around the wire core in such a way that the presence of the tantalum may have influenced the nature of the deposit. From the analysis of the red crystals of another deposit it seems clear that no significant amount of tantalum is necessarily present in the crystals. There remains the possibility that tantalum may be acting as a "getter" for impurities and thus promoting the growth of a red phase locally. Again, the presence of tantalum is not a necessary condition for the red glassy phase was observed in the center of the "bull's eyes" which grew on the exterior of the deposit as shown in Fig. 5.

The question of why the various kinds of growth and different colors occur in these deposits is a fascinating subject for speculation. The color of the crystals is very likely related to the impurity content. Apparently only one crystalline phase is involved, yet there must be subtle differences in the way the crystals grow in order to cause the segregation observed.

Acknowledgment

The authors are indebted to F. H. Horn for his interest and work on the properties of "red" boron. J. S. Kasper and Mrs. B. F. Decker performed most of the x-ray crystallographic work. A. E. Newkirk has been interested in the morphology of boron deposits for many years. His advice and encouragement were extremely valuable.

Manuscript received June 12, 1959.

Any discussion of this paper will appear in a Discussion Section to be published in the December 1960 JOURNAL.

REFERENCES

1. A. W. Laubengayer, A. E. Newkirk, and R. L. Brandaur, *J. Chem. Ed.*, **19**, 382 (1942).
2. A. W. Laubengayer, D. T. Hurd, A. E. Newkirk, and J. L. Hoard, *J. Am. Chem. Soc.*, **65**, 1924 (1943).
3. J. S. Spevack, U.S. Pat. No. 2,685,501 (1954).
4. Heinz Hoag, U.S. Pat. No. 2,794,708 (1957).
5. N. F. Murphy, R. S. Tinsley, and G. F. Meenaghan, *Bull. Va. Polytech. Inst.*, **50**, Eng. Expt. Sta. Ser. No. 115, **4**, 18 pp. (1957).
6. G. H. Fetterly, U.S. Pat. No. 2,542,916 (1951).
7. D. R. Stern and L. Lynds, *This Journal*, **105**, 676 (1958).
8. H. Moissan, *Compt. rend.*, **112**, 717 (1891).
9. "Chemistry and Metallurgy of Miscellaneous Materials: Thermodynamics," National Nuclear Energy Series IV-19B, Laurence L. Quill, Editor, McGraw-Hill Book Co. (1950). Cf. paper 6 by L. Brewer, L. A. Bromley, P. W. Gilles, and N. L. Lofgren.
10. W. C. Schumb, E. L. Gamble and M. D. Banus, *J. Am. Chem. Soc.*, **71**, 3225 (1949).
11. F. B. Litton and H. C. Andersen, *This Journal*, **101**, 287 (1954).
12. L. V. McCarty, *ibid.*, **106**, 1036 (1959).
13. L. V. McCarty, J. S. Kasper, F. H. Horn, B. F. Decker, and A. E. Newkirk, *J. Am. Chem. Soc.*, **80**, 2592 (1958).
14. B. F. Decker and J. S. Kasper, *Acta Cryst.*, **12**, 503 (1959).
15. F. H. Horn, *J. Appl. Physics*, **30**, 1611 (1959).
16. H. Richter, *Physik Z.*, **44**, 406 (1943).
17. W. Kaiser, P. H. Keck, and C. F. Lange, *Phys. Rev.*, **101**, 1264 (1956).
18. W. C. Shaw, D. E. Hudson, and G. C. Danielson, *Phys. Rev.*, **107**, 419 (1957).
19. F. H. Horn, Private communication.

Electrolytic Reduction of Thorium Oxide

L. H. Meyer

Savannah River Laboratory, E. I. du Pont de Nemours & Company, Aiken, South Carolina

ABSTRACT

Thorium metal was prepared by electrolytic reduction of thorium oxide in two systems, a fused KF-ThF_4 mixture and a fused NaCl-KCl-$ThCl_4$ mixture. The average decomposition potential measured in both systems was 1.92 v. Electrolysis in the fluoride melt proved to be a superior process, the metal product having higher purity and larger average particle size than the product from the chloride melt. In addition, the recovery of thorium from recycle streams proved to be much simpler in the fluoride process than in the chloride process. The feasibility was demonstrated for all the essential steps of a complete process for production of the metal in the fluoride system.

A satisfactory method for production of thorium metal requires (*a*) a simple preparation of feed material, (*b*) a successful reduction of the thorium feed compound to thorium metal, and (*c*) an efficient recovery of the metal after reduction. A simple recycle of nonrecoverable metal fines and other thorium-containing materials is also frequently desirable. Existing techniques utilize electrolytic or metallothermic reduction of a thorium halide as a means of producing the metal. However, preparation of an anhydrous thorium halide suitable for feed to a continuous reduction process is at best a difficult operation. Production of thorium metal through reduction of its oxide offers the advantage of eliminating the halogenation step and substituting for it the relatively simple preparation of thorium oxide.

This investigation was undertaken to determine the feasibility of a process based on electrolytic reduction of thorium oxide. This technique, which is closely analogous to the Hall process for producing aluminum, was suggested as a possible method for thorium production in a 1931 patent by Driggs (1). Electrolytic rather than metallothermic reduction of the oxide was selected because the former lends itself more readily to continuous operation and because other attempts (2) at the latter have resulted in a product with an average particle size of only 7-8 μ. Previous work (3) indicated that electrolytic reduction should produce a metal having larger particle size and lower impurity content.

The results of this experimental study form the basis for a proposed process for producing thorium metal by electrolytic reduction of its oxide. All steps essential to continuous operation have been demonstrated.

Experimental

Apparatus.—Electrolysis cells.—The cells, which also served as the anodes during electrolysis, were CS-312 graphite crucibles, 18 in. high and 5 in. in diameter with 0.5-in. walls. They were obtained from the National Carbon Company. During operation, the cell was inserted into a stainless steel sleeve to prevent loss of the melt in event of cell rupture.

Housing.—The cell was contained in a dry box provided with equipment to handle the internal manipulations. During operation the box atmosphere could be maintained at 99+% helium.

Instrumentation.—The instrumentation was standard. The Pt-Pt, 10% Rh thermocouple was housed in a stainless steel well which was immersed in the melt.

Materials.—Potassium thorium fluoride.—The compound $KThF_5$ was prepared by the method of Driggs and Lilliendahl (4). The anhydrous double salt precipitated upon adding an excess of aqueous potassium fluoride to aqueous thorium nitrate. The precipitation of Th^{+4} from the solution was virtually complete, the filtrate analyzing $<6\times10^{-6}$M Th^{+4}.

Thorium chloride.—The anhydrous NaCl-KCl-$ThCl_4$ mixture was obtained from Horizons, Inc., Cleveland, Ohio.

Thorium oxide.—Fisher Scientific Co. C. P. thorium oxide was used in all runs.

Cathode metals.—Six-millimeter molybdenum rod was used as cathode material in most of the electrolyses. The molybdenum and the tantalum were obtained from the Fansteel Metallurgical Corporation, North Chicago, Illinois. Titanium was obtained from Rem-Cru Titanium, Inc., Midland, Pennsylvania; and the thorium used for cathodes was obtained from the Atomic Energy Commission.

Procedures.—Electrolysis.—Prior to each electrolysis, the cell was filled with salt plus the desired quantity of oxide. The cathodes were hung on racks, and all electrical connections were made. The front window then was put in place, and the helium purge and heating were started simultaneously. Two to three hours were required to reach operating temperature.

After thermal equilibrium at the desired temperature had been attained, the cathode was immersed in the melt and electrolysis started immediately. At the conclusion of the electrolysis, the cathode was withdrawn slowly to allow maximum drainage of the molten salt. The cathode with its metallic deposit was hung on a rack to cool. A second cathode then

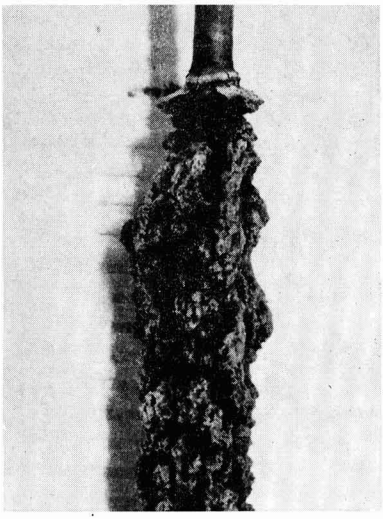

Fig. 1. Typical cathode deposit obtained by electrolysis of ThO_2 in a KF-ThF_4 melt.

could be immersed and the process could be repeated. A helium atmosphere was maintained throughout the cooling period to prevent oxidation of the deposited metal. Figure 1 is a photograph of a typical cathode deposit.

Metal recovery.—Fluoride system.—The metal produced by electrolysis in the fluoride system was recovered by stripping the deposit from the cathode, crushing, screening, and leaching. After the deposit was crushed, 20 to 40% passed a 200-mesh screen. This fraction, containing from 5 to 14% of the metal, was not processed further. The +200 mesh fraction was leached for 10 to 20 min in boiling aqueous aluminum nitrate (~1M). A white or gray near-colloidal dispersion formed in the supernatant liquor during the leaching operation. This dispersion, which consisted of finely divided thorium oxide and thorium metal, could be coagulated and precipitated by centrifugation. After the leaching operation, the metal was visibly free of salt, as shown in Fig. 2.

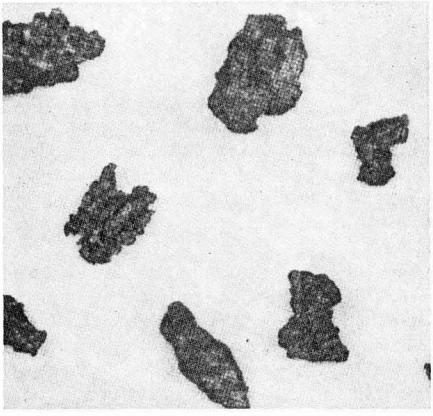

Fig. 2. Thorium metal particles (+10 mesh) produced by electrolysis of ThO_2 in a KF-ThF_4 melt, following leach with hot aqueous aluminum nitrate.

Table I. Anode gas analyses during electrolysis of ThO_2 in a KF-ThF_4 melt*

Constituent	Before start	8 min after start	18 min after start	3 min after conclusion	16 min after conclusion
He	95.4	70.0	72.1	94.1	96.6
CO	1.77	22.2	25.8	4.62	2.33
CO_2	0.17	7.02	1.23	0.10	0
N_2	0.15	Trace	Trace	Trace	Trace
O_2	0.03	0	0	0	0
H_2	2.45	0.69	0.88	1.10	1.10
F-containing gas	0	0	0	0	0

* All figures given in mole per cent.

Table II. Anode gas analyses during electrolysis of ThO_2 in a NaCl-KCl-$ThCl_4$ melt*

Constituent	Before start	5 min after start	20 min after start	Immediately after conclusion	10 min after conclusion
He	98.4	71.6	73.2	93.8	98.0
CO	0	5.33	6.96	2.53	0.15
CO_2	0.10	20.4	17.8	1.78	0.24
N_2	0.10	0.41	0.51	0.22	0.09
O_2	0	0.05	0	0	0
H_2	1.35	2.10	1.55	1.64	1.56
Cl-containing gas	0	0	0	0	0

* All figures given in mole per cent.

Metal recovery.—Chloride system.—The recovery scheme following electrolysis in the chloride melt differed from that for the fluoride system. The procedure consisted of stripping the deposit from the cathode, crushing, and leaching with water. Screening yielded no effective separation of metal from salt due to the very small average particle size of the metal. Leaching was accomplished easily, since the chloride salts of the melt are all highly soluble in water.

Cathode pretreatment.—During the course of the experimentation, it was found that pretreating the cathode decreased the porosity and improved the adherence of the metallic deposit. This pretreatment consisted of sanding to roughen the surface, degreasing with trichloroethylene vapor, and pickling for 3-5 min with an agent suitable for the cathode material. Following the pickling, the cathodes were washed in distilled water and dried in air.

Results and Discussion

Electrolysis of thorium oxide.—The composition of the anode gas evolved during electrolysis in both the fused fluoride and the fused chloride systems established thorium oxide as the compound undergoing decomposition. The oxygen resulting from decomposition of the oxide was liberated at the graphite anodes as carbon dioxide and carbon monoxide. The large increase in the oxide content of the gas surrounding the anode during electrolysis is evident from the analyses listed in Tables I and II. The anode gas contained no fluorine or chlorine compounds. The presence of such compounds would have been observed had the halides been decomposed during the electrolysis.

Decomposition potential.—The decomposition potential of thorium oxide in both systems was determined

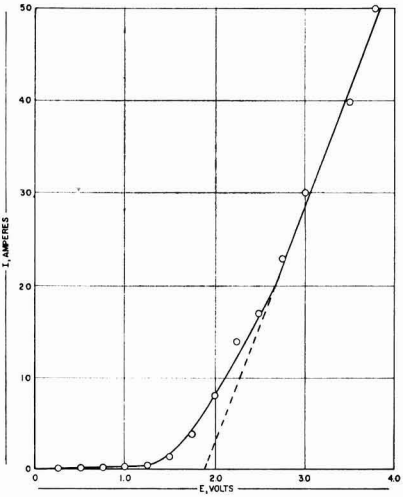

Fig. 3. Current-voltage curve for electrolysis of ThO_2 in a $KF\text{-}ThF_4$ melt.

in the conventional manner from current-voltage graphs. A typical plot is shown in Fig. 3. A variation from 1.67 to 2.15 v was found over fourteen independent determinations in the fused fluoride system, yielding a value of 1.92 ±0.11 v. Ten determinations in the fused chloride system gave a value of 1.92 ±0.27 v.

Solubility of thorium oxide.—The solubility of thorium oxide in a $KF\text{-}ThF_4$ melt, 70% ThF_4 by weight, was found to be approximately 1%. No reliable result was obtained for the solubility of thorium oxide in the $NaCl\text{-}KCl\text{-}ThCl_4$ melt.

Leaching agents.—A solvent was required for the constituents of each of the melts in order to leach the occluded salt from the metal. No problem was encountered in the chloride system, since all the salts in the melt are water soluble. Thorium fluoride and its double salts with potassium fluoride are insoluble in water but dissolve satisfactorily in boiling aqueous aluminum nitrate.

Product purity.—The product was identified as thorium metal by x-ray diffraction. Determination of the HCl-insoluble content yielded the amount of dissolved or occluded thorium oxide, which averaged 0.63% in the product from the fluoride process, but ran as high as 12.2% in the product from the chloride process. One complete spectroscopic analysis of the metal produced by electrolysis in the fluoride melt (Run 3D) is listed below:

600 ppm Al	35 ppm Mg
9 ppm B	40 ppm Mn
90 ppm Ca	300 ppm Ni
<0.5 ppm Cd	400 ppm Si
700 ppm Cr	<1 ppm U
250 ppm Cu	80 ppm Zn
1000 ppm Fe	<50 ppm Zr

Remainder Th

The source of impurities was assumed to be the fluoride salt.

Operating and performance data.—Fused fluoride system.—Table III lists the operating and performance data for seventeen electrolyses carried out in the fused fluoride system. Runs with a common numeral were made in the same salt bath. The recovery efficiency listed in the table is the per cent recovery of the metal theoretically deposited by the passage of the given charge, assuming a quadrivalent thorium ion in the molten salt solution. The HCl-insoluble content indicates the quantity of oxide dissolved in the metal.

Examination of the data reveals that the first electrolysis with each salt bath resulted in poor yields. This effect is ascribable to impurities in the salt, the presence of which decreases the mean particle size

Table III. Operating and performance data for the electrolyses of ThO_2 in a $KF\text{-}ThF_4$ melt

Run	Cathode material	Cathode pretreatment	Temperature, °C	Current density amp/dm²	Recovery efficiency, %	Wt. fraction of recovered metal*	Wt. % recovered metal +40 mesh	Wt. % deposit −200 mesh	Wt. % metal in −200 mesh deposit	Per cent HCl-insolubles
1A	Mo	None	990	160	2.5	0.025	0	—	—	—
1B	Mo	None	1000	280	9.6	0.221	38.7	—	—	2.30
1C	Mo	None	980	56	14.7	0.228	16.7	—	—	—
1D	Mo	None	950	63	8.2	0.276	69.0	—	—	1.10
1E	Mo	None	940	103	24.6	0.583	95.0	—	—	0.43
1F	Mo	None	960	280	10.3	0.210	63.4	—	—	0.14
2A	Mo	None	1000	193	0	—	—	—	—	—
2B	Mo	None	1000	380	18.5	0.182	32.4	—	—	0.44
2C	Mo	None	990	380	21.5	0.473	69.0	34.3	6.9	0.94
3A	Mo	8M HNO_3	950	174	12.0	—	1.5	—	18.8	2.70
3B	Mo	8M HNO_3	965	104	7.8	0.478	63.5	39.2	—	0.32
3C	Mo	8M HNO_3	970	35	19.1	0.596	65.1	27.2	—	0.26
3D	Mo	8M HNO_3	980	174	41.0	0.679	91.4	18.8	—	0.10
3E	Mo	8M HNO_3	1010	182	25.8	0.400	74.1	31.4	20.7	0.23
3F	Th	6M HCl	1000	53	8.2	0.129	2.0	66.7	21.8	0.21
3G	Ti	6M HCl	1000	136	10.2	0.084	0	80.6	39.0	2.60
3H	Ta	8M HNO_3	1000	167	12.3	0.058	0	88.0	40.0	0.25

* $\frac{\text{Weight of recovered metal}}{\text{Total weight of deposit}}$ (includes occluded salt and oxide)

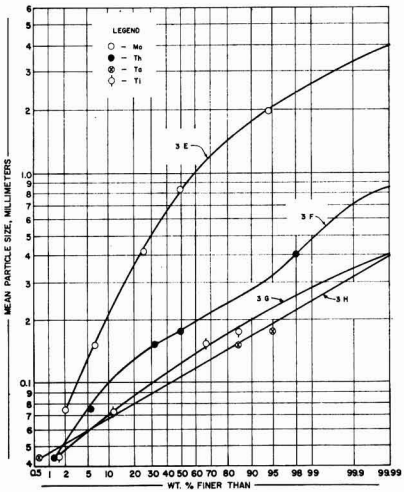

Fig. 4. Particle-size distribution for electrolyses with varied cathode material.

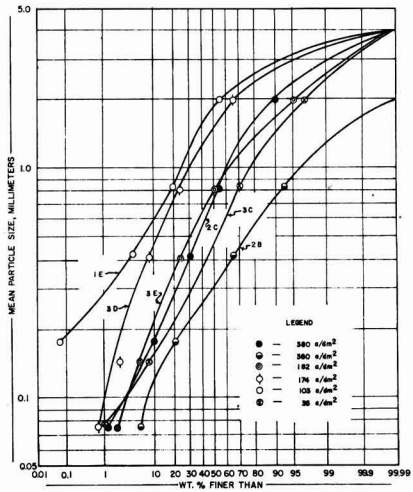

Fig. 5. Particle-size distribution for electrolyses at varied current densities.

(5) and consequently the recovery efficiency. The first electrolysis with each bath apparently served as a scavenging run, after which performance improved.

From the data in Table III the superiority of molybdenum as a cathode material over the other metals tested is apparent. If the results of the scavenging runs are discounted, the recovery efficiency, based on a quadrivalent thorium cation, for the electrolyses with molybdenum cathodes varied from 8.2 to 41.0%, averaging 18.3%.[1] The ratio of the weight of the recovered metal to the total weight of the deposit (including occluded salt and ThO_2) averaged 39.3%, with a total variation from 18.2 to 67.9%. An average of 61.7% of the recovered metal exceeded 40 mesh in size, and the amount of metal fines in the −200 mesh fraction ranged from only 2 to 7% of the total weight of the deposit. The HCl-insoluble content varied from 0.10 to 2.30%, averaging 0.63%. Performance with thorium, titanium, and tantalum cathodes was much less satisfactory. In particular, the particle size distribution of the product was less favorable than with the molybdenum cathodes, since much larger fractions of the thorium metal were produced as irrecoverable fines with the other three cathode materials tested. Figure 4 illustrates the differences in particle size distributions for the four cathode materials.

Current density was varied from 35 to 380 amp/dm² for the electrolyses listed in Table III. No good correlation was observed, however, between current density and any of the performance criteria. Figure 5 shows the particle size distributions for electrolyses run at different current densities.

Beginning with Run 3A, the cathodes were given a pretreatment with a pickling agent in an attempt to improve the adherence of the deposit. Improvement was not pronounced; however, the metal particles plated on pickled electrodes had a firmer structure, which facilitated separation of the metal from the salt.

Operating and performance data.—Fused chloride system.—Fourteen electrolyses were performed in the chloride system. Recovery efficiency, based on Th^{+4} in solution, varied from 13.9 to 55.0%, averaging 27.2%. The ratio of the weight of recovered metal to the total weight of the deposit averaged 22.5%, ranging from 10.9 to 43.3%. The HCl-insoluble content was high, 1.92 to 12.2%. The particle size distribution was considerably less favorable than that resulting from the electrolyses in the fluoride system. In only one of the fourteen runs did any of the metal particles exceed 80 mesh in size. Virtually all the product was −100 mesh, with sizable fractions in the 10 to 50 μ range.

Comparison of Processes in the Fluoride and Chloride System

The experimental results indicate that the production of thorium metal by electrolysis of thorium oxide in the fused fluoride system is superior to the analogous process in the chloride system. The chloride melt has a lower fusion temperature (~800°C) than the fluoride system (~1000°C), plus a high water solubility of the bath constituents, which facilitates the leaching operation. However, these advantages are inadequate to compensate for the lower purity and smaller particle size of the product. Moreover, there is no simple technique for recycling the occluded chloride salts that are removed with the cathode deposit. Unless methods can be found for depositing larger metal particles from the chloride melt, electrolysis of thorium oxide in this system does not appear to be competitive with the fluoride process.

Flowsheet for Proposed Process

Figure 6 is the proposed flowsheet of the complete process for the production of thorium metal in the fused fluoride system. A brief discussion of each of the steps is presented below.

[1] A sizable loss resulted from lack of proper equipment to strip the tightly adhering thorium deposit efficiently from the cathodes.

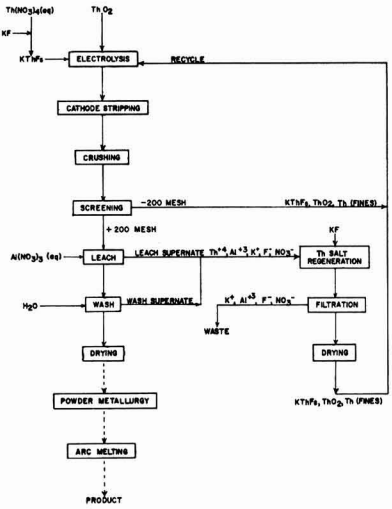

Fig. 6. Proposed flowsheet for production of thorium metal in fused fluoride system.

Electrolysis.—Electrolysis is performed in graphite-lined cast iron cells. The liners, serving as anodes, are replaced as they are consumed. An inert atmosphere chamber must be provided for removal and cooling of the cathodes following electrolysis.

Cathode stripping.—Conventional techniques and equipment are available for stripping the deposit from the cathodes.

Crushing and screening.—The gross physical separation of metal from salt is based on the fact that the salt crystals are reduced in size easily by crushing, while the metal particles are not. It is proposed that the metal in the +200 mesh (U. S. Standard Series) fraction, which contains 80 to 95% metal by weight, be leached, while the −200 mesh fraction which averages only 15% metal be recycled.

Leaching.—The salt not removed by the physical separation can be dissolved in hot aqueous aluminum nitrate. Boiling 10 to 20 min in 1M aluminum nitrate gives satisfactory removal of salt.

Metal processing.—After the leaching operation, the metal is separated from the supernatant liquor by decantation. The metal then is washed with water and air dried. The drying step is followed by a powder metallurgical forming of electrodes for subsequent arc melting.

Recycle (−200 mesh screening fraction).—The composition of this fraction averages 15% thorium metal, 0.4% thorium oxide, and the remainder salt. Two alternatives are available for treatment of these fines. An oxygen roast converts the metal to thorium oxide, after which this fraction can be returned to the electrolysis cells; or the −200 mesh fraction may be recycled directly to the cells, and a periodic oxygen sparge may be employed to re-oxidize the thorium metal. The latter alternative is favored, since an oxygen sparge is probably necessary to re-oxidize the nonadhering metal product, which collects at the bottom of the cells during electrolysis. Any such treatment with oxygen requires careful control to prevent excessive attack on the graphite liners.

Recycle (leach and wash supernatant liquors).—The leach and wash supernatant liquors contain thorium in the form of soluble Th^{+4} ion plus dispersed oxide and metal fines. The dissolved thorium can be recovered by adding KF in quantity sufficient to precipitate all the thorium as $KThF_5$. Some care must be observed in order not to precipitate any of the potassium aluminum fluorides. Control is not too critical, however, since less than 80% of the KF required for incipient precipitation from a blank 1M aluminum nitrate solution precipitates essentially all of the Th^{+4} from a 1M aluminum nitrate solution saturated with $KThF_5$. A well-agitated precipitation should succeed in coagulating and carrying down the dispersed particles as well. Following filtration, the precipitate is dried and recycled to the electrolysis cells.

Waste.—The only waste stream in the process is the filtrate from the $KThF_5$ regeneration step. Thorium concentration in this stream is less than 10^{-5}M.

Manuscript received May 25, 1959. The information contained in this article was developed during the course of work under contract AT(07-2)-1 with the U.S. Atomic Energy Commission.

Any discussion of this paper will appear in a Discussion Section to be published in the December 1960 JOURNAL.

REFERENCES

1. F. H. Driggs, U. S. Pat. 1,815,054 (1931).
2. B. Kopelman, International Conference on the Peaceful Uses of Atomic Energy, Paper No. 531 (1955).
3. W. C. Lilliendahl, "Rare Metals Handbook," C. F. Hampel, Editor, pp. 429-454, Reinhold Publishing Corp., New York (1954).
4. F. H. Driggs and W. C. Lilliendahl, *Ind. Eng. Chem.*, **22**, 1302 (1930).
5. C. C. Ma, *ibid.*, **44**, 342 (1952).

Mass Transfer at the Streaming (Jet) Mercury Electrode

Theoretical Calculation of Limiting Currents

Kameo Asada, Fumio Hine, Shiro Yoshizawa, and Shinzo Okada

Department of Industrial Chemistry, Faculty of Engineering, Kyoto University, Kyoto, Japan

ABSTRACT

Mass transfer at the streaming or jet mercury electrode has been studied theoretically. Momentum equations for both the mercury jet and the surrounding solution layer have been solved simultaneously on the assumption of laminar flow in both mercury jet and surrounding solution envelope. Limiting currents were measured for the reduction of Tl^{+}, Pb^{++}, and Zn^{++} at 25°C with 0.1M KCl as supporting electrolyte. Experimental results are in good agreement with predictions based on theoretical analysis.

The streaming or jet mercury electrode has been studied and used in various forms of polarography (1-12). Its application to routine analytical purposes is restricted by the large amount of mercury consumed, the high charging currents, and the inconvenience in reproducing stream geometry. On the other hand, the streaming electrode, if used along with the dropping electrode, appears promising in studies of kinetic currents (6, 7) and irreversible electrode processes (12). Furthermore, the rapid renewal of the mercury surface makes it useful in studies of the mercury-solution interface (2, 4, 8, 11). Toshima and Mizuno (13) successfully applied a mercury stream to the production of caustic soda from crude brine.

It is of interest to know how the mercury jet drags the solution around it and how the rate of mass transfer of the ions (limiting current) is related to the conditions of operation, such as flow rate of mercury, length of jet, etc. Ríus, *et al.* (8) obtained an expression for the limiting current based on the assumption that the radius of the mercury jet is constant, the curvature negligible, and the velocity of the jet and of the adjacent solution uniform everywhere. Weaver and Parry (12) showed the invalidity of these assumptions and presented a semi-empirical equation for the limiting current, using observed values of the jet diameter, interfacial velocity, and velocity gradient. The present paper gives an analysis of jet characteristics by methods of fluid dynamics, which have already been applied successfully to many instances of ionic mass transfer (14-17), and describes methods for the calculation of limiting currents without the use of empirical information on jet geometry.

Stream Characteristics

Theoretical.—Although the turbulent flow of gases from nozzles (18) and the breakup of liquid streams (19) have both been considered in fluid mechanics, no theory adaptable to working conditions of the streaming mercury electrode was available. Throughout this paper it will be assumed that (*a*) the flow of the mercury within the capillary is laminar (Hagen-Poiseulle flow without slip), (*b*) the mercury jet, after leaving the capillary, and the solution boundary layer formed around it are cylindrical and undergo laminar flow, and (*c*) there is no slip between the mercury jet and the solution boundary layer. The cylindrical coordinates are chosen as shown in Fig. 1, z being the logitudinal distance from the capillary tip and r the radial distance from the center of the jet.[1] The mercury jet and the solution flow are distinguished from each other by subscripts m and s, respectively.

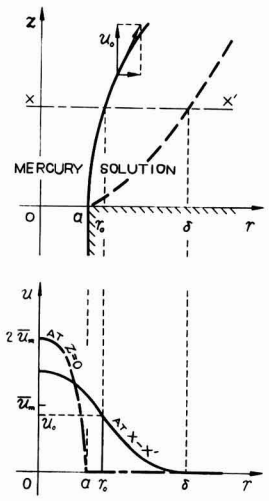

Fig. 1. Model for theoretical analysis; coordinates and velocity profiles.

As a rigorous simultaneous solution of the Navier-Stokes equations and the continuity equations for noncompressible fluids is very difficult, the Kármán momentum equation method (20, 21) is applied, a boundary layer of definite thickness being assumed. In order to simplify the mathematical model, parabolic velocity profiles are assumed, that is, the ve-

[1] A glossary of symbols is given at the end of this paper.

locity components in the z direction, u_m and u_s, are expressed by

$$\left.\begin{aligned} u_m/u_o &= 1 + [(\mu_s/\mu_m)r_o/(\delta - r_o)][1 - (r/r_o)^2] \\ u_s/u_o &= [(\delta - r)/(\delta - r_o)]^2 \end{aligned}\right\} \quad [1]$$

which satisfies the following conditions

$$\left.\begin{aligned} &\text{at } r = 0,\ \partial u_m/\partial r = 0 \\ &\text{at } r = r_o,\ u_m = u_s \equiv u_o \text{ and} \\ &\quad \mu_m \cdot \partial u_m/\partial r = \mu_s \cdot \partial u_s/\partial r \\ &\text{at } r = \delta,\ u_s = \partial u_s/\partial r = 0 \end{aligned}\right\} \quad [2]$$

In the above μ is the dynamic viscosity, r_o the radius of the mercury stream, δ the thickness of the boundary layer measured from the center of the stream ($r = 0$), and u_o the interface velocity component in the z direction. The last three quantities are unknown parameters dependent on z alone and are determined by the momentum equations

$$\left.\begin{aligned} &-d[\rho_m \textstyle\int_0^{r_o} u_m^2\, r\, dr]/dz + g(\rho_m - \rho_s)r_o^2/2 \\ &= -\mu_m r_o (\partial u_m/\partial r)_{r=r_o} = -\mu_s r_o (\partial u_s/\partial r)_{r=r_o} \\ &= d[\rho_s \textstyle\int_{r_o}^{\delta} u_s^2\, r\, dr]/dz \end{aligned}\right\} \quad [3]$$

and by the equation of conservation of mass for the mercury stream

$$d[\textstyle\int_0^{r_o} u_m r\, dr]/dz = 0 \quad [4]$$

ρ being the density and g the acceleration due to gravity (g is negative when the stream flows upward).[2] In Eq. [3] the bracketed terms are equivalent to the momenta of the mercury jet and of the solution envelope. The third and fourth terms correspond to the shearing stresses per unit length. Hence Eq. [3] implies that the momentum of the moving mercury jet, after ejection from the capillary, is consumed by work against gravitational force (or *vice versa*) or is transferred to the surrounding solution through the shearing stress at the interface. The second equality in Eq. [3] means absence of slippage at the interface [assumption (c)] and so perfect momentum transfer. It follows from assumption (a) that the boundary conditions in the z coordinate are

$$\text{at } z = 0,\ u_m/\overline{u_m} = 2[1 - (r/a)^2] \text{ and } u_s = 0 \quad [5]$$

where u_m is the mean velocity of the mercury jet and a the inner radius of the capillary.

Equation [1] is introduced into Eqs. [3] and [4], which then are integrated with respect to r and Eq. [5] is taken into consideration. One obtains

$$\left.\begin{aligned} &dM_s/dz' = 3(u_o/\overline{u_m})\mu'\phi/(1 - \phi) \\ &M_m + M_s = 1 + g' \textstyle\int_0^{z'} (r_o/a)^2\, dz' \\ &(r_o/a)^2(u_o/\overline{u_m})[2 + \mu'\phi/(1 - \phi)] = 2 \end{aligned}\right\} \quad [6]$$

where

$$\left.\begin{aligned} &z' = \nu_m z/a^2\overline{u_m},\ \mu' = \mu_s/\mu_m,\ \rho' = \rho_s/\rho_m,\ \phi = r_o/\delta \\ &M_m = \tfrac{1}{4}(r_o/a)^2(u_o/\overline{u_m})^2 \cdot \\ &\quad [3 + 3\mu'\phi/(1 - \phi) + (\mu')^2\phi^2/(1 - \phi)^2] \\ &M_s = (\rho'/20)(r_o/a)^2(u_o/\overline{u_m})^2 \cdot \\ &\quad (1 - \phi)(1 + 5\phi)/\phi^2 \\ &g' = \tfrac{3}{4}(1 - \rho')\, ga^2/\nu_m\overline{u_m} \end{aligned}\right\} \quad [7]$$

ν being the kinematic viscosity ($=\mu/\rho$). The quantities M_m and M_s are the momenta of the mercury jet and of the solution envelope, respectively, expressed as fractions of the initial momentum of the mercury on ejection from the capillary.

The ratios r_o/a and $u_o/\overline{u_m}$ may be eliminated from Eq. [6] if the gravity term of the second expression is left in the integral form. When the effect of gravity is assumed negligible ($g' = 0$), one has an ordinary differential equation with separable variables, whose numerical integral is available (22) if values of μ' and ρ' are specified. Calculations including the gravity term may be carried out by means of successive approximations.

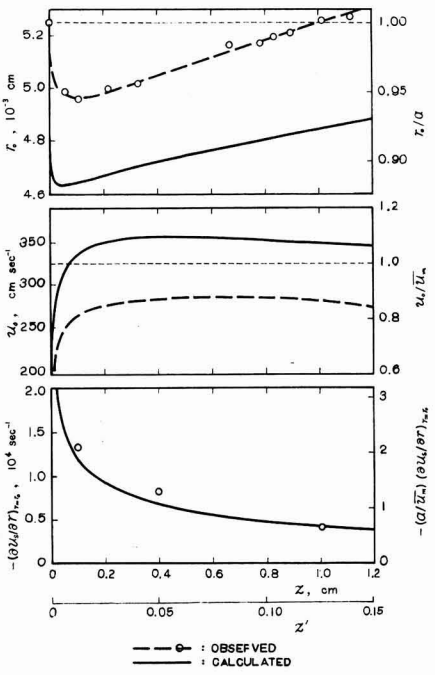

Fig. 2. Mercury jet diameter, interface velocity, and interface velocity gradient, from top to bottom; comparison between calculated and observed results for an upward mercury jet with $a = 0.0052_5$ cm and $\overline{u_m} = 325$ cm sec^{-1}. (Although the dashed curve in the middle figure is not for u_o but for the interface velocity, there is no appreciable difference except near the base of the stream.)

Results and Discussion

The above analysis was applied to some practical systems, and the results were discussed in comparison with experimental findings of Weaver and Parry (12). These authors obtained the jet diameter photographically, the interface velocity by measurements of charging currents, and the interface velocity gradient at the solution side by adding aluminum dust therein. Theoretical results for the foregoing three quantities for a 0.1M KCl solution at 25°C[3]

[2] Equations [3] and [4] may be obtained by integration of the Navier-Stokes equations and the equations of continuity.

[3] The following values were adopted for the physical properties of this system: $\mu_s = 0.008298$ g cm^{-1} sec^{-1}, $\mu_m = 0.01527$ g cm^{-1} sec^{-1}, $\rho_s = 1.0018$ g cm^{-3}, and $\rho_m = 13.534$ g cm^{-3} (from International Critical Tables and Landolt-Börnstein Tabellen).

Table I. Comparison of observed and calculated results of $(r_o/a)^2(u_o/\bar{u}_m)$

z'	Observed	Calculated	Deviation, % calc.—obs.
0.01	0.72	0.779	+9
0.02	0.75	0.837	+12
0.04	0.79	0.875	+11
0.06	0.82	0.894	+9
0.1	0.85	0.914	+7
0.15	0.87	0.927	+6
0.2	—	0.935	—

(the gravity term is neglected) are shown in Fig. 2 together with the experimental values of Weaver and Parry.

Qualitative agreement is good and supports the model described by Eqs. [3]-[5]. The initial increase of u_o is simply a result of acceleration of the outer slow layers of the mercury jet by the inner fast ones through viscous shear. This means that the velocity distribution within the jet becomes more and more uniform; hence the mercury jet should tend to contract in order to conserve its mass velocity, so far as its momentum remains unchanged. But, since momentum transfer from the mercury jet to the solution envelope occurs gradually, the jet slows down and its diameter enlarges because, in the extreme example of infinitesimal momentum, an infinitely wide stream alone can sustain definite mass velocity.

Quantitative failure in the values of r_o and u_o arises in part from the parabolic velocity distribution approximation (Eq. [1]).[4] Since momentum is being transferred at the interface, the deceleration of the mercury jet due to drag of the solution moves from the interface into the interior; thus the velocity distribution profile should have an inflection point. Attempts to improve the velocity distribution function through introduction of higher terms (definite in number) led to a discontinuity in Eq. [5]. However, the momentum equation method is not designed to give individual values for r_o and u_o but is designed to yield products such as $r_o^2u_o$ and $r_o^2u_o^2$. Since the rate of reversible reduction (mass transfer) of ions at the streaming mercury electrode depends chiefly on the former product (12) and since the theoretical values of this product are in reasonable agreement with the experimental (Table I), this failure does not preclude an application of the analysis to problems of mass transfer (and thus to electrochemical measurements).

Although gravitational force was considered as a variable in the original analysis, its effect on an actual situation is negligible. For example, consideration of the gravity term raises r_o by 0.3% and reduces u_o by 0.6% at $z' = 0.14$ in the case of Fig. 2.

Limiting Current

Theoretical.—Limiting currents were evaluated by the following four methods:

1. The approximate solution of the problem by Ríus and his coauthors [(8) see also (16)]

$$I = 4n\mathbf{F}C_o a(\pi D\bar{u}_m l)^{\frac{1}{2}} \qquad [8]$$

[4] Although the experimental values are not specified as to temperature, minute change in physical properties does not account for such a large deviation.

where I is the limiting current, n the number of Faradays per mole or gram-ion reacting, $\mathbf{F}$ the Faraday, C_o the bulk concentration of the reactive species in moles per cubic centimeter, D its diffusion coefficient, and l the effective length of the jet or streaming mercury electrode.

2. Introduction of the jet characteristics observed by Weaver and Parry (dashed curves on Fig. 2) into their rigorous equation (12)

$$I = \pi n\mathbf{F}DC_o\left\{2\int_o^{\delta'} r_o^2u_o[\pi D\int_o^z r_o^2u_o dz]^{-\frac{1}{2}}dz + l + \tfrac{1}{2}\int_o^l (r_o/u_o)(\partial u_o/\partial r)_{r=r_o}\,dz + \ldots\right\}^{-\frac{1}{2}} \qquad [9]$$

3. Introduction of the calculated characteristics (solid curves on Fig. 2) into Eq. [9],

4. Solution of the equation of mass transfer with an approximate method similar to that applied to the stream, as shown in the following.

A profile of the concentration C of the reactive species

$$C/C_o = 1 - [(\delta' - r)/(\delta' - r_o)]^2 \qquad [10]$$

is adopted, where δ' is the thickness of the diffusion layer in the same sense as $\delta(\delta' < \delta)$. If Eq. [1] and [10] are put into

$$d[\int_{r_o}^{\delta'} u_o(C - C_o)r\,dr]/dz = -Dr_o(\partial C/\partial r)_{r=r_o} \qquad [11]$$

one obtains (the gravity term on Eq. [6] is neglected)

$$\frac{60\psi}{\sigma(1-\psi)} = \frac{d}{dz'}\cdot\left\{\frac{(1-\psi)}{[2(1-\phi)+\mu'\phi](1-\phi)\psi^4}\cdot [5\psi^2(1+3\psi) - 4\phi\psi(1+3\psi+6\psi^2) + \phi^2(1+3\psi+10\psi^3)]\right\} \qquad [12]$$

where $\sigma = \nu_m/D$ and $\psi = r_o/\delta'$. Equation [12] can be solved numerically (22), and limiting currents are calculated through

$$I = n\mathbf{F}D\int_o^l 2\pi r_o(\partial C/\partial r)_{r=r_o}\,dz \qquad [13a]$$

or

$$I' = I\nu_m/4\pi n\mathbf{F}DC_o a^2\bar{u}_m = \int_o^{l'} \psi(1-\psi)^{-1}\,dz' \qquad [13b]$$

where $l' = \nu_m l/a^2\bar{u}_m$.

The dimensionless group I' in Eq. [13] corresponds to a Nusselt number divided by the Reynolds number of the mercury stream within the capillary. The mass transfer correlation is expressed as a relationship among the dimensionless parameters I', l', σ, μ', ρ', and g', the last three being of minor influence. It is not easy to measure a and $\bar{u}_m$ separately, but they appear both in I' and l' as the product $a^2\bar{u}_m$, which may be replaced by the mass velocity

$$\bar{m} = \pi\rho_m a^2\bar{u}_m \qquad [14]$$

Experimental, Results and Discussion

Valenta (9) reported that the limiting current was proportional to the square root of $\bar{m}l$ in accordance with Eq. [8], while Weaver and Parry (12) demonstrated that this proportionality required some correction with their equation, Eq. [9] above.

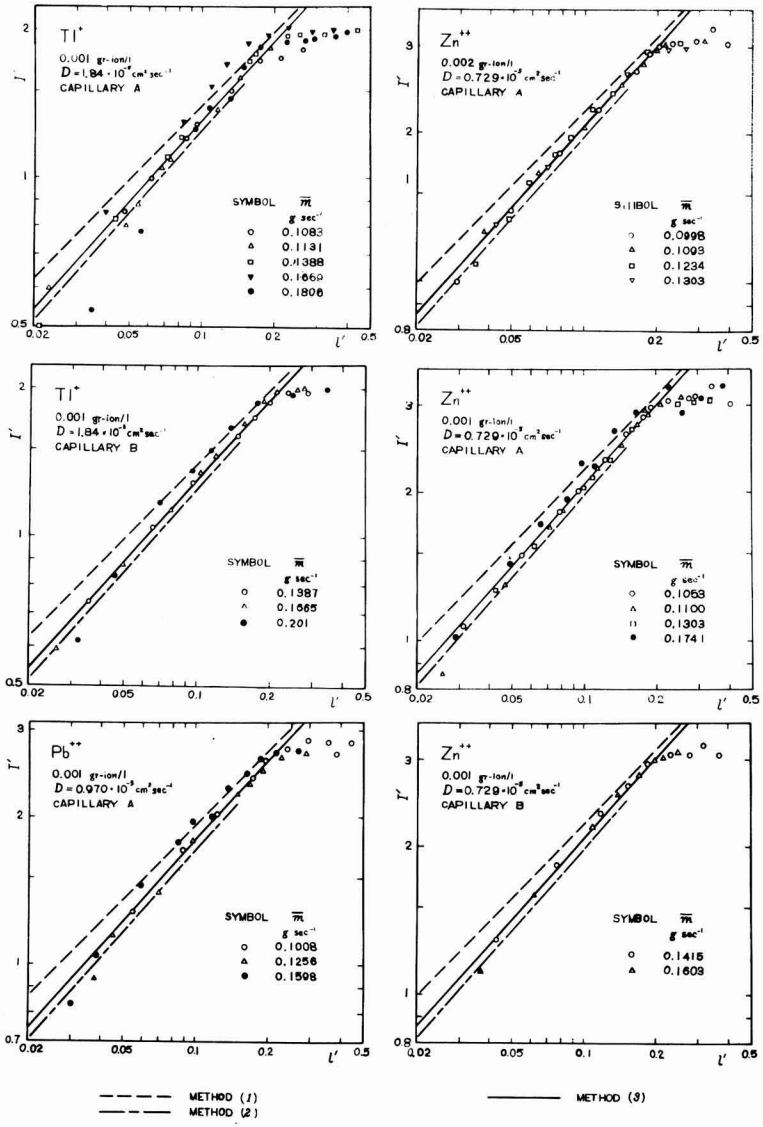

Fig. 3. Mass transfer correlation. Open symbols refer to laminar mercury streaming; solid symbols, to turbulent.

As neither of these data was specified as to temperature, measurements were made with an apparatus essentially similar to that used by Bieber and Trümpler (5), mounted in a bath controlled at 25°C. The solutions studied were 0.1M in KCl and 0.001 or 0.002M in TlCl, $PbCl_2$, or $ZnCl_2$. These systems were chosen since diffusion coefficients of the tracer ions of the reactive species are known: 10^5D (cm^2 sec^{-1}) = 1.84 (Tl^+), 0.970 (Pb^{++}), 0.729 (Zn^{++}) in 0.1M KCl (23). The limiting current I was measured at different values of the mass velocity $\overline{m}$ and the electrode length l, and the results are summarized in Fig. 3 in a dimensionless correlation between I' and l'.

In measuring I, a polarographic apparatus was not employed because anodic polarization and ohmic drop were large. Since charging currents are relatively high at streaming mercury electrodes (7), it was necessary to evaluate them separately. This was achieved by making measurements on solutions with and without the reactive species present.

The mercury mass velocity $\overline{m}$ is dependent both on the characteristics of the capillary and on the mercury head. Two capillaries designated A and B were used; although the mercury flow rate for B was almost twice as large as that for A under the same pressure head, no differences between A and B appear in Fig. 3. $\overline{m}$ was measured by weighing the ejected mercury, and results were plotted against the pressure head in order to check linearity between them or to confirm assumption (a). If this assumption is valid, assumption (b) is expected to be true, for the path of the mercury stream is rather short. On Fig. 3. open symbols refer to runs within the limit of laminar flow, while solid symbols refer to runs in

which $\overline{m}$ was larger and the mercury stream was turbulent. In the latter case the data were scattered.

The length l (more precisely speaking, the length of the upward mercury jet between the capillary tip and the solution level) was varied from 0.05 through 2.5 cm and measured by use of a cathetometer. When l was very small, polarization curves had discontinuities due to disappearance of charging currents. According to Valenta (9) it is caused by slippage at the interface, and so has a close connection with assumption (c) (accordingly, with Eq. [3]). Slippage at the mercury solution interface is dependent on surface tension; application of surface active agents has been supposed necessary to prevent it, in connection with polarographic maxima (24) and the rotated dropping mercury electrode (25). Although no surface active agent was added in the present study, the discontinuity was observed rather rarely, and besides the experimental results in Fig. 2 show clearly the drag of the solution; hence, slippage would not invalidate the theory. But rather low results for runs for $l' < 0.05$ may be due to this slippage (9). Although slipping was no serious problem, another trouble appeared. The solution coned up around the mercury stream above the solution level (9, 12) and some correction (reduction) was required for observed limiting currents. When l was too large or $\overline{m}$ too small, the limiting current increased no more because of decay and breakup of the stream. The critical value of l' was found to be around 0.2 at −1.4 v vs. S.C.E.

Within these restrictions (turbulence, and upper and lower limits of l'), the observed values ranged themselves on a single correlation for a species, justifying the choice of the dimensionless groups.

The limiting current was calculated by the four methods listed in the theoretical part and represented on Fig. 3 and Table II (method 4 was applied only to reduction of thallous ions). Equation [8] by Ríus and his coauthors (method 1) gives values which are too high. Methods 3 and 4, based on theoretical stream characteristics, gave results within about 2% of each other, suggesting that the approximations used are of fairly high reliability. Methods 2 and 3 give curves which, although nearly parallel, deviate from each other by about 6%. The experimental data follow well curves for these two methods. But no correction for coning of the solution was applied to the measured I values. The fractional correction should vary with the electrode length (larger as l' becomes smaller). It is not easy to obtain the magnitude of the "tail-cone correction," but Weaver and Parry estimated it at about 5-7% for $l' = 0.126$ in 0.1M KCl solution. In conclusion, the present theory of the stream characteristics allows prediction of limiting currents with an accuracy of a few per cent at worst.

Table II. Comparison of methods for calculating l' (reduction of Tl^+, $D = 1.84 \times 10^{-5}$ cm^2 sec^{-1})

l'	Method 1	Method 2	Method 3	Method 4
0.01	0.442	0.35	0.367	0.373
0.02	0.625	0.51	0.541	0.552
0.04	0.884	0.75	0.793	0.810
0.06	1.082	0.94	0.989	1.009
0.1	1.397	1.24	1.310	1.333
0.15	1.711	1.55	1.623	1.649
0.2	1.976	—	1.893	1.921

Acknowledgment

The authors are grateful to Dr. T. Sato of Kyoto University for his kind advice on fluid dynamics. Their thanks also go to Dr. R. W. Parry of the University of Michigan, who reviewed and offered a number of helpful suggestions in the preparation of the manuscript.

Manuscript received Sept. 17, 1958. This paper was abstracted from the dissertation of one of the authors (K.A.), Kyoto University, 1958. The theoretical part of the paper was presented before the Polarographic Discussion Meeting, Tokyo, Nov. 20 and 21, 1956.

Any discussion of this paper will appear in a Discussion Section to be published in the December 1960 JOURNAL.

REFERENCES

1. J. Heyrovsky and J. Forejt, *Z. phys. Chem.*, **193**, 77 (1943).
2. J. Heyrovsky, F. Sorm, and J. Forejt, *Coll. Czech. Chem. Comm.*, **12**, 11 (1947).
3. J. Heyrovsky, *Faraday Soc. Discussions*, **1**, 212 (1947).
4. J. Heyrovsky and M. Matyás, *Coll. Czech. Chem. Comm.*, **16**, 455 (1951).
5. R. Bieber and G. Trümpler, *Helv. chim. Acta*, **30**, 971 (1951).
6. J. Koryta and I. Kossler, *Coll. Czech. Chem. Comm.*, **15**, 241 (1950).
7. J. Koryta, *ibid.*, **19**, 433 (1954); **20**, 1125 (1955).
8. A. Rius, *et al., Chem. Abstr.*, **41**, 4725g (1947); **44**, 5233i, 8267a (1950); **45**, 50a, 7454g,h (1951); **46**, 10963e (1952); **47**, 11037h (1953); **48**, 6289g (1954).
9. P. Valenta, *Coll. Czech. Chem. Comm.*, **16**, 239 (1951).
10. P. Léveque, *J. chim. phys.*, **49**, 269 (1952).
11. J. W. Loveland and P. J. Elving, *J. Phys. Chem.*, **56**, 250 (1952).
12. J. R. Weaver and R. W. Parry, *J. Am. Chem. Soc.*, **76**, 6258 (1954); **78**, 5542 (1956).
13. S. Mizuno and S. Toshima, *J. Electrochem. Soc., Japan*, **27**, 391 (1959).
14. J. N. Agar, *Faraday Soc. Discussions*, **1**, 26 (1947).
15. C. W. Tobias, M. Eisenberg, and C. R. Wilke, *This Journal*, **99**, 359C (1952).
16. P. Delahay, "New Instrumental Methods in Electrochemistry," Chap. 9, Interscience Publishing Co., New York (1954).
17. S. Yoshizawa, *J. Electrochem. Soc., Japan*, **25**, 584 (1957).
18. W. Forstall and A. H. Shapiro, *J. Appl. Mech.*, **17**, 399 (1950).
19. R. M. Christiansen and A. N. Hixon, *Ind. Eng. Chem.*, **49**, 1017 (1957).
20. S. Goldstein, Editor, "Modern Developments in Fluid Dynamics," Clarendon Press, Oxford (1938).
21. E. R. G. Eckert, "Introduction to Transfer of Heat and Mass," McGraw-Hill Book Co., New York (1950).
22. K. Hidaka, "Suchi-sekibun-ho (Numerical Integration)," vol. I, Iwanami Book Co., Tokyo (1936).
23. J. H. Wang, *J. Am. Chem. Soc.*, **76**, 1528, 1584 (1954).
24. B. Levich, *Faraday Soc. Discussions*, **1**, 37 (1947).
25. Y. Okinaka and I. M. Kolthoff, *J. Am. Chem. Soc.*, **79**, 3326 (1957).

GLOSSARY OF SYMBOLS

a — radius of capillary (cm)
C — concentration of reactive species (moles/cm³)
C_o — bulk concentration of reactive species (moles/cm³)
D — diffusion coefficient of reactive species (cm²/sec)
$\mathbf{F}$ — the Faraday (amp sec/eq)
g — acceleration of gravity (cm/sec²)
g' — modified Froude number, defined by Eq. [7] (dimensionless)
I — limiting current (amp)
I' — reduced limiting current, defined by Eq. [13] (dimensionless)
l — electrode length (cm)
l' — reduced electrode length, defined by Eq. [13] (dimensionless)
$\overline{m}$ — mass velocity of mercury stream (g/sec)
M — fractional momentum, relative to that possessed by the mercury jet on ejection from capillary (dimensionless)
n — number of Faradays per mole or gram-ion (eq/mole)
r — radial distance (cm)
r_o — radius of mercury jet (cm)
u — velocity component in the z-direction (cm/sec)
u_o — interface velocity component in the z-direction (cm/sec)
$\bar{u}_m$ — mean velocity of mercury jet (cm/sec)
z — distance in the direction of streaming (cm)
z' — $= \nu_m z/a^2\bar{u}_m$ (dimensionless)
δ — thickness of boundary layer (cm)
δ' — thickness of diffusion layer (cm)
μ — dynamic viscosity (g/cm-sec)
μ' — $= \mu_s/\mu_m$ (dimensionless)
ν — kinematic viscosity ($= \mu/\rho$) (cm²/sec)
σ — $= \nu_m/D$ (dimensionless)
ρ — density (g/cm³)
ρ' — $= \rho_s/\rho_m$ (dimensionless)
ϕ — $= r_o/\delta$ (dimensionless)
ψ — $= r_o/\delta'$ (dimensionless)
$_m$ — mercury (jet)
$_s$ — solution (flow)

On the Parabolic Rate Law

W. B. Jepson

Department of Chemistry, University of Exeter, Exeter, England

ABSTRACT

The parabolic rate constant k_p is reformulated in terms of the defect concentration at one interface only by introducing the free energy change of the oxidation reaction ΔG. The pressure dependence of k_p then follows naturally, and k_p is shown to have an exponential dependence on ΔG.

Of the various rate laws which have been found to describe the oxidation kinetics of metals, the parabolic relation

$$X^2 = k_p t \qquad [1]$$

connecting the thickness of the layer of reaction product X with the time of oxidation t is probably the most familiar and widely applicable. The relation between the parabolic rate constant k_p and the mobility of the moving particles has attracted considerable interest, and there have been a number of derivations (1-5).

The purpose of this paper is to re-formulate k_p in terms of the defect concentration at one interface only.

We consider a metal whose rate of oxidation is controlled by the rate of diffusion of metal ions across the oxide layer; the attacking gas is oxygen and any simultaneous anionic diffusion is assumed to be negligible. The derivation by Mott (4, 5) of k_p is easily extended to give, for an n-type oxide, the result:

$$k_p = AD_i[n_i(\mathrm{O}) - n_i(\mathrm{X})]$$
$$\mathrm{A} = 2(z+1)\Omega \qquad [2]$$

for an interstitial ion of valence z where D_i is the diffusion coefficient of the interstitial ion, Ω is the volume of oxide per metal ion, and $n_i(\mathrm{O})$ and $n_i(\mathrm{X})$ are the concentrations of interstitial metal ions at the metal/oxide and gas/oxide interface, respectively. In deriving Eq. [2], the following assumptions are made: (*a*) the regions of space charge at the two interfaces can be neglected (4); (*b*) the problem can be treated as one of steady-state diffusion through a slab of constant thickness (6, 7); and (*c*) the dissolved metal atoms are fully dissociated into ions and quasi-free electrons which in turn form an ideal-dilute solution in the oxide; to the same approximation the concentration gradient of interstitial ions across the oxide layer is linear.

Now the defect concentrations at the two interfaces are determined by the equilibria:

$$2\mathrm{M} = 2\mathrm{M}_o^{z+} + 2ze \qquad [3]$$

$$\frac{z}{2}\mathrm{O}_2 + 2\mathrm{M}_o^{z+} + 2ze = \mathrm{M}_2\mathrm{O}_z \qquad [4]$$

at the metal/oxide and gas/oxide interfaces, respectively, the symbol M_o^{z+} denotes a metal ion occupying an interstitial position. It is easy to show that

$$2\ln n_i(\mathrm{X})n_e^z(\mathrm{X}) - 2\ln n_i(\mathrm{O})n_e^z(\mathrm{O}) = \Delta G/RT \qquad [5]$$

where $n_e(\mathrm{O})$ and $n_e(\mathrm{X})$ are the concentrations of quasi-free electrons at the metal/oxide and gas/oxide interfaces, respectively, and ΔG is the free energy change per mole of the oxidation reaction

$$2\mathrm{M} + \frac{z}{2}\mathrm{O}_2 = \mathrm{M}_2\mathrm{O}_z \qquad [6]$$

at temperature T and an oxygen pressure of p atm. By assumption (a), $n_o = zn_i$ so that, after simplifying Eq. [5] and inserting in Eq. [2], we obtain:

$$k_p = AD_i n_i(\mathrm{O}) \left[1 - \exp\left\{\frac{\Delta G}{2(1+z)RT}\right\}\right] \quad [7]$$

which shows the dependence of k_p on the driving force of the reaction.

Since $n_i(\mathrm{O})$ is determined by the equilibrium represented in Eq. [3], the only pressure dependent term in Eq. [7] is ΔG,

$$\Delta G = \Delta G_o - \frac{z}{2} RT \ln p \quad [8]$$

where ΔG_o is the standard free energy change per mole of the oxidation reaction. Hence

$$k_p = AD_i n_i(\mathrm{O})[1 - \alpha p^{-s}] \quad [9]$$

where

$$\alpha = \exp \frac{\Delta G_o}{2(1+z)RT}$$

$$s = \frac{z}{4(1+z)} \quad [10]$$

If the metal ions are diffusing between vacant cation sites then, making the same approximations as before, the result is

$$k_p = AD_v n_v(\mathrm{X})\ [1 - \alpha p^{-s}] \quad [11]$$

where D_v is the diffusion coefficient of the vacancy (of valence z) and α and s are as defined in Eq. [10]; $n_v(\mathrm{X})$ the concentration of vacant cation sites at the gas/oxide interface is determined by the equilibrium:

$$2\mathrm{M}^{z+} + 2ze + \frac{z}{2}\mathrm{O}_2 = \mathrm{M}_2\mathrm{O}_z + 2\mathrm{M}^{z+}\square + 2ze\square \quad [12]$$

where $\mathrm{M}^{z+}\square$ and $e\square$ denote a vacant cation site and a positive hole, respectively. Equation [12] is sometimes formulated with the oxygen in the adsorbed state (12). By Eq. [12],

$$n_v(\mathrm{X}) = n_v^{\circ} p^s \quad [13]$$

where n_v° is the concentration of vacant cation sites in equilibrium with an oxygen pressure of one atmosphere. Equations [11] and [13] give

$$k_p = AD_v n_v^{\circ} p^s (1 - \alpha p^{-s}) \quad [14]$$

The relations in Eq. [9] and [14] are of course equivalent to the alternative formulation (8) in terms of the partial pressures of oxygen at the metal/oxide and gas/oxide interfaces, but in the author's opinion they have two advantages: the dependence of k_p on the driving force of the reaction ΔG is clearly brought out (cf. Eq. [7]) and both the pressure dependence of k_p for an n-type oxide and what may be termed the additional pressure dependence for a p-type oxide follow naturally from Eq. [8]. Thus if $\alpha << p^s$, k_p will either be independent of pressure [n-type oxide] or will vary according to p^s [p-type oxide].[1] Values of α are given in Table I for some metal oxidation reactions which satisfy the parabolic rate law and whose pressure dependence has been examined. For the first three examples it is clear that the term αp^{-s} is negligible except at very low pressures: taking nickel oxidation as an example, the term αp^{-s} is only 0.076 with $p = 10^{-3}$ atm. For copper oxidation on the other hand, $\alpha = 0.163$ and k_p is not proportional to p^s (with $p = 10^{-2}$ atm., $\alpha p^{-s} = 0.290$); the procedure adopted by Baur, Bridges, and Fassell (12) of plotting log k_p against log p to determine s as an experimental quantity is therefore incorrect. It would also appear that the generalized rate expression for pressure sensitive oxidation reactions, developed by the same authors, should be modified to include the term in αp^{-s}.

Finally, it is of interest to note that if ΔG is sufficiently small for the exponential term in Eq. [7] to be written

$$\exp\left\{\frac{\Delta G}{2(1+z)RT}\right\} = 1 + \frac{\Delta G}{2(1+z)RT}$$

the parabolic rate constant becomes

$$k_p = A \frac{D_i n_i(\mathrm{O})}{2(1+z)RT} (-\Delta G)$$

so that k_p is now proportional to the driving force of the reaction or alternatively to the electromotive force of the equivalent electrical cell, a result equivalent to that derived by Hoar and Price (3) for a film substance of constant specific conductivity.

Manuscript received July 13, 1959.

Any discussion of this paper will appear in a Discussion Section to be published in the December 1960 JOURNAL.

REFERENCES

1. C. Wagner, *Z. phys. Chem.*, **21B**, 25 (1933).
2. W. Jost, "Diffusion in Solids, Liquids and Gases," p. 383, Academic Press Inc., New York (1952).
3. T. P. Hoar and L. E. Price, *Trans. Faraday Soc.*, **34**, 867 (1938).

[1] The value of s found experimentally is usually different from that predicted (see Table I): for copper oxidation, the discrepancy has been attributed to the fact that the defects do not form an ideal-dilute solution in the oxide (8).

Table I. Values of the parameter α (11)

Oxidation reaction	Ref.	Temp, °C	α	s Predicted	s Observed
$2Ni + O_2 = 2NiO$	(8)	1000	2.4×10^{-3}	1/6	1/4
$2Co + O_2 = 2CoO$	(9)	1148	2.8×10^{-3}	1/6	1/3
$2Fe + S_2 = 2FeS$	(10)	670	1.4×10^{-2}	1/6	1/7, 1/4
$2Cu + \frac{1}{2}O_2 = Cu_2O$	(8)	1000	1.63×10^{-1}	1/8	1/7
$2Zn + O_2 = 2ZnO$	(8)	400	5.4×10^{-8}	(0)	(0)

4. N. F. Mott, *J. chim. phys.*, **44**, 172 (1947).
5. N. Cabrera and N. F. Mott, *Repts. Prog. in Phys.*, **12**, 163 (1949).
6. F. Booth, *Trans. Faraday Soc.*, **44**, 796 (1948).
7. W. J. Moore, *This Journal*, **100**, 302 (1953).
8. C. Wagner and K. Gruenewald, *Z. phys. Chem.*, **40B**, 455 (1938).
9. R. E. Carter and F. D. Richardson, *J. Metals*, Trans. AIME, 336 (1955).
10. K. Hauffe and A. Rahmel, *Z. phys. Chem.*, **199**, 152 (1952).
11. Calculated from the data listed by: O. Kubaschewski and E. LL. Evans, "Metallurgical Thermochemistry," Pergamon Press, New York (1956).
12. J. P. Baur, D. W. Bridges, and W. M. Fassell, Jr., *This Journal*, **103**, 273 (1956).

Magnetism of the Electrodeposited Films as Revealed by Electron Diffraction

S. Yamaguchi

Institute of Physical and Chemical Research, Tokyo, Japan

The path of an electron beam is deflected in a magnetic field as the result of the Lorentz effect. This phenomenon is observable in electron diffraction of a ferromagnetic substance. The magnetic induction of a ferromagnetic film was measurable from the diffraction pattern obtained from it.

Experimental

A process of double exposure was utilized in order to measure the deflection of an electron beam caused by a ferromagnetic specimen. The diffraction pattern from a nonferromagnetic substance (gold foil) was photographed beforehand, and then that of a ferromagnetic specimen was superposed on it. In this process the wave length of the electrons applied as well as the position of the photographic plate were kept fixed. Diffraction rings from these two substances were not cocentric, because the specimen had the Lorentz effect on the electrons, whereas the nonferromagnetic gold foil showed no magnetic effect on them.

Nickel Film

Nickel was deposited electrolytically on a foil of brass from an aqueous solution of nickel sulfate (1). The deposited layer of nickel was divorced from the brass foil with a dilute solution of nitric acid. The area and thickness of the nickel film prepared for the experiment were 10 x 10 mm and about 5 μ, respectively. The specimen was magnetized as illustrated in Fig. 1a. A small piece of permanent magnet (size: about 0.5 mm, coercive force: 400 Oersted) was attracted at the edge of the film. An electron beam passed through a pin hole (about 0.1 mm) found in the nickel film (see Fig. 1a). Such pin holes were formed frequently in an electrodeposited film. Figure 2a was obtained by the double exposure process with the specimen and with a nonferromagnetic gold foil. In this double diagram it is recognizable that the diffraction rings from the specimen and those from

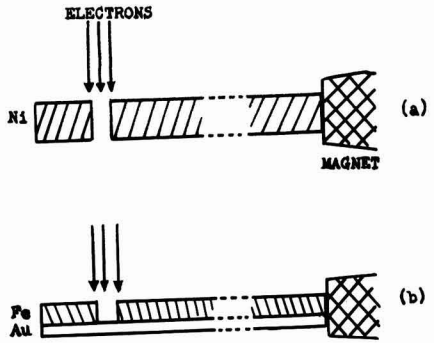

Fig. 1. Experimental arrangement: (a) for an isolated film, (b) for a composite film.

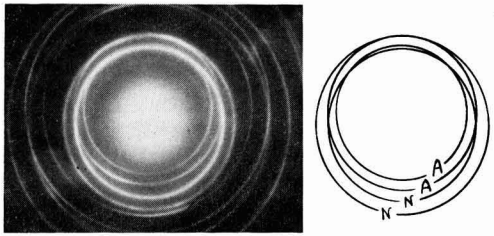

Fig. 2a (left). Diffraction pattern of a magnetized film of nickel and that of gold are superposed. The diffraction rings are eccentric as the result of the Lorentz effect. Wave length: 0.0327Å; camera length: 495 mm: Positive enlarged 2.3 times before reduction for publication. Fig. 2b (right). The main rings corresponding to Ni and to Au in (a) are indicated. N: Ni. A: Au.

the gold foil are eccentric as the result of the Lorentz effect. The main rings corresponding to the two substances are indicated in Fig. 2b (N: the nickel specimen, A: gold).

The deflection ΔZ of the incident beam caused by the magnetic specimen is measurable from the ring

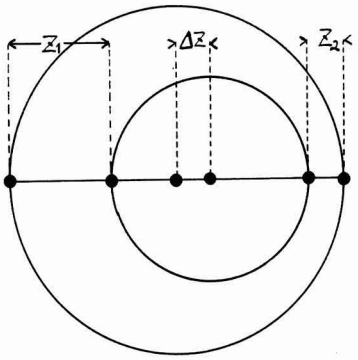

Fig. 3. Illustration for the calculation of the magnetic deflection ΔZ of the incident beam from the ring eccentricity.

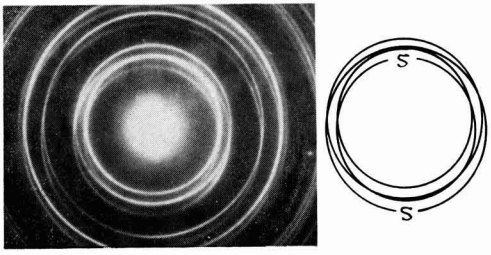

Fig. 4a (left). Diffraction pattern of the composite Fe-Au film and that of gold are superposed. Wave length: 0.0332Å. Lorentz effect. Fig. 4b (right). S shows the rings from the Fe-Au film.

eccentricity, as illustrated in Fig. 3. That is

$$\Delta Z = \frac{1}{2}(Z_1 - Z_2)$$

Under the experimental arrangement in Fig. 1 and 2 we have a relation between ΔZ and the magnetic induction B:

$$\Delta Z = \frac{eL}{mv}\int_0^l B\,dl = \frac{eL\lambda}{h}\int_0^l B\,dl \qquad [1]$$

where e is electron charge (1.6×10^{-20} emu), m is electron mass, v the velocity of the electrons, L the camera length (495 mm), λ the wave length of the electrons, and l the magnetic field region traversed by the electron beam. λ was determined with the diffraction rings of gold observed in Fig. 2. As seen from Fig. 1, l is approximately equal to the film thickness of the specimen (5 μ). In Fig. 2 we measure $\Delta Z = 0.142$ cm and $\lambda = 0.0327$Å. We obtain, therefore, $B \cong 7 \times 10^3$ gausses for the nickel film according to Eq. [1].

Iron Film

Iron was electrodeposited on a gold foil from an aqueous solution of ammonium ferrous sulfate. A composite Fe-Au film thus prepared, in which the thickness of the iron layer and that of the gold film were about 10^4Å and 5×10^2Å, respectively, was readily investigated by the present process (see Fig. 1b). Figure 4a is a double diagram obtained with the specimen and with a single film of gold. In Fig. 4b the main rings from the specimen are indicated with "S." In this diagram we recognize the ring eccentricity resulted from the magnetic effect. Here we measure $\Delta Z = 0.109$ cm and $\lambda = 0.0332$Å. According to Eq. [1], therefore, we obtain $B \cong 3 \times 10^4$ gausses.

Discussion

Figure 4 shows mainly the existence of the diffraction rings from gold. In this figure it is difficult to determine the rings characteristic of iron. This is because the electrodeposited layer of iron is not so crystalline as the gold film. In the present process, the magnetic state of the ferromagnetic layer is studied indirectly through the diffraction rings from the crystalline gold layer in the composite film. This method is suitable for the study of the magnetism of an amorphous film.

The magnetic inductions of the nickel and the iron film here measured (7×10^3 and 3×10^4 gausses) coincide with the known saturation inductions of these two substances (2). As seen from Eq. [1], it is possible to measure the thickness l of a film if the induction B of the film is known.

The successful result of a blank test for the present magnetic analysis was already shown with the two nonferromagnetic substances, i.e., here all diffraction rings were cocentric in a double exposure diagram (3).

It is of significance that the B-values determined in the present process are absolute, because Eq. [1] contains only the universal constants.

Manuscript received Oct. 20, 1958.

Any discussion of this paper will appear in a Discussion Section to be published in the December 1960 JOURNAL.

REFERENCES

1. Cf. A. G. Gray, "Modern Electroplating," p. 299, John Wiley & Sons, Inc., New York (1953).
2. R. M. Bozorth, "Ferromagnetism," p. 870, D. Van Nostrand Co., Princeton, New Jersey (1956).
3. S. Yamaguchi, *This Journal*, **106**, 268 (1959).

Polarography in Formamide

I. Some Transition Metal Ions, Zinc and Cadmium Ions

Glenn H. Brown and Hsiao-shu Hsiung

Department of Chemistry, University of Cincinnati, Cincinnati, Ohio

Formamide is a good solvent for a large number of inorganic salts as well as organic compounds. It has a very high dielectric constant (109.5 at 25°C) (1), a convenient liquid range (freezing point 2.5°C, boiling point 193°C), a very low vapor pressure (1 mm Hg at 70.5°C), and its solutions have a moderate electrical resistance. Formamide is very easily deoxygenated thus making it a good solvent for use in polarography. Moreover, formamide with anhydrous sodium perchlorate as a supporting electrolyte has a decomposition potential of −1.6 v vs. a saturated calomel electrode. Even though this voltage does not allow the voltage range of usefulness afforded by N-N′-dimethylformamide (2) (−2.4 v vs. a mercury pool) it is nevertheless a sufficiently high voltage to make it a useful solvent for polarography of many inorganic salts. The solvent has a high viscosity (3.359 cp at 25°C), but this is not a serious objection to its use.

Formamide is a very good solvent for a large number of different kinds of inorganic compounds; Colton and Brooker (3) have obtained solubility values for 47 salts. Although we have not made quantitative measurements of solubility for our polarographic studies, we have found that perchlorates are quite soluble in formamide. Also, the salts K_2NbF_7, K_2ZrF_6, K_2TaF_7, and K_2HfF_6 are all somewhat soluble in the solvent.

There appear to be only four papers in the literature concerned with the polarography of inorganic salts in formamide. Zan'ko and Mannsova (4) studied the polarography of cadmium sulfate, lead nitrate, tin (II) chloride, and zinc chloride. No supporting electrolyte was used in this study since the authors report that there is sufficient ammonium chloride (origin in synthesis of formamide) in the formamide to function as a supporting electrolyte. Letaw and Gropp (5) investigated the polarography of organic compounds such as acetophenone and anisaldehyde in formamide. They also obtained polarographic data on zinc sulfate, thallium (I) sulfate, and lead nitrate. Their supporting electrolyte was 0.1M KCl for the zinc and lead and 0.1M KNO_3 for thallium. Hook, Letaw, and Gropp (6) studied these same metal ions in formamide-acetamide mixtures. Their $E_{1/2}$ values in formamide are close to those for the same ions in water, and those in the mixed solvent are close to those in formamide.

Bruss and DeVries (7) in a study of the effect of solvents on the polarographic reduction of cations observed the $E_{1/2}$ values of bismuth, cadmium, chromium (III), and zinc ions against a silver-silver chloride electrode in a number of different solvents of which formamide was one. Their values for cadmium and zinc ions check with ours when one considers the different reference electrodes used. However, they did not report on $E_{1/2}$ value for Cr (II) to Cr (0), but did report an $E_{1/2}$ value for Cr (III) to Cr (II). We found the wave for the Cr (III) to Cr (II) to be ill-defined but were able to assign an approximate value of −0.9 v vs. S.C.E. to this transition which is close to the value of −0.83 v vs. Ag-AgCl electrode reported by Bruss and DeVries.

This paper deals with the polarography of some transition metal ions, zinc and cadmium in formamide. In this study we chose the hydrates of the salts of the electroreducible ions instead of anhydrous salts. Further studies of stability constants in nonaqueous solvents are now in progress using different ligands with some of the ions reported herein. When these studies are completed, data on the anhydrous salts will be discussed in light of the systems under observation.

Experimental

Materials.—The practical grade of formamide, obtained from Matheson Company, Inc., was purified by double vacuum distillation (2-3 mm Hg, bp 90°C). However, small amounts of water do not alter the decomposition potential of the solvent. It was found in this work that up to 3 ml of water in 25 ml of formamide did not change the decomposition potential of the formamide.

Anhydrous sodium perchlorate was used as the supporting electrolyte in this study. Anhydrous sodium perchlorate of "reagent" quality purchased from the G. Frederick Smith Chemical Company was used without further purification. The decomposition potential of a 0.2M solution of sodium perchlorate in formamide is −1.6 v vs. a saturated calomel electrode.

All perchlorates used in this study were "reagent" quality, obtained from the G. Frederick Smith Chemical Company and were used without further purification. These salts were dried in a current of dry air and dissolved as the hydrates. The cadmium sulfate was the "Baker Analyzed" reagent manufactured by the J. T. Baker Chemical Company. It was used without further purification.

In a few cases, maxima occurred in the polarographic wave and when these were found, they could be depressed by the use of gelatin.

Apparatus.—All polarograms were obtained using a L&N recording "Electro-Chemograph." The electromotive force recorded by the instrument was

checked with a "Queen Model" E-3040, three-range potentiometer manufactured by the Gray Instrument Co., Philadelphia, Pennsylvania. All diffusion currents were corrected for residual current, which never exceeded 1.5 μamp for any potential at which the diffusion current was measured.

The polarographic cell was constructed according to one described by Kolthoff and Coetzee (8) in order to eliminate the transference of water or potassium chloride into the electrolysis cell during the time required to complete the polarogram. The half-wave potentials were measured against a saturated calomel electrode.

All diffusion currents were corrected for iR drop across the electrolysis cell. The resistance of the solutions was measured with an Industrial Instruments, Inc., Model R C 16 conductance bridge. A 0.2M sodium perchlorate solution in formamide gave a resistance of 9600 ±50 ohms. In the iR corrections average values of i and R were used.

The capillary was made of Corning marine barometer tubing, which has a capillary of 28.4 μ radius, and was 10 cm in length. The capillary (open circuit) had the following characteristics: $m = 1.01$ mg/sec, and $t = 5.83$ sec/drop for $h = 64$ cm. The relationship of $m^{2/3}t^{1/6}$ was studied as a function of applied voltage for the capillary. These values for several applied voltages are: −0.4 v, 1.34; −0.8 v, 1.33; −1.20 v, 1.31; and −1.60 v, 1.26. These values were used at the appropriate places in the handling of the data.

The cell was immersed in a water bath at a temperature of 25 ±0.5°C. The electrolytic solutions were deaerated by bubbling tank nitrogen, obtained from the National Cylinder Company, through them.

Results and Discussion

Well-defined waves were obtained for the metal ions considered in this investigation. The concentrations of the electroreducible ions were varied from 0.6 to 4 mM in 0.2M $NaClO_4$ as the supporting electrolyte. In all cases the diffusion currents were proportional to the concentration. If one uses the criterion that an experimental value of the slope of a

$$\text{plot of } -E_{d.e.} \text{ vs. } \log \frac{i}{i_d - i} \text{ is } \frac{0.0591}{n} \text{ volts at } 25°C$$

and must agree with the theoretical value within 3-5 mv for a system to be reversible (9), then only one of the ions studied undergoes a reversible process (i.e., manganese). Zinc and cadmium approach reversibility while each of the other ions shows irreversibility in its electroreducible process. The copper reduction gave only a one-step wave, the same as in water.

The polarographic data on the ions investigated are to be found in Table I. The I_d values were calculated using values for t which were taken at the decomposition potential of the particular ion.

In formamide, as in water, the reduction stage of iron which gives a true curve is that from iron (II) to iron (0). On starting with iron (III) the first wave is not a true one since the reduction of iron (III) sets in at a potential which is more positive than the anodic dissolution of mercury.

Chromium (III) ion gives a stepwise reduction to chromium (II) and then to chromium (0). The first wave is not well-defined and makes the determination of the $E_{1/2}$ (approximately −0.9 v) for this step uncertain. Also, it might be pointed out that the height of the second wave is somewhat greater than twice that of the first. The chromium (II) to chromium (0) wave is well defined and can be used for evaluation of polarographic data.

Table I. Polarographic characteristics of some transition metal ions, zinc and cadmium in formamide (0.2M $NaClO_4$ as supporting electrolyte).

Salt	conc, mM/l	I_d	$-E_{1/2}$ v vs. S.C.E.	D cm²/sec x 10^5	0.059/n
$Cr(ClO_4)_3 \cdot 6H_2O$	2	1.65	1.56*	0.184	0.119
$Mn(ClO_4)_2 \cdot 6H_2O$	2	1.78	1.57	0.216	0.035
$Fe(ClO_4)_2 \cdot 6H_2O$	2	0.91	1.40†	0.056	0.059
$Co(ClO_4)_2 \cdot 6H_2O$	1	1.81	1.20	0.292	0.072
$Ni(ClO_4)_2 \cdot 6H_2O$	2	0.99	0.98	0.066	0.083
$Cu(ClO_4)_2 \cdot 6H_2O$	2	1.28	0.12	0.110	0.077
$Zn(ClO_4)_2 \cdot 6H_2O$	2	1.71	1.07	0.197	0.043
$3CdSO_4 \cdot 8H_2O$	2	1.85	0.69	0.229	0.049

* Value is for chromium (II) to chromium (0).
† Value is for iron (II) to iron (0).

Manuscript received May 22, 1959.

Any discussion of this paper will appear in a Discussion Section to be published in the December 1960 JOURNAL.

REFERENCES

1. G. R. Leader, *J. Am. Chem. Soc.*, **73**, 856 (1951).
2. G. H. Brown and R. Al-Urfali, *ibid.*, **80**, 2113 (1958).
3. E. Colton and R. E. Brooker, *J. Phys. Chem.*, **62**, 1595 (1958).
4. A. M. Zan'ko and F. A. Mannsova, *J. Gen. Chem. (U.S.S.R.)*, **10**, 1171 (1940); *C.A.*, **35**, 2808 (1941).
5. H. Letaw, Jr., and A. H. Gropp, *J. Phys. Chem.*, **57**, 964 (1953).
6. J. H. Hook, H. Letaw, Jr., and A. H. Gropp, *ibid.*, **58**, 81 (1954).
7. D. B. Bruss and T. DeVries, *J. Am. Chem. Soc.*, **78**, 733 (1956).
8. I. M. Kolthoff and J. F. Coetzee, *ibid.*, **79**, 870 (1957).
9. L. Meites, "Polarographic Techniques," p. 104, Interscience Publishers, Inc., New York (1955).

Fabrication, Properties, and Applications of Some Metallic Silicides

R. D. Grinthal

American Electro Metal Division of Firth Sterling Inc., Yonkers, New York

Recent requirements for higher and higher operating temperatures in the rocket and missile field, nuclear reactors, and many other applications have led to the consideration of the so-called "refractory hardmetals" for use as one class of structural materials in the temperature ranges where today's superalloys are no longer useful.

The term refractory hardmetals includes compounds of the transition metals with boron, carbon, nitrogen, silicon, and sulfur. These materials are characterized in general as hard, brittle interstitial compounds which have very high melting points. They differ from the corresponding oxides mainly in their electrical and thermal behavior which is distinctly metallic. They are good conductors of electricity and heat. Many are even better in this respect than austenitic stainless steel and titanium which are among the poorer conducting metals. Thus the term refractory hardmetals serves to distinguish this class of materials from high melting metals such as tungsten and molybdenum and from the more refractory oxides.

Table I. Physical properties of some metallic silicides.

Silicide	Crystal structure	Density g/cm³	Melting point, °C	Hardness, kg/mm² (100 g load)	Electrical resistivity, micro-ohm-cm
Ti_5Si_3				986	170
$TiSi_2$	Orthorhombic	4.4	1540	618	123
$ZrSi_2$	Orthorhombic	4.9	1520	1030	161
V_3Si	Cubic	5.7	2000		
VSi_2	Hexagonal	4.7	1750	1090	9.5
$NbSi_2$	Hexagonal	5.3	1950	1050	6.3
$TaSi_2$	Hexagonal	8.8	2400	1560	8.5
Cr_3Si	Cubic	6.5	1730	1100	43
CrSi	Cubic	5.3	1600	1230	139
$CrSi_2$	Hexagonal	4.4	1570	1150	600
Mo_3Si	Cubic	9.0	2100	1310	
$MoSi_2$	Tetragonal	6.2	1870	1260	21.5
WSi_2	Tetragonal	9.3	2150	1090	334
$ThSi_2$	Tetragonal	7.8	1600	1120	
USi	Orthorhombic	10.4	1600		
$USi_2(\alpha)$	Tetragonal	9.0			
$USi_2(\beta)$	Hexagonal	9.2	1700		
YSi_2	Orthorhombic	4.5	1500		
$LaSi_2$	Tetragonal	5.0	1500		
$EuSi_2$	Tetragonal	5.5	1500		
$GdSi_2$	Orthorhombic	6.4	1500		
$DySi_2$	Orthorhombic	6.8	1500		

Their stability in oxidizing atmospheres at high temperature falls between that of the refractory metals and the oxides. Some of these hardmetals have excellent resistance to oxidation at elevated temperatures while others must be protected or used in nonoxidizing atmospheres. This discussion is concerned only with metallic silicides, which are among the most stable of the refractory hardmetals under oxidizing conditions.

Table I lists physical properties of some silicides of the transition metals and metals of the lanthanide and actinide series. A great variety of crystal structures are encountered in these materials, from the orthorhombic $TiSi_2$ through the cubic V_3Si, tetragonal $MoSi_2$, and hexagonal $CrSi_2$. While most monocarbides and mononitrides are isomorphous with each other and most diborides are isomorphous with each other, this is not true of the silicides.

The melting points of the silicides which are known are quite high, although not as high as the corresponding borides or carbides in most cases. The disilicides in particular, however, have outstanding chemical stability, and resistance against oxidation and attack by acids is maintained over large temperature ranges.

Production

Silicides are produced by several methods, the most important of which are as follows.

Direct combination of the metal and silicon.—This can be accomplished by either fusion or sintering. Fusion temperatures are extremely high, necessitating electric arc or carbon tube furnaces. Sintering of mixtures of powders produces a violently exothermic reaction at temperatures ranging from 900°-1500°C, depending on the material. In many instances the metal hydride can be substituted for the metal powder. Protective atmospheres of argon, hydrogen, or vacuum are necessary to prevent oxidation.

Reduction of metal oxides with silicon.—Silicon can reduce metal oxides in the same manner as boron or carbon, but extremely high temperatures (above 1500°C) are necessary, and the silica which forms as a reaction product is difficult to remove completely. If the reduction is carried out in vacuum, however, the silica contamination is held to a minimum by

removal of the more volatile SiO before it can condense on the furnace charge.

Reaction between metal oxides and silica in the presence of carbon.—This process is similar to direct reduction with silicon except that the carbon serves to reduce both the metal oxide and the silica, forming CO and CO_2 which do not contaminate the reaction product. This process is best carried out at high temperature in an electric arc furnace.

The aluminothermic process.—The reaction of metal oxide, quartz, and either aluminum or magnesium, performed in clay crucibles in the presence of sulfur, yields fused silicides which can be treated chemically to remove undesirable reaction products. The sulfur serves to form a liquid slag which is decomposed readily by water.

Reaction of metal with silicon halide.—Silicon tetrachloride, when passed over heated metal powder in the presence of hydrogen, reacts to form the metal silicide and HCl at temperatures ranging from 1100°-1800°C, depending on the material. This method is also used to siliconize metal surfaces and produce protective coatings in place.

Fused salt electrolysis.—By electrolysis of fused alkali fluosilicate baths containing metal oxides, silicide crystallites are deposited on the cathode.

Fabrication

Bodies may be fabricated from the silicide powders by several powder metallurgical methods. Hot pressing (simultaneous application of heat and pressure) is done in graphite dies and produces dense parts. Limitations of this process, however, only allow production of fairly small, simple shapes which have regular cross section, no undercuts, and no thin walls. Since the graphite dies cannot be used more than once or twice, this is not a means of achieving high production rates.

Cold pressing followed by sintering allows the use of steel or carbide dies and can be adapted for fairly high volume production. The same limitations in size and shape apply here as were described for hot pressing. Long time sintering in a protective atmosphere consolidates and densifies the part, but the shrinkage which occurs makes it more difficult to hold close dimensional tolerances. This can be compensated for in long run production by allowing for shrinkage in the die design. Cold pressed and sintered parts may have slightly different mechanical properties than hot pressed parts.

Extrusion of the silicide powder after it has been mixed with plastic is also possible. This method is limited to simple cross sections which have straight sides, but for certain parts it can be a high volume production process. The sintered piece may be slightly porous due to voids left when the plastic burns out, but this is not a serious drawback in most cases.

Slip casting is a ceramic process which is currently being applied successfully to metal powders. The shape of the part produced by this method is far more unrestricted than any previously described, but the process at present is in a developmental state and, although some materials are produced in quantity, most would require considerable experimentation before usable parts could be produced on a volume basis. Using this method, however, re-entry angles, undercuts, thin-walled sections are all possible. Size is restricted only by the weight that the green piece can support without collapsing during sintering.

Another fabrication method which may be employed in special cases is flame spray forming. Here the silicide is extruded into rod, which is sintered, then fed through a flame spray gun and deposited on a pattern as a coating. The coating is built up to any desired thickness and the substrate removed chemically, leaving a strong, formed body which does not require further sintering. Density is 80-90% of theoretical. If this is not satisfactory for the application, it can be improved somewhat by sintering. This method may also be used, of course, to produce protective coatings on substrate materials which are subjected to oxidizing conditions which they cannot withstand normally. The coatings are slightly porous and quite brittle, but the porosity is not interconnected and is usually sealed by the protective silicate which forms during high-temperature oxidation.

Properties

The mechanical properties of these materials are generally similar. They are hard, brittle, and have appreciable compressive and transverse rupture strength which is retained at temperatures up to 1000°-1200°C. Like most interstitial compounds, they are sensitive to impact loading and cannot be relied on in applications where tensile strength is necessary. The properties of any given material can be varied somewhat by changes in the fabrication method or by the presence of small amounts of impurities which may come from various methods of preparation. Porosity exerts a major influence in this respect and, since most test samples are prepared by powder metallurgical methods, some porosity is almost always present.

Some of the properties of $MoSi_2$, chosen here as a typical example, are listed in Table II. This material is perhaps the best known silicide and may be closest to having real commercial application. The figures given should be taken only as representative values, since the properties can vary over a wide range when variations in fabrication technique or impurity content are employed.

Modifications

Several attempts have been made to apply the cermet principal to the hardmetals and improve impact strength by addition of a third metal, which is intended to act as a binder as in the case of WC-Co

Table II. Mechanical properties of $MoSi_2$

Hardness		80-87 RA
Compressive strength		100-350,000 psi
Modulus of elasticity		59×10^6 psi
Modulus of transverse rupture	20°C	36-67,000 pst
	1000°C	51-86,000 psi
Tensile strength	1300°C	41,000 psi
Stress to rupture (100 hr life)	1000°C	13,000 psi
Oxidation resistance	Excellent to 1700°C	

and TiC-Ni. These two cases, however, have proved to be the exception rather than the rule. Several factors must be considered in choosing a metal addition to a silicide system. First, the metal to be added should be one which does not form silicides readily and, second, the silicide should be the lowest possible in the system. If, for instance, copper should be added to $MoSi_2$, the result would not be a two-phase system consisting of $MoSi_2$ in a copper matrix. The copper would react with the $MoSi_2$ forming a copper silicide and leaving a lower molybdenum silicide such as Mo_3Si_2 or Mo_5Si. These materials are all brittle and, in addition, do not have the excellent oxidation resistance of $MoSi_2$. The same results are obtained when cobalt, platinum, nickel, chromium, or titanium are added to $MoSi_2$. When metallurgical equilibrium is obtained, the starting materials are never present in their original form but always react to form new compounds, solid solutions, or ternary compounds which are sometimes even more brittle and less stable than the original materials.

Several investigators have worked with the silicide-silicide systems which, in many cases, act like binary systems between elements. It is possible in this manner to produce modifications of some silicide structures by addition of only a few mole per cent of a second silicide. For instance, $TiSi_2$ and $MoSi_2$ are not isomorphous, and $TiSi_2$ is practically insoluble in $MoSi_2$. However, a few mole per cent $MoSi_2$ added to $TiSi_2$ changes the orthorhombic structure to a hexagonal one which is intermediate between $TiSi_2$ and the tetragonal $MoSi_2$. The two compounds form a third phase which has a wide range of homogeneity and, although similar to the parent compounds, it possesses unique properties of its own.

$MoSi_2$ and WSi_2 are isomorphous, and behavior similar to the above was also noted with $TiSi_2$ and WSi_2. $CrSi_2$ and $MoSi_2$ are mutually soluble in one another in very large amounts, with a narrow two-phase region between them in the center of the diagram. Other pseudobinary systems investigated include $ZrSi_2$-$TiSi_2$, WSi_2-$CrSi_2$, VSi_2-$TiSi_2$, $CrSi_2$-$TaSi_2$, USi_2-$MoSi_2$, $MoSi_2$-WSi_2. The last pair forms a complete series of solid solutions. Investigation of systems like these may lead to methods of changing physical, electrical, or mechanical properties of these materials so that they can be tailored to suit specific applications.

Applications

Many of the silicides have been tested for potential applications in various fields. $MoSi_2$ is perhaps the best known of the group and the one closest to commercial use. A new type of heating element has been developed which is based on this material. It can be heated in air for long periods at temperatures up to 1650°C without damage. The excellent stability of $MoSi_2$ has led to its use as a protective coating for molybdenum. This coating can be applied by flame spraying or by siliconizing a molybdenum surface. It has also been found to be resistant to corrosion by molten boron oxide at elevated temperatures. Other potential applications where impact loading is not a factor may be in rocket nozzles, afterburners (as a coating), or as refractory brick.

Some investigation has been carried out concerning the possible use of solid solutions of $MoSi_2$ and USi_2 as nuclear fuel elements. This may allow high reactor temperatures and minimize the distortion usually encountered when uranium metal or alloys are used as fuel elements.

A great deal of interest has developed lately in the use of the so-called refractory metals molybdenum, tungsten, tantalum, and niobium for very high-temperature applications. If the atmosphere is oxidizing, these materials must be protected, and the possibility of coating each with its corresponding silicide is certainly an interesting one.

$CrSi_2$ and $TiSi_2$ may find applications where the combination of high temperature stability and light weight are of interest.

Among the rare earth silicides, gadolinium disilicide has been considered as a possible control rod material, dysprosium disilicide has been used as a counter for neutron flux density measurements, and europium disilicide has been fabricated for a nuclear application.

As more information is compiled about these materials, other applications will undoubtedly be suggested and investigated, and one or two will find commercial outlets. When this happens, the whole class of hardmetal materials will begin to come into more popular use, and it is hoped that the fear of using brittle materials will subside finally.

Manuscript received June 4, 1959. This paper was prepared for delivery before the Philadelphia Meeting, May 3-7, 1959.

Any discussion of this paper will appear in a Discussion Section to be published in the December 1960 JOURNAL.

REFERENCES

1. P. Schwarzkopf and R. Kieffer, "Refractory Hard Metals," Macmillan Co., New York (1953).
2. R. D. Grinthal, WADC, TR 53-190, Part VI, "New High Temperature Materials" (May 1958).
3. I. Campbell, Editor, "High Temperature Technology," John Wiley & Sons, Inc., New York (1956).
4. Climax Molybdenum Co., Bulletin Cdb-6, (January 1956).
5. R. Kieffer and F. Benesovsky, "Silicides of the Transition Metals of the 4th, 5th, and 6th Group of the Periodic Table." Powder Metallurgy (1954), The Iron and Steel Institute (Dec. 1954).

Brief Communication

Nodule Growth on Al_2O_3 Coatings

R. J. Jaccodine

Bell Telephone Laboratories, Incorporated, Allentown, Pennsylvania

This communication concerns the growth of nodules or hillocks on surfaces of heaters sprayed with Al_2O_3 coatings.

In studying heater-cathode breakdown phenomena, the method used (1) involved helically winding a bare tungsten heater or other bare metals about the Al_2O_3 coated heater: these were pumped and sealed off at 10^{-6} mm Hg. A variable heater voltage then was applied to both heaters to obtain the desired thermal conditions (Al_2O_3 coated heater at 1200°C optical and bare tungsten heater 900°C optical), and a d-c voltage of 180 v with coated heater positive was applied between both heaters to set up a potential gradient. During the course of this study, it was observed that nodules or hillocks of Al_2O_3 surface to the outside tungsten heater. These growths appeared gradually over a period of several months. The size of the nodule seemed to be limited by the gap formed between the outside base tungsten heater and the alumina surface. Figure 1 shows the hillock growth with the helically wound outside heater in place. Figure 2 shows the nodules with the outside heater removed. As can be noted, the nodules are aligned helically and occur only under the outside heater. The tops of the hillocks appear loosely packed and powdered as compared to the more substantial-looking base region. However, upon probing with a fine metal probe, the whole hillock and the region immediately adjacent to and under its base was found to be powdered, less adherent, and more loosely packed than adjacent normal regions of the coating.

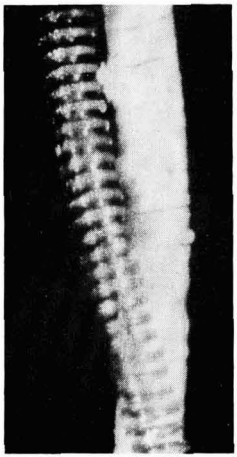

Fig. 1. Hillock growth with helically wound outside heater in place.

Fig. 2. Nodules with outside heater removed

The presence of hillocks might be explained by several possible mechanisms. There may be an Al_2O_3-W (or impurities in W) reaction; bulk and/or surface diffusion under the influence of thermal and electrical gradients and also reaction involving vapor phase constituents.

The question of an Al_2O_3-W reaction at elevated temperatures remains open. Brewer and Searcy (2) claim Mo and W are nonreactive toward Al_2O_3. Wartenberg (3) and also Ackermann and Thorn (4) claim Al_2O_3 and W do react at high temperatures and form AlO.

Vapor phase reactions have been noted by various workers. Brewer and Searcy (2) give data on the Al-Al_2O_3 system, particularly the pressure of gaseous species over liquid Al_2O_3 and over liquid Al and solid Al_2O_3 mixture. Webb and Forgeng (5) account for the growth of single crystal Al_2O_3 whiskers by a vapor phase reaction in which AlO is adsorbed on an aluminum oxide surface where disproportionation takes place according to the reaction

$$3AlO(g) = 3AlO(surface) = Al_2O_3(s) + Al(l)$$

They noted globules of aluminum metal at the tips of their Al_2O_3 single crystal whiskers.

There seems a good possibility that the nodules grow as a result of an interaction of the above mechanisms. A reaction of Al_2O_3 with tungsten or the impurities in tungsten (carbon, for example) to give AlO and other vapor species, and the chemical disproportionation might be indicated by the identification of aluminum which coats in spots the wound outside heater and after longer periods slightly darkens the inside of the tube bulb. Chemical identification of these bright metallic spots was made by removing the outside tungsten heater and having qualitative spectrochemical analysis made of these areas. In Fig. 1, some of these spots can be seen on the outside base tungsten heater. Diffusion mechanism can be invoked to aid in the buildup of the nodules and could account for the observation that the regions immediately adjacent to the base of the nodules are loosely packed and in some instances are concave or moat-like.

These hillocks have also been observed in tubes in which the outside "heater" was made of nickel.

Manuscript received Sept. 3, 1959.

Any discussion of this paper will appear in a Discussion Section to be published in the December 1960 JOURNAL.

REFERENCES

1. R. J. Jaccodine, *This Journal*, **106**, 530 (1959).
2. L. Brewer and A. W. Searcy, *J. Am. Chem. Soc.*, **73**, 5308 (1951).
3. H. V. Wartenberg, *Ceramic Abstracts*, **7**, 110 (1928).
4. R. J. Ackermann and R. J. Thorn, *J. Am. Chem. Soc.*, **78**, 4169 (1956).
5. W. W. Webb and W. D. Forgeng, *J. Appl. Phys.*, **28**, 1448 (1957).

FUTURE MEETINGS OF
The Electrochemical Society

Chicago, Ill., May 1, 2, 3, 4, and 5, 1960

Headquarters at the Lasalle Hotel
Sessions probably will be scheduled on
Electric Insulation (including a symposium on "Electrolytic Capacitors"), Electronics (including Luminescence and Semiconductors), Electrothermics and Metallurgy (including symposia on "High-Purity Vanadium—Its Preparation, Properties, and Alloys" and on Rhenium, and a round table on "Methods of Reducing Iron Ores"), Industrial Electrolytics, and Theoretical Electrochemistry

★ ★ ★

Houston, Texas, October 9, 10, 11, 12, and 13, 1960

Headquarters at the Shamrock Hotel
Sessions probably will be scheduled on
Batteries, Corrosion, Electrodeposition, Electronics (Semiconductors), Electro-Organics, and Electrothermics and Metallurgy

★ ★ ★

Indianapolis, Ind., April 30, May 1, 2, 3, and 4, 1961

Headquarters at the Claypool Hotel

★ ★ ★

Detroit, Mich., October 1, 2, 3, 4, and 5, 1961

Headquarters at the Statler Hotel

Papers are now being solicited for the meeting to be held in Houston, Texas, October 9-13, 1960. Triplicate copies of each abstract *(not exceeding 75 words in length)* are due at Society Headquarters, 1860 Broadway, New York 23, N. Y., *not later than June 1, 1960* in order to be included in the program. *Please indicate on abstract for which Division's symposium the paper is to be scheduled and underline the name of the author who will present the paper.* Complete manuscripts should be sent in triplicate to the Managing Editor of the JOURNAL at 1860 Broadway, New York 23, N. Y.

Papers submitted for presentation at the meeting become the property of The Electrochemical Society and may not be published elsewhere, in whole or in part, unless permission is requested and granted by the Society. Papers already published elsewhere, or submitted for publication elsewhere, are not acceptable for oral presentation except on invitation by a Divisional program Chairman.

Some Practical Aspects of Copper Refining in a Multiple System Tank House

M. A. Mosher

Raritan Copper Works, Perth Amboy, New Jersey

Weird Character of the Tank House

In this day of rapid revolution, startling innovation, and overnight obsolescence in industrial processes and equipment, the electrolytic copper tank house stands and has stood for nearly three-quarters of a century as a fixed and stubborn example of resistance to radical change. In the great copper, zinc, and nickel industries so completely dependent on it, the tank house seems to be considered a fundamental thing, comparable in our physiology to the process of metabolism, and in nature to "Old Man River" who "just keeps rollin' along."

The typical copper tank house with its hundreds of cells and thousands of electrodes and millions of gallons of circulating solution, is for the greater part of each 24-hr day a quiet and unspectacular place, with only the faint purring of pumps and the gentle flow of electrolyte through the tanks to indicate that it is actually functioning. Almost unique among the great producing units of modern industry, the tank house makes most of its production in majestic and peaceful silence, in marked contrast to the ceaseless roar of furnaces, the din of machinery, and the noisome reactions of large chemical processes.

Of course there are a few hectic hours in each day when a tank house, like a restless infant, has to be fed and changed, but that is only to keep it healthy and behaving properly.

The Tank House Boss

In line with these unique characteristics of the operation, long exposure to tank house work tends to develop a rather peculiar type of chief operator or superintendent, and having been one of these, I will briefly describe him for you, even though by comparison with the masterful and dynamic operators of other types of processes, he may seem drab and uninteresting.

He tends to become a slave of the established routine which he has worked out, the hard way, to get the best results. He learns to live with and keep alert to a staggering number of small easily overlooked operating details, because he knows from bitter experience that disregard of any of them may upset his whole show. He is slow to arrive at conclusions about process difficulties because he knows that dozens of inter-related factors are involved in every operating crisis he has to deal with. He develops a militant aversion to any radical innovations or changes in his methods of operation because he feels their adoption may result in complications which will jeopardize vital production. And, finally, he develops a great patience in the face of operating adversity, realizing that, in most cases of process sickness in a tank house, there is no miracle-drug cure.

Contrary as these characteristics of a good tank house operator may seem, there is much justification for them in tank house work for the following reasons:

1. The tank house process is essential for economically providing the standardized high-purity product on which his company or division depends for its existence. This is a tremendous responsibility for its operator, and consciousness of this fact naturally makes him conservative and jealous of his time-proven methods and procedures.

2. The tank house operator knows that it takes months or even years successfully to work out worthwhile changes or innovations, because every move must be made with care and patience to avoid upsetting the scheduled flow of large-scale continuous production.

3. No matter how eagerly the tank house operator may want process improvement through research, he knows from many a disappointment that the best of research results can fail miserably when applied to full-scale commercial operation. In fact there are few other industrial operations where laboratory or small-scale tests will provide so little usable data for full-scale application.

Tank House Improvements

You may wonder why I have tried to give you a picture of the typical tank house superintendent, but through it I think we have arrived at the main reason why changes and improvements in tank house operation for the past half century have been somewhat limited in scope, and chiefly in the area of construction materials, physical arrangement, and improved mechanical equipment for handling anode input and cathode production. These advances can be listed as follows:

Improved building walls and roof construction, using such materials as glazed hollow tile and Porete roof slabs that afford insulation against loss of heat and minimize condensation when outside temperature is low.

Conversion to reinforced concrete cell construction to replace wood.

Improved types of solution line insulation to provide protection against the passage of stray electrolytic current, such as the use of plastic pipe and tubing to replace lead and rubber.

Use of heat exchangers constructed of corrosion-proof materials, in place of lead pipe heating coils. This more efficient solution heating equipment has made possible an increase of about 10°F (5.6°C) in the accepted temperature for electrolyte entering the cells.

Larger cells to permit the use of higher circuit amperage and to reduce the number of unit loads of anodes and cathodes to be handled by crane.

Improved addition agents and better addition agent control.

Improved methods for inspection of cells in operation, particularly the introduction of the Gaussmeter for the detection of shorted cathodes.

Continuous filtration of make-up solutions.

Improved pump design and construction, using stabilized stainless steel.

The racking of anodes at the casting furnace and the mechanical washing and loading of cathode production in the tank house were introduced about 35 years ago. At about the same time the method of stripping starting sheets was changed from horizontal to vertical handling. That about sums up the improvements in mechanical handling since overhead electric cranes for tank-load lifts were introduced in the early 1900's.

Present Day Equipment and Operation

The general acceptance and adoption of most of these advancements by the various refineries in the last two decades has resulted in a fair degree of standardization in both equipment and operation. We can therefore discuss these accepted essentials of present day tank house equipment and operation with assurance of their almost general application.

Our discussion will be confined to the Walker Multiple System lay-out with the electrodes in parallel in each cell and the cells themselves in series in the electrolytic circuit. In the original Walker system current was passed from tank to tank by means of a conductor bar of small cross section placed on the common partition between adjacent tanks. The contact end of the cathode rods of the first tank rested on the conductor bar in alternation with the contact lugs of the anodes in the second tank. This arrangement has been largely superseded by the Whitehead contact which eliminates the conductor bar by having the contact end of the cathode rods rest directly in a slot in the contact lug of the anodes. As much as 5 mv of *IR* drop per cell is saved by this direct contact.

Electrolytic Cells

Two general types of reinforced concrete construction have proved satisfactory. One type comprises the assembly of precast slabs to form a row or tier of cells with partitions common to two tanks. The use of replaceable planks of heavy wood for the bottoms of these cells is generally favored. The precast concrete elements are so fitted and interlocked that only a few bolts and stays are required to make the entire tier a rigid construction unit. All types of cells have a bottom outlet for the removal of electrolytic slime, and in many designs another outlet is provided in the end wall of the cell a few inches above the bottom for the decantation of electrolyte prior to the removal of slime. Bottom outlets discharge into a system of launders which convey the slime slurry by gravity to pumps in the cellar. The other type of construction is the cast-in-place monolithic tier of reinforced concrete.

Insulating slabs of glass or stoneware are placed between the tank bottoms and the supporting piers which rise from a 7 to 8 ft cellar. Tiers or rows are usually designed in pairs as sections. The section is the operating unit in practically all tank houses, as the electrolytic current bus bars are so arranged that the current can be conveniently applied to or cut off from it to permit removal or replacement of anodes, cathodes or electrolyte.

Eight-pound 6% antimonial lead is still universally used for cell linings, but there is considerable testing and experimentation with several types of acid-resisting plastic materials.

Solution Lines and Tanks

Solution lines for conveying electrolyte to and from the cells have traditionally been of lead with lengths of insulating rubber tubing at the cell inlet and outlet. However, polyvinyl tubing is replacing rubber in many tank houses and there have recently been several installations in which p.v.c. pipe and p.v.c. lined launders have replaced lead pipe and lead linings. Increasing use of plastics in place of lead has resulted from the need to eliminate conducting paths through which destructive current can stray from the electrolytic circuit.

Lead-lined steel or steel skeleton tanks are still favored for storage, settling, and mixing of tank house solutions, although there have been many trial installations of plastic-lined tanks.

Pumps

Centrifugal pumps of all types, both horizontal and vertical, are in general use, but lead construction has been almost entirely abandoned in favor of stabilized stainless steel alloys. Use of the latter metal makes it necessary to protect fully the pumps from electrolytic corrosion resulting from stray current which gives the pump positive polarity.

Electrolyte—Composition and Temperature

The aqueous solution of copper sulfate and sulfuric acid used in electrolytic copper refining can vary widely in chemical composition, specific gravity, and temperature and still give satisfactory results in the production of high-purity cathode copper.

The content of these electrolyte constituents is usually adjusted to compensate for the presence of contaminating salts which accumulate from the solution of anode impurities. For example, sulfuric acid content can range from 150 to 220 g/l, but in most tank houses is maintained near 200 g/l since this concentration has a high electrical conductivity and usually avoids the anode polarization which results from the reduced solubility of impurity salts caused by high acid content. Likewise copper content as sulfate may range from 40 to 55 g/l but is usually maintained at 45 g/l. This content insures pure copper deposition, yet allows for the presence of reasonable amounts of soluble impurities. The copper content of the electrolyte tends to increase by about 1.5% of the copper deposited. A sufficient amount of electrolyte is therefore continually passed through plating-out or liberator cells equipped with lead anodes. This maintains the desired level of copper content in the entire body of electrolyte, and the copper thus removed is of normal high purity.

The beneficial effect of temperature in maintaining solubility of the salts is important. Electrolyte temperature can range from 120°F (48.9°C) to 150°F (65.6°C) and most tank houses use 140°F (60°C) or higher at the cell inlet to insure high solubility as well as to lower specific gravity, which facilitates movement of the electrolyte through the cell.

Of the soluble impurities which accumulate from normal corrosion of the anode, arsenic, antimony, bismuth, and nickel give the operator the most concern and make it necessary for him to keep close control of copper and acid content as well as temperature. Of these four anode impurities, nickel remains almost entirely soluble in the electrolyte. Much of the arsenic, antimony, and bismuth forms complex compounds, probably arsenates, which are insoluble and precipitate with the slime. While the electrolyte can safely tolerate nickel up to 20 g/l and arsenic up to 15 g/l, antimony and bismuth can become troublesome when they exceed 0.5 g/l. Difficulty with

electrolytic impurities can be minimized by reducing the sulfuric acid content to as low as 125 g/l, and holding copper content down to 45 g/l. The total amount of soluble impurity elements should not be permitted to exceed 30 g/l.

Any appreciable amount of soluble selenium and tellurium, introduced through return solutions from the leaching of electrolytic slime, can cause havoc in the tank house, since these elements cement out on the cathode surfaces and destroy the continuity of crystal growth. The result is a coarse, granular deposit which in extreme cases becomes nonadherent and falls from the cathode.

It should be noted that soluble impurities in the electrolyte appreciably increase its resistivity and can become a significant factor in the cost of electric power.

Electrolyte Purification

Except for minor modifications, the general procedure for removing arsenic, antimony, and nickel to maintain reasonable electrolyte purity is as follows:

The required volume of electrolyte is diverted continuously through liberating cells for plating out the copper. The solution is then further electrolyzed in outdoor tanks to deposit arsenic and antimony. The resulting high-acid nickel-bearing solution is evaporated to approximately 60° Be', which precipitates the nickel as a crude sulfate. With proper washing and centrifuging this product is marketable. The resulting "black acid" and wash waters are returned to the electrolyte, or subjected to acid distillation to remove iron, calcium, magnesium, sodium, and potassium salts. It is possible to remove appreciable amounts of calcium and magnesium salts by isolating batches of decopperized solution and letting these salts crystallize out at outdoor temperature.

Electrolyte Conditioning

Early in the development of electrolytic copper refining it was found that the electrolyte required certain additions to produce consistently firm and relatively smooth cathode deposits free from entrapped impurities and sprouting growths which would short circuit to the anodes. Common salt to introduce chloride ions was the first of these additions and is supposed to have been adopted after the benefits of an accidental intake of sea water for solution make-up had been noted at an east-coast refinery. Most refineries now add salt or hydrochloric acid to maintain a chlorine content of 0.02 to 0.035 g/l. The exact function of the chloride ion is not well understood, but it precipitates dissolved silver and improves the physical characteristics of the cathode deposit. Several refineries have noted difficulty with sandy, nonadherent cathode deposit when chlorine content was permitted to fall below 0.008 g/l.

Organic additions are also necessary in order to obtain a fine-grained, firm cathode deposit which remains relatively free from sprouts and protrusions during many days of plating. Animal glue, a complex protein, has long served as the most effective organic addition agents, apparently due to the slight cathode polarization which it causes. Other organic compounds work well in conjunction with glue but not to the extent of displacing it entirely. Among these are casein, thiourea, and sulfonated products such as goulac and bindarene from sulfite liquors, and Avitone, a sulfonated petroleum derivative. Orzan A, an ammonium ligno-sulfonate and Separan, a flocculating agent, are also used by certain refineries. These sulfonated compounds appear to modify the action of glue, tending to decrease its polarization effect and counteracting the excessive hardness and sprouting of the deposit which can result from an overdose of glue alone. Several refineries find that an addition of light petroleum oil emulsified in electrolyte is beneficial in tempering the action of glue. Each refinery has developed from experience an organic addition agent formula which gives the best results under its own process conditions, and the amounts added vary widely. Per ton of cathode deposition, glue additions range from 0.01 to 0.3 lb, the usual amount being about 0.1 lb. Modifying agents are added in a ratio of 2, 3, or 4 times the weight of glue. Addition agents are dissolved or emulsified in relatively large volumes of water and continuously introduced in the circulating electrolyte reservoirs, preferably by mechanical reagent feeders.

Daily evaporation of water from the electrolyte averages 2-3% of the total volume being heated and circulated through the cells. This evaporation has to be carefully and continuously replaced, either with clean water or "make-up" solution, which results from the washing of cathodes and anode scrap, or from the leaching and washing of electrolytic slime. Make-up solution must be thoroughly blended and kept warm, so that it will mix readily when added continuously to the circulating electrolyte. If water is required in addition to available make-up solution, it should be clean and warm and added in a small stream at a point where it will mix in thoroughly. Making up evaporation is a critical item in tank house operation, since careless addition of solution or water causes localized dilution of the electrolyte. This can quickly upset the proper functioning of all cells receiving it.

The cathode surfaces in cells receiving diluted electrolyte even for a short period will show areas of needle or whisker-like copper deposit, which will later develop into short-circuiting growths.

Electrolyte Heating

Low pressure steam is universally used by means of heat exchangers, immersion heaters, or closed coils. Depending on building construction and climate, steam requirements average roughly one pound for each pound of cathode production. It is important that during cold weather building ventilation be regulated to maintain a minimum temperature of 80°F (26.7°C).

Karbate (resin-bonded carbon) tubes are used for conducting the electrolyte through heat exchangers. Stabilized stainless steel jackets carry the stream in immersion or plate coil heaters, and lead pipe is used for closed coils. The Karbate tube heat exchanger has been in favor in recent years because of its compactness and high rate of heat transfer.

Whatever the type of heating apparatus used, the condensate water is usually collected and utilized through a separate hot water system for all process washing and electrolyte make-up purposes. This avoids eventual contamination of the electrolyte with prolonged use of raw water and is an important factor in the economy of using steam for heating.

Electrolyte temperature much below 120°F (48.9°C) will, with most refinery electrolytes, permit salting-out of sulfates and bring on anode polarization which upsets the electrolysis by increasing the cell voltage to the decomposition voltage of the copper sulfate electrolyte. When this occurs the operators dub the cells "crazy."

Circulation of Electrolyte

The heated electrolyte must circulate through each cell at a rate which will prevent too great a loss of temperature between the inlet and outlet and maintain the proper ion concentrations at the electrode surfaces. For good operation this temperature drop is seldom permitted to exceed 10°F or 5.6°C. The required rate of flow

varies with the size of the tank and the room temperature but usually falls within the range of 3.5-6 gal/min. Excessive rate of flow tends to interfere with the settling of the electrolytic slime which sloughs from the anodes.

Once a satisfactory rate of electrolyte flow has been established, it is most important that it be maintained constantly and kept uniform in all cells. Otherwise not only the electrolyte temperature, but the beneficial effects of the organic addition agents will vary from cell to cell.

In most refineries the circulating electrolyte is pumped to a head tank from which it feeds by gravity to the sections of electrolytic tanks. Some refineries, however, pump directly into the supply lines. In this case care must be taken to avoid intake of air at the pump, as air entrained in the electrolyte will form small bubbles on the cathode surfaces and prevent copper deposition wherever they cling, thus having the effect of increasing the current density.

Anodes

The impure anodes, cast from blister or converter copper after it has been furnace refined to remove sulfur, usually have a copper content of 99+%. Oxygen content is usually within the 0.10 to 0.30% range, and in most cases the percentages of the various impurity elements, exclusive of silver, are in the second or third decimal place. Silver plus gold seldom exceeds 30 oz/ton or 0.10%.

In different refineries, anode dimensions vary from 27 to 36 in. in width, from 31 to 39 in. in length, and from 1¼ to 2 in. in thickness. Anodes are universally cast flat with two ears or lugs at one end. This permits them to be hung vertically, and the longer of the two lugs acts as the conductor for the inflow of current. Weight per anode ranges from 440 to 700 lb, and anode life under electrolysis is scheduled at from 21 to 42 days, leaving a scrap remainder of 12 to 20%. Scrap anodes are washed free of adhering slime and returned to the anode furnace for remelting.

In most refineries anode life is about 4 weeks, during which period the cells produce two sets of deposited cathodes. This affords an economical operating schedule and permits the use of a standard rotation for taking out cathode production, replacing anodes, and removing slime from the cells. In some cases where nodularized cathode deposition results from the requirement to electrolyze with high current density or with troublesome anode impurities, it is necessary to plate three or four sets of cathodes during the life of the anode.

After casting, anodes are hung by their lugs and evenly spaced in racks which hold a cell load, so that they can be placed in the cells in unit crane lifts of several tons. While in the racks it is important that the individual anodes be plumbed to hang vertically. This is accomplished by a slight bending of the lugs, using a heavy hammer. Also at this time the contact area of the long lugs is cleaned or polished.

Cathodes

The thin starting sheets of electrolytic copper which are hung between the anodes, and in most refineries at each end of the cell, are usually produced as a 24-hr deposit on smooth, oiled plates or blanks of hard rolled copper which are themselves hung as cathodes in special cells operated for this purpose. In order to eliminate the necessity for surface oiling, there has been considerable experimentation with stainless steel blanks, but passivity to corrosion has been found to decrease with use, and surface repolishing becomes necessary. A deposited sheet, 0.02 to 0.03 in. thick, is peeled from each side of each blank every working day. After stripping, the blanks are re-oiled if necessary and returned to their cells. Strips cut from the same sheet deposit are formed into loops and affixed to each sheet by punching or spot welding so that a copper rod can be threaded through them. These rods support the sheets when they are later hung in the production cells; they also serve as current conductors.

The anodes used in the cells for depositing sheets are usually 2 in. wider and 1 in. longer than the anodes in production tanks. This insures adequate deposition around the edges of the blanks even after 75% of the anode has been corroded away. Starting sheets are usually 2 in. wider and 1 in. longer than the anodes used in production cells. This avoids the formation of a heavy border of deposition during the early days of production plating while the regular anodes still retain their full area.

Before being hung in production cells as cathodes, starting sheets must be "flapped" or flattened so that they will hang straight and not touch the adjacent anodes. In most refineries the flapping is done by hand, but machines are being developed which perform both flattening and affixing of loops.

To permit effective flattening, the sheets must be soft and pliable and free of springiness. The deposition surface must be free of roughness which would promote nodular growth. As a result of these requirements, the composition and conditioning of the electrolyte for the starting sheet cells must be controlled closely and handled through a circulation separate from those which supply the production cells. It is best to use only glue as addition agent. Due to the presence of oil on the blanks, the amount of glue necessary may be 0.2-0.3 lb/ton in order to insure a smooth, tough, fine-grained deposit. Copper content of starting sheet electrolyte is usually maintained between 45 and 50 g/l and acid content between 180 and 190 g/l. The temperature of the electrolyte entering cells should be no less than 140°F (60°C). Cathode current density in excess of 23 amp/ft² tends to cause rough deposition.

Production Cathodes

In the production cells, the starting sheets are spaced carefully in relation to the adjacent anodes, and anode lugs and cathode rod ends are all checked for good current contact. With electrolyte up to normal level and at proper temperature and flow, the section is ready for operation. Current is applied, and deposition continues until the scheduled growth of the cathodes has been completed. Current is then shut off from the section of cells and the cathodes are withdrawn by crane, thoroughly washed with hot water by immersion or spray, and loaded for transportation to furnaces or the market.

The copper content of the completed cathode should be 99.98+% with the percentages of most of the impurity elements in the fourth decimal place. Sulfur and iron content as high as 0.002% can be tolerated. Silver content should not exceed 0.35 oz/ton.

Cathode Current Density

The amount of current through each cell can be set to obtain the desired production of cathode deposit within a fairly wide range of current density. For economic reasons the operation is seldom carried on at less than 10 amp/ft² of cathode surface. Under high production demand, many refineries have operated at 25 or 26 amp/ft², but 15 to 20 amp/ft² is generally preferred. Higher current density tends to produce a rougher deposit and often causes excessive short circuiting from sprouting cathode growths.

Cathode Current Efficiency

Current efficiency is considered a measure of good tank house operation since it is an index of the production obtained for the investment in power and labor, the two chief items of operating cost. Under ideal conditions 1 amp deposits 0.06274 lb of copper per 24-hr day per cell. Using the average of hourly amperage readings taken during the life in days of the cathodes in a cell or section of cells, a theoretical weight of deposition is calculated. When the completed cathodes are removed they are weighed, and the net weight of deposition is divided by the calculated theoretical deposition. A current efficiency of 90% is considered good, but many refineries average 94% or better. The chief cause of reduced current efficiency is short circuiting between adjacent cathodes and anodes. Another cause of lowered efficiency is stray current loss through tank linings and solution lines, which, however, seldom exceeds 2 or 3%.

Power Yield

Since power is measured and paid for in kilowatts, some concern has to be given to the voltage component by minimizing resistances wherever possible in the electrolytic circuit. The source of d-c power is located as close as possible to the cell room, main bus lines are of ample size, anode-to-cathode spacing is set at the minimum which will avoid short-circuiting, and all conductor contacts are kept clean. Both electrolyte temperature and acid content are maintained at values which reduce electrolyte resistivity. As current density is increased, power yield tends to decrease, and this explains why most refineries prefer to operate at moderate current density provided it will enable them to meet their production requirements. Power yield varies widely among different companies in a range of from 6 to 12 lb of copper per kilowatt hour.

Scheduling

The section of tanks, made up of two tiers or rows through which the electrolytic current flows across and back again to the main bus, is the normal unit of operation in the tank house. The tiers are seldom more than a foot apart, and to permit the current to leave the main bus bar and flow across the first tier and return to the bus across the second tier, there is a gap in the bus bar similar to the space between the tiers. This gap is easily bridged by dropping a short piece of bus bar across it and clamping it to maintain good contact. This short piece of bus is called a "lock" or "jumper" and when it is clamped in place the section is "locked out" or "jumpered"; the current is shunted past the section through the lock. This permits removal of completed cathodes and anode scrap, the cleaning of tanks, and finally reloading with new anodes and starting sheets. A scheduled removal of completed cathodes is called a "pulling" or "drawing." When only full-grown production cathodes are removed to be replaced with starting sheets, it is often called a "copper." When both cathodes and fully corroded anodes or scrap are removed and the slime cleaned from the tanks, the drawing is called a "mud."

It is highly desirable for smooth tank house operation to be able to pull the sections on a regular schedule so that they are unloaded and reloaded in the same rotation, cycle after cycle. Such a schedule evens out the work for the loading and unloading crews as well as for the inspection groups who keep the cells operating properly while under electrolysis. To establish and operate a pattern schedule efficiently it is necessary that the anodes be of uniform weight, that current amperage be held closely to the designated figure, and that the ampere efficiency be maintained at a predetermined satisfactory figure. The latter requirement is the most difficult to control since it involves consistently good performance of both the loading and inspection crews as well as the maintenance of uniformly satisfactory conditioning and circulation of electrolyte. Within limits it is possible to adjust a pattern schedule to an increase or decrease in production requirements, but a full cycle is required to complete the adjustment.

Where it is not possible to maintain a regular schedule due to uncontrollable variations, it is general practice to schedule section pullings approximately two weeks in advance.

Cell Inspection and Correction during Electrolysis

All of the items of tank house materials, equipment, and procedure center around the proper operation of the individual cells under electrolysis, so that their inspection and the prompt correction of any malfunctioning become of paramount importance. Competent and sustained good performance on the part of both supervision and operators assigned to cell inspection is most essential.

Satisfactory electrolysis requires that the flow of current be equal and uniform through each anode and cathode in the cell. To achieve this, two things are necessary: first, all electrode contacts must be kept clean for good conduction and, second, cathodes and anodes must be kept evenly spaced with no contact in the cell, either above or in the electrolyte.

Whenever these conditions are not maintained, the distribution of current among the electrodes becomes uneven due to their being in parallel. The current which faulty electrodes fail to receive is taken by electrodes with good contact, resulting in wide variations in current density. Cathodes operating under high current density develop undesirable surface growths which may result in short-circuiting contacts, through which the current flow is excessive and deposits no copper. The ampere efficiency of the cell is lowered proportionately.

The same condition develops when starting sheets come in contact with adjacent anodes because of surface irregularities or poor spacing. To the operator all anode-to-cathode contacts are known as "shorts" or "hot sheets" as the supporting rod of a shorted cathode becomes hot to the touch due to the excessive current it is carrying.

To perform their inspection and correction work, the operators, designated as "inspectors," "metermen," "hotsheetmen," or "section men," work on top of the tanks, their weight being suported by the closely spaced cathode rods.

The meterman uses a millivoltmeter whose terminals are connected to two copper prongs attached to a 3-ft stick so that he can walk along each cell and make contact with the prongs between each anode and cathode just beneath the surface of the electrolyte. Because of the parallel arrangement, normal anode-to-cathode voltage is approximately the same as the cell voltage and ranges from 0.18 to 0.35 v. When the meterman observes a low reading he chalk-marks the electrodes involved so that the condition causing it can be corrected by a hotsheetman. He usually checks the cathode rod by touch, and, if it is cool, the cathode rod or anode lug contact is fouled. If the rod is hot, the cathode is shorted to one or the other of its adjacent anodes.

Until a few years ago the hotsheetman detected shorted cathodes by going over the cells and touching all cathode rods to locate those which were hot. This method has been largely superseded by the use of the Gaussmeter, which is mounted on a stick and passed over the cathode rods as the operator proceeds along the cell. The stronger magnetic field surrounding the rod of a shorted

cathode with its excessive current flow shows a high reading on the Gaussmeter.

As promptly as possible after faulty contacts have been located and marked, the section men make the necessary corrections. Contacts are wiped or shined with sandpaper. While they are still not too heavy, usually up to the fourth day of deposition, shorted cathodes are lifted out of the electrolyte for correction. The operator uses a flat iron blade or "knife" to remove shorting growths and smooth out any irregularities. Corrected cathodes are returned with special care as to spacing to avoid recurrence of the shorting.

It is highly essential that inspection and correction work be performed thoroughly and competently during the first three or four days of deposition. A section of cells with new starting sheets may have as high as 25% of shorts and faulty contacts. In order to obtain proper over-all current efficiency shorts should be reduced to less than 3% for the fourth day of deposition.

In order to check their performance properly, hotsheetmen usually work in small groups or in pairs on designated sections of cells. The work is laid out so that all cells can be gone over for correction at least twice, and the sections of young copper three or four times each day. Most refineries confine the correction work to the day shift, but some find it worthwhile to have a small crew of competent operators follow up on the second shift to give additional attention to sections of young cathodes. A single meterman usually can check by millivoltmeter the sections of cells covered by several groups of hotsheetmen. One voltmeter inspection per section per day is considered adequate.

It should be noted that too much inspection can defeat its own purpose since the additional walking on the cathode rods may move them out of alignment and cause new shorts. This is especially true when the cathodes are still light in weight.

Recommendations

This tedious review of some of the hundreds of little details involved in good tank house operation has touched only lightly on the electrochemistry of the copper refining process. Competent research has done a good job of keeping abreast of the needs of the various refiners for special adaptations and modifications of the basic process to suit it to their individual requirements for the production of pure electrolytic copper from their particular type of crude blister. I hope I have made clear what I stated at the outset, that despite the world's dependence on tremendous tonnages of electrolytically refined copper, the techniques of good tank house operation have seen little change in recent times and still depend to a great extent on hand labor performed under rather unfavorable working conditions.

With the decreasing availability of the required type of labor and the constantly increasing rate of wages, especially in this country, it is time that more serious consideration be given to radical improvements in tank house operation, particularly to the problem of efficient cell performance during electrolysis. Here are a few suggestions of things to come and many of them are on the drawing boards or being developed on the job at the present time:

1. Anodes with uniformly good physical characteristics. This means positive control of weight within narrow limits during casting, sound lugs of uniform thickness, and perfect flatness so that they hang vertically when racked in tank loads. They must be free of blisters, protrusions, and fins, and the contact surface of the long lug should be ground or shined to clean metal.
2. Starting sheets should be produced, stripped, flattened, looped with rods in place and hung in racks by mechanical means to eliminate the present arduous hand-handling. It is not too much to suggest that means could be devised to place them in the cells by crane a tank-load at a time, instead of one at a time by hand.
3. Improved control facilities should be installed to insure proper conditioning and supply of electrolyte so that composition, clarity, temperature, and flow can be held within narrow limits of variation with a minimum of hand juggling.
4. Anode scrap as well as cathode production should be washed, bundled, and loaded out by mechanical means.
5. In the construction of tank house buildings more consideration should be given to insulation against variations in outside temperature, and adequate ventilation facilities should be provided to improve working conditions and to minimize vapor condensation as well as variations in humidity and rate of evaporation.
6. Full advantage should be taken of the rapid development of acid-resisting steels and plastics to replace iron and lead in tank house equipment. In this connection, cells should be fully protected on the outside as well as inside, especially when made of concrete.

We have taken a brief look into the aging anatomy, complex functions, and obvious needs of the tank house, the work-horse of the copper industry. If doing so has been mildly interesting to the uninitiated, a little helpful to the embryo operator, and a bit provocative to the tank house graduate, it will more than have served its modest purpose.

Current Affairs

High Lights of the Meeting of the Board of Directors

(Held October 18, 1959, Deshler Hilton Hotel, Columbus, Ohio)

The following matters were considered and acted on by the Board of Directors at its meeting in Columbus, Ohio, on October 18, 1959.

Communications from the President

Committee Appointments.—Dr. Gardiner announced the following committee appointments, which were approved:

Convention Advisory Committee: To consider long-term planning for future meetings of the Society, including continuing review and revision of our policies and procedures and the preparation of a manual of our procedures. The personnel of the committee will consist of the Treasurer, Secretary, the three previous Meeting Committee Chairmen, and the Executive Secretary serving as an ex-officio member. Ernest G. Enck will serve as Chairman.

Protocol Committee: To assist in connection with luncheons, dinners, medal awards, and special lectures at National Meetings; Robert M. Burns, Chairman, Paul Delahay, and Sherlock Swann, Jr.

Tellers of Election: A. C. Loonam, Chairman, S. H. Reynolds, and Fred P. Peters; Alternates, Hans R. Neumark, John C. Trackman, and C. H. Chappell.

Nominating Committee: Norman Hackerman, Chairman, Frederick W. Fink, Arthur C. Haskell, M. F. Quaely, E. M. Sherwood.

Committee C-67 ASA: Upton B. Thomas to replace Guy H. Fetterly, deceased.

Chemical Industry Medal Dinner.—It was announced that Cecil V. King represented the Society at the dinner of the Society of Chemical Industry at which time the Chemical Industry Medal was presented to Dr. Harry B. McClure.

100th Anniversary of The Cooper Union.—Frances S. Lang, Chairman of our New York Section, represented the Society at the 100th Anniversary and Academic Convocation of The Cooper Union held in New York City on November 2, 1959.

Report of the Treasurer

Dr. Gilbertson, Treasurer, submitted the Financial Statement for the six-month period ending September 30, 1959 which indicated an excess of expenses over income. It was pointed out that the period in question represented our low-income months and that beginning in November we would enter our high-income period, following which our receipts would serve to offset the present excess of expenses over income.

Report of Audit

Dr. Gilbertson, Treasurer, presented the Report of Audit for the fiscal year ending March 31, 1959; it was approved by the Board.

Communications from the Secretary

Votes by Mail Ballot.—Dr. Campbell, Secretary, reported that the following proposals had been approved by the Board by mail ballot since its previous meeting: committee appointments by the President; Report of the Nominating Committee for the election of officers for 1960-1961; suggestion of the names of Dr. J. C. Warner and General L. E. Simon to the Engineers Joint Council as our candidates for appointment on the Board of Directors of the National Science Foundation; holding of a joint symposium on the subject "The Principals of Electrochemical Engineering" by the Theoretical Electrochemistry and Industrial Electrolytic Divisions, including permission to solicit financial support from some agency of the Government and an appropriation of $500 from Society funds; acceptance of the book entitled "Metal Iodides and Iodide Metals" by Dr. Robert F. Rolsten as part of our Monograph Series.

Financial Report of Philadelphia Meeting.—Dr. Campbell reported that 1489 people had attended our 1959 Spring Meeting in Philadelphia which was the largest meeting the Society ever held. The report indicated income and expenditures as well as the amount received by the Society and the division of surplus funds between the Society and the Philadelphia Section. The report is replete with information from the Chairmen of subcommittees which should prove most helpful to future meeting committees of the Society. A special vote of appreciation was extended to the Philadelphia Meeting Committee for arranging one of the finest meetings which the Society ever held.

Toronto Meeting.—The Secretary announced that arrangements had been consummated for holding the 1964 Spring Meeting of the Society in Toronto, Canada, at the Royal York Hotel, May 3-7.

Research Council on Causes and Methods of Preservation of Internal Corrosion of Water Pipes.—Dr. Campbell presented a report from Frank L. LaQue, our Society's representative on the Council, which indicated that the work accomplished under the direction of Professor Eliassen of M.I.T. had resulted in a number of papers being published. The work having been completed, it is now assumed that this report will terminate the services of our representative on the Council.

Inaugural Ceremonies, New President University of West Virginia.—At the request of Dr. Gardiner, the Secretary announced that he had represented the Society at the Inaugural Ceremonies of the new President of the University of West Virginia.

National Office Affairs.—Dr. Campbell announced that a special memorandum had been prepared and sent to all Division Chairmen and Vice-Chairmen in which are outlined a number of important matters dealing with our policies and procedures involving Divisional relationships with the Society; copies will also be sent to newly elected officers and it is hoped that in this way a closer liaison will be established between our Divisions and the Society.

Future Meetings

The General Chairmen for our meetings in Columbus, Chicago, Los

Angeles, Pittsburgh, and New York reported progress in planning for these future meetings of the Society.

Report of Ways and Means Committee

The following changes in the By-laws of the Society were approved on recommendation of the Ways and Means Committee:

Article XVI, Section 2, (part 3): "Local Sections will receive from the National Society $1.00 from the first year's dues for each new member received into the Society within their geographical boundaries."

Article VI, Section 1: "A Publication Committee shall be appointed by the President with the approval of the Board of Directors. Appointments shall be for a three-year term. The Committee shall consist of a Chairman, the Secretary of the Society, the Editor of Monographs and Special Publications, the Editor of the JOURNAL, and the Technical Editor of the JOURNAL. This Committee shall be responsible to the Board of Directors for the financial and managerial policy of all Society publications."

Philadelphia Meeting Fall 1966.—The invitation extended by the Philadelphia Section to hold our Fall 1966 Meeting in this city was unanimously approved.

Summer Conference on Electro-Organic Chemistry.—It was voted to approve the recommendation of the Electro-Organic Division for petitioning the National Science Foundation for their financial support of a program to hold summer conferences having as their objective the strengthening of the teacher's professional knowledge in the newer developments of this science.

Membership Lists.—A statement of policy was approved by the Board concerning the sending of membership lists to nonmembers of the Society, which granted to the Secretary authority to determine whether such requests were in the interests of the Society or its members.

Articles of Incorporation.—It was reported that an investigation had uncovered the fact that the Society's Articles of Incorporation (granted under the Membership Corporations Law of the State of New York) were not in conformity with the provisions of the Constitution of the Society; that the Articles provide for 19 members on the Board of Directors while our Constitution provides for 18 members. It was voted to amend our Constitution to provide that the second immediate Past President shall be added to the Board in order to conform to the number required by the statute.

Report of Finance Committee

Dr. Gilbertson, Chairman, reported that the Society is currently spending slightly in excess of $5000 over our Budget for printing and mailing the JOURNAL; that this is due to the large number of papers submitted and cleared for publication. He reported that at the next meeting of the Board the Finance Committee will submit a recommendation for an increased appropriation to reflect our current requirements in this respect, but that we were operating in the meantime in the belief that the Board will not wish to curtail the publication of these papers.

Report of Publication Committee

Monographs and Special Publications.—Dr. Uhlig, Chairman, reported that the Society now has in the course of compilation the following new monographs and special publications: Metal Iodides and Iodide Metals; Primary Batteries; Mechanical Properties of Intermetallic Compounds; Chemistry of Metal and Semiconductor Surfaces; Electrode Processes. The Board also approved the publication of papers delivered at the Liquid Dielectrics Symposium held in Philadelphia in the spring of 1958.

Papers Presented at Society Meetings.—Approval was given to the following statement of policy which was recommended by the Committee concerning the presentation of papers at our National Meetings:

"Papers submitted for presentation at the meeting become the property of The Electrochemical Society and may not be published elsewhere, in whole or in part, unless permission is requested and granted by the Society. Papers already published elsewhere, or submitted for publication elsewhere, are not acceptable for oral presentation except on invitation by a Divisional Program Chairman."

Report of Membership Committee

Fred W. Koerker reported that our membership now stands at an all-time high of 3144 members.

Report of Sustaining Membership Committee

Mr. John T. Owen reported that six new Sustaining Members had been secured, but that one had not renewed, leaving a net gain of five. Sustaining Memberships now total 156 and Patron Memberships five.

Report of Honors and Awards Committee

Dr. Harold M. Scholberg, Chairman, reported that the Committee had been giving special consideration to the re-establishment of Fellowships by the Society. The Board voted to approve the institution of a Fellowship on an experimental basis for the summer months in the amount of $800, payable from the Consolidated Fellowship Fund, and that it be established not on the basis of need. The recommendation of the Committee concerning the establishment of a Fellowship in the amount of $4500 for an academic year for a period of one year, not on the basis of need, was disapproved. It was voted to present to all living Past Presidents of the Society a Certificate of Appreciation; this was done at the Banquet.

Report of Palladium Medal Award Committee

On recommendation of the Committee, it was voted to postpone the Award of the Palladium Medal to

Brief Communications

The JOURNAL accepts short technical reports having unusual importance or timely interest, where speed of publication is a consideration. The communication may summarize results of important research justifying announcement before such time as a more detailed manuscript can be published. Consideration also will be given to reports of significant unfinished research which the author cannot pursue further, but the results of which are of potential use to others. Comments on papers already published in the JOURNAL should be reserved for the Discussion Section published biannually.

Submit communications in triplicate, typewritten double-spaced, to the Editor, Journal of The Electrochemical Society, 1860 Broadway, New York 23, N. Y.

Professor Frumkin until our Chicago Meeting in the spring of 1960 because of his inability to attend our Columbus Meeting.

Unfinished Business

Dr. Uhlig reported progress in arranging for the Second International Conference on Passivity; that it will be held in September 1962, but that the place of the meeting had not yet been determined.

New Business

It was reorted that the mid-winter meeting of the Board of Directors will be held at Society Headquarters in New York on Friday, January 8, 1960; the Programming Session for our Spring Meeting in Chicago will be held the preceding day.

Robert K. Shannon,
Executive Secretary

Nominations for Honors and Awards of The Electrochemical Society

The Honors and Awards Committee in planning its work for the coming year reminds the membership that their suggestions for honors and awards are solicited by the Committee. Please note the following:

Honorary Members

Bylaws, Article X, Section 3.—"The Honors and Awards Committee shall make recommendations to the Board of Directors for Honorary Membership in the Society of individuals who, in the opinion of the Committee, have made valuable contributions to electrochemistry or who deserve special recognition by the Society."

Constitution, Article II, Section 4.—"Honorary Members shall be those individuals who, by reason of valuable contributions to electrochemistry, deserve special recognition by the Society."

Honorary Members are as follows:

Charles F. Chandler,*
New York, N. Y.
Edgar F. Smith,*
Philadelphia, Pa.
Carl Hering,* Philadelphia, Pa.
Edward G. Acheson,*
Niagara Falls, N. Y .
Wilder D. Bancroft,*
Ithaca, N. Y.
Edward Weston,* Montclair, N.J.
Thomas A. Edison,* Orange, N.J.
W. Lash Miller,*
Toronto, Ont., Canada
Edward Dean Adams,*
New York, N. Y.
Charles F. Burgess,*
Chicago, Ill.
Frederick M. Becket,*
New York, N. Y.
L. H. Baekeland,*
New York, N. Y.
Robert A. Witherspoon,*
Montreal, Que., Canada
Archer E. Wheeler,†
New York, N. Y.
W. R. Whitney,*
Schenectady, N. Y.
Paul J. Kruesi,
Chattanooga, Tenn.
Colin G. Fink,*
New York, N. Y.
Oliver W. Brown,
Bloomington, Ind.
John W. Marden,
Bloomfield, N. J.
William Blum, Washington, D. C.
George W. Heise, Cleveland, Ohio
Frank C. Mathers,
Bloomington, Ind.
Robert M. Burns, Summit, N. J.

* Deceased.
† Whereabouts unknown.

The listing of those deceased is given to remind you of the men who have been selected for Honorary Membership. The Committee wishes to retain this high standard.

The number of Honorary Members is limited to ten.

Nominations must be accompanied with nine copies of a suitable biography setting forth the qualifications of the nominee.

Acheson Medal Award

The Acheson Award can be made no oftener than every two years. The next opportunity for the Society to so honor someone is at the Houston Meeting in the fall of 1960.

The Honors and Awards Committee is charged by the Bylaws to recommend a selection to the Board. The rules adopted by the Society, amended as of March 3, 1949, require that the award shall be made without distinction on account of sex, citizenship, race, or residence.

In addition to the above with regard to the selection, these rules have the following proviso:

1. Nominations shall be accepted, also, from the membership at large. Announcement to this effect shall be made by the Secretary through the JOURNAL of The Electrochemical Society as promptly as possible after the appointment of the Committee, together with such instructions taken from these Rules as the Secretary may consider necessary for the guidance of the membership.

2. All nominations, whether made by a member of the Nominating Committee or by any other member of the Society, must be accompanied by a full record of qualifications of the nominee for the Award. Such supporting documents from friends of the candidate or from his organization shall be in order.

3. The nominator must assume the responsibility for providing the Chairman of the Nominating Committee with nine copies of the supporting documents, one for each member.

It is desired that such suggestions be in the hands of the Chairman *not later than February 1, 1960.*

Following is a list of Acheson Medalists since the Award was founded:

Edward G. Acheson*—1929
Edwin F. Northrup*—1931
Colin G. Fink*—1933
Frank J. Tone*—1935
Frederick M. Becket*—1937
Francis C. Frary—1939
Charles F. Burgess*—1942
William Blum—1944
H. Jermain Creighton—1946
Duncan A. MacInnes—1948
George W. Vinal—1951
John W. Marden—1953
George W. Heise—1954
Robert M. Burns—1956
William J. Kroll—1958

* Deceased.

Please address all nominations on both of the above subjects to Ralph M. Hunter, The Dow Chemical Co., Midland, Mich.

Ralph M. Hunter, *Chairman*
Honors and Awards Committee

ECS Assistance Award

Dr. Ralph M. Hunter, Chairman of the Honors and Awards Committee, announces that in accordance with approval by the Board of Directors of the Society an Assistance Award will be made to a fellow or teaching assistant pursuing work between the degree of B.S. and Ph.D. on a subject in a field of interest to The Electrochemical Society.

The Assistance Award will amount to $800 for one year only and will be awarded for the period June-September 1960. It is intended that this Award shall be made to the possessor of a nine-month grant for

the academic year 1960-1961 and who shall have been the holder of a similar grant for the academic year 1959-1960. The Assistance Award is intended to cover a period during which the recipient has no financial support for the continuance of his work.

Palladium Medal Award to Professor Frumkin Postponed until Chicago Meeting

At the Board of Directors Meeting held in Columbus, Ohio, on October 18, 1959, it was announced that Professor A. N. Frumkin, Director of the Institute of Electrochemistry of the U.S.S.R. Academy of Sciences and Professor of Electrochemistry at the University of Moscow, would be unable, for reasons of health, to attend our Columbus Meeting to receive the Palladium Medal Award for 1959 and deliver the Palladium Medal Address.

The Board of Directors unanimously approved of the recommendation of the Award Committee that the ceremonies be postponed until our Chicago Meeting in the spring of 1960, by which time it is hoped that Professor Frumkin's health will have improved so that he will be able to attend and accept the Medal and deliver the Address.

Division News

Corrosion Division

A Corrosion Division news luncheon and business meeting was held at the Neil House, Columbus, Ohio, on October 22, 1959.

Several announcements were made concerning new books which are being planned and which should be available soon; future meetings which pertain to corrosion; and new laboratories where work on corrosion is conducted.

The Division Bylaws were amended to extend the term of office of the Chairman, Vice-Chairman, and Secretary-Treasurer to two years starting with the election which will be held in October 1960.

The following Division officers were elected for a one-year term:

Chairman—M. A. Streicher, Engineering Research Lab., DuPont Experimental Station, Wilmington, Del.

Vice-Chairman—R. T. Foley, General Electric Co., Schenectady, N. Y.

Secretary-Treasurer — M. Stern, Metals Research Labs., Union Carbide Metals Co., Niagara Falls, N. Y.

The Secretary-Treasurer reported a cash balance of $21.68, a sum which has remained constant for at least three years.

M. Stern, *Secretary-Treasurer*

Electrodeposition Division

The annual luncheon meeting of the Electrodeposition Division was held in Columbus on October 21, 1959 with 55 members present.

Dr. Petrocelli reported that his committee (to consider shortening the tenure of Division officers from two years to one) has recommended maintaining the two-year term of office. This recommendation was accepted by a unanimous vote.

Dr. Lowenheim, Editor of the revised edition of "Modern Electroplating," stated that 23 of the 44 chapters of the Monograph were in his hands. The previous estimated publication date of mid-1961 remains unchanged.

The election of new officers will take place at the next meeting. Chairman Brenner appointed the following members to the Nominating Committee: Sidney Barnartt, Fred Lowenheim, and Cloyd Snavely.

Abner Brenner made two suggestions for future Division symposia: (*a*) Electroless plating of metals, and (*b*) Gas-phase metal deposition. Fred Lowenheim suggested that symposia be planned two to three years in advance instead of just one year. He proposed putting the responsibility for organizing future symposia on the Vice-Chairman. Chairman Brenner proposed that another symposium on Electro-Organic Chemistry be held two to three years from now. Dennis Turner suggested that a Symposium on Addition Agents in Electroplating probably would be of considerable interest.

Dennis R. Turner,
Secretary-Treasurer

Section News

Detroit Section

A meeting of the Detroit Section was held on October 14, 1959 at McGregor Memorial, Wayne State University, Detroit. Professor H. Gerischer spoke on "Mechanisms of Electrolytic Deposition and Dissolution of Metals."

In his exceptionally well-presented talk, Professor Gerischer considered the various reaction paths by which a metal, silver for example, may be dissolved electrolytically. On the basis of metal ions in a half-crystal position and in an adsorbed position, there is experimental evidence for the presence of intermediates and therefore a two-step process. These same general considerations were extended to cover the situation involving the formation of complexes. He also discussed briefly some possible mechanisms accounting for the dissolution of semiconductors.

Manuel Ben, Chairman of the 1961 Convention, reported that Dr. Lee O. Case, Mr. Wright Wilson, and Dr. Dan Trivich had agreed to serve as Advisors for it.

The Program Chairman, J. P. Hoare, announced that the Section would have seven meetings during the year; the speaker on November 19, 1959 to be Dr. D. Trivich of Wayne State University, whose topic would be "Electrochemical Research in Europe."

News from India

India's New Steel Plants.—The commissioning of the first blast furnace of the new steel plants at Rourkela and Bhilai took place in February 1959. In addition to foundry iron, both the plants will turn out a wide range of products. The Rourkela plant, employing both the openhearth and L.D. processes, will have an initial capacity of 1.1 million tons of pig iron per year, whereas Bhilai has a capacity of 1 million tons of ingot steel per year by the openhearth process. The existing plants of the Tata Iron and Steel Co., Jamshedpur; Indian Iron and Steel Works, Burnpur; and Mysore Iron and Steel Works, Bhadravathi, have also taken up expansion programs. These developments are aimed toward the fulfillment of the production target of 6 million tons of ingot steel by the end of the Second Five-Year Plan of the country. It is hoped that, with the third plant at Durgapur going into production by 1960-1961, the shortage of steel in India will be removed.

Electroplating Course in the CECRI.—A three-month course in electroplating was organized by the Central Electrochemical Research Institute, Karaikudi, during March-June 1959. The lecture program covered the theory and practice, preparatory treatments, industrial plating, and anodizing. The trainees had, in addition, an intensive course in practical work, including visits to factories.

Process for Electrolytic Manganese Dioxide.—The National Metallurgical Laboratory, Jamshedpur, has evolved a process, Indian Patent No. 47982, for producing battery grade 99.99% purity manganese dioxide from low-grade manganese ores. This has been satisfactorily operated on a pilot-plant scale. It consists of producing acidic manganese sulfate solution from manganese ores and electrolyzing it to yield manganese dioxide. Most of the plant and equipment required for the manufacture can be fabricated in India. Details can be had from the National Research Development Corp., New Delhi.

Symposium on Polarography.—A Symposium on Polarography was organized by the Dept. of Inorganic and Physical Chemistry, Indian Institute of Science, Bangalore, from August 12 to 14, 1959, as part of the Golden Jubilee Celebrations of the Institute. There were 16 papers covering: effect of surface active substances, diffusion coefficients, organic reactions, a-c polarography, application to analysis, reversible and irreversible processes, and complex formation, with foreign contributions from the U.S.A., West Germany, and the U.K.

Defense Electronics Convention in Bangalore.—The First Defense Electronics Convention was held in Bangalore from September 28 to October 1, 1959. The technical sessions covered 40 papers on: defense electronics, problems of service electronic equipment, special problems and industrial potential, and education of electronic engineers. There were representatives from the Defense Services, LRDE, CSIR, AEC, government and private industries, research institutions, scientific societies, and other organizations. Dr. M. S. Thacker, Chairman of the India Section, addressed the Convention.

India Section.—The Eighth Annual Meeting of the India Section was held on July 24, 1959 at the Indian Institute of Science, Bangalore, with Dr. S. Krishnamurthy in the Chair since the Chairman, Dr. M. S. Thacker, was out of India.

The following officers of the Section were elected for the 1959-1960 term:

Chairman—M.S. Thacker, Council of Scientific & Industrial Research, Old Mill Rd., New Delhi 2, India
Vice-Chairman—A. Jogarao, Central Electrochemical Research Institute, Sekkalai P.O., Karaikudi, S.I. Ry., South India
Vice-Chairman—N. R. Srinivasan, Bhilai Steel Plant, P.O. Bhilai-1, Drug Dist. (M.P.), India
Secretary-Treasurer—S. Krishnamurthy, 637 17th Cross, Malleswaram, Bangalore 3, India.

T. L. Rama Char,
India Correspondent

Philadelphia Section

At its first meeting of the season, held in November 1959, the Philadelphia Section was addressed by Dr. Paul Rüetschi of the Electric Storage Battery Co., and recent winner of the Society's Young Author's Prize. Dr. Rüetschi's talk, "The Obsolete Lead-Acid Storage Battery," was received with considerable interest, and he led a lively discussion period following the presentation.

H. C. Mandell, Jr., *Secretary*

Personals

G. M. Butler, Jr., manager, Engineering Research Branch of the Research and Development Div., Carborundum Co., Niagara Falls, N. Y., has resigned from that position, effective January 1, 1960, to become the director of engineering and research for a large corporation located in California. Dr. Butler had been with Carborundum for 12 years in various positions in research.

H. A. Cataldi has been appointed supervisor-physical chemistry in the Materials and Processes Lab. of the General Electric Co.'s Large Steam Turbine-Generator Dept., Schenectady, N. Y. His new assignment will be in the field of physical and electro- chemistry.

Arthur J. Freedman has been named research project leader at Nalco Chemical Co., Chicago, Ill. He has been prominent in refinery

Manuscripts and Abstracts for Fall 1960 Meeting

Papers are now being solicited for the Fall Meeting of the Society, to be held at the Shamrock Hotel in Houston, Texas, October 9, 10, 11, 12, and 13, 1960. Technical sessions probably will be scheduled on Batteries, Corrosion, Electrodeposition, Electronics (Semiconductors), Electro-Organics, and Electrothermics and Metallurgy.

To be considered for this meeting, triplicate copies of abstracts (*not exceeding 75 words in length*) must be received at Society Headquarters, 1860 Broadway, New York 23, N. Y., *not later than June 1, 1960. Please indicate on abstract for which Division's symposium the paper is to be scheduled, and underline the name of the author who will present the paper.* Complete manuscripts should be sent in triplicate to the Managing Editor of the JOURNAL at the same address.

Papers submitted for presentation at the meeting become the property of The Electrochemical Society and may not be published elsewhere, in whole or in part, unless permission is requested and granted by the Society. Papers already published elsewhere, or submitted for publication elsewhere, are not acceptable for oral presentation except on invitation by a Divisional program Chairman.

* * *

The Spring 1961 Meeting will be held in Indianapolis, Ind., April 30, May 1, 2, 3, and 4, 1961, at the Claypool Hotel. Sessions will be announced in a later issue.

process corrosion research and inhibitor development for a number of years, more recently on electrical resistance methods for monitoring corrosion rates. Prior to joining Nalco, he was in the Engineering Research Dept. at Standard Oil of Indiana.

S. Ramaswamy has been designated as general superintendent, The Mettur Chemical and Industrial Corp. Ltd., Mettur Dam, R.S., India.

T. L. Rama Char has been nominated as Correspondent for India, Sub-Committee on Relations with Foreign Organizations of the Inter-Society Corrosion Committee, National Association of Corrosion Engineers, U.S.A. He also has been selected as a member of the Committee of the newly formed Mysore Regional Centre of the Indian Institute of Chemical Engineers.

New Members

In November 1959, the following were elected to membership in The Electrochemical Society by the Admissions Committee:

Active Members

H. K. Bishop, Union Carbide Consumer Products Co.; Mail add: 4080 W. 161 St., Cleveland 35, Ohio (Battery)

J. J. Bordeaux, Rheem Semiconductor Corp.; Mail add: 1143 Pome Ave., Sunnyvale, Calif. (Electronics)

J. E. Clifford, Battelle Memorial Institute; Mail add: 357 Carilla Lane, Columbus 4, Ohio (Theoretical Electrochemistry)

J. R. Davis, Jr., Wesson Metal Corp.; Mail add: P.O. Box 707, Lexington, Ky. (Electronics)

Pierre de la Breteque, Campagne Blanchard, Ch. des Aygalades, Marseilles 15, France

J. L. Devitt, Cook Batteries, Subsidiary of Telecomputing Corp.; Mail add: 4622 E. Mexico Ave., Denver 22, Colo. (Battery)

G. R. Drengler, Union Carbide Consumer Products Co.; Mail add: 5091 Andrus Ave., North Olmsted, Ohio (Battery, Theoretical Electrochemistry)

H. W. Fishburn, Jr., E. J. Lavino and Co., Box 29, Plymouth Meeting, Pa. (Battery)

S. S. M. Fok, Shockley Transistor Corp.; Mail add: 820 Talisman Dr., Palo Alto, Calif. (Electronics)

Allen Gee, Texas Instruments, Inc., 13500 N. Central Expressway, Dallas, Texas (Electronics)

Michael Golben, Gould-National Batteries, Inc.; Mail add: 691 S. Cleveland Ave., St. Paul 16, Minn. (Battery)

A. E. Hultquist, Union Carbide Metals Co., P.O. Box 5000, Niagara Falls, N. Y. (Electrothermics & Metallurgy)

Maurice Indig, Delco-Remy Div., General Motors Corp.; Mail add: R.R. 1, Box 65, Anderson, Ind. (Battery, Theoretical Electrochemistry)

Allan Kahn, International Business Machines Corp.; Mail add: 2034 Margot Place, San Jose, Calif. (Electronics)

D. L. Klein, Bell Telephone Labs., Inc.; Mail add: 1725 Westover Rd., Clark, N. J. (Electronics)

J. H. Klein, Cook Batteries, Subsidiary of Telecomputing Corp.; Mail add: 1852 Crestridge Dr., Littleton, Colo. (Battery)

E. C. Kopper, McGraw-Edison Co.; Mail add: 8 Cliff St., Verona, N. J. (Battery)

Seymour Kraut, General Electric Co.; Mail add: 579 Starin Ave., Buffalo 23, N. Y. (Electronics)

J. R. Madigan, Hoffman Electronics Corp.; Mail add: 806 W. Milburn Ave., Mt. Prospect, Ill. (Electronics)

K. J. Miller, Bell Telephone Labs., Inc.; Mail add: 498 Long Hill Rd., Gillette, N. J. (Electronics)

R. C. Plumb, Worcester Polytechnic Institute, Worcester, Mass. (Corrosion)

Taro Sekine, Tokyo Institute of Technology; Mail add: c/o Mrs. Aksamit, 902 McMillan Ave., Winnipeg, Manitoba, Canada (Electro-Organic)

S. W. Smith, Delco-Remy Div., General Motors Corp.; Mail add: 1314 Central Ave., Anderson, Ind. (Theoretical Electrochemistry)

J. L. Sprague, Sprague Electric Co.; Mail add: 25 Moorland St., Williamstown, Mass. (Corrosion, Electronics)

R. E. Stark, Union Carbide Consumer Products Co.; Mail add: 3094 Warren Rd., Cleveland 11, Ohio (Battery)

R. D. Stewart, American Potash & Chemical Corp.; Mail add: 14973 Meta Dr., Whittier, Calif. (Industrial Electrolytic)

R. F. Sympson, Ohio University; Mail add: 34 Columbia Ave., Athens, Ohio (Corrosion, Theoretical Electrochemistry)

E. R. York, International Business Machines Corp.; Mail add: 322 Pierce Ave., Endwell, N. Y. (Electrodeposition)

Associate Members

R. J. Kersey, Sprague Electric Co., Marshall St., North Adams, Mass. (Corrosion, Electronics)

D. E. Rosen, C.B.S.-Electronics; Mail add: 10 Watts St., Chelsea, Mass. (Electronics)

Deceased Members

G. H. Fetterley, Chippawa, Ont., Canada

I. J. Moltkehansen, Brussels, Belgium

M. C. Taylor, Niagara Falls, N. Y.

By action of the Board of Directors of the Society, all prospective members must include first year's dues with their applications for membership.

Also, please note that, if sponsors sign the application form itself, processing can be expedited considerably.

Book Reviews

Chemical Engineering Calculations, by E. J. Henley and Herman Bieber. Published by McGraw-Hill Book Co. Inc., New York, 1959. 441 pages; $9.00.

This is a beginning text in chemical engineering. Chapters 1-9 cover material usually found in a stoichiometry text. Chapters 10-14 discuss the first law of thermodynamics. Also included is a short history of chemical engineering.

A great deal of effort is expended on problem solving. Mathematical techniques of computation and methods of approximation are stressed. Over 600 problems, illustrating the principles discussed, are included.

It is quite a good book, although not the ultimate.

H. E. List

The Upper Atmosphere, by H. S. W. Massey and R. L. F. Boyd. Published by Philosophical Library, Inc., New York, 1959. xii + 333 pages; $17.50.

"The high atmosphere," say the authors of this book, "is a unique laboratory of vast extent, at low pressure and without walls." Their work is a fascinating account of the methods that afford access to that laboratory and of the results obtained up to the middle of 1958.

It is intended neither as a text nor as a monograph; its appeal is to the general scientific reader. Since information for such a reader has been mostly fragmentary and lacking in perspective, this book, from

the hands of two well-known investigators, comes as a welcome addition to scientific literature.

Those parts of physics which are relevant to the study of the upper atmosphere are summarized in a separate chapter which can be read by anyone with a knowledge of elementary mathematics and physics. On the whole, the presentation seems reasonable, even though the treatment of some topics (like group velocity) leaves something to be desired.

A brief and very useful chapter sets forth what is currently known about the atmosphere. The text is a straightforward and comprehensive exposition of results, omitting, for the moment, discussion of the methods of investigation or of the puzzles that abound in this difficult field.

Methods and instruments are dealt with in two chapters. It is made clear that much more than is commonly known can be found out about the upper atmosphere without leaving the ground or sending instruments aloft. Probing with sound waves and with radio waves provides a wealth of information about temperatures and winds high in the air, as well as about the well-known ionized layers found there. All of these somewhat classical procedures are explained as are the more recent and dramatic ones that involve balloons, rockets, and artificial satellites.

The major part of the book presents the data so far obtained in some detail and discusses the conclusions that can be drawn from them. An impressive array of subjects is dealt with: atmospheric ozone, photochemical action of sunlight, the aurora, the night glow, aerial tides, magnetic storms, radio fade-outs, meteors, and cosmic rays.

A special chapter is devoted to artificial satellites. All the technical terms used in describing their motions, and the techniques of orbiting them and obtaining information from their motions and signals, are described in an admirably clear and complete manner.

The book closes, as all such books must close, with a look into future possibilities. Already, one of the questions the authors raise, "Has the moon a magnetic field?," has received at least a preliminary answer. (The Russians detected no field.) Progress in the study of the upper atmosphere is precipitate, but the systematic and lucid account presented here will be of value for a long time.

R. I. Wolff

Scientific Russian. Edited by George E. Condoyannis. Published by John Wiley & Sons, Inc., New York, 1959. 225 pages; $3.50.

This book satisfies the long-time need for a Russian manual for the scientist who needs to be able to read texts and papers but who cannot devote much of his time to language study. The book is very well organized and from the beginning it helps the student use the dictionary with ease.

The part on pronunciation is well and simply done. Transliterations are excellent and the sections on cognates are a very useful addition to the scientific text readings. Maybe one could question the actual selections of text material. In this reviewer's opinion, they should be of graded difficulty, the easiest ones first, and so on. The aspects of the verb are well and compactly treated, although verb treatment could be more detailed. Also, unfortunately, the explanatory notes are rather confusing in part. They should have brief grammar references with them. However, these are minor faults. The only serious defect is the large number of misprints, especially in explanatory notes. On the credit side must be noted the excellent organization and the treatment of the grammatical tables.

All in all, this book should be welcomed by both teachers and students of scientific Russian.

Marie Tolstoy

High-Temperature Materials. Edited by R. F. Hehemann and G. Mervin Ault. Published by John Wiley & Sons, Inc., New York, 1959. 544 pages; $17.50.

The book presents 34 papers originally presented at a symposium on recent developments in high-temperature materials, April 16 and 17, 1957, sponsored by the High-Temperature Materials Committee of the American Institute of Mining, Metallurgical, and Petroleum Engineers. The delay in publishing the volume is unfortunate in an era when progress in this field is so rapid. The papers cover a wide variety of materials and topics; hence, the book has been separated into seven parts on cobalt and nickel-base alloys, cermets and intermetallics, refractory metals, dispersion strengthening, vacuum melting, effect of environment on high-temperature properties, and oxidation resistance. The book should be of interest to researchers in the field of high-temperature metallurgy and should also find use as a supplemental text or reference in graduate course work in this field.

The editors have done an admirable job of arranging and indexing the volume. As might be expected, a few of the papers are fraught with poor grammar and the technical content of some is inadequate for presentation in this type of volume. It is unfortunate that formal discussions of the papers were not presented at the symposium and published. However, most of the papers are well written and contain technical matter worthy of note.

J. R. Weir

News Items

New ECS Sustaining Member

Globe-Union, Inc., Milwaukee, Wis., recently became a Sustaining Member of The Electrochemical Society.

1959 Annual Index

The Annual Index for Vol. 106 (1959) of the JOURNAL will appear in the February 1960 issue. Reprints of the Index can be obtained about the middle of March by writing to The Electrochemical Society, 1860 Broadway, New York 23, N. Y.

New Technique Permits Zone Melting of Boron

The discovery of a method for pressing rods of commercially available powdered boron has led in turn to successful floating-zone melting of that extremely high-melting element. The technique will provide larger crystals for basic research studies of this semiconductor than have been available before. A paper describing the new method was presented by Dr. E. S. Greiner of Bell Telephone Laboratories to the Metallurgical Society of the AIME in Chicago on November 3, 1959.

Because of its physical properties, boron does not lend itself to floating-zone melting, since it is not possible to form the powder into a suitable shape by pressure alone. The pressed forms are so friable that they crumble as soon as any attempt is made to remove them from the forming dies.

In one aspect of Dr. Greiner's new technique, boron powder, —20 to 100 mesh in size, is placed in boiling boric acid solution, and the mixture boiled to dryness. This coats the boron granules with boric acid, and

the powder can then be pressed into forms which can be handled without breaking.

The formed bars, or compacts, are heated in two stages under vacuum for 1 hr, at temperatures of 300° to 600°C to decompose the boric acid into boron oxide. This compound forms a liquid coating on the boron particles. When the compact is cooled, this liquid hardens, and bonds the powder into a strong bar.

The bar of boron powder is mounted vertically for floating-zone melting, and a high-frequency induction coil is used to melt a narrow band or zone of the material. The molten zone is moved down the rod by raising the bar through the coil, while the melted boron freezes or crystallizes above the coil. During this operation, the boron oxide binder sublimes before the melting point of boron (about 2000°C) is reached. Crystals as large as 0.1 in. were obtained, many of which were twinned.

The apparatus used in the floating-zone refining is similar to that used in the treatment of other materials, except that the rod of boron is enclosed within two concentric transparent quartz tubes. The inner tube is slotted; when the subliming boron oxide coats the tubes enough to restrict vision, the slotted tube is rotated to give a clear field again. This modification to the equipment has been used previously in the floating-zone melting of gallium arsenide at Bell Labs. by J. M. Whelan and G. H. Wheatley.

Preparatory to mounting the compact, the corners of the square bar are ground off, to minimize the "cage" effect, in which the corners do not melt. Also, in order to lower the resistivity of the boron, to allow it to be heated and melted by high-frequency induction, the top end of the bar is mounted in a graphite cup, which can be readily heated by such means.

Second Battery Symposium to be Held in England in October 1960

A Battery Symposium, the first of its kind to be held in England, was held at Bournemouth, Hampshire, in 1958, by the Inter-Departmental Committee on Batteries, Admiralty Engineering Laboratory, West Drayton, Middlesex. This Symposium was so successful that the Committee has undertaken to hold similar events every two years.

The next Battery Symposium will be held at Bournemouth on October 18, 19, and 20, 1960. Visitors from North America will be welcomed, as are offers of papers for the Symposium. However, since some 30 papers had been offered as of the middle of October 1959, the list may be closed. Papers have been received from Australia, Canada, France, Germany, the U.S.A., and Norway, and cover a wide field of battery research and development work as well as battery applications. A detailed program will be available early in 1960.

Australian Electroplating Shows Rapid Growth

The rate of growth of electroplating "down under" is out-pacing the United States, according to Peter L. Berkelaar, technical sales representative, United Chromium (Aust.) Pty., Ltd., Sydney, who recently spent a month in this country being brought up to date on the latest technical developments in both electroplating and organic coatings. Mr. Berkelaar estimates that Australian electroplating activity has more than doubled since World War II, and should double again within the next ten years.

United Chromium (Aust.) Pty., Ltd. has been an active participant in Australian metalworking and electroplating since the end of the War. Formed in 1946 by Metal & Thermit Corp., New York, and Polymer Corp. Pty., Ltd., in Sidney, it manufactures plating solutions, chromate dips, and plastisol and organosol finishes.

Australian plating practices are practically identical to those in the United States, Mr. Berkelaar pointed out. He attributes this to the excellent transmission of technical and application information from this country. The main difference is that production runs "down under" are far smaller than in the U.S., meaning less automation of plating equipment. And, he added, "it's difficult to compare the U.S. automobile industry—traditionally the biggest user of chromium plating solutions—with its Australian counterpart: we use chromium plate primarily for decorative and corrosion-resistant purposes. Die castings, hardware, tubular furniture, domestic appliances, and general decorative applications are the big market," he said.

Notice to Members and Subscribers

(Re Changes of Address)

To insure receipt of each issue of the JOURNAL, please be sure to give us your old address, as well as your new one, when you move. Our records are filed by states and cities, not by individual names. The Post Office does not forward magazines.

New Jersey Health Dept. Registering Sources of Radiation in State

The New Jersey State Department of Health began in late October 1959 to register sources of radiation in New Jersey, according to Dr. Roscoe P. Kandle, State Commissioner of Health and a member of the New Jersey Commission on Radiation Protection.

The first step was the registration of radiation-producing machines such as x-ray machines and high-voltage rectifiers, followed later by registration of radiation-producing materials, such as isotopes.

The Department began by sending a card, and a registration document to complete, to members of groups, such as physicians, dentists, veterinarians, industrialists, and hospitals, who are known to use radiation-producing machines.

Since registration of sources of radiation is required by Chapter 116, Public Laws of 1958, a non-salaried Commission was set up and has been working since October 1958 to develop a code of reasonable and practical measures to protect the public against injurious radiation.

Hoffman Electronics Developing Silicon Transistor Line

Hoffman Electronics Corp. announced plans recently to develop and market a line of silicon transistors.

The company's entry into the transistor field will give Hoffman a complete silicon semiconductor line capable of meeting a broad range of requirements in both military and commercial fields.

Hoffman will specialize in silicon transistors, to capitalize on the company's wide experience in developing and producing silicon junction devices. The company, beginning in 1952, was the first to produce silicon diodes commercially.

Vitro Consolidates Chemical and Metallurgical Operations

The formation of Vitro Chemical Co., a subsidiary, was announced recently by the Vitro Corp. of America.

The new company consolidates the chemical and metallurgical oper-

ations in the United States, including those conducted by Vitro Uranium Co., Salt Lake City, Utah; Heavy Minerals Co., Chattanooga, Tenn.; and Vitro Rare Metals Co., Canonsburg, Pa.

William B. Hall has been named president of Vitro Chemical Co. A chemical engineering graduate of Princeton University, Mr. Hall joined Vitro in 1951. From 1955 to 1958 he served as president of Vitro Uranium Co., Salt Lake City, Utah. He was appointed vice-president of Vitro Corp. of America in January 1959, a post he will continue to hold.

The new chemical company is engaged at present in the milling of uranium ores; production of thorium, rare earth chemicals, rare metals and metal alloys, and industrial chemicals; and is also engaged in chemical and metallurgical research and development.

Additional Buildings Acquired by Ohio Semiconductors, Inc.

Ohio Semiconductors, Inc., Columbus, Ohio, has announced the acquisition of additional quarters. The newly acquired space will be used for administrative offices and the development and production of materials and devices. The firm is engaged in the research, development, manufacture, and national distribution of semiconductor materials and devices for infrared, thermoelectric, and electronic applications.

The new location, consisting of three buildings covering approximately 23,000 square feet, will supplement the company's two present locations in Grandview Heights, a Columbus area community. The additional buildings bring the total floor area occupied by the company to six times that of its original headquarters occupied at the company's inception in 1956.

First Phase of Pennsalt Chlor-Caustic Modernization Completed

Pennsalt Chemicals Corp. recently completed the first phase of a $6,000,000 modernization program of its Wyandotte, Mich., chlorine-caustic soda facilities. The first section of improvements includes new 50% caustic soda evaporating facilities designed to reduce costs and improve quality.

The second major phase will be the replacement of several thousand Gibbs diaphragm-type electrolytic cells with a much smaller number of 30,000-amp, more economic cells, along with improvements to auxiliary cell-room equipment. When the new cells go on stream in mid-1960, the facility is expected to produce chlorine and caustic soda with product quality and operating efficiency equal or superior to any existing diaphragm cell operation.

Olin Mathieson to Expand Plant at McIntosh, Ala.

The Chemicals Division of Olin Mathieson Chemical Corp. has announced it is planning to further expand its electrolytic caustic-chlorine plant at McIntosh, Ala. The announcement was made by Edward Block, senior vice-president and general manager of the Chemicals Division.

The initial installation was made at McIntosh in 1952. The plant was doubled by the addition of a second unit which was completed in early 1957. It is proposed to add a new cell bank to the two already installed. The projected expansion is to meet the needs of the customers in the mid-South, particularly the rayon and the pulp and paper industries, and should accommodate these needs for the foreseeable future.

In addition to caustic and chlorine, the McIntosh plant manufactures various insecticide products.

Announcements from Publishers

"Gmelins Handbuch der Anorganischen Chemie, 8. Fluorine, Supplement Volume (System No. 5)." Published by Verlag Chemie, GmbH., Weinheim/Bergstr., West Germany, 1959. XVIII + 258 pages; $36.00.

This supplements the 1926 volume, covering in general the period up to 1949 with occasional references as late as 1955. ECS members will be interested in sections on the electrolytic preparation and electrochemical behavior of F_2, HF, F_2O, and NF_3. There is an English-German index and the chapter and paragraph headings have been translated into English.

"Gmelins Handbuch der Anorganischen Chemie, 8. Silicon, Part C (System No. 15)." Published by Verlag Chemie, GmbH., Wein-

June 1960 Discussion Section

A Discussion Section, covering papers published in the July—December 1959 JOURNALS, is scheduled for publication in the June 1960 issue. Any discussion which did not reach the Editor in time for inclusion in the December 1959 Discussion Section will be included in the June 1960 issue.

Those who plan to contribute remarks for this Discussion Section should submit their comments or questions in triplicate to the Managing Editor of the JOURNAL, 1860 Broadway, New York 23, N. Y., *not later than March 1, 1960.* All discussion will be forwarded to the author(s) for reply before being printed in the JOURNAL.

heim/Bergstr., West Germany, 1958. XII + 501 pages; $67.44.

This volume covers the preparation and properties of over 3000 organosilicon compounds. In addition, there is a discussion of the manufacturing problems and industrial application of silicones. The index is in German but the paragraph and chapter headings have been translated. Compound types covered are silanes, silanoles, siloxanes, and silicic acid esters.

"The Preparation and Characteristics of Thin Ferromagnetic Films," Air Force Cambridge Research Center, Nov. 1958. Report PB 151525,* 139 pages; $2.75.

"Properties of Ferrites and Their Applications to Microwave Systems," F. Reggia and R. D. Hatcher, Diamond Ordnance Fuze Labs., U. S. Army, Feb. 1959. Report PB 151749,* 59 pages; $1.50.

"Special Measurement Techniques for Thermoelectric Materials with Results for Bi_2TE_3 and Alloys with Bi_2Se_3," T. C. Harman and J. J. Logan, Battelle Memorial Institute, for Office of Naval Research, June 1958. Report PB 151656,* 19 pages; 50 cents.

"The Efficiency of Thermoelectric Generators," J. M. Borrego and others, Wright Air Development Center, U. S. Air Force, Sept. 1958. Report PB 151748,* 81 pages; $2.25.

"Status Report on Fuel Cells," B. R. Stein, Army Research Office, June 1959. Report PB 151804,* 119 pages; $1.25.

"An Electrolytic Saw," M. Metzger, University of Illinois, for Office of Naval Research, March 1958. Report PB 151574,* 8 pages; 50 cents.

"The Preparation of Polycrystalline Ferrites for Microwave Applications," J. E. Pippin and C. L. Hogan, Gordon McKay Lab., Harvard University, for Air Force Cambridge Research Center, Jan. 1958. Report PB 151020,* 65 pages; $1.50.

"Ionic Mobilities in Selected Fused Salt Systems," Aug. 1957. AEC Report ISC-992,* 60 pages; $1.75.

"Preparation of Ferromagnetic Fine Particles from Bimetallic Oxalates," W. J. Shuele, The Franklin Institute, for Wright Air Development Center, U. S. Air Force, April 1958. Report PB 151468,* 16 pages; 50 cents.

"Ferroelectric Devices," R. A. Fotland and E. F. Mayer, Horizons, Inc., for Wright Air Development Center, U. S. Air Force, Oct. 1958. Report PB 151484,* 75 pages; $2.00.

"Thermoelectric Properties of the Noble Metals and their Alloys" ("Termoelektricheskie Svoistva Blagorodnykh Metallov i ikh Splavov"), A. A. Rudnitskii, Institute of Metallurgy, Institute of General and Inorganic Chemistry, Academy of Sciences, U.S.S.R.. 1956. Russian report translated by the U.S. Atomic Energy Commission from a publication of the Publishing House of the Academy of Sciences, U.S.S.R. Report AEC-tr-3724,* 237 pages; $2.50.

* Order from Office of Technical Services, U. S. Dept. of Commerce, Washington 25, D. C.

Catalog Lists Reports of Battery Research

A new "Catalog of Technical Reports" listing all reports in the field of batteries available to the public from the collection of the Office of Technical Services has been published.

The catalog identifies reports on storage, alkaline, nuclear, and general types of batteries, and battery chargers. Many of the reports resulted from research conducted for the Army, Navy, Air Force, Atomic Energy Commission, and other agencies of the U. S. Government. Others are German documents captured during World War II. All are for sale to the public, some in printed form and others in microfilm or photocopy.

The listing, CTR-372 "Batteries, 1933-58," may be ordered from Office of Technical Services, U. S. Dept. of Commerce, Washington 25, D.C., at 10 cents each.

Tenth Edition of "American Men of Science"

The Tenth Edition of "American Men of Science" is in preparation and will contain biographies of more than 130,000 living Americans and Canadians who are actively contributing to the advancement of science. Over 40,000 of these biographies will be appearing in the directory for the first time. This increase has necessitated a revision in format from the last edition. The Tenth Edition will be published in five parts on an accelerated four-year cycle as follows: The Physical and Biological Sciences—A-E, F-K, L-R, S-Z; The Social and Behavioral Sciences—A-Z.

The A-E Volume was scheduled for completion by late 1959 with other volumes to appear on a nine-month schedule.

For further information, please contact Jaques Cattell, Editor, "American Men of Science," Arizona State University, Annex 15, Tempe, Ariz.

Abstracted Versions of More Russian Journals Published by OTS

Several more Russian technical journals are being published in abstract form in English by the Office of Technical Services, two of which are of particular interest to JOURNAL readers. Listed below are the order numbers and titles, frequency of issuance, and prices for single issue or for a subscription period.

PB 141058T, "Chemical Science and Industry" ("Khimicheskaya Nauka i Promyshlennost'"). Bimonthly; 70 cents single issue, $4.00 for 6 issues.

PB 141076T, "Journal of Applied

AERONUTRONIC

a Division of Ford Motor Company

Has an immediate opening for an

ELECTROCHEMIST

to assume direct responsibility for research in the fabrication of solid state digital devices.

HE MUST:

- be capable of doing research on new types of solid state devices.
- have at least a BS degree in chemistry; an advanced degree is preferable.
- have experience in analytical chemistry, printed circuits, electrochemical reactions and chemical reactions associated with solid state device fabrication.

This responsible position offers challenging work opportunities at Aeronutronic's new $22 million Engineering and Research Center, now being completed on a 200-acre site at Newport Beach, in Southern California—the West's most ideal area for living, working and raising a family.

Ford resources provide the finest facilities for carrying out complete research, engineering and manufacturing operations on advanced projects which can prove stimulating, as well as exceptionally rewarding, to the right man.

If your qualifications meet the above requirements, send an inquiry or resume to Mr. R. E. Durant, Computer Operations, Aeronutronic, Box N-Z-486, Newport Beach, California.

COMPUTER OPERATIONS

AERONUTRONIC

a Division of FORD MOTOR COMPANY
Ford Road, Newport Beach

NEWPORT BEACH • SANTA ANA • MAYWOOD, CALIFORNIA
NATICK, MASSACHUSETTS

Chemistry" ("Zhurnal Prikladnoy Khimii"). Monthly; 90 cents single issue, $5.00 for 6 issues.

Orders should be addressed to Office of Technical Services, U.S. Dept. of Commerce, Washington 25, D.C.

A complete list of Russian journals published in abstract form by OTS will be furnished on request.

New Products

Ultrahigh-Purity Silicon Monocrystals. Grace Electronic Chemicals, Inc., 101 N. Charles St., Baltimore 1, Md., has announced the availability of float zone refined silicon monocrystals, semiconductor grade, doped to customer specifications. According to a company spokesman, the new product, produced in a plant in the Baltimore area, has a boron level of less than ½ ppb. Undoped monocrystals are characterized by resistivities of 800 ohm-cm or higher, and lifetimes in excess of 200 μsec. Polycrystalline rods of the same purity, which have been given one floating zone pass, are available for those who wish to grow their own monocrystals in floating zone equipment. In addition to monocrystals, the company will continue to supply ultrahigh-purity Grade I and Grade II polycrystalline silicon.

Teflon Jackets for Diode Cases. For circuitry where bank-mounting or other close-quarter mounting procedures are used, the entire range of International Rectifier Corp. silicon pigtail diodes are now available with an insulating Teflon coating over the diode case. In such applications as printed circuit boards, computers, and data-processing equipment, the high-temperature chemical-resistant jacket permits extremely close positioning of diodes, while eliminating the possibility of diode cases shorting to other components or to chassis. For further information write to International Rectifier Corp., 1521 E. Grand Ave., El Segundo, Calif.

Literature from Industry

Metex Electropolish BB, an acidic solution used to produce a brilliant luster on lead-free wrought brass, is fully described in a two-page usage and instruction sheet, Technical Data Sheet No. 41. **Alumetex Process,** a process for preparing commercially used aluminum alloys for any type of electrodeposit, is fully described in Technical Data Sheet No. 13. This simple, easy to control process permits all commonly electroplated metals to be safely deposited on aluminum. The Alumetex Process consists of an alkaline, non-etch cleaner, two acid etches, an immersion coating, and a final copper strike. Both Data Sheets are available from MacDermid Inc., Waterbury, Conn.

G. E. Bulletin on Nuclear Irradiation Services. The General Electric Atomic Power Equipment Dept. has announced a new bulletin describing department facilities for irradiation services. APED services include the handling of complete radiation effects programs, from planning through irradiation and post-irradiation analysis and reporting. The bulletin includes photographs and detailed descriptions of irradiation services, particularly in the General Electric Test Reactor (GETR), this country's largest privately owned materials testing reactor. Request Bulletin GEA-6934 from the General Electric Apparatus Sales Division, Schenectady 5, N. Y.

Advertiser's Index

Employment Situations

Positions Available

Chemists and Chemical Engineers—We need physical, organic and inorganic chemists, and chemical engineers to carry out engineering and development work in the rapidly growing power sources field. Research & Development center located in Minneapolis near University of Minnesota. Battery experience preferred but not required. Send résumés to: J. W. Baxter, Employee & Labor Relations, Gould-National Batteries, Inc., E. 1326 First National Bank Bldg., St. Paul 1, Minnesota.

The Electrochemical Society

Patron Members

Aluminum Co. of Canada, Ltd.,
Montreal, Que., Canada
International Nickel Co., Inc.,
New York, N. Y.
Olin Mathieson Chemical Corp.,
Niagara Falls, N. Y.
Industrial Chemicals Div., Research
and Development Dept.
Union Carbide Corp.
Divisions:
Union Carbide Metals Co.,
New York, N. Y.
National Carbon Co., New York, N. Y.
Westinghouse Electric Corp., Pittsburgh, Pa.

Sustaining Members

Air Reduction Co., Inc.,
New York, N. Y.
Ajax Electro Metallurgical Corp.,
Philadelphia, Pa.
Allen-Bradley Co., Milwaukee, Wis.
Allied Chemical & Dye Corp.
General Chemical Div., Morristown, N. J.
Solvay Process Div., Syracuse, N. Y.
(3 memberships)
Allied Research Products, Inc.,
Detroit, Mich.
Alloy Steel Products Co., Inc., Linden, N. J.
Aluminum Co. of America,
New Kensington, Pa.
American Machine & Foundry Co.,
Raleigh, N. C.
American Metal Climax, Inc.,
New York, N. Y.
American Potash & Chemical Corp.,
Los Angeles, Calif. (2 memberships)
American Zinc Co. of Illinois,
East St. Louis, Ill.
American Zinc, Lead & Smelting Co.,
St. Louis, Mo.
American Zinc Oxide Co., Columbus, Ohio
M. Ames Chemical Works, Inc.,
Glens Falls, N. Y.
Auto City Plating Company Foundation,
Detroit, Mich.
Basic Inc., Maple Grove, Ohio
Bell Telephone Laboratories, Inc.,
New York, N. Y. (2 memberships)
Bethlehem Steel Co., Bethlehem, Pa.
(2 memberships)
Boeing Airplane Co., Seattle, Wash.
Burgess Battery Co., Freeport, Ill.
(4 memberships)
C & D Batteries, Inc., Conshohocken, Pa.
Canadian Industries Ltd., Montreal, Que.,
Canada
Carborundum Co., Niagara Falls, N. Y.
Catalyst Research Corp., Baltimore, Md.
Chrysler Corp., Detroit, Mich.
Ciba Pharmaceutical Products, Inc., Summit,
N. J.
Columbian Carbon Co., New York, N. Y.
Columbia-Southern Chemical Corp.,
Pittsburgh, Pa.
Consolidated Mining & Smelting Co. of
Canada, Ltd., Trail, B. C., Canada
(2 memberships)
Continental Can Co., Inc., Chicago, Ill.
Cooper Metallurgical Associates, Cleveland,
Ohio
Corning Glass Works, Corning, N. Y.
Crane Co., Chicago, Ill.
Diamond Alkali Co., Painesville, Ohio
(2 memberships)
Dow Chemical Co., Midland, Mich.
Wilbur B. Driver Co., Newark, N. J.
(2 memberships)
E. I. du Pont de Nemours & Co., Inc.,
Wilmington, Del.
Eagle-Picher Co., Chemical Div., Joplin, Mo.
Eastman Kodak Co., Rochester, N. Y.
Electric Auto-Lite Co., Toledo, Ohio
Electric Storage Battery Co.,
Philadelphia, Pa.
Englehard Industries, Inc., Newark, N. J.
(2 memberships)
The Eppley Laboratory, Inc., Newport, R. I.
(2 memberships)
Erie Resistor Corp., Erie, Pa.
Exmet Corp., Tuckahoe, N.Y.
Fairchild Semiconductor Corp., Palo Alto,
Calif.
Federal Telecommunication Laboratories,
Nutley, N. J.
Food Machinery & Chemical Corp.
Becco Chemical Div., Buffalo, N. Y.
Westvaco Chlor-Alkali Div., South
Charleston, W. Va.
Foote Mineral Co., Paoli, Pa.
Ford Motor Co., Dearborn, Mich.
General Electric Co., Schenectady, N. Y.
Chemistry & Chemical Engineering
Component, General Engineering
Laboratory
Chemistry Research Dept.
General Physics Research Dept.
Metallurgy & Ceramics Research Dept.
General Instrument Corp., Newark, N. J.

(Sustaining Members cont'd)

General Motors Corp.
Brown-Lipe-Chapin Div., Syracuse, N. Y. (2 memberships)
Guide Lamp Div., Anderson, Ind.
Research Laboratories Div., Detroit, Mich.
General Transistor Corp., Jamaica, N. Y.
Gillette Safety Razor Co., Boston, Mass.
Globe-Union, Inc., Milwaukee, Wis.
Gould-National Batteries, Inc., Depew, N. Y.
Grace Electronic Chemicals, Inc., Baltimore, Md.
Great Lakes Carbon Corp., New York, N. Y.
Hanson-Van Winkle-Munning Co., Matawan, N. J. (3 memberships)
Harshaw Chemical Co., Cleveland, Ohio (2 memberships)
Hercules Powder Co., Wilmington, Del.
Hill Cross Co., Inc., New York, N. Y.
Hoffman Electronics Corp., Evanston, Ill.
Hooker Chemical Corp., Niagara Falls, N. Y. (3 memberships)
Houdaille Industries, Inc., Detroit, Mich.
Hughes Aircraft Co., Culver City, Calif.
International Business Machines Corp., Poughkeepsie, N. Y.
International Minerals & Chemical Corp., Chicago, Ill.
Jones & Laughlin Steel Corp., Pittsburgh, Pa.
K. W. Battery Co., Skokie, Ill.
Kaiser Aluminum & Chemical Corp.
Chemical Research Dept., Permanente, Calif.
Div. of Metallurgical Research, Spokane, Wash.
Kennecott Copper Corp., New York, N. Y.
Keokuk Electro-Metals Co., Keokuk, Iowa
Libbey-Owens-Ford Glass Co., Toledo, Ohio
P. R. Mallory & Co., Indianapolis, Ind.
McGean Chemical Co., Cleveland, Ohio
Merck & Co., Inc., Rahway, N. J.
Metal & Thermit Corp., Detroit, Mich.
Minnesota Mining & Manufacturing Co., St. Paul, Minn.
Monsanto Chemical Co., St. Louis, Mo.
Motorola, Inc., Chicago, Ill.
National Cash Register Co., Dayton, Ohio
National Lead Co., New York, N. Y.
National Research Corp., Cambridge, Mass.
National Steel Corp., Weirton, W. Va.
New York Air Brake Co., Vacuum Equipment Div., Camden, N. J.
Northern Electric Co., Montreal, Que., Canada
Norton Co., Worcester, Mass.
Olin Mathieson Chemical Corp., Niagara Falls, N. Y.
High Energy Fuels Organization (2 memberships)
Peerless Roll Leaf Co., Inc., Union City, N. J.
Pennsalt Chemicals Corp., Philadelphia, Pa.
Phelps Dodge Refining Corp., Maspeth, N. Y.
Philco Corp., Philadelphia, Pa.
Philips Laboratories, Inc., Irvington-on-Hudson, N. Y.
Pittsburgh Metallurgical Co., Inc., Niagara Falls, N. Y.
Poor & Co., Promat Div., Waukegan, Ill.
Potash Co. of America, Carlsbad, N. Mex.
Radio Corp. of America, Harrison, N. J.
Ray-O-Vac Co., Madison, Wis.
Raytheon Manufacturing Co., Waltham, Mass.
Reynolds Metals Co., Richmond, Va. (2 memberships)
Rheem Semiconductor Corp., Mountain View, Calif.
Schering Corporation, Bloomfield, N. J.
Shawinigan Chemicals Ltd., Montreal, Que., Canada
Speer Carbon Co.
International Graphite & Electrode Div., St. Marys, Pa. (2 memberships)
Sprague Electric Co., North Adams, Mass.
Stackpole Carbon Co., St. Marys, Pa.
Stauffer Chemical Co., New York, N. Y.
Sumner Chemical Co., Div. of Miles Laboratories, Inc., Elkhart, Ind.
Sylvania Electric Products Inc., Bayside, N. Y. (2 memberships)
Tennessee Products & Chemical Corp., Nashville, Tenn.
Texas Instruments, Inc., Dallas, Texas
Metals & Controls Div., Attleboro, Mass.
Three Point Four Corp., Yonkers, N. Y.
Titanium Metals Corp. of America, Henderson, Nev.
Tung-Sol Electric Inc., Newark, N. J.
Udylite Corp., Detroit, Mich. (4 memberships)
Universal-Cyclops Steel Corp., Bridgeville, Pa.
Upjohn Co., Kalamazoo, Mich.
Victor Chemical Works, Chicago, Ill.
Western Electric Co., Inc., Chicago, Ill.
Wyandotte Chemicals Corp., Wyandotte, Mich.
Yardney Electric Corp., New York, N. Y.